



**University of
Nottingham**
UK | CHINA | MALAYSIA



DOCTOR OF PHILOSOPHY
(2023)

**Further studies in rat models of neural
disinhibition: behavioural, in vivo
electrophysiological, and translational
imaging studies**

Joanna Loayza

School of Psychology
University of Nottingham
United Kingdom

*Doctoral thesis to be submitted to Student Services of the University of
Nottingham by the 9th of June 2023.*

Every good and perfect gift is from above,
coming down from the Father of the heavenly lights,
who does not change like shifting shadows.

James 1:17

Abstract

Neural disinhibition, i.e., reduced inhibitory GABA transmission, has been implicated in various neuropsychiatric disorders. In particular, GABA-ergic abnormalities in the hippocampus and the striatum have been associated with schizophrenia and Tourette Syndrome, respectively. Regional neural disinhibition may affect behaviour by disrupting regional neural function and by causing changes in projection sites of the disinhibited region. In schizophrenia, one of such projection sites is the septum and in Tourette Syndrome the motor cortex. To further examine the impact of regional disinhibition (ventral hippocampus or anterior dorsal striatum), we combined intra-cerebral microinfusions of a GABA-A receptor antagonist (picrotoxin) with translational neural imaging (MRS, rsFC MRI), electrophysiological measurements and behavioural methods (locomotor activity and prepulse inhibition) in Lister hooded rats.

First, we used ^1H -Magnetic Resonance Spectroscopy (MRS) at 7T, to measure neuro-metabolites in the septum following ventral hippocampal disinhibition (Chapter 2). This study was based on our previous Single-photon emission computed tomography (SPECT) imaging study that revealed marked metabolic activation in several extra-hippocampal sites, including the septum, after ventral hippocampus disinhibition (Williams et al., in preparation). This experiment demonstrated no clear effects of ventral hippocampal disinhibition on any of the neuro-metabolites measured in the septum, including glutamate, glutamine and GABA, indicating that marked acute metabolic activation in the lateral septum (as detected by SPECT) is potentially not accompanied by neuro-metabolites changes measurable by MRS (possibly reflecting homeostatic metabolic mechanisms).

Second, we used electrophysiological measurements in anaesthetised rats (Chapter 3) to examine the effects of striatal disinhibition, induced by picrotoxin infusions (300 ng picrotoxin in 0.5 μl saline) into the anterior dorsal striatum, on neural activity in the vicinity of the infusion site. Our findings revealed large local field potential (LFP) spike-wave discharges, consisting of a single negative spike followed by a positive wave. Furthermore, picrotoxin in the dorsal striatum enhanced multi-unit burst firing, reflected by significant increases in mean spike frequency in burst per block, mean peak spike frequency in burst and percentage spikes in burst and by increased frequency of bursts, reflected by significant decreases of mean interburst interval per block. This is a new finding in the striatum and is consistent with disinhibition-induced enhancement of burst firing that we previously reported in the prefrontal cortex and hippocampus (Pezze et al., 2014; McGarrity et al., 2017), suggesting that in all these regions, GABA-A receptor-mediated inhibition is particularly important to control neural burst firing. No tic-like movements were visible in the anaesthetised rats.

Third, we characterised tic-like forelimb movements caused by infusing picrotoxin into the right anterior dorsal striatum (300 ng and 200 ng picrotoxin in 0.5 μ l saline) of rats (Chapter 4). Such infusions reliably induced tic-like movements in the left forelimb within the same rat and across rats. Most rats expressed highest frequency of tic-like movements in the first 5 to 35 min post-infusion. Tic-like movements were characterised. The most common tic-like movement involved the rat to lift its left forelimb, thereby rotating its head and torso to the right around the body's long axis, before putting the left forelimb back down again, and thereby moving its head and torso into its starting position. There were also some more pronounced forelimb movements that lasted for several seconds and led to a whole rotation of the body around its long axis. The movements observed in this study were compared to tics in Tourette syndrome.

Fourth, we investigated the impact of anterior dorsal striatal disinhibition (300 ng picrotoxin in 0.5 μ l saline) on prepulse inhibition (PPI) of the acoustic startle response and locomotor activity (Chapter 5). Picrotoxin infusion caused tic-like movements, had no effect on prepulse inhibition, tended to reduce startle and significantly increased locomotor activity and fine motor count. No PPI deficit following striatal disinhibition indicates that GABAergic inhibition in the dorsal striatum is not critical for prepulse inhibition. Our finding that marked tic-like movements were produced alongside intact PPI does not support the possibility that PPI disruption is necessary for tic-like movements (as suggested by Swerdlow and colleagues). The timeline of the fine motor count was similar to the timeline of the tic-like movements, and therefore, fine motor counts may thus be used as an automated measure of tic-like movements. The locomotor hyperactivity alongside tic-like movements indicates that dorsal striatal activity is not only involved in generating movements of individual body parts, but also in modulating locomotor activity and suggests that striatal disinhibition that contributes to tic-like movements may also contribute to hyperactivity, which is often comorbid with Tourette Syndrome (Robertson, 2015).

Lastly, we aimed to provide proof of principle that standard resting state functional connectivity Magnetic Resonance Imaging (rsFC MRI) measurements are possible in rats with pre-implanted guide cannulae and microinfusions in the anterior dorsal striatum (Chapter 6). Although we obtained sufficient quality rsFC MRI data to reveal the resting-state default mode network of an unoperated rat using the anterior cingulate as a seed, we were unable to obtain any resting-state default mode network of an operated rat, due to the significant signal loss from the guide cannula. We also tried to obtain spectra from the motor cortex following striatal disinhibition (using MRS), however, were unable to get good Signal to Noise ratio values for the water signal of the voxel placed in the motor cortex (SNR_H₂O). Although some neuro-metabolites, including glutam-

ate, were measurable in the motor cortex of rats with a dorsal striatal guide cannula, others, including GABA, were not. When comparing the SNR_{H₂O} values between our studies, it appears that SNR_{H₂O} values decrease with increased distance between regions (disinhibited region and ROI for spectrum).

Concluding, disinhibiting the ventral hippocampus, has no clear effects on any neuro-metabolites in the septum, as measured by MRS. Dorsal striatal disinhibition causes large spike wave discharges and enhances burst firing in the striatum under anaesthesia. In behaving rats, striatal disinhibition causes tic-like movements, increases locomotor activity and fine movement counts, and has no effect on prepulse inhibition. Obtaining sufficient quality rsFC MRI data to reveal the resting-state default mode network is not possible following implantation of a guide cannula, as the cannula leads to too much signal loss. The signal for MRS is too poor with striatal cannula implants and a voxel placed in the motor cortex.

Acknowledgements

The PhD would not have been possible without the support of many people. I would like to thank Tobias Bast, my PhD supervisor, for his guidance throughout the project. I am grateful for your advice, patience, encouragement, knowledge and support. Thank you for taking me on as a student and for reading through my numerous revisions. I could not have hoped for a better supervisor!

Thank you, Stephen Jackson, for introducing me to the field of Tourette Syndrome and for encouraging me to do a PhD. Researching Tourette Syndrome will forever have a special place in my heart! Thank you Malcolm Prior, for your patience and constant support for making our MR studies possible. And thank you Tracy Farr for helping us with the rsFC MRI study.

A big thank you goes to my lab group: Charlie, Jacco, Rachel and Stuart. I could not have done all the surgeries and experiments without you. Thank you for your time and for creating a warm lab environment. I had a lot of fun! I would also like to thank the Jackson Lab for being so welcoming and inviting me to all the pub trips! Special thanks to Kat Gialopsou, you have constantly supported me and kept me calm in times of stress, especially during my last weeks of writing my thesis. Thank you!

I would like to thank the animal unit (Bio Support Unit, BSU) and the School of Life Sciences Imaging Facility (SLIM) and staff for their contribution to this thesis. Thank you to the Medical Research Council for not only awarding me a doctoral training program and for providing me with the financial means to complete this project, but for also providing us with many opportunities. Thank you, Karen Robinson, Dan Tennant and Louise Wain, for going out of your way to create a close-knit cohort of students from Nottingham, Birmingham and Leicester. I have very fond memories!

And finally, a big thank you to my family, James and numerous friends who endured this long process with me and who always offered love and support. I will cherish this time forever.

Thank you!

Contents

1	Introduction	12
1.1	Brief overview of GABA	12
1.2	Evidence for neural disinhibition in neuropsychiatric disorders	13
1.3	Animal models of neural disinhibition	22
1.4	Aims of the PhD project	30
2	A Magnetic Resonance Spectroscopy study of neurochemical changes in the septum in a rat model of hippocampal disinhibition	33
2.1	Introduction	33
2.2	Methods	37
2.3	Results	45
2.4	Discussion	55
3	Further characterisation of the rat striatal disinhibition model: In vivo electrophysiological characterisation of neural activity changes in the striatum under anaesthesia	60
3.1	Introduction	60
3.2	Methods	63
3.3	Results	70
3.4	Discussion	76
4	Further characterisation of the rat striatal disinhibition model: tic-like movements	79
4.1	Introduction	79
4.2	Methods	82
4.3	Results	87
4.4	Discussion	95
5	Further characterisation of the rat striatal disinhibition model: No deficit in prepulse inhibition of the acoustic startle response, and increased locomotor activity	97
5.1	Introduction	97
5.2	Methods	101
5.3	Results	107
5.4	Discussion	111
6	Pilot studies to examine the feasibility of resting state functional connectivity MRI and Magnetic Resonance Spectroscopy in the rat striatal disinhibition model	114
6.1	Introduction	114
6.2	Methods	115
6.3	Results	122

6.4 Discussion	123
7 General discussion	126
8 Conclusions and future directions	129

List of Figures

1	Model of the cortical-striatal-thalamic-cortical pathway . . .	18
2	Graphical visualisation of screws and cement placement to secure hippocampal guide cannulae	39
3	Coronal view of voxel placement in the septum and example spectrum generated with LCModel	42
4	MRS study timeline	43
5	Data exclusion criteria	44
6	Infusion sites in the ventral hippocampus	45
7	Comparison of shim values and SNR_H ₂ O in the voxel placed in the septum in rats with and without front screws	46
8	Example of rats showing artefacts in MR scan	47
9	Scan pre- and post-signal dropout of the same rat	47
10	Example of blood in rats that were included in the analysis	47
11	Difference scores (post-infusion minus pre-infusion concentration) for all measured metabolites following saline and picrotoxin infusion	50
12	Main effect of time	52
13	No longer main effect of time	53
14	Comparing our results to Williams et al. (in preparation)	53
15	Comparing our results to Iltis et al. (2009)	54
16	Electrode and infusion cannula placements	65
17	Enhanced LFP spike-wave discharges and multiunit burst-firing	70
18	Enhanced burst firing	74
19	No picrotoxin related changes	75
20	Graphical visualisation of cannula, screw and stylet implants	83
21	Study timeline of tic-like movements caused by striatal disinhibition	85
22	Set up of recording for tic-like movements	86
23	Infusion sites in the anterior dorsal striatum	87
24	Screenshots from the video recording showing tic-like movements	89
25	Time course of tic-like movements following striatal disinhibition by picrotoxin	91
26	Between-subjects variability in number of tic-like movements following striatal disinhibition	93
27	Comparing number of tic-like movements between infusions per rat	94
28	Prepulse inhibition of the startle response	98
29	Connectivity between PPTg, basal ganglia and thalamus	99
30	Test chambers to measure startle reflex and prepulse inhibition	103
31	Pulse-alone and prepulse-plus-pulse trials	104
32	Activity boxes with photobeams	105

33	Study timeline for PPI and LMA experiment	105
34	Infusion cannula tip placements in the anterior dorsal striatum	107
35	Startle and percentage prepulse inhibition following striatal infusion of saline or picrotoxin	108
36	Baseline measurements of locomotor activity and fine movement activity	109
37	Locomotor measurements following saline/picrotoxin . . .	110
38	Graphical visualisation of guide cannula and screw implants	117
39	Photograph of head coil set up for rsFC MRI scanning . .	118
40	Coronal view of voxel placement in motor cortex	120
41	Registration of Ratlas to the unoperated rat brain	121
42	Coronal view of gradient echo images taken from the unoperated (a) and an operated (b) rat	122
43	Seed based analysis with the anterior cingulate	123

List of Tables

1	Metabolite concentrations with CRLB pre/post saline/picrotoxin infusion	49
2	Baseline values of multi-unit and LFP parameters recorded from the dorsal striatum in the present study, alongside values recorded previously from medial prefrontal cortex (Pezze et al., 2014) and ventral hippocampus (McGarrity et al., 2017)	72
3	Rodent studies reporting tic-like limb movements, caused by striatal disinhibition, caused by intra-striatal drug microinfusions	81
4	Comparing tic onset and duration between picrotoxin infusions	90
5	Number of body twisting per infusion	92

1 Introduction

This thesis focuses on rodent models of reduced GABAergic neural inhibition, so-called neural disinhibition, within the hippocampus and striatum. Such hippocampal and striatal disinhibition has been implicated as part of the pathophysiology of various neuropsychiatric disorders, such as schizophrenia and Tourette Syndrome (Bast et al., 2017; G. M. Jackson et al., 2015; Leke & Schousboe, 2016). Evidence of such disruption is provided in the Introduction Chapter, first from human studies, followed by animal models of disinhibition. A range of brain regions have been identified that show dysfunctional GABAergic inhibition in psychiatric disorders, including the hippocampus and the striatum. Particular focus is placed on those two brain areas when discussing schizophrenia and Tourette Syndrome respectively. This Introduction Chapter starts by giving a brief background on GABA and closes by discussing the aims of my project.

1.1 Brief overview of GABA

For healthy cognition and behaviour, neural activity needs to be coordinated and balanced within specific as well as across different brain areas (Uhlhaas & Singer, 2010). This is achieved through the mutually controlling excitatory and inhibitory neurotransmitter systems (Kalkman & Loetscher, 2003), which determine both spatially and temporally the amount of input a neuron receives (Vogels & Abbott, 2009). This regulation allows for effective information flow (Cline, 2005) as overall firing properties of brain networks are controlled (Lisman et al., 2008; Danton & Dietrich, 2005; Hattori et al., 2017). The major inhibitory neurotransmitter of the brain is γ – aminobutyric acid (GABA) (Kalkman & Loetscher, 2003). Its concentration has been estimated at 1.5-3 mM in the synaptic cleft (Mozrzymas et al., 2003). The synthesis of GABA is dependent on glutamate decarboxylase, an enzyme that distinguishes GABAergic cells from non-GABAergic cells (Sonnwald et al., 2006). GAD is present as two isoenzymes, GAD65 and GAD67, which are encoded by different independently regulated genes (Soghomonian & Martin, 1998). There is evidence that most GABAergic neurons co-express both isoforms (Stone et al., 1999). However, some neurons may express one isoform more than the other or may only express GAD67 (Esclapez et al., 1993). Both isoforms can synthesise GABA (Bu et al., 1992).

The hippocampus and striatum are important brain regions, that are discussed further in Sections 1.2.1.1 and 1.2.2.1 and are thus also mentioned in this context. In the cerebral cortex, the ratio of inhibitory to excitatory transmission is higher than in the hippocampus (Heckers & Konradi, 2015). In the hippocampus the majority of neurons are glutamatergic (approximately 90%) (Freund & Buzsáki, 1996). This makes the hippo-

campus more vulnerable to excitation and seizures (Heckers & Konradi, 2015). Despite the small proportion of GABAergic neurons, whole populations of pyramidal cells are inhibited, and their firing is being synchronized, as an individual interneuron makes multiple postsynaptic contacts onto a thousand pyramidal cells (Sweatt, 2007; Uhlhaas & Singer, 2010). In the striatum, the majority of neurons are medium spiny GABAergic projection neurons (Kreitzer, 2009; Bernácer et al., 2012) and less than 4% of the total neuron population are GABA interneurons (Lenington et al., 2016). GABAergic interneurons are neurons that control the activity of excitatory or inhibitory projections neurons within individual brain regions (Sweatt, 2007), including hippocampus (where projection neurons are excitatory glutamatergic neurons (Chauhan et al., 2021)) and striatum (where projections neurons are GABAergic (Gerfen & Bolam, 2010)).

GABAergic interneurons in the neocortex and hippocampus have often been subdivided based on different criteria such as their morphology (basket cells and chandelier cells), electrophysiology (fast-spiking and low-threshold spiking), synaptic connectivity (soma and distal dendrites), and gene expression (parvalbumin-containing and somatostatin-containing interneurons) (Markram et al., 2004; Pelkey et al., 2017). It has been suggested that the diversity of interneurons arises from specific interactions of genetic and environmental factors (Batista-Brito & Fishell, 2009). Different subtypes form different synapses and thus each class of interneurons modulates and impacts pyramidal cells differently (Freund & Buzsáki, 1996; Somogyi & Klausberger, 2005). Therefore, a deficit in a specific GABAergic subtype may have different consequences than a deficit in another subtype (Marín, 2012).

1.2 Evidence for neural disinhibition in neuropsychiatric disorders

1.2.1 Schizophrenia

Schizophrenia affects around 1% of the world's population (Perälä et al., 2007) and is typically diagnosed in late adolescence or early adulthood (Gogtay et al., 2011). It is characterised by positive (e.g. hallucinations, delusions), negative (e.g. lack of motivation, poverty of speech), cognitive (e.g. difficulties in attention, memory, and executive functioning) and affective (depression, mania) symptoms (van Os & Kapur, 2009). The aetiology of schizophrenia is currently unknown, however, neurotransmitter systems such as the GABAergic system have been identified that show impairments in schizophrenia (Benes & Berretta, 2001; Gilmour et al., 2012). An early post-mortem study found significant reductions of cortical GABA in the nucleus accumbens (ventral striatum) and thalamus in individuals with schizophrenia (T. L. Perry et al., 1979). Another line of evidence for the disruption of the GABAergic system in schizo-

phrenia comes from studies investigating glutamate decarboxylase (GAD) levels post-mortem in people with schizophrenia. In schizophrenia, reduced GAD67 mRNA levels is a robust finding and has been found in several brain regions, such as prefrontal cortex (PFC) (Akbarian et al., 1995; Volk et al., 2000; Guidotti et al., 2000), hippocampus (Benes et al., 2007; Heckers et al., 2002), temporal cortex (Impagnatiello et al., 1998) and cerebellum (Guidotti et al., 2000). This indicates that changes may not be confined to one brain region but may take place throughout the whole brain. Some of these changes have also been found in patients with other psychotic disorders such as bipolar disorder, suggesting that the two disorders may have overlapping molecular pathways (Heckers et al., 2002; Guidotti et al., 2000; Lakhan et al., 2013).

Furthermore, parvalbumin-expressing interneurons (PV+), appear to be affected in schizophrenia (Marín, 2012). Although the overall number of neurons within hippocampus and PFC of post-mortem brains of people with schizophrenia is typically not found to be changed (Akbarian et al., 1995; Dwork, 1997; Heckers et al., 1991; Schmitt et al., 2009; Walker et al., 2002), reduced numbers of PV+ interneurons is consistently reported in several brain areas (Beasley et al., 2002; Benes & Todtenkopf, 1998; Eyles et al., 2002; Torrey et al., 2005). Similarly, Konradi et al. (2011) did not find reductions in the total number of hippocampal neurons in the pyramidal cell layer, however, reported reduced somatostatin and PV+ interneurons as well as reduced somatostatin, parvalbumin and GAD67 mRNA in individuals with schizophrenia. Reductions in the density of PV+ neurons in the hippocampus of schizophrenic patients have also been observed (Zhang & Reynolds, 2002). Both Volk et al. (2002) and Benes et al. (1996) found an upregulation of postsynaptic GABA-A receptors in schizophrenia, in the PFC and hippocampus respectively. This increased expression may be a compensatory mechanism for the diminished expression of GABA-related molecules.

Parvalbumin-expressing GABAergic interneurons have shown to play a key role in the generation of high frequency gamma oscillations (typically 30 to 80 Hz) (Uhlhaas & Singer, 2013). Therefore, one would expect that abnormalities in PV+ interneurons would be accompanied by abnormalities in gamma oscillation (and vice versa). In patients with schizophrenia, aberrant gamma oscillations (both amplitude and synchrony) have been consistently reported using magnetoencephalography (MEG) or electroencephalography (EEG) (Gandal et al., 2012; M. H. Hall et al., 2011; Krishnan et al., 2009; Uhlhaas & Singer, 2010, 2013). Impairments have been found during different cognitive tasks (Basar-Eroglu et al., 2009; Haenschel et al., 2009; Minzenberg et al., 2010; K. M. Spencer et al., 2003; Uhlhaas et al., 2006) as well as at rest (Kikuchi et al., 2011; Rutter et al., 2009). Many of these reports mentioned above found impairments in gamma oscillations and some correlated schizophrenic symptoms with reduced gamma oscillations (Ferrarelli et al., 2012; Grützner et al., 2013).

Given that inhibitory GABA neurons play a key role in the generation and synchronisation of oscillations, aberrant oscillations may arise partly from GABA dysfunction (Bast et al., 2017; Lisman et al., 2008; Tregellas, 2014). Furthermore, GABAergic interneurons that fail to inhibit might contribute to the cognitive deficits and perhaps other symptoms that are associated with schizophrenia (Lisman et al., 2008; Marín, 2012). Additionally, impaired function of GABAergic interneurons may also be reflected by transcranial magnetic stimulation studies that found reduced cortical inhibitory function in schizophrenia patients (Daskalakis et al., 2002; Wobrock et al., 2008).

1.2.1.1 Hippocampal GABA dysfunction in schizophrenia

As patients with schizophrenia often suffer from severe deficits in memory, attention and executive function (Sitskoorn et al., 2004) it seems likely that there are abnormalities in the PFC and hippocampus. Several studies have investigated hippocampal activity in patients with schizophrenia during cognitive tasks, using various imaging techniques such as functional Magnetic Resonance Imaging (fMRI) and positron emission tomography (PET), and found impaired task-dependent activation (Buchsbaum et al., 1992; Heckers et al., 1998; Holt et al., 2005, 2006; Jessen et al., 2003; Nordahl et al., 1996; Weiss et al., 2004; L. E. Williams et al., 2013).

At rest, schizophrenia patients consistently show increased activation in the hippocampus (Lieberman et al., 2018; Malaspina et al., 2004; Medoff et al., 2001; Talati et al., 2014), but also see Tamminga et al. (1992), who reported decreased regional cerebral glucose metabolic rates in the hippocampus using PET, which does not support the evidence for resting hippocampal hyperexcitability. Schobel et al. (2013), who also found increases in the cerebral blood volume (CBV) in the hippocampus, additionally investigated hippocampal metabolic changes that take place during the onset and course of schizophrenia. In their longitudinal study, they found that during the prodromal pre-psychotic stages, increases in CBV occurred mainly in the CA1 subregion, which spread to the subiculum as patients progressed to psychosis. The increases were interpreted as evidence for a hypermetabolic state in schizophrenia. In their previous study they also reported that regional CBV in the CA1 region of the hippocampus predicted progression to psychosis (Schobel et al., 2009). Furthermore, several studies found significant correlations between hippocampal activity and schizophrenic symptoms (Friston et al., 1992; Kawasaki et al., 1994; Liddle et al., 1992; Tregellas et al., 2014). Overall, consistent with evidence for reduced GABAergic inhibition in the hippocampus, there is substantial evidence for increased resting activity of the hippocampus in schizophrenia, although in patients it has not been demonstrated (and it may not be possible to demonstrate) that disinhibition causes the metabolic overactivity (Heckers & Konradi, 2015).

GABA dysfunction may also be a consequence of N-methyl-d-aspartate (NMDA) receptor hypofunction, which has also been suggested as a key etiological factor implicated in schizophrenia (Nakazawa & Sapkota, 2020). NMDA channels contribute strongly to excitatory postsynaptic potentials in parvalbumin-containing GABAergic interneurons (Grunze et al., 1996). Blockage of these channels appear to hyperpolarise neurons by reducing ambient glutamate, hindering excitability of GABAergic interneurons and thus reducing their inhibitory output (Binshtok et al., 2006). Using electrophysiological recordings on awake rats, Homayoun & Moghaddam (2007) demonstrated that inhibiting NMDA receptors with MK801 causes decreased activity of GABA interneurons and increased firing rate of pyramidal neurons. Furthermore, Lisman et al. (2008) proposed that interneurons may use NMDARs to sense pyramidal cell activity. Hypofunction of NMDAR may be misinterpreted as inactive, and interneurons may attempt to compensate by reducing their inhibitory output by lowering GAD67 levels, the enzyme responsible for the synthesis of GABA. The diminished expression of GAD67 (discussed above in Section 1.2.1) may reduce extracellular GABA levels, disinhibiting pyramidal cells (Kalkman & Loetscher, 2003).

Magnetic Resonance Spectroscopy can measure neuro-metabolites and neurotransmitters such as GABA and glutamate. However, due to the low abundance of GABA, measuring GABA is much more challenging compared to glutamate, which is available in high concentration (Duarte & Xin, 2019). There are also challenges when interpreting GABA measurements from MRS as the measured GABA may not reflect only GABA that serves as a neurotransmitter in GABAergic interneurons, but also GABA that is part of metabolic cycles in neuronal and non-neuronal brain cells (Stagg et al., 2011). Therefore, the link between MRS GABA and GABAergic neurotransmission is not clear.

Egerton et al. (2017) conducted a meta-analysis on neuroimaging studies of GABA in schizophrenia to identify whether the GABAergic dysfunction that has been reported previously in post-mortem samples can be reflected in data from in vivo studies. The analysis revealed no significant difference in GABA concentrations between schizophrenic patients and healthy controls in the medial PFC, parietal/occipital cortex, and striatum. Hippocampal GABA concentrations in patients with schizophrenia could not be compared to healthy controls in the meta-analysis due to insufficient data. Only one study examined GABA in the hippocampus and they found no significant group difference (Stan et al., 2015). It may be the case that no change was visible due to the robust metabolic system with compensatory mechanisms that try to maintain homeostasis (Tkac et al., 2012). This result also indicates that studies are not conclusive, and that further research is necessary to fill the gaps in our current understanding of the mechanisms underlying changes in MRS neuro-metabolites.

1.2.2 Tourette Syndrome

Tourette Syndrome is a neurodevelopmental condition first described by Georges de la Tourette in 1885. It lies on the more severe side of the tic disorder spectrum and is characterised by the presence of chronic motor and vocal tics (T. Spencer et al., 1995). A single tic and a single spontaneous movement are indistinguishable (Finis et al., 2012). However, tics occur in bouts throughout the day, are involuntary, repetitive, stereotyped and uncontrolled behaviours and therefore, often misplaced in context and time (Cohen et al., 2013). Tourette Syndrome has been estimated to affect up to 1% of the population and large epidemiological studies and meta-analyses show a prevalence between 0.3% and 0.9% (Scharf et al., 2015). In child populations with Tourette Syndrome the ratio of males to females is estimated at 4 to 1 (Draper et al., 2015). However, this sex bias decreases in adult samples, with tic improvement in males and tic worsening in females (Lichter & Finnegan, 2015). The reason for this development is unknown, although they are likely due to a combination of psychosocial influences and biological factors (Lichter & Finnegan, 2015).

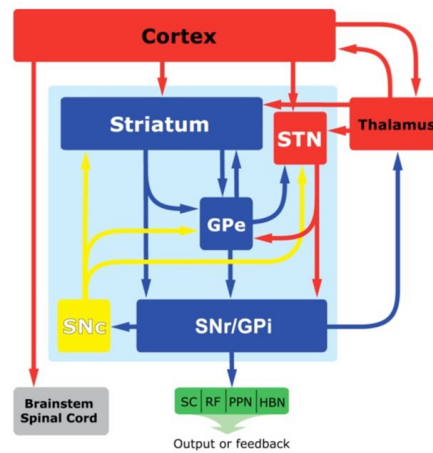
The aetiology and exact neurobiological background of Tourette Syndrome still remains unclear, however, neurological abnormalities of the cortical-striatal-thalamic-cortical (CSTC) circuit appear to play a central role in Tourette Syndrome (Albin & Mink, 2006). In particular, dysfunctional GABAergic signalling in the CSTC is a prominent theory of Tourette Syndrome. It is suggested that motor tics arise from the loss of inhibitory function (i.e. GABA) in the striatum, which in turn leads to disinhibition of the thalamus and hyperexcitability of the motor cortex, leading to tics (Gilbert, 2006). It is thought that striatal neurons become active within inappropriate context, leading to inappropriate action selection which is further reinforced through dopamine in Tourette Syndrome (Albin & Mink, 2006). In line with this suggestion, there is evidence for GABA dysfunction, particularly in the striatum, in Tourette Syndrome (Tremblay et al., 2015). I consider this evidence in the next sections, following a consideration of the functional anatomy of the basal ganglia (BG) (as reviewed by Tepper et al. (2007)), with particular focus on aspects that are relevant for Tourette Syndrome.

1.2.2.1 The Basal Ganglia

The basal ganglia are a group of nuclei composed of the striatum, the globus pallidus (GP), the substantia nigra (SN) and the subthalamic nucleus (STN). The striatum can be divided into a dorsal and ventral part (discussed further below) (Tremblay et al., 2015). The GP is composed of an external (GPe) and internal (GPi) segment. In rodents the GP refers to the GPe, whereas the entopeduncular nucleus corresponds to the GPi. The two divisions of the pallidal complex have different inputs and outputs and are functionally distinct. Similarly, the SN consists of two

major sub-nuclei; the pars compacta (SNc) and the pars reticulata (SNr). Both receive similar inputs but have mostly different outputs (Gerfen & Wilson, 1996). Figure 1 provides a simplified overview of the role of the BG in context of the rest of the brain. The BG receive their input mainly from the cortex and send their output to the cortex via the thalamus. The majority of BG nuclei have GABAergic projection neurons, and thus communication between nuclei is mostly through inhibitory signals. From the study by Oorschot (1996), it is estimated that 98% of neurons in the BG are GABAergic (Lopes et al., 2019).

Figure 1: Model of the cortical-striatal-thalamic-cortical pathway



Note: Taken from Tepper et al. (2007).

The main input structure of the BG is the striatum, which receives excitatory, GABAergic and dopaminergic input, but also sends GABAergic projections to various nuclei; and contains interneurons. As a result, the output from the striatum is influenced by a variety of neurotransmitters. It is speculated that three quarters of the total neuronal population in the striatum are projection neurons and around one quarter is interneurons (Bernácer et al., 2012). GABAergic medium spiny neurons (MSNs) are the main projection neurons of the striatum and can send their axons to more distant locations in the brain and exert feedback inhibition (Fjodorova et al., 2015; Lévesque & Parent, 2005; Tepper et al., 2008). In feedback inhibition, a population of excitatory neurons (e.g. from the cortex) depolarises inhibitory cells (e.g. MSNs in the striatum), which in turn inhibit the same population of excitatory cells (Kee et al., 2015). On the other hand, interneurons exert control over projection neurons through feedforward inhibition (Tepper et al., 2008; Tepper & Bolam, 2004). Feedforward inhibition typically occurs between different brain regions. Cortical input excites interneurons (often PV+ fast spiking interneurons), which in turn inhibit spiny projection neurons (Gittis et al., 2010; Kee et al., 2015; Plenz, 2003). Cholinergic interneurons can also be found in the striatum and only comprise around 1-3% of all striatal

cells (Goldberg & Wilson, 2016; Kim et al., 2019; Mallet et al., 2019). They are the main source of acetylcholine and can directly modulate the activity of MSNs and inhibit them via muscarinic acetylcholine receptors (Goldberg & Wilson, 2016; Mallet et al., 2019). Cholinergic interneurons are thought to critically regulate striatal activity and output because of their tonic activity (Lemos et al., 2019; Mallet et al., 2019; Sullivan et al., 2008).

The striatum can be divided into a dorsal part, which includes the caudate nucleus and putamen, and a ventral part with the nucleus accumbens and olfactory tubercle (Robbins & Everitt, 1992). The striatum receives cortical projections in a topographical manner, which define three cortico-BG circuits with different functional processes (Tremblay et al., 2015). The putamen has been associated with sensorimotor functions, the caudate with associative functions and the nucleus accumbens with limbic functions (Tremblay et al., 2015; Worbe et al., 2009). Consistent with such divisions, the BG has also been divided into three pathways: (i) The motor pathway is thought to cover the dorso-lateral regions of the BG and consists of the SMA, putamen, ventrolateral GPe and GPi. (ii) The cognitive pathway, which covers central BG regions and includes dorsolateral PFC, caudate, dorsomedial GPe, GPi and SNr. (iii) The limbic pathway is thought to cover the ventral regions of the BG and consists of the anterior cingulate cortex, ventral striatum, ventral pallidum and SNr (Tremblay et al., 2015). Projection neurons in the striatum, GPi, GPe and SNr are GABAergic. Projection nuclei that use other neurotransmitters include the (i) STN which has glutamatergic (excitatory) connections to the GP and the SNr, and (ii) the SNc which has dopaminergic projection neurons connecting to the striatum, GPe and STN.

The major output structures of the BG are the SNr and the GPi, which connect to the thalamus. There are two distinct pathways that process information from the striatum and send signals to the rest of the BG through GABAergic MSNs (Gerfen & Surmeier, 2011). MSNs in the direct pathway express dopamine D1 family receptors and project onto the SNr and GPi (Fujita & Eidelberg, 2017). This inhibition in turn disinhibits the thalamus, allowing the excitatory glutamatergic neurons from the thalamus to be projected to the cortex, making excitation more likely. On the other hand, in the indirect pathway the striatal neurons express dopamine D2 family receptors and inhibit the GPe, which disinhibits the STN. The STN then makes excitatory connections to the GPi, allowing the GPi to inhibit the thalamus, therefore, decreasing stimulation of the motor cortex by the thalamus (Tepper et al., 2007). Thus, the direct pathway has an excitatory effect to cortical regions, facilitating movement, in contrast to the indirect pathway, which is more inhibitory (Fujita & Eidelberg, 2017; Y. Smith et al., 1998).

The role of the basal ganglia in motor control is not fully understood yet.

However, it appears that the BG may function as a gate where desired actions (from action plans that originate in the motor cortex) are supported through the direct pathway and competing actions are inhibited via the indirect pathway (Albin & Mink, 2006; Y. Smith et al., 1998; Yin, 2017). Consequentially, when the BG is dysregulated, they may fail to suppress unwanted behaviours and behaviours are thus expressed in a contextual inappropriate manner (Albin & Mink, 2006).

1.2.2.2 Abnormalities of the cortical-striatal-thalamic-cortical circuit and GABA in Tourette Syndrome

A growing body of evidence points to abnormalities in the cortical-striatal-thalamic-cortical (CSTC) circuit and their neurotransmitter systems. In particular, GABA related changes have been consistently observed in the striatum. Kalanithi et al. (2005) conducted a post-mortem study on brains from individuals with persistent and severe Tourette Syndrome as well as healthy controls. Looking at the total number of neurons, they found significant changes in the GPe (46% decrease) and the GPi (68% increase) in Tourette Syndrome subjects. Furthermore, they reported significant imbalance of parvalbumin containing interneurons in the basal ganglia. Specifically, fewer PV+ GABAergic neurons were detected in the striatum and the GPe. PV+ neuron density was decreased in the caudate by 51% and in the putamen by 37%, suggesting reduced control over neuronal excitability. On the other hand, the GPi showed an increase of PV+ neurons, which may reflect a migration error and an imbalance. Kataoka et al. (2010) also found reductions of PV+ interneurons in the striatum of Tourette Syndrome patients, alongside reductions of cholinergic interneurons. These findings are further supported by Lenington et al. (2016) who analysed the transcriptome of the BG through RNA sequencing and found up- and down-regulated genes in the caudate and putamen of Tourette Syndrome individuals and decreased numbers of cholinergic and GABAergic interneurons, confirmed by immunohistochemistry. A reduction in interneurons may be linked to findings from Peterson et al. (2003) and Plessen et al. (2009) who reported reduced caudate volumes. Reduced volumes may thus provide further support for the reduced inhibition in the striatum that leads to the hyperexcitation of the cortical motor area. Furthermore, in a longitudinal study, Bloch et al. (2005) demonstrated that the volumes of the caudate nucleus correlated inversely with tic severity in early adulthood. Thinning of sensorimotor cortices in children with Tourette Syndrome which correlated with tic symptoms has also been reported (Sowell et al., 2008). Furthermore, smaller volumes of the left GP have also been found in individuals with Tourette Syndrome comorbid with attention-deficit hyperactivity disorder (ADHD) (Singer et al., 1993), which may reflect some of the changes that have been reported by Kalanithi et al. (2005), as discussed above.

A PET study by Stern et al. (2000) identified several brain areas, including

the caudate, putamen, insula, and anterior cingulate cortex, whose activity correlated with tic occurrence. Widespread alterations in GABA-A receptor bindings have been reported by Lerner et al. (2012). Decreased bindings were found bilaterally in the ventral striatum, globus pallidus, thalamus, amygdala and right insula and increased GABA-A receptor bindings was found in the bilateral substantia nigra, left periaqueductal grey, right posterior cingulate cortex and bilateral cerebellum. These are interesting findings as several of the brain regions mentioned have been identified as key areas for the generation of tics. For example, the striatum and thalamus form critical parts of the CSTC loop (Albin & Mink, 2006) and the insular cortex is involved in processing bodily sensations and urges and is thought to represent premonitory urges in Tourette Syndrome individuals (Tinaz et al., 2015). Interestingly, reduced numbers of GABAergic interneurons have also been observed in the insular cortex in individuals with Tourette Syndrome (Vaccarino et al., 2013).

1.2.2.3 Tonic inhibition and compensatory mechanisms

It has been proposed that there are two types of inhibition; (1) phasic inhibition, which involves GABA in the synapse and has transient effects and (2) tonic inhibition, where GABA is in the extracellular space through a spill-over from the synaptic cleft (Wei et al., 2003) and binds to extra-synaptic, high affinity GABA receptors (Glykys & Mody, 2007; G. M. Jackson et al., 2015). The latter is thought to dampen down and modulate the inhibitory tone of a neuron or whole populations of neurons, and to have long-lasting effects (Héja et al., 2012; G. M. Jackson et al., 2015). As Tourette Syndrome follows a developmental time course (Leckman et al., 1998) where many adolescents gain greater control over their tics (Cohen et al., 2013), it has been proposed that this gain in control is due to tonic inhibition. Tonic inhibition has been suggested to be an adaptive compensatory response for enhanced control over motor outputs for the suppression of tics (Draper et al., 2014).

The study by S. R. Jackson et al. (2011) provides evidence for compensatory brain reorganisation that may underlie the increased gain of control for tics. Tourette Syndrome individuals showed enhanced control over motor outputs on a task-switching paradigm, which also correlated positively with tic severity. Additionally, they found widespread alterations in the microstructure of their cortical white matter tracts in the corpus callosum and forceps minor (in the frontal lobe) which were also strongly associated with tic severity. Furthermore, using fMRI, the Blood-oxygen-level-dependent (BOLD) response in PFC was significantly greater in the Tourette Syndrome group during the task. In addition, that BOLD response correlated with performance on the task-switching paradigm in individuals with Tourette Syndrome, suggesting that enhanced cognitive control in Tourette Syndrome is accompanied by adaptive functional and structural changes, particularly in the PFC. Greater cognitive control in

individuals with Tourette Syndrome compared to age-matched controls was reported by Mueller et al. (2006) in an oculomotor switching task. They suggest that the constant need for tic suppression may result in an enhanced executive function for inhibitory control. Further evidence for enhanced control in individuals with Tourette Syndrome comes from J. Y. Jung et al. (2015). In their study, patients and controls responded equally fast, but patients were significantly more accurate in the task. The research group also found that greater cognitive control was associated with lower levels of tics.

In a 7T MRS study by Draper et al. (2014), GABA levels were significantly elevated in the supplementary motor area (SMA) of individuals with Tourette Syndrome compared to healthy controls. This region is thought to be particularly important for tic generation (Bohlhalter et al., 2006). Furthermore, this elevation was predicted by motor tic severity and white matter structure of a region in the corpus callosum that projects to the SMA. In addition, the elevation was negatively correlated with (i) fMRI BOLD activation and (ii) cortical excitability in the primary motor cortex. The researchers suggest that extra-synaptic GABA contributes to localized tonic inhibition in the SMA, which may lead to tic suppression. Lastly, a structural MRI study found significantly different dorsal PFC volumes in Tourette Syndrome patients depending on age, with children having larger and adults having smaller volumes (Peterson et al., 2001). Contrastingly, they found that premotor volumes were significantly smaller in Tourette Syndrome boys and larger in Tourette Syndrome men. The authors suggest these changes may reflect a compensatory function to regulate tic occurrence. These changes, in areas remote from the striatum, are an important issue and something that we aimed to investigate using the rat model of striatal disinhibition and imaging methods.

1.3 Animal models of neural disinhibition

1.3.1 Validity of using animal models

Animal models provide a unique way for new discoveries, testing hypotheses and validation of human data (Barré-Sinoussi & Montagutelli, 2015). A great advantage of animal models is the ability to carefully design the research, to mimic biological conditions of humans and to control certain variables, such as age (Andersen & Winter, 2019). Animal experiments provide an opportunity to gain clarity over some human studies. Research involving human participants, can often have mixed findings due to confounding variables such as comorbidities, type of task, effects of medication, age and time of analysis (G. M. Jackson et al., 2015). For example, some studies report impaired inhibitory control in Tourette Syndrome (Dursun et al., 2000; Georgiou et al., 1995), others did not find a significant difference between Tourette Syndrome individuals and healthy controls (Ozonoff et al., 1998) and some report greater cognitive control

in Tourette Syndrome patients (G. M. Jackson et al., 2007; S. R. Jackson et al., 2011; J. Y. Jung et al., 2015; Mueller et al., 2006). In animal research, most variables are typically kept constant whilst one variable is manipulated. From this design, it can be expected that the changes observed are due to the manipulation. Therefore, a key advantage of animal models, especially in the context of the present project, is that they allow examination of causality. For example, in this thesis we examined the changes caused by hippocampal or striatal disinhibition in the regional disinhibited area and/or in projection sites. The overarching aim of animal research is to increase knowledge, unravel mechanisms of human physiology and contribute to finding solutions to biomedical questions, to develop new methods so that new therapeutic advances and opportunities can be created (Alderton, 2020; Andersen & Winter, 2019).

Validation of animal models on human disorders is often based on (i) face, (ii) predictive and (iii) construct validity (Yael et al., 2016). (i) Face validity looks at the similarity between human clinical symptoms and the symptoms in the animal model. As reviewed by Feifel & Shilling (2010), developing animal models of schizophrenia with good face validity of psychotic features is highly problematic. It is not possible to reliably measure, for example positive symptoms like hallucinations, as they are internal and subjective phenomena. Furthermore, the lack of vocalisation makes it impossible to model symptoms such as disorganised speech in animals. Some negative symptoms such as avolition (lack of motivation) can be measured, however they are also seen in other psychiatric disorders such as depression and are thus not specific enough to schizophrenia.

In the case of Tourette Syndrome, there is also some difficulty due to the nature of Tourette Syndrome being a movement and psychiatric disorder (e.g. premonitory urge and comorbid symptoms) (Yael et al., 2016). Firstly, most animal experiments try and evoke simple, tic-like movements to a confined area such as the hindlimb. However, tic expression in humans is more complex. For instance, tics can be simple or complex in appearance with simple tics involving one muscle group (e.g. eye blinking, nose twitching, throat clearing) and complex tics involving multiple muscle groups that follow coordinated sequences (e.g. echopraxia (imitating observed behaviours), echolalia (copying what others say) and coprolalia (obscene utterances)) (Leckman et al., 1989). Usually, simple tics precede complex tics and manifest first in the head and face (Hollis et al., 2016). As mentioned, most animal models try to evoke a simple tic and ignore complex tics. This is partly due to the difficulty of measuring certain tics such as verbal complex tics in animal models. Another key feature of Tourette Syndrome is that patients can control, defer, and suppress the expression of tics to some extent (Bortolato & Pittenger, 2017), however, these aspects cannot be measured in animal models.

Secondly, most animal models of psychiatric disorders use acute, instead

of chronic, injections. Although acute injections allow examination of causality, a chronic model reflects the true nature of the disorder better, by evoking for example compensatory mechanisms, which can also be observed in the disorder. Tourette Syndrome, for example, typically follows a developmental time course (Leckman et al., 1998) with an onset of tics occurring in early childhood, typically around the age of 4 and 7 years, worsening between the ages of 11 and 14 years and improving in their frequency and severity by early adulthood (Cohen et al., 2013). Approximately 70-80% of Tourette Syndrome have mild tics or are absent of tics by the age of 18 years (Leckman et al., 2006). Importantly, with age, most individuals with Tourette Syndrome seem to develop a way to control and suppress their tics, which is accompanied by compensatory, neuroplastic alternations in the brain structure and function (discussed in Section 1.2.2.3). These important changes are considered as key features of the pathology of Tourette Syndrome, however, they are not captured in an acute animal model.

Thirdly, assessing Tourette Syndrome as a psychiatric disorder, i.e. capturing the presence of premonitory urges to move (Sanger et al., 2010) in animals is challenging. Around 90% of individuals with Tourette Syndrome report having premonitory urges, a term often described as an unpleasant bodily sensation (tension or pressure) preceding tics (Leckman et al., 1993). The premonitory urge is typically limited to a specific area of the body, with only the minority of individuals with Tourette Syndrome perceiving it as a general inner tension (Cavanna et al., 2017). While the suppression of tics is possible for many individuals, it becomes distressing and uncomfortable. The urge to tic increases and becomes uncontrollable after a period of time (Hollis et al., 2016). After tic expression the urge is temporarily relieved (Martino et al., 2013), producing negative reinforcement of tics, and thus may become habitual (Woods et al., 2009). With animal models these specific features cannot be identified directly (due to lack of vocalisation), however, it has been suggested that premonitory urges may be reflected as deficits in sensorimotor gating, which could be assessed through prepulse inhibition (PPI) (Yael et al., 2016) (sensorimotor gating and PPI are discussed in Chapter 5).

Fourthly, although tics are the defining symptom of Tourette Syndrome, approximately 90% of individuals also present psychiatric comorbidities and 57.7% have two or more psychiatric disorders (Hirschtritt et al., 2015). The most commonly comorbid disorders are ADHD (54.3%) and Obsessive-compulsive disorder (OCD) (50%), with 72.1% of Tourette Syndrome individuals meeting the criteria for either disorder. Nearly one third has Tourette Syndrome, OCD and ADHD (29.5%). The common neurodevelopmental comorbidities suggest that they share a common neurobiological underlying mechanism with Tourette Syndrome (Hollis et al., 2016). These comorbidities demonstrate the complex nature of the disorder, however, most animal neural disinhibition studies for Tourette

Syndrome focus solely on tic-like movements. It could be argued that this presents a limitation, as the disorder is not tested as a whole. On the other hand, singling out one aspect of a disorder allows for a better analysis and understanding. Grabli et al. (2004) arguably strengthened the validity of the animal model of Tourette Syndrome by demonstrating that they were able to evoke comorbid behaviours as well as tics, through the use of bicuculline. In addition to abnormal movements, the research group was able to observe attention deficit and/or hyperactivity as well as stereotypy in monkeys. Similarly, Worbe et al. (2009) demonstrated that depending on the location of the microinfusions into the striatum, bicuculline produced different movements and behaviours in monkeys, including tic-like behaviour, stereotyped behaviour (persistent repetition of behaviour) and hyperactivity that resembled Tourette Syndrome, OCD and ADHD. The posterior putamen corresponded to the sensorimotor territory, the dorsal part of the anterior striatum to associative function and the ventral striatum to limbic function. These findings support the face validity of animal models in regard to comorbidities.

(ii) Predictive validity relates to treatment effects. Typically, the degree to which an animal's response to medication can predict the human response, is investigated. In animal models of psychiatric disorders, the predictive validity is often hard to assess, given the lack of good treatments in several disorders (i.e. no positive controls). Another problem related to predictive validity is that this criterion may, to some extent, bias research efforts towards 'old' treatment mechanisms such as using only dopaminergic treatments in schizophrenia (Leonard, 2002). (iii) Construct validity looks at the theoretical rationale of the animal model and whether it matches the known pathophysiology. However, construct validity of animal models of psychiatric disorders is often speculative, as the underlying pathophysiology is not yet known (Nespoli et al., 2016; Yael et al., 2016). As different animal species are used in research, different properties can be investigated to gain a better understanding of underlying mechanisms of specific disorders. Mice are often used for genetic manipulation, rats for investigating the relationship between pharmacology, physiology and behaviour and primates to study complex behaviour (Yael et al., 2016).

Our experiments with rats allow us to temporarily and chronically manipulate specific brain sites, their functions as well as their projection sites, through pharmacological manipulations. By implanting cannulae, we can precisely choose the timing of our manipulation of drugs such as picrotoxin (GABA-A receptor antagonist) to temporarily disinhibit neural activity. This method allows the study of GABAergic systems and their effects on brain sites. When discussing face validity, I described the downsides of using acute pharmacological manipulation. However, there are also major advantage such as its reversibility. Within-subjects designs can be used to better determine the effects of a drug. Temporal manipulations are perhaps more suitable than lesion studies for analysing the effects of

a brain area, as lesions are often accompanied by compensatory mechanisms, which make an interpretation more challenging (Bast & Feldon, 2003). On the other hand, compensatory mechanisms represent a key part of the pathology and may thus reflect the nature of the disorder more accurately (as discussed above in Section 1.2.2.3).

1.3.2 Hippocampal and prefrontal disinhibition

Hippocampal and prefrontal neural disinhibition have been implicated as part of the pathophysiology of various neuropsychiatric disorders, like schizophrenia and age-related cognitive decline (Bast et al., 2017). Focusing on schizophrenia, animal models offer the opportunity to examine if hippocampal disinhibition and resulting overactivity cause schizophrenia-relevant behavioural and cognitive changes and by which mechanisms. Hippocampal overactivity, due to GABAergic disinhibition, has been recognised as a central feature of schizophrenia (Heckers & Konradi, 2015). Some studies induced hippocampal hyperactivity through excitatory or disinhibitory drugs and have found supporting evidence for sensorimotor deficits that are related to psychosis (Bast & Feldon, 2003). Sensorimotor gating is considered as a key mechanism for the processing of information in the brain and thus forms the basis of behaviour (Bast & Feldon, 2003; Braff et al., 2001; Braff & Geyer, 1990). Therefore, individuals with sensorimotor dysfunction may fail to filter out irrelevant stimuli and consequentially have reduced responsiveness to the most salient stimuli (Braff et al., 2001; Braff & Geyer, 1990) and may thus theoretically increase their vulnerability to developing schizophrenia symptoms (Braff & Geyer, 1990). Prepulse inhibition (PPI) (further discussed in Chapter 5) is viewed as an operational measure that reflects sensorimotor mechanisms (Braff et al., 2001). In schizophrenia, reduced PPI is well documented and has been proposed to contribute to sensory overload as well as to other psychotic symptoms (Braff et al., 2001; Braff & Geyer, 1990). For example, PPI deficits have been found to significantly correlate with thought disorder in schizophrenic patients (W. Perry et al., 1999; W. Perry & Braff, 1994). However, the level of PPI cannot predict clinical course, specific symptoms, or individual medication responses (Swerdlow et al., 2008). Brain mechanisms underlying reduced PPI in rats have been suggested to be relevant to brain mechanisms underlying psychosis in humans. (Bast & Feldon, 2003).

Although tightly controlled temporal reductions in the GABAergic inhibition may facilitate learning and memory (Letzkus et al., 2015), tonic regional neural disinhibition may disrupt both regional and distal function in efferent brain sites, which may contribute to some behavioural changes caused by regional disinhibition (Bast et al., 2017). This concept was supported by McGarrity et al. (2017) who disinhibited the hippocampus with picrotoxin (GABA-A receptor antagonist) of rats. Under anaesthesia, electrophysiological recordings around the infusion site showed regional

changes such as enhanced burst firing and an increase percentage of spikes fired within the bursts in the hippocampus. Furthermore, they reported clinically relevant cognitive impairments in hippocampus dependent memory performance (rapid place learning) and attentional performance, which typically depends on the PFC. These results are consistent with the idea that regional disinhibition influences projection sites and can therefore disrupt their function also. Pezze et al. (2014) investigated the effects of an GABA-A receptor agonist (muscimol) and antagonist (picrotoxin) in the PFC in rats. Both drugs impaired attention, and furthermore, muscimol reduced locomotor activity whereas picrotoxin increased it. Using in vivo electrophysiological recordings, they found that PFC firing was inhibited by muscimol and increased by picrotoxin. Additionally, bursts were reduced by the muscimol and enhanced by picrotoxin. Both drugs changed the temporal pattern of bursting and picrotoxin also significantly increased local field potential (LFP) power. LFP are extracellular signals that reflect the summation of postsynaptic potentials from a population of neurons in the vicinity of the recording site (Buzsáki, 2006). Overall, these two studies support the idea that disrupting local GABA function, and thus burst firing in the hippocampus and PFC, can disrupt both regional and distal cognitive functions (Bast et al., 2017). Furthermore, results from Pezze et al. (2014) suggest that both too little and too much neural activity in the PFC disrupts attention. Therefore, some cognitive functions appear to require appropriately tuned neural activity. To simply suppress neural activity to treat cognitive deficits may not be as effective, and instead rebalancing aberrant neural activity appears to be necessary (Bast et al., 2017). In accordance with the findings from Pezze et al. (2014), single-neuron recordings in animal models demonstrate that intact GABA transmission is necessary for task appropriate neural tuning (Isaacson & Scanziani, 2011; Rao et al., 2000).

Even though there are several studies that demonstrate the negative effects of reduced GABA function on cognition, there are also some that report positive effects. For example, G. R. Dawson et al. (2006) used an inverse agonist ($\alpha 5$ IA) that binds to the benzodiazepine site of GABA-A receptors in rats and found that it increased hippocampal plasticity in the CA1 region and improved performance on the hippocampus dependent test of learning and memory; the delayed-matching to-place task of the Morris water maze.

A few rodent studies directly investigated the relationship between parvalbumin-expressing interneurons and gamma oscillations. Activating fast-spiking interneurons appears to amplify gamma oscillations (Cardin et al., 2009). In contrast, inhibiting (Sohal et al., 2009) or losing (Lodge et al., 2009) PV+ interneurons suppresses gamma oscillations. Based on the findings of Glickstein et al. (2007), who reported loss of PV+ interneurons in cyclin D2 knockout mice, Gilani et al. (2014) found that the loss of PV+ interneurons was particularly present in the CA1 region of the hip-

pocampus. They also observed deficits in synaptic inhibition, increased in vivo spike activity of excitatory projection neurons, and increased in vivo basal metabolic activity (assessed via fMRI). These findings are line with studies that have found similar changes in schizophrenia patients and highlight the importance of hippocampal GABAergic interneurons further. Royer et al. (2012) silenced parvalbumin and somatostatin expressing interneurons in the CA1 area of the hippocampus in mice and recorded increased firing rates of pyramidal cells in both cases. Although silencing somatostatin-expressing interneurons significantly increased burst firing, the authors suggest that silencing PV+ interneurons had a greater effect on regulating spike timing. Similarly, an in vitro study also reported enhanced hippocampal burst firing in the CA1 region after pharmacogenetically silencing interneurons (Lovett-Barron et al., 2012). The amygdala has also been identified to contribute to changes in GABAergic neurons in schizophrenia (Berretta et al., 2001). Berretta et al. (2001) found decreases in the density of GAD65 positive terminals in the CA3 and CA2 region of the hippocampus following picrotoxin infusion into the amygdala in rats, recreating remarkably similar abnormalities that can also be observed in schizophrenia.

1.3.3 Striatal disinhibition

Over the last five decades, the effects of neural disinhibition in the striatum have been investigated directly through the use of microinfusions of a GABA-A antagonist like picrotoxin and bicuculline in rodents (McKenzie et al., 1972; Tarsy et al., 1978; Patel & Slater, 1987; Bronfeld, Yael et al., 2013; Israelashvili & Bar-Gad, 2015; Pogorelov et al., 2015; Klaus & Plenz, 2016; Vinner et al., 2017; Vinner Harduf et al., 2021), as well as in primates (Crossman, 1987; McCairn et al., 2009; Worbe et al., 2009; Bronfeld, Israelashvili & Bar-Gad, 2013). Earlier research characterised the movements caused by striatal disinhibition as 'hyperkinetic syndrome' (McKenzie et al., 1972), or described them with more specific terms like 'choreiform movements' (McKenzie et al., 1972), 'myoclonus' (Tarsy et al., 1978; Patel & Slater, 1987) and/or 'dyskinesia' (Crossman, 1987; Muramatsu et al., 1990). Although some early animal studies discussed involuntary movements caused by picrotoxin in context with Tourette Syndrome (and Huntington's chorea) (McKenzie et al. (1972)), the striatal disinhibition model has only been highlighted as a model of Tourette Syndrome over the last few years (Yael et al., 2016). The first to describe such movements as tics were Bronfeld, Yael et al. (2013).

The similarities between different hyperkinetic disorders make it challenging for a correct identification, nevertheless it seems necessary and attempts for an accurate classification should be made (Sanger et al., 2010). Sanger et al. (2010) compared different movement disorders and distinguished them from tics as follows: "Tics can be distinguished from (...) chorea, and myoclonus by the lack of continuity of the movement,

the intervening periods of normal movement, and the lack of interference with ongoing tasks.” As well as by the “predictability and repeatability of the movements.” The above mentioned objective differences between different hyperkinetic disorders should be considered when researching animal models of movement disorders.

Tic-like movements are expressed on the contralateral side of the disinhibited area and are mostly confined to a single body part, depending on the somatotopic location of the striatal infusion (Bronfeld, Israelashvili & Bar-Gad, 2013). For example, bicuculline infusions into the anterior striatum cause tic-like forelimb movements, whereas infusions into the posterior striatum cause tic-like hindlimb movements in rats (Bronfeld, Yael et al., 2013). In addition, selectively blocking synaptic excitation of fast-spiking interneurons in the mouse striatum has also shown to elicit dystonia (Gittis et al., 2011). Importantly, even when animals express tic-like movements, they appear to continue with their normal ongoing behaviours, such as exploration and grooming (Bronfeld, Yael et al., 2013). These findings are important, as tics typically do not interfere with voluntary movements (Sanger et al., 2010) (although in some people, tics may be disabling and interfering with daily living (Ohm, 2006)). Furthermore, the ongoing behaviour indicates that striatal disinhibition in animals is not grossly debilitating.

1.4 Aims of the PhD project

This thesis had the overarching goal to further characterise the neural and behavioural impact of hippocampal (Chapter 2) and striatal (Chapters 3 to 6) disinhibition in rats.

Aim 1 (Chapter 2): Impact of hippocampal disinhibition on septal neurochemicals, as assessed using Magnetic Resonance Spectroscopy

Hippocampal metabolic hyperactivity and neural disinhibition (i.e., impaired GABAergic inhibition) are key features of schizophrenia (Heckers & Konradi, 2015). Regional neural disinhibition may affect processing in projection sites of the disinhibited region, which may contribute to some behavioural changes caused by regional disinhibition. Our previous Single-Photon Emission Computed Tomography (SPECT) study in rats revealed marked metabolic activation in several extra-hippocampal sites, including the septum, after ventral hippocampus disinhibition (Williams et al., in preparation). Our aim was to examine the changes in the septum by measuring the impact of ventral hippocampal disinhibition on a range of neuro-metabolites in the septum, using MRS. Although MRS is widely used, including in schizophrenia studies, there are still substantial gaps in our understanding of the mechanisms underlying changes in MRS neuro-metabolites and how regional disinhibited areas affect projection sites.

Aim 2 (Chapter 3): Impact of striatal disinhibition on neural activity

Another key aim of this thesis was to further characterise the rat striatal disinhibition model, related to Tourette Syndrome. In freely moving rats and non-human primates, large amplitude local field potential (LFP) spike-wave discharges have been reported after striatal disinhibition, alongside increased neural firing within the striatum (e.g. Israelashvili & Bar-Gad (2015); Klaus & Plenz (2016); McCairn et al. (2009)). Such LFP spike-waves have been shown to highly correlate with tics (Israelashvili & Bar-Gad, 2015; McCairn et al., 2009), but have also been reported during intertic intervals (McCairn et al., 2013). We aimed to confirm that striatal picrotoxin infusions (reliably) induces LFP spike-wave discharges in anaesthetised rats and aimed to characterise the impact of striatal disinhibition on regional multi-unit firing activity.

Aim 3 (Chapter 4): Further characterisation of tic-like movements caused by striatal disinhibition

The effects of neural disinhibition in the striatum have been investigated directly, through the use of microinfusions of a GABA-A antagonist, like picrotoxin and bicuculline in rodents (Bronfeld, Yael et al., 2013; Klaus & Plenz, 2016), as well as in primates (McCairn et al., 2009; Worbe et al., 2009). Our study aimed to confirm that striatal disinhibition, by

local microinfusion of the GABA-A receptor antagonist picrotoxin (300 ng and 200 ng of picrotoxin in 0.5 μ l saline), causes tic-like movements in rats. We aimed to investigate the reliability of such movements following picrotoxin infusion and wanted to characterise the time course and some key features of tic-like movements.

Aim 4 (Chapter 5): Impact of striatal disinhibition on prepulse inhibition

A number of neuropsychiatric disorders are characterised by sensorimotor gating deficits, including Tourette Syndrome (Baldan Ramsey et al., 2011). Swerdlow and colleagues suggested that motor or vocal tics are due to failed automatic gating of sensory information (experienced as unwanted and bothersome premonitory urges) (Swerdlow, 2013; Swerdlow & Sutherland, 2005). Prepulse inhibition (PPI) of the startle reflex is often used as a measure of sensorimotor gating (Baldan Ramsey et al., 2011). As PPI deficits have been reported in patients with Tourette syndrome (Castellanos et al., 1996; S. J. Smith & Lees, 1989), we aimed to investigate the impact of striatal disinhibition on PPI in Lister hooded rats.

Aim 5 (Chapter 5): Impact of striatal disinhibition on locomotor activity

Locomotor activity appears to be partly regulated by the ventral striatum, specifically the nucleus accumbens (Lorens et al., 1970; Morgenshtern et al., 1984; Pijnenburg & van Rossum, 1973). The dorsal striatum on the other hand, has been mainly highlighted to cause tic-like movements when disinhibited (Israelashvili et al., 2020; Bronfeld, Yael et al., 2013). However, some evidence suggests that dorsal striatal disinhibition increases locomotor activity (Yoshida et al., 1991) and numerous studies on dorsal striatal disinhibition in rats have reported increased locomotor activity alongside tic like movements (Yael et al., 2016; Bronfeld, Yael et al., 2013; Israelashvili et al., 2020). Therefore, we aimed to investigate the impact of striatal disinhibition on locomotor activity.

Aim 6 (Chapter 6): Examining the feasibility of resting state functional connectivity MRI and Magnetic Resonance Spectroscopy in the rat striatal disinhibition model

Resting state functional connectivity MRI has been used on patients with Tourette Syndrome to better understand the brain's functional connectivity changes in the disorder (Ganos et al., 2014; Ramkiran et al., 2019; Worbe et al., 2012; Cui et al., 2014; Liu et al., 2017; Tikoo et al., 2020; Openneer et al., 2020). MRS has been used to investigate changes in glutamate and GABA in patients with Tourette Syndrome, in areas such as the premotor cortex (Mahone et al., 2018), thalamus (Kanaan et al., 2017) and striatum (Kanaan et al., 2017). Both MR methods can also be used on animals, however, the striatal disinhibition model of Tourette

Syndrome involves striatal cannula implants and microinfusions in rats. Both the cannula and the drug infusion may interfere with rsFC MRI measurements. Therefore, we aimed to provide proof of principle that standard rsFC MRI measurements and MRS measurements of neuro-metabolites, including glutamate and GABA, in the motor cortex are possible in rats with pre-implanted cannulae and microinfusions in the dorsal striatum.

2 A Magnetic Resonance Spectroscopy study of neurochemical changes in the septum in a rat model of hippocampal disinhibition

Declaration: I conducted surgeries, monitored anaesthesia, collected MRS data, perfused rats, and analysed and interpreted data. Malcolm Prior operated the scanner. Stuart Williams, Charlotte Taylor and Jacco Renstrom contributed to surgery and monitoring anaesthesia. Stuart Williams also contributed to MRS data collection (in the first batch of rats).

2.1 Introduction

Hippocampal metabolic hyperactivity and neural disinhibition (i.e., impaired GABAergic inhibition) are key features of schizophrenia pathophysiology (Heckers & Konradi, 2015). Regional neural disinhibition may affect processing in projection sites of the disinhibited region, which may contribute to some behavioural changes caused by regional disinhibition (Bast et al., 2017). Although Magnetic Resonance Spectroscopy (MRS) is widely used, including in schizophrenia studies, there are still substantial gaps in our understanding of the mechanisms underlying changes in MRS neuro-metabolites and how regional disinhibited areas affect projection sites. Our current MRS study builds on our previous findings (Williams et al., in preparation) where we investigated brain-wide activation changes caused by ventral hippocampus infusion of the GABA-A receptor antagonist picrotoxin, using Single-Photon Emission Computed Tomography (SPECT) imaging in rats. SPECT allows imaging of cerebral blood flow (CBF) in awake behaving rodents. It involves injecting a tracer, which after passing through the blood brain barrier, accumulates in the brain in a flow-dependent manner and gets trapped in the brain (Oelschlegel & Goldschmidt, 2020). This method provides spatial patterns of CBF during the time of the tracer injection (Oelschlegel & Goldschmidt, 2020). Among other findings, SPECT imaging revealed increased neural activation (reflected by increased blood flow) in the vicinity of the infusion site, which resembles metabolic hippocampal hyperactivity reported in schizophrenia (Heckers & Konradi, 2015), as well as marked metabolic activation in several extra-hippocampal sites, including the medial prefrontal cortex (mPFC), thalamus and lateral septum, after ventral hippocampus disinhibition (Williams et al., in preparation). To complement the SPECT findings, our previous study investigated the neurochemical impact of ventral hippocampal disinhibition on mPFC. An increase in myo-inositol and a decrease in GABA concentrations were found. In the present study, we continued this research by investigating the effects of hippocampal disinhibition on neuro-metabolites in the septum, the re-

gion that showed the most marked increase in metabolic activity following ventral hippocampal disinhibition.

The septum is considered to serve as a relay station between brain areas (Sarwar, 1989) with particularly strong reciprocal anatomical links to the hippocampus (Caputi et al., 2013; Müller & Remy, 2018; Risold & Swanson, 1997). The hippocampus sends strong projections to the septum, dominantly to the lateral septum, and receives projections from the medial septum (Gray & McNaughton, 1983; L. W. Swanson, 1977; Leranth et al., 1992; Toth et al., 1993). The projections from the hippocampus to the lateral septum are significantly denser (20 – 800 times) than other projections from the hippocampus (Tingley & Buzsáki, 2018), which is consistent with our SPECT study showing that the septum had the most marked activation changes following hippocampal disinhibition.

There is potential functional relevance of the hippocampal-septal connectivity. It has been proposed that the septum acts as an intermediary between signals received from the hippocampus and behavioural responses (H. S. Wirtshafter & Wilson, 2019). For example, contextual (fear) conditioning appears to depend on hippocampal-lateral septum synaptic neurotransmission (Calandrea et al., 2010; Vouimba et al., 1998). The ventral hippocampus has been identified as an important structure for the formation of classical fear conditioning (Bast et al., 2001b). N-methyl-d-aspartate (NMDA) receptor antagonists in the ventral hippocampus have shown to block fear conditioning (Bast et al., 2001b). On the other hand, lesioning the lateral septum induces fear, and stimulating it can inhibit fear (Sheehan et al., 2004). The authors suggest a negative correlation between the excitability of lateral septal neurons in response to hippocampal input and the expression of fear-related behaviours (Sheehan et al., 2004). Hippocampal-lateral septum connectivity has also been implicated with locomotor activity. Bender et al. (2015) found that running speed is increased by inhibition of hippocampal projections to the lateral septum and decreased by theta-rhythmic activation of lateral septum projections to the hippocampus. This finding may explain the reports of increased locomotor activity through hippocampal disinhibition (Bast et al., 2001a,b). Furthermore, it has been shown that social aggression can be caused by hippocampal (CA2) arginine vasopressin receptor activation, which in turn acts through the lateral septum-hypothalamus disinhibitory circuit (Leroy et al., 2018).

There is also potential clinical relevance of the strong septo-hippocampal connectivity. Structural changes; reduced hippocampal volumes (Bogerts et al., 1985; Brown et al., 1986; Falkai & Bogerts, 1986; Roeske et al., 2021; Shenton et al., 1992; Steen et al., 2006; Whitworth et al., 1998) and increased prevalence or size of the cavum septum pellucidum (CSP) (Degreef et al., 1992; DeLisi et al., 1993; Galarza et al., 2004; Kwon et al., 1998; Lewis & Mezey, 1985; Nopoulos et al., 1997; Shioiri et al., 1996)

have been reported in patients with schizophrenia. Furthermore, such structural changes in the hippocampus (Ho et al., 2017; Ledoux et al., 2014; Vargas et al., 2018) and in the CSP (Flashman et al., 2007) have been correlated with schizophrenia symptoms.

As indicated above, a key pathological feature of schizophrenia is hippocampal hyperactivity (Kawasaki et al., 1992; Malaspina et al., 2004; Medoff et al., 2001; Talati et al., 2014), which has also been linked to symptom severity and cognitive impairments (Friston et al., 1992; Kawasaki et al., 1994; Liddle et al., 1992; Tregellas et al., 2014). Although the underlying mechanisms for structural changes in schizophrenia patients are not known, it has been hypothesised that hippocampal volume loss is a consequence of neuronal hyperactivity driven by an excitation-inhibition imbalance, due to dysfunction of GABAergic inhibitory interneurons (Heckers & Konradi, 2015; Lieberman et al., 2018). Such imbalance in the hippocampus may affect the septum due to their strong connectivity and may thus potentially lead to structural changes in the septum. This interpretation may be supported by the significant correlation of smaller left para-hippocampal gyrus grey matter volumes and larger CSP, in patients with schizophrenia (Kasai et al., 2004).

MRS may serve as a translational bridge between human and rodent model findings. There is a substantial amount of studies on humans that used MRS to identify the neuro-metabolic profile of patients with schizophrenia, however, most focus on the PFC (Bartha et al., 1997; Kegeles et al., 2012; Liemburg et al., 2016; Marsman et al., 2014; Modinos et al., 2018; Natsubori et al., 2014; Tebartz Van Elst et al., 2005) or on the anterior cingulate cortex (Bustillo et al., 2010, 2014; Egerton et al., 2012; Kumar et al., 2020; Öngür et al., 2010; Reid et al., 2019; Rowland et al., 2013; Théberge et al., 2002, 2007; Wijtenburg et al., 2017). The findings of the studies mentioned above have been mixed and appear to depend on multiple factors such as symptom severity, medication and brain region (Egerton et al., 2017; Reddy-Thootkur et al., 2022; Wenneberg et al., 2020; Merritt et al., 2016). Often, changes in glutamate have been found, however, findings are not consistent, as both increases and decreases have been reported (Merritt et al., 2016). This is likely due to the factors mentioned above. To our knowledge, there are no MRS studies that investigated the neuro-metabolic profile of the septum in schizophrenia.

Two MRS studies in anaesthetised rats examined the impact of acute NMDA receptor blockade by systemic injection of the NMDA receptor antagonist phencyclidine (Iltis et al., 2009) or ketamine (Napolitano et al., 2014). NMDA-R hypofunction plays a key role in pathophysiology of schizophrenia (Nakazawa & Sapkota, 2020). NMDA antagonists are thought to reduce excitation of fast spiking GABAergic neurons, which leads to disinhibition of glutamatergic pyramidal cells, resulting in excitation (with an increase in glutamate) (Iltis et al., 2009; Lisman et al.,

2008). Iltis et al. (2009) examined neuro-metabolic changes in the PFC after acute phencyclidine (PCP) injection in rats. The study suggests that manipulations of excitatory neurotransmission can lead to neuro-metabolic changes, measurable by MRS in anaesthetised rats. It further provides evidence that regional brain activation caused by an NMDA receptor antagonist may be associated with increased glutamine/glutamate ratio. Furthermore, they found increases in glucose and glutamine and decreases in lactate and GABA. The other study mimicking aspects of schizophrenia in rodents is by Napolitano et al. (2014). Using a different NMDA receptor antagonist (ketamine) led to a significant increase in glutamine in the mPFC. Furthermore, they found that ketamine in combination with social isolation decreased GABA in the mPFC.

Our aim was to examine the effects of ventral hippocampal disinhibition on neuro-metabolites in the septum using MRS. Predictions for our study are not straight forward, based on limited available data and major gaps in understanding of what mechanisms underlie changes in MRS neuro-metabolites. However, based on the metabolic activation found using SPECT, a general upregulation of neuro-metabolites may be predicted. Alternatively, it can be hypothesised that ventral hippocampal disinhibition causes similar, or even stronger effects in the septum than in our MRS data of the mPFC, given the stronger activation of the septum compared to the mPFC in our SPECT study (Williams et al., in preparation). From our mPFC findings, a significant decrease in GABA and an increase in myo-inositol concentration is predicted. On the other hand, findings from Iltis et al. (2009) indicate more specific and neuro-metabolite-specific changes caused by regional activation. From the Iltis et al. (2009) study, decreases of glutamate and GABA and increases in glutamine (alongside increased glucose) are predicted.

Although MRS is widely used, including in schizophrenia studies, there are still substantial gaps in our current understanding of the mechanisms underlying changes in MRS neuro-metabolites and how regional disinhibited areas affect projection sites. Our MRS study will enhance our understanding on the mechanisms underlying changes in MRS neuro-metabolites, how the regional disinhibited hippocampus affects one of its main projection sites –septum– and we will gain further insight on how MRS measures relate to blood-flow measures, such as measured by SPECT.

2.1.1 Aims

Our aim was to examine the effects of ventral hippocampal disinhibition, by local microinfusion of the GABA-A receptor antagonist picrotoxin (150 ng/ μ l/side), on neuro-metabolites in the septum using Magnetic Resonance Spectroscopy.

2.2 Methods

2.2.1 Rats

Thirty-two male adult Lister hooded rats (Envigo, UK), weighing between 300 g and 350 g and aged 10-11 weeks at the time of surgery were used. Six rats had to be terminated before completion of the experiment due to onset of the Covid19 pandemic and additional 13 rats had to be excluded for other reasons, so that overall 13 rats contributed to our MRS data. For a justification of sample size and details on the reasons for excluding rats, please see Section 2.2.7.

Rats were housed in groups of four in two-level high top cages (462 mm x 403 mm x 404 mm; Techniplast, UK). To minimize the risk of damaging cannula implants, food hoppers were removed and replaced with pots lying on the floor after surgery. Food (Teklad global 18% protein diet 2019, Harlan, UK) and water was provided ad libitum. Rats were housed in an alternating light/dark cycle of 12 h per phase (lights were on between 7 am and 7 pm), at a temperature of 21 ± 1.5 °C and a humidity of $50 \pm 8\%$. All experimental work was carried out during the light phase. Prior to the start of any experimental procedures, rats were given at least 5 days to acclimate to the new environment and were handled daily to habituate them to the experimenters. All procedures were conducted in accordance with the requirements of the United Kingdom (UK) Animals (Scientific Procedures) Act 1986. All efforts were made to minimise animal suffering and to reduce the number of animals used. Procedures were carried out under the personal licence number I71997928, granted by the Home Office.

2.2.2 Surgery - Stereotaxic implantation of guide cannulae into the ventral hippocampus

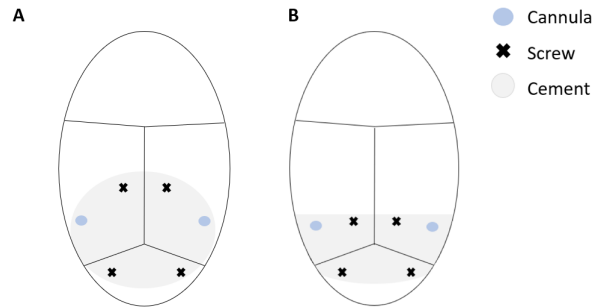
All rats underwent stereotaxic surgery to implant infusion guide cannulae into the ventral hippocampus, following our previous studies (McGarrity et al., 2017; Williams et al., unpublished). In preparation for the surgery, rats received analgesia (Rimadyl large animal solution, 1:9 dilution, 0.1 ml/100 g, s.c., Zoetis, UK) and an antibiotic to act as a prophylactic against meningitis (Synolux, 14% Amoxicillin, Zoetis, UK 0.2 ml/100 g). Rats were anaesthetised with isoflurane (3%), delivered in oxygen (1%). Isoflurane levels were adapted according to breathing rate. The breathing rate provides an indication of the depth of anaesthesia and was kept around 40-60 breaths per minute. Every 5 minutes breathing rate was recorded, and isoflurane levels were maintained at 2-3% throughout surgery. Rats were positioned in a stereotaxic frame. EMLA cream, containing a local anaesthetic (lidocaine, prilocaine, 5%, AstraZeneca, UK), was applied onto the ear bars to reduce pain and an eye gel (Lubrithal; Dechra, UK) was used to prevent ocular drying. An incision was made in the scalp, the skull was exposed and bregma and lambda were aligned hori-

zontally. Holes were drilled bilaterally above the infusion site, which had the following target coordinates: 5.2 mm posterior to bregma, ± 4.8 mm lateral from the midline and 6.5 mm ventral from the dura (McGarrity et al., 2017). MR compatible infusion guide cannulae (PEEK, 26 gauge, 8.5 mm below pedestal; Plastics One, USA) were implanted into the ventral hippocampus and stainless-steel stylets (26-gauge, projecting 8.5 mm from a plastic pedestal; Plastics One, Bilaney, UK) were inserted into the guides to prevent occlusion and closed with dust caps. The tips of the stylets protruded 0.5 mm beyond the tips of the guide cannulae (as did the infusion cannulae).

Guide cannulae were secured in place to the skull using two dental cements (HS Natural Elegance Flowable Composite A2 2 g 4pk, order no: 199952, Henry Schein Minerva Dental Care, Kent, UK and Simplex Rapid Powder with Simplex Rapid liquid, Kemdent, UK) and 4 MR compatible nylon screws (Plastic Ones, USA). Due to a discontinuation of the light curing cement by the supplier, we used a new light curing cement (HS Maxima Natural Elegance Nanohybrid Flow Composite Syringe A2/B2 2.3 g, order number: 9003854, Henry Schein Henry Schein Minerva Dental Care, Kent, UK), which turned out to disrupt the MR signal. No light curing cement was therefore used for subsequent cohorts of rats. For the first 16 rats, screws were placed in front and behind the cannulae, to ensure stabilisation of the implant (Figure 2A). For the last 16 rats, two of the screws were placed in line with the cannulae, two behind the cannulae and cement was minimised at the front of the cannulae (Figure 2B). Screw placement was changed, as our MRS measurement in the first batch of rats indicated that the screws placed before the cannulae reduced the signal of the MR measurements in the lateral septum. At the end of the experiment, analysis of screw location on spectroscopy values was performed (Results 2.3.2).

The open wound was then stitched to reduce its size. For rehydration, rats received an injection of saline (1 ml) subcutaneously and were monitored as they recovered from the anaesthetic. Following surgery, rats were checked, handled, weighed, and injected with antibiotics (Synulox, 14% Amoxicillin, Zoetis, UK, 0.2 ml/100 g) daily. Rats were given at least five days to recover before commencing the experiment.

Figure 2: Graphical visualisation of screws and cement placement to secure hippocampal guide cannulae



Note: **A** Rats 1-16 with two screws in front of the cannulae. **B** Rats 17-32 with two screws in line with the cannulae.

2.2.3 Animal preparation for MRS

Rats were initially anaesthetised with 3% isoflurane in oxygen (1%) and stainless-steel stylets were removed. After transporting the rat over to a pre-warmed cradle in the MR scanner, the head of the rat was restrained using tooth and ear bars. An eye gel (Lubrithal; Dechra, UK) was applied to prevent eyes from drying out during scanning. In the scanner, isoflurane was delivered through a nose cone with a mixture of O₂ and N₂O as carrier gases (in the ratio 0.33:0.66 L/min, respectively). The level of the anaesthetic was adjusted (isoflurane 1 – 3%) to maintain a stable respiratory rate (60 ± 10 per minute). Respiratory rate was monitored using an ERT control/gating module (Model 1032, SA Instruments, Stony Brook, USA) of which the sensors were positioned under the abdomen of the rat, below the diaphragm, which detect movement of the rib cages when the rat breathes. The rat's body temperature was measured using a rectal thermal probe and controlled by a water-pump system that is connected to tubing embedded in the base of the rat cradle. Temperature was maintained around $37 \pm 1^\circ\text{C}$. The infusion cannulae for the ventral hippocampal infusions were inserted into the guides, before the rats were moved into the scanner bore (details for infusion are given in Section 2.2.5). Once the rat was placed into the scanner bore, anatomical reference images were obtained and a voxel for MRS data acquisition was positioned in the septum (details for MRS acquisition in the following Section 2.2.4). Study timeline is illustrated in Figure 4.

2.2.4 MRS acquisition

MRS measurements were conducted on a 7-Tesla Bruker Biospec 70/30 USR horizontal bore small animal scanner (Bruker, Germany). A surface receive-only head coil, consisting of 4 channels (Bruker, Germany), was placed as closely to the cannula as possible. To ensure that the septum was in the centre of the magnet, a quick gradient echo acquisition scan

was performed (TE = 6 ms, TR = 100 ms). Anatomical reference images were obtained in three orthogonal planes using a rapid acquisition with relaxation enhancement (RARE) sequence (Hennig et al., 1986) with TR = 5 s, flip angle = 90° and rare factor = 8. The axial MRI scan slice (which corresponds to coronal view) had the following values: TE = 14 ms, TE_{effective} = 28 ms, FOV = 40x40 mm, spatial resolution = 0.156 x 0.156, slice thickness = 0.5 mm. The values for the dorso-ventral views were TE = 25 ms, TE_{effective} = 50 ms, FOV = 40 x 40, spatial resolution = 0.156 x 0.156 slice thickness = 1 mm, and for the sagittal views were TE = 25 ms, TE_{effective} = 50 ms, FOV = 50 x 36 mm, spatial resolution = 0.195 x 0.141, slice thickness = 1 mm. A voxel of 2x2x2 mm³ was positioned in the septum for the acquisition of MRS data (Figure 3A). A gradient echo sequence was used to calculate a phase difference, to map the homogeneity of the overall magnetic field, allowing enhancement of B₀ homogeneity. Local magnetic field homogeneity was adjusted within the septum by applying FASTMAP (Gruetter, 1993). The average water line width for all spectra was 8.55 ± 0.19 (mean \pm SEM) Hz (full-width half maximum) of the unsuppressed water peak across the spectroscopy voxel. The average Signal to Noise ratio of the water signal from the voxel was SNR_{H₂O} = 185.29 ± 10.46 (mean \pm SEM). Localised proton MR spectroscopy was obtained using a Point Resolved Spectroscopy (PRESS) sequence (Bottomley, 1987), with an acquisition time of 34 min (acquisition parameters: TE = 13.5 ms, TR = 2000 ms, spectral width of 4006.41 Hz with 2048 points and 1024 averages with Eddy current compensation) after water suppression with variable power and optimized relaxation delays (VAPOR) (Tkáč et al., 1999).

2.2.5 Hippocampal microinfusion

Prior to the experiment, MR compatible infusion cannulae (PEEK, 33-gauge, to fit the guides with 0.5 mm protrusion; Plastics One, USA) were glued to flexible Teflon tubing (0.65 mm OD x 0.12 mm ID; BASi, UK). On the day of the experiment, the tubing was filled with picrotoxin (C30H34O13; Sigma Aldrich, UK) in saline (150 ng/ μ l/side) or 0.9% sterile saline (control). Hamilton syringes (1 μ l) were filled with 0.75 μ l distilled water and 0.25 μ l air before they were connected to the Teflon tubing. Then, once connected to the Teflon tubing, the piston was pushed to 0.5 μ l, before being pulled back to 0.75 μ l. This method creates a 0.25 μ l air bubble at the end of the Teflon tubing where it is connected to the syringe tip. The air bubble by the infusion cannula tip acts as an 'air plug' to reduce the risk of infusion solution leaking into the brain, and the air bubble close to the syringe tip was monitored for movement during infusion, to verify that infusion was successful. Infusion cannula tips were inserted into the guide cannulae, protruding 0.5 mm below the guides into the hippocampus. The air plug (0.25 μ l), plus a volume of 0.5 μ l/side of either saline or picrotoxin was infused bilaterally over the course

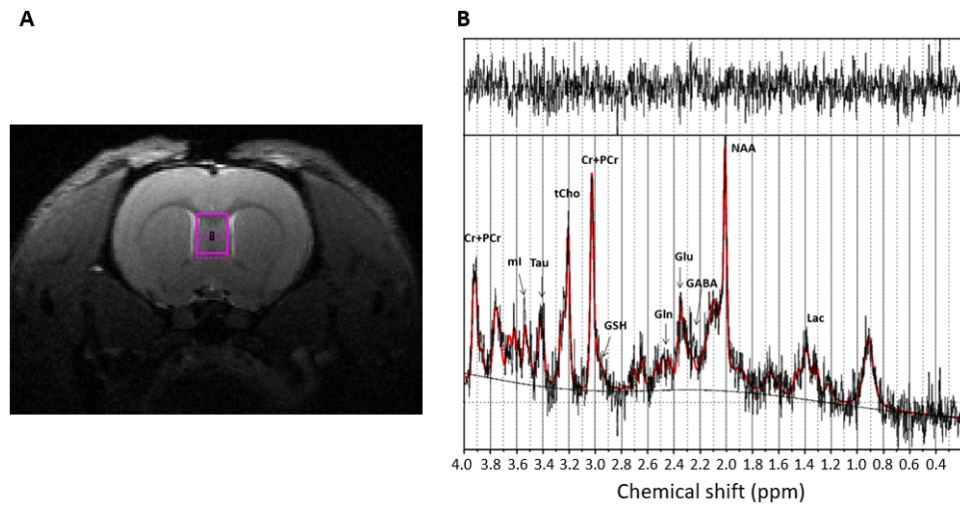
of approximately 90 s (30 s for air plug + 60 s for picrotoxin/saline). The Teflon tubing was long enough for the syringes to remain placed outside the scanner after the rat was positioned in the MR scanner, so that the rat could remain positioned in the scanner during the intra-hippocampal infusions. When rats came back from anaesthesia they were visually inspected to check for seizure-related signs (S. A. Williams et al., 2022). No such signs were observed.

2.2.6 Processing of MRS data

MRS data was analysed using LCModel software (S. W. Provencher, 1993) in a fully automated pipeline. Figure 3B demonstrates an example of the in vivo MRS spectrum acquired from the voxel positioned in the septum. The analysis window ranged from 0.2 to 4.0 ppm. Data was fitted to a basis set containing 21 metabolites: alanine (Ala), aspartate (Asp), creatine (Cr), phosphocreatine (PCr), gamma-aminobutyric acid (GABA), glucose (Glc), glutamine (Gln), glutamate (Glu), glycerophosphorylcholine (GPC), phosphorylcholine (PCh), glutathione (GSH), myo-inositol (m-Ins), lactate (Lac), n-acetyl aspartate (NAA), n-acetyl aspartate glutamate (NAAG), scyllo-inositol (Scyllo), taurine (Tau), total creatine (Cr+PCr), total choline (GPC+PCh), NAA+NAAG (tNAA) and glutamate + glutamine (Glx). Metabolite concentrations were determined as a ratio to total creatine (Cr+PCr) (S. W. Provencher, 1993) as creatine is thought to be a reliable marker of intact brain energy metabolism (Danielsen & Ross, 1999). The assumption of its stability is used to quantify metabolite levels as ratios, rather than absolute concentrations (Li et al., 2003; Soares & Law, 2009).

Cramér-Rao lower bounds (CRLB) provide quantitative error estimates for metabolic quantification, to assess reliability of the metabolite concentration (Öz et al., 2014). CRLB values of under 20% are deemed as reliable spectra fitting, however, this is not a strict criterion (S. Provencher, 2021). Higher CRLB values could be used for metabolites that exist at lower concentrations (Just & Faber, 2019). We included any metabolite measurement with a CRLB of 50%. The following metabolites were undetectable: Ala, Asp, PCh, -CrCH₂, Scyllo as well as lipids. Macromolecule components were not analysed for this study.

Figure 3: Coronal view of voxel placement in the septum and example spectrum generated with LCMoDel



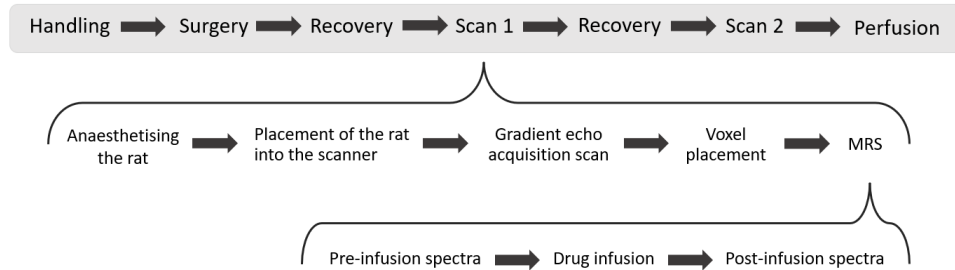
Note: **A** Coronal view (axial slice) of rat brain. Purple box shows localisation of the voxel of interest ($2 \times 2 \times 2 \text{ mm}^3$) in the septum and delineates the area in which spectra were acquired. It was used to quantify the relative metabolite concentrations. **B** Example spectrum generated with LCMoDel. At the top is the residual error obtained after LCMoDel fitting (the data minus the fit to the data). The black line at the bottom represents the original spectrum data. The red line shows the LCMoDel fit to the data. Numbers on x-axis show chemical shift, measured in parts per million. Manually labelled peaks indicate the following metabolites: Creatine + phosphocreatine (Cr+PCr), Glutamate (Glu), Glutamine (Gln), myo-inositol (m-I), Taurine (Tau), Total Choline (tCho), gamma-aminobutyric acid (GABA), Glutathione (GSH), N-acetylaspartate (NAA), Lactate (Lac).

2.2.7 Experimental design (including sample size and exclusion justification)

The effects of hippocampal neural disinhibition on the septum were examined in a within-subjects, counterbalanced, crossover design, using two conditions: saline ($0.5 \mu\text{l}/\text{side}$) and picrotoxin ($150 \text{ ng}/0.5 \mu\text{l}/\text{side}$) (Sigma-Aldrich, UK). This dose is the same as in our SPECT study (William et al., in preparation) and has shown to cause marked cognitive and behavioural, as well as electrophysiological effects (McGarrity et al., 2017; S. A. Williams et al., 2022). No blinding occurred. Rats received one of the two infusions (saline or picrotoxin) during their first MR scanning session and the other one during their second scanning session, which was run at least two days later. Pre-infusion baseline spectra were acquired from the voxel positioned in the septum prior to the start of hippocampal drug microinfusions. Infusions took place immediately following the com-

pletion of the baseline scan. Post-infusion spectra were acquired 9 min following the end of hippocampal infusion (which had a 1 min duration). This timing of spectra acquisition was chosen based on electrophysiological measures to capture the peak effect of picrotoxin infusion on hippocampal neuron firing (McGarrity et al., 2017). Study timeline illustrated in Figure 4.

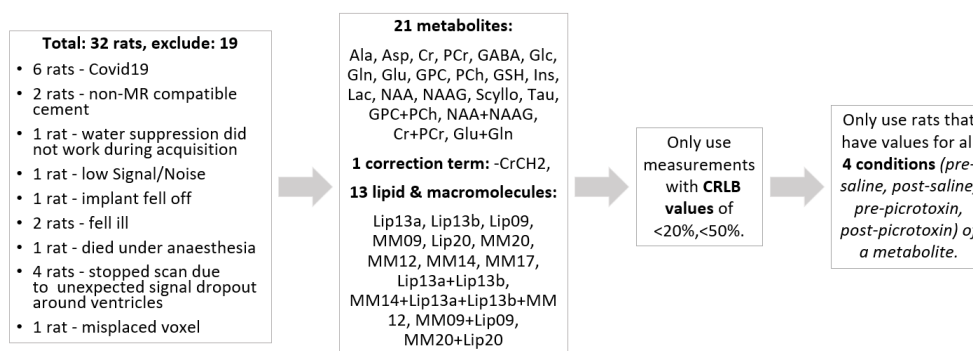
Figure 4: MRS study timeline



Note: Voxel was positioned in the septum. When rat was anaesthetised, stylets were removed. Once the rat was placed in the scanner, infusion cannulae filled with saline or picrotoxin were inserted into guides. If spectra were not successfully acquired, more scans would take place following a day of recovery, before perfusion was carried out.

We aimed for a sample size of at least $n=10$ to give $>80\%$ power to detect an effect size of $d=1$ at a significance threshold of $p=0.05$, using pairwise comparisons (power analysis conducted with GPower 3.1 (Faul et al., 2007)). The experiment was run in multiple batches of at least four rats (as rats were housed in cages of four). Of the 32 rats that were used in the study, only 13 rats contributed to the MRS data. This was because 6 rats had to be culled because the experiment had to be terminated due to Covid19, in 2 rats there were MR susceptibility artefacts due to the dental cement, in 1 rat the water suppression did not work during acquisition and the metabolite signals were not visible, 1 rat had a low Signal to Noise ratio, and 1 rat was excluded because it lost its head cap, possibly due to screw placement (however, this is speculative given the small numbers). Furthermore, 2 rats fell ill, 1 rat died under anaesthesia during scanning and scanning was stopped for 4 rats due to unexpected signal dropout around the ventricles (discussed in 2.3.3, Figure 8). Lastly, for 1 rat the voxel was misplaced. Data/metabolites were also excluded based on CRLB values for the 4 scans (discussed in Section 2.2.6). If a metabolite was not measurable for all four of a rat’s scans (i.e. pre- and post-infusion for saline and picrotoxin), this rat was excluded from the analysis for this metabolite. For a visual representation of how data was excluded see Figure 5. The final numbers of rats that contributed to the analysis of the different metabolites are indicated in Table 1.

Figure 5: Data exclusion criteria



2.2.8 Data analysis

Difference scores (post-infusion score minus pre-infusion score) were calculated for each metabolite to identify any differences between pre-infusion and post-infusion in the saline and picROTOXIN condition. Statistical analysis of difference scores for each metabolite was performed using two-tailed paired t-tests. Moreover, metabolite concentrations (Cr+PCr) were analysed using a 2x2 repeated measures ANOVA with drug infusion condition (saline or picROTOXIN) and time (pre- or post-infusion period) as within-subjects factors. The accepted level of significance was $p < 0.05$. Analysis was done on IBM SPSS Statistics 24, Excel and GraphPad prism (Version 9, GraphPad software, USA).

2.2.9 Histology

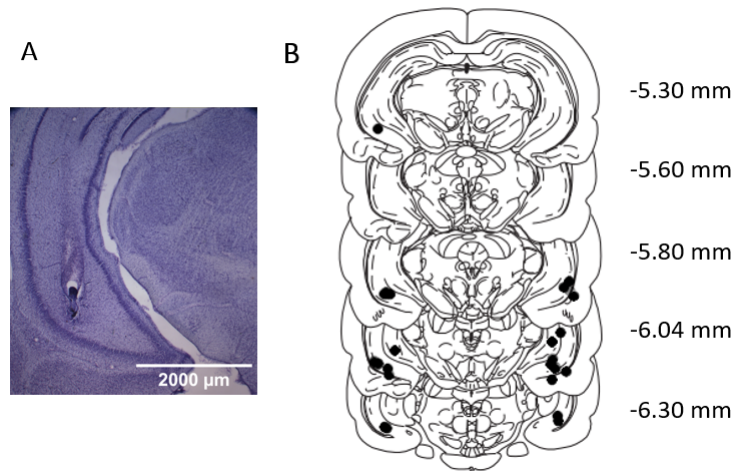
Rats were overdosed with sodium pentobarbital (Dolethal, Vetoquinol, UK) and transcardially perfused using 0.9% saline followed by 4% paraformaldehyde (PFA) solution right after their last scan. Brains were extracted and stored in 4% PFA. Brains were sliced into 80 μm thick coronal sections using a vibratome (Leica VT1000 S) and placed onto microscope slides. Infusion cannula placements were verified using a Leica light microscope (Leica DM1000, Leica DFC295, 1.25x/0.04 with a Leica HCX PL Fluotar 1.25x/0.04 microscope objective) and mapped onto coronal sections adapted from the rat brain atlas by Paxinos & Watson (1998). Some slides were stained with cresyl violet and coverslipped to take photos, captured with a Zeiss Axioplan light microscope using a QImaging MicroPublishers 5.0 RTV and the Micro Manager software. Images were taken using a 1.25x/0.035NA objective. The images were then white balanced and a scale bar applied using the FIJI software.

2.3 Results

2.3.1 Histology - verification of ventral hippocampus infusion cannulae placements

In total, data from 13 rats was used for analysis. Cannulae tip positions were mapped onto coronal sections of an adapted Paxinos & Watson (1998) rat brain atlas (Figure 6). All cannula tips were located in the ventral hippocampus between 5.30 mm and 6.30 mm posterior to bregma. One cannula placement on the right side of the brain could not be identified based on the histology slices and therefore, placement was made using the MR images as guide.

Figure 6: Infusion sites in the ventral hippocampus

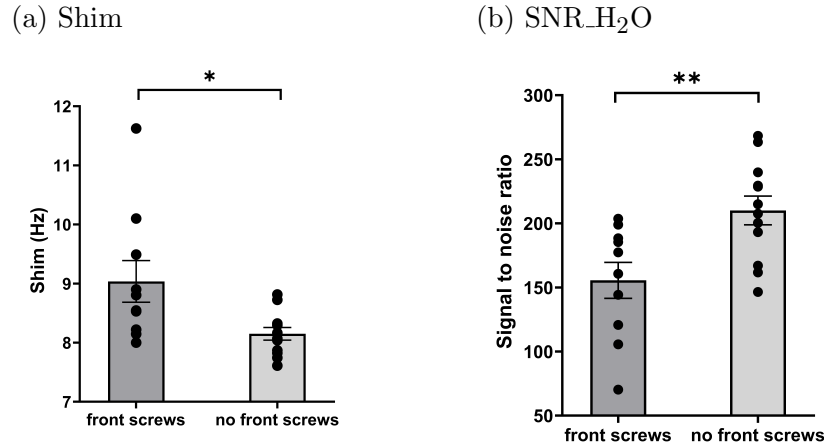


Note: **A:** Photograph of a coronal brain section showing guide cannula track. **B:** Approximate locations of infusion tips in the ventral hippocampus using light microscopy. Locations are shown on coronal plates adapted from the atlas by Paxinos & Watson (1998), with numbers indicating distance from bregma in millimetres as shown in the atlas.

2.3.2 Effects of screw location on spectroscopy

In rats without front screws, shim values (the water line width of the unsuppressed water peak across the voxel placed in the septum) were lower ($t(20) = 2.604, p = 0.017$) ($n=10$) (Figure 7a) and the SNR_{H₂O} were higher ($t(20) = -3.077, p = 0.006$) (Figure 7b) than in rats with front screws ($n=12$).

Figure 7: Comparison of shim values and SNR_H₂O in the voxel placed in the septum in rats with and without front screws



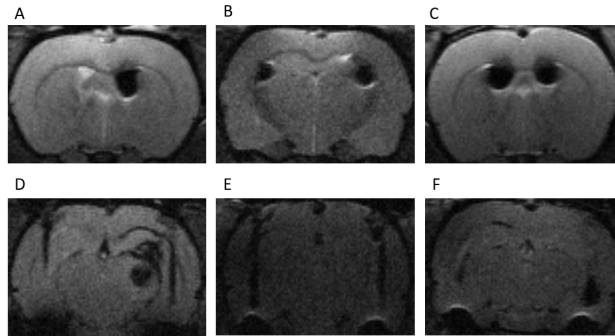
Note: Rats without front screws had on average lower shim values (a) and higher SNR_H₂O (b).

2.3.3 Signal dropouts and bleeding

Although many rats did not contribute to the analysis of infusion effects on MRS metabolite values (see reasons for exclusions in Section 2.2.7), 27 rats prepared for the present study underwent at least one structural MR scan (4 rats were culled due to Covid19, and 1 rat due to illness). These structural MR scans revealed MR signal dropout, not only around the cannulae and infusion sites (where we would have expected such susceptibility artefacts), but also in other parts of the brain. In 8 rats, we found signal dropout in MR images (Figure 8) which was either unilateral (A), or bilateral (B,C); mainly in the lateral ventricles as well as around the external capsule. For some rats we did not extract the brains, and for others we looked for the signal dropout, but did not find evidence for bleeding. The last three images in Figure 8 (D,E,F) correspond to the first 3 images in Figure 10 (A,B,C) respectively. One rat showed an enlarged left ventricle (Figure 9), which after 6 days of the first scan showed a similar looking signal dropout to Figure 8. The susceptibility artefact roughly covered the CA3 as well as the external capsule.

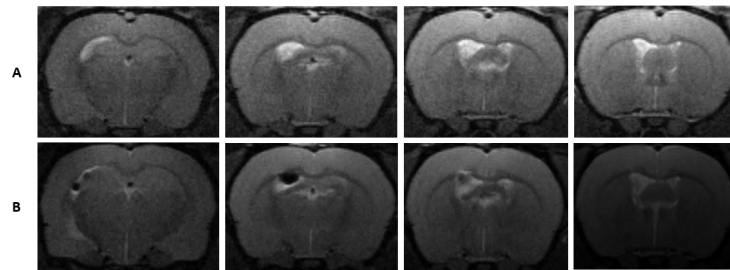
For 3 of the rats that showed MR signal dropout, we were able to confirm blood clots histologically (Figure 10). One other rat showed blood clots, however, due to illness, it had to be culled before an MR scan was obtained. Blood clots were found in the corpus callosum (white arrow) and/or hippocampus (black arrow) for all the rats that showed bleeding. For Rat A, the blood clot covered parts of the posterior dorsal hippocampus and thalamus and rat B also had the blood in the external capsule, in more posterior slides.

Figure 8: Example of rats showing artefacts in MR scan



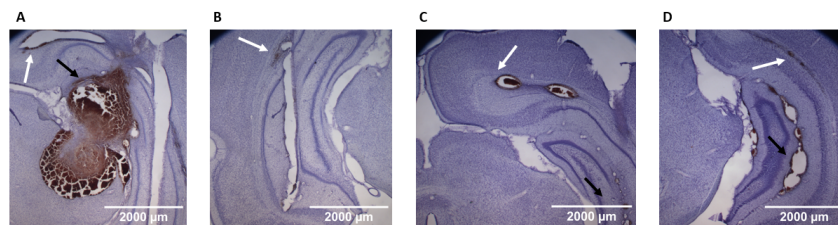
Note: Unilateral (**A**), and bilateral (**B,C**) signal dropouts and blood next to (**D,E**) or just below the right cannula (**F**) (histologically verified).

Figure 9: Scan pre- and post-signal dropout of the same rat



Note: **A** depicts a scan 6 days before scan **B** of the same rat. Left lateral ventricle is enlarged, and large signal dropout in the left ventricle at the later scan.

Figure 10: Example of blood in rats that were included in the analysis



Note: White arrows point to blood clots in the corpus callosum and black to the hippocampus. For **A** the large blood clot also covers the thalamus and the posterior dorsal hippocampus.

2.3.4 Metabolite concentrations

In total, 16 metabolites were quantified. For Cr, PCr, GABA, Gln, Glu, Glx, m-Ins, NAA, Tau, GPC+PCh and NAA+NAAG we used a CRLB of 20% or lower as inclusion criterion and for Glc, GPC, GSH, Lac and NAAG we used a CRLB of 50% or lower, as with a threshold of 20% we would not be able to include any rat for the latter metabolites. Table 1 presents the metabolite concentration as a ratio to the concentration of tCr (Cr+PCr) and CRLB values before and after hippocampal infusion of saline or picrotoxin.

Table 1: Metabolite concentrations with CRLB pre/post saline/picrotoxin infusion

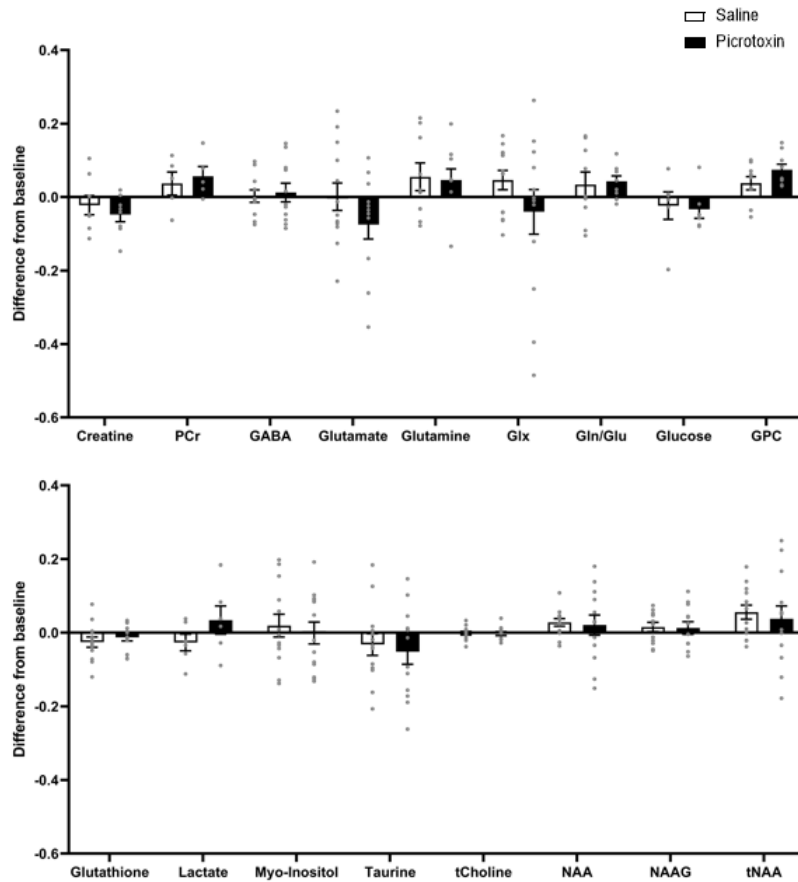
	Inclusion Criterion used CRLB	n	Saline Pre-infusion		Saline Post-infusion		Picrotoxin Pre-infusion		Picrotoxin Post-infusion	
			Concentration/tCr	CRLB (%)	Concentration/tCr	CRLB (%)	Concentration/tCr	CRLB (%)	Concentration/tCr	CRLB (%)
Cr	20%	8	0.52±0.02	12.3±0.6	0.50±0.03	13.0±0.3	0.61±0.05	13.0±1.0	0.57±0.06	13.0±0.6
PCr	20%	5	0.50±0.02	12.6±0.7	0.53±0.02	12.0±0.8	0.44±0.02	16.0±1.4	0.50±0.03	13.8±1.6
GABA	20%	11	0.44±0.02	14.6±0.6	0.44±0.01	14.5±0.1	0.42±0.03	15.7±1.1	0.44±0.02	14.8±0.8
Gln	20%	9	0.56±0.02	15.2±0.6	0.62±0.03	14.2±0.8	0.54±0.04	16.1±0.7	0.59±0.02	14.8±0.6
Glu	20%	13	1.45±0.02	6.1±0.2	1.45±0.03	6.3±0.2	1.47±0.04	6.5±0.5	1.42±0.04	6.5±0.5
Glx	20%	13	2.00±0.02	5.9±0.1	2.05±0.04	6.0±0.2	2.02±0.06	6.3±0.4	1.98±0.04	6.3±0.3
m-Ins	20%	13	0.79±0.02	8.2±0.4	0.81±0.02	8.2±0.4	0.80±0.03	8.7±0.6	0.80±0.03	8.4±0.5
NAA	20%	13	1.04±0.02	4.8±0.2	1.07±0.01	4.9±0.2	1.02±0.02	5.5±0.3	1.04±0.02	5.2±0.3
Tau	20%	13	0.66±0.03	10.1±0.6	0.63±0.03	10.6±0.6	0.70±0.02	9.9±0.6	0.65±0.03	10.5±0.6
GPC+PCh	20%	13	0.25±0.01	6.0±0.3	0.25±0.01	6.15±0.3	0.26±0.01	6.8±0.5	0.25±0.01	6.2±0.5
NAA+NAAG	20%	13	1.21±0.02	5.1±0.1	1.27±0.02	5.00±0.2	1.19±0.03	5.5±0.2	1.23±0.02	4.9±0.2
Glc	50%	6	0.26±0.04	30.5±4.2	0.24±0.03	33.3±4.3	0.28±0.02	28.2±2.6	0.25±0.04	33.5±4.7
GPC	50%	9	0.18±0.02	26.3±4.4	0.21±0.01	21.6±4.2	0.15±0.01	36.9±2.7	0.22±0.01	19.6±3.6
GSH	50%	13	0.19±0.01	22.2±1.1	0.16±0.01	27.3±2.2	0.19±0.01	24.1±1.7	0.18±0.01	25.2±1.5
Lac	50%	6	0.28±0.02	26.3±2.4	0.26±0.02	31.5±2.1	0.27±0.02	33.0±4.0	0.30±0.03	25.8±2.3
NAAG	50%	12	0.18±0.01	24.9±2.1	0.20±0.02	23.7±1.8	0.18±0.02	29.7±2.6	0.19±0.01	24.8±1.4

Note: Average (mean ± SEM) concentration as a ratio to total creatine (phosphocreatine and creatine) and corresponding CRLB values for each metabolite measured using ¹H-spectroscopy for both saline and picrotoxin infusion groups before and after drug infusion. CRLB value <20%: Cr, PCr, GABA, Gln, Glu, Glx, m-Ins, NAA, Tau, GPC+PCh, NAA+NAAG. CRLB value <50%: Glc, GPC, GSH, Lac and NAAG.

2.3.5 Difference scores

Figure 11 shows the difference scores, calculated by subtracting pre-infusion scores from post-infusion scores for each metabolite. These were calculated separately for saline and picrotoxin infusions. There was no evidence for any specific effect of picrotoxin compared to saline infusions on any of the neuro-metabolites, with paired t-tests revealing no significant difference between the difference scores in the picrotoxin and saline condition for any of the neuro-metabolites studied, including for glutamine/glutamate ratio (all $t < 1.954$, $p > 0.104$).

Figure 11: Difference scores (post-infusion minus pre-infusion concentration) for all measured metabolites following saline and picrotoxin infusion



Note: Changes in the metabolite concentrations induced by hippocampal picrotoxin and saline infusion are displayed. Infusion-induced changes are expressed as difference scores, i.e. difference between pre-infusion concentration and post-infusion concentration (as a total to creatine). Data are depicted as mean \pm SEM, with sample sizes and CRLB values presented in Table 1 for each metabolite. There were no significant differences in the difference scores following saline or picrotoxin infusion for any of the metabolites.

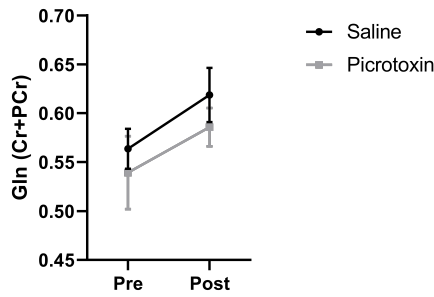
2.3.6 2x2 ANOVAs - No infusion effects on metabolites

To further investigate the changes in metabolite concentrations (Cr+PCr) after infusion with saline/picrotoxin we conducted 2x2 (drug infusion x time) ANOVAs for each metabolite. The ANOVAs, in line with the difference score analysis, did not support any specific impact of the picrotoxin infusion on any neuro-metabolite (interaction infusion x time, all $F < 3.817, p > 0.104$). Some metabolites changed from pre- to post-infusion period, regardless of the infusion condition, as reflected by a significant main effect of time. **Glutamine** increased over time ($F_{(1,8)} = 6.137, p = 0.038$) (Figure 12a) as did **glutamine/glutamate ratio** ($F_{(1,8)} = 6.804, p = 0.031$) (Figure 12b), **glycerophosphoryl-choline** ($F_{(1,8)} = 18.819, p = 0.002$) (Figure 12d) and **NAA+NAAG** ($F_{(1,12)} = 5.343, p = 0.039$) (Figure 12e). **Taurine** decreased over time ($F_{(1,12)} = 5.508, p = 0.037$) (Figure 12c). There was a numerical tendency for a decrease of **creatine** ($F_{(1,7)} = 3.776, p = 0.093$) (Figure 12f) and **glutathione** ($F_{(1,12)} = 3.747, p = 0.077$) (Figure 12g) with time but no statistical support for this. We ran supplementary analyses, with a more liberal CRLB threshold for glutamine and glutamine/glutamate ratio (30% instead of 20%), which increased the numbers of rats included in the analyses. The effect of time was no longer significant for both glutamine ($F_{(1,12)} = 1.130, p = 0.309$) (Figure 13a) and glutamine/glutamate ratio ($F_{(1,12)} = 2.273, p = 0.157$) (Figure 13b).

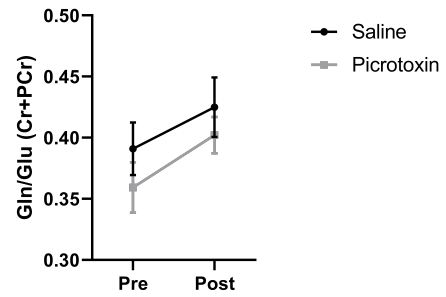
Figure 14 is depicted to compare our findings with Williams et al. (in preparation) and Figure 15 to compare our results to Iltis et al. (2009). Septal **GABA** (Figure 14a) and **myo-inositol** (Figure 14b) were not affected by hippocampal picrotoxin infusion (main effect of drug and interaction drug x time, all $F < 0.193, p > 0.670$). Septal **glutamate** (Figure 15a) and **glucose** (Figure 15b) were not affected by hippocampal picrotoxin infusion (main effect of drug and interaction drug x time, all $F < 0.804, p > 0.387$). However, these results of glucose are not robust due to the sample size of 6, in combination with the CRLB threshold at 50%.

Figure 12: Main effect of time

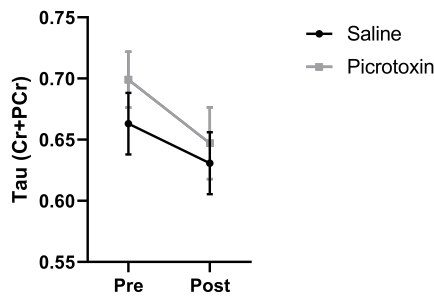
(a) Glutamine (CRLB: 20%)



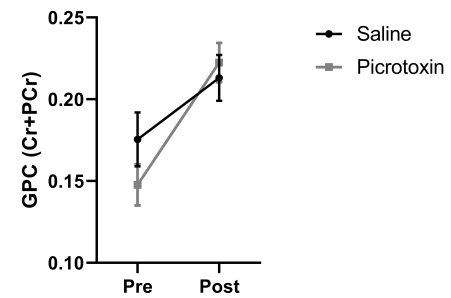
(b) Gln/Glu (CRLB: 20%)



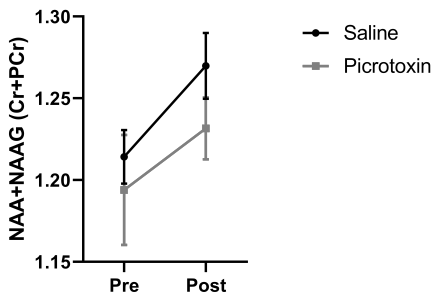
(c) Taurine (CRLB: 20%)



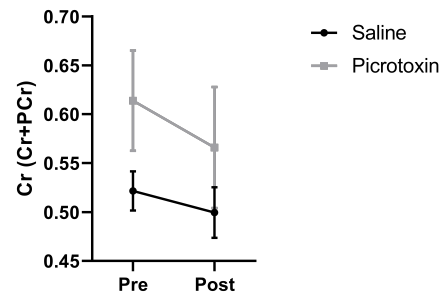
(d) GPC (CRLB: 50%)



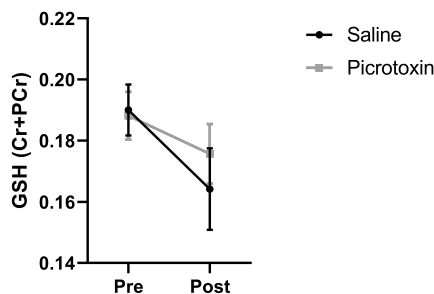
(e) NAA +NAAG (CRLB: 20%)



(f) Creatine (CRLB: 20%)



(g) Glutathione (CRLB: 50%)

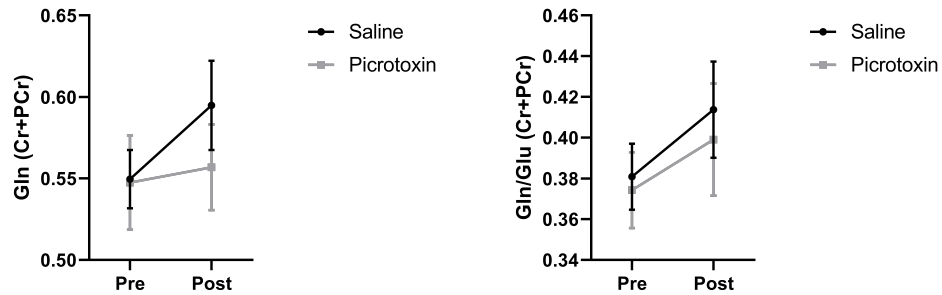


Note: Metabolite concentrations (mean \pm SEM) shown as a ratio to total creatine (Cr+PCr) for saline (black) and picrotoxin (grey), measured before and after hippocampal drug infusion.

Figure 13: No longer main effect of time

(a) Glutamine (CRLB: 30%)

(b) Gln/Glu (CRLB: 30%)

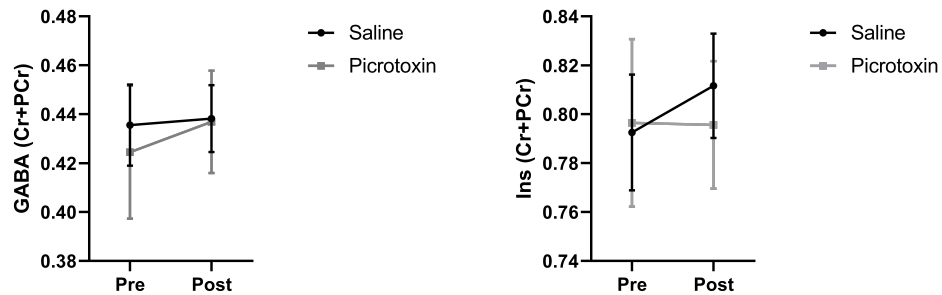


Note: (a) Glutamine (CRLB: 30%) and glutamine/glutamate (CRLB: 30%) concentration (mean \pm SEM) as a ratio to total creatine (Cr+PCr) for saline (black) and picrotoxin (grey), measured before and after hippocampal drug infusion.

Figure 14: Comparing our results to Williams et al. (in preparation)

(a) GABA (CRLB: 20%)

(b) Myo-inositol (CRLB: 20%)

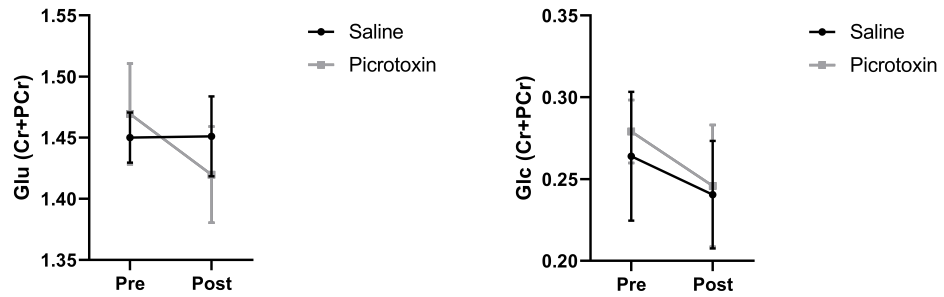


Note: (a) GABA and (b) myo-inositol concentration (mean \pm SEM) as a ratio to total creatine (Cr+PCr) for saline (black) and picrotoxin (grey), measured before and after hippocampal drug infusion, depicted with a CRLB threshold of 20%. There were no significant main effects of drug, time and no significant interaction (drug x time)

Figure 15: Comparing our results to Iltis et al. (2009)

(a) Glutamate (CRLB: 20%)

(b) Glucose (CRLB: 50%)



Note: (a) glutamate (CRLB: 20%) and (b) glucose (CRLB: 50%) concentration (mean \pm SEM) as a ratio to total creatine (Cr+PCr) for saline (black) and picrotoxin (grey), measured before and after hippocampal drug infusion.

2.4 Discussion

Our findings do not support a significant impact of ventral hippocampus disinhibition on the various metabolites that we measured in the septum, including creatine (Cr), phosphocreatine (PCr), gamma-aminobutyric acid (GABA), glutamine (Gln), glutamate (Glu), glutamate + glutamine (Glx), myo-inositol (m-Ins), n-acetyl aspartate (NAA), taurine (Tau), total choline (GPC+PCh), NAA+NAAG (tNAA), glucose (Glc), glycerophosphorylcholine (GPC), glutathione (GSH), lactate (Lac) and acetyl aspartate glutamate (NAAG). There was some evidence for changes of some neuro-metabolite concentration across time, from pre- to post-infusion measurements, regardless of drug. There was a significant decrease of taurine and a significant increase of glutamine, the glutamine/glutamate ratio, GPC and NAA+NAAG over time. The reliability of these changes is discussed in the next Section (2.4.1). There was a numerical tendency for a decrease of GSH and creatine with time, however no statistical support for this.

2.4.1 Decrease of taurine and increase of glutamine, gln/glu, GPC and NAA+NAAG concentrations over time

Taurine is one of the most abundant amino acids in the brain (R. Wang & Reddy, 2017). It has been suggested that taurine balances glutamate activity, particularly under excitotoxic conditions to prevent cell death (El Idrissi & Trenkner, 1999; Trenkner, 1990). Apart from neuroprotection it has shown to be involved in osmoregulation (Schaffer et al., 2000), modulation of calcium movements (Foos & Wu, 2002; Chen et al., 2001; El Idrissi & Trenkner, 1999, 2003), anti-inflammatory processes (Sun et al., 2012; Miao et al., 2012) and neuromodulation (Oja & Saransaari, 1996). Taurine has also shown inhibitory function by activating GABA-A or glycine receptors in rat hippocampal neurons (Z. Y. Wu & Xu, 2003; Del Olmo et al., 2000). The decreased levels seem somewhat surprising, based on its function discussed above. However, it is important to note that the decrease of taurine with time was for both saline and picrotoxin.

Increased levels of **glutamine** and **glutamine/glutamate ratio** (as found in our results) has been previously reported in patients with schizophrenia (Bustillo et al., 2014) and could reflect increased glutamate release and turnover to glutamine with time (Napolitano et al., 2014). However, we observed no significant change in glutamate nor was the increase with time drug related. **Glycerophosphorylcholine (GPC)** along with phosphorylcholine (PCh) and free choline are the main metabolites that contribute to the choline resonance peak (Hammen & Kuzniecky, 2012; Bivard et al., 2013). The compounds are involved in cell membrane synthesis and degradation (Bivard et al., 2013). Although, the effect of time is significant ($p=0.002$), it is important to note the CRLB level of 50%, which suggest unreliable readings. Furthermore, when looking at total choline (GPC+PCh) we were able to use a CRLB of 20% and include all

rats, however, did not find a significant interaction of drug x time nor effect of time. In MRS, the **N-acetyl aspartate glutamate (NAAG)** compound strongly overlaps with the signal of NAA (its precursor) (Jessen et al., 2013). NAAG is thought to have neuroprotective function by activating the 3 metabotropic glutamate receptors which facilitate glutamate reuptake and suppress glutamate release (Guo et al., 2015; Zhong et al., 2014). In disorders such as schizophrenia, reduced levels of NAA are found in various brain regions (Moffett et al., 2013). However, our findings not only show an increase in NAA+NAAG with time, they were also drug independent.

To the best of our knowledge, previous studies have not reported temporal changes without a significant interaction of drug/disorder x time. It is likely that the changes that we observed in taurine, glutamine, GPC and NAA+NAAG over time reflect a baseline drift from pre-infusion to post-infusion measurement, which may be due to physiological changes or changes of the scanner. It is also important to note that when increasing the CRLB bound for glutamine and glutamine/glutamate ratio to 30% to include more rats (from 9 to 13), the effect of time was no longer significant.

2.4.2 Neuro-metabolite concentrations in the septum: comparison to previous studies in other brain regions

Although a direct comparison with other studies is difficult due to methodological differences, our baseline measurements of neuro-metabolites using MRS in the septum are largely consistent with what would be expected based on previous MRS studies in the rat brain. For example, the concentrations as a ratio to total creatine, and CRLB values of neuro-metabolites including NAA, glu, and gln are similar to Napolitano et al. (2014) (difference is ≤ 0.05 (number chosen arbitrary)). Their GABA value is slightly higher than ours (0.65 vs 0.44). When comparing our data with that of our previous study on the mPFC (Williams et al., in preparation), most of our values are similar (difference is ≤ 0.07 (number chosen arbitrary)), except of glutamine, glutamate+glutamine and taurine, where our values are smaller by 0.31, 0.35 and 0.28 respectively and GABA, where our concentrations are bigger (0.44 vs 0.29). The increased concentration is consistent with the nature of the septum containing mainly GABAergic neurons (D. Wang et al., 2021). Our data also reflects the naturally higher occurring concentrations of NAA (Pouwels & Frahm, 1997) compared to GABA and glutamine.

2.4.3 Hippocampal disinhibition did not affect neuro-metabolites in the septum - Possible explanations for our findings

We hypothesised a general upregulation of neuro-metabolites. Our findings do not support these predictions. We also hypothesised similar or stronger effects to our previous findings in the mPFC as the septum has stronger connectivity to the hippocampus (Gray & McNaughton, 1983; Müller & Remy, 2018; Risold & Swanson, 1997) and our previous SPECT study (Williams et al. in preparation) showed greater activation in the septum than in the mPFC. No significant change in GABA or myo-inositol was found. Lastly, we predicted similar findings to Iltis et al. (2009). A decrease in GABA and glutamate and an increase in glucose was not found. Although there was a significant increase in glutamine, this increase was observed for both drug infusions.

There may be several explanations why our measurements in the septum may not reveal a significant impact of ventral hippocampal disinhibition. In light of our SPECT study, where ventral hippocampus disinhibition caused marked metabolic activation in the lateral septum, the failure of our MRS measurements to detect any changes in neuro-metabolites in the lateral septum under anaesthesia indicates that marked acute metabolic activation in the lateral septum (as detected by SPECT) is not accompanied by neuro-metabolite changes measurable by MRS (possibly reflecting homeostatic metabolic mechanisms). Alternatively, given that the SPECT measurements reflected lateral septum activation in freely moving rats, whereas the MRS measurements were taken under anaesthesia, it is possible that the anaesthesia may have interfered with the lateral septum activation. Lastly, the different outcomes of the MRS measurements in mPFC and septum, in spite of both regions showing significant metabolic activation following ventral hippocampal disinhibition in the SPECT study, may reflect that the link between metabolic activation, as revealed by SPECT, and neuro-metabolite concentration, as revealed by MRS, is region specific (septum versus PFC).

2.4.4 Impact of cannula implant on MR signal quality, signal dropout and bleeding

During the study we changed screw location in relation to the cannulae. Our findings support statistically that having screws in line with cannulae (instead of in front) improves shimming as well as MR signal. Furthermore, it suggests that cement or screws close to the region of interest in MR measurements causes susceptibility artefacts. These findings have implications for future surgeries as screw location did not affect implant stability greatly.

Our structural MR scans revealed MR susceptibility artefacts, not only around the cannulae and infusion sites (where we would have expected such artefacts due to phase transitions), but also in other parts of the

brain, mainly in the lateral ventricles as well as around the external capsule. We did not find evidence for bleeding for brains that showed signal dropouts in these regions. These signal dropouts may have developed over time, as suggested by our MR scans of one of the rats that only showed signal dropouts on the third scan. Other rats showed signal dropout in the corpus callosum and hippocampus, which was later confirmed histologically to be blood clots. Reasons for these blood clots are unknown but may be a consequence of the cannula implantation.

2.4.5 Limitations

MRS can possibly provide a direct translation between pre-clinical and clinical studies as it is a powerful tool that can detect the presence and can quantify neuro-metabolite concentrations in *in vivo* tissues non-invasively (Puts & Edden, 2012). However, there are a few limitations that need to be considered. A major confounding variable is the use of anaesthesia. Although it is necessary for an animal to be under anaesthesia while scanning to remove movement artefacts and to minimise stress of restraint and stress of the acoustic noise generated by the scanner (Haensel et al., 2015), anaesthetics have shown to decrease neural activity (Heinke & Koelsch, 2005; Moreland, 2014). Modulation of synaptic activity (Aksenov et al., 2015), suppression of neurotransmitters (Shichino et al., 1997) and reduction of the amplitude of evoked field potentials (Masamoto et al., 2007) have been reported in relation to anaesthesia. Neurovascular coupling is affected by anaesthesia (Masamoto & Kanno, 2012), with most anaesthetics decreasing cerebral blood flow and blood oxygenation level-dependent (BOLD) signals (Aksenov et al., 2015; Masamoto et al., 2007). Such findings are in line with the reported decreased concentration of glucose and oxygen with anaesthesia (Alkire et al., 1997; Toyama et al., 2004). Other metabolites are also affected, such as GABA and lactate, where an increase was observed following delivery of isoflurane (Boretius et al., 2013). Anaesthetics are thought to enhance GABA-A receptor mediated inhibition (Garcia et al., 2010; Nishikawa & MacIver, 2001). Together, these findings suggest that anaesthetic use during MRS acquisition could potentially mask infusion related effects on neural activity and metabolism, and may thus be unsuitable to detect changes caused by acute ventral hippocampal disinhibition. Nevertheless, our previous study (Williams et al., in preparation) and other studies such as Iltis et al. (2009) and Napolitano et al. (2014) have identified changes in neuro-metabolites using acute pharmacological injections under anaesthesia.

2.4.6 Conclusion

Contrary to our expectations, our MRS did not reveal any neuro-metabolite changes in the septum, including in glutamate, GABA, glucose and myoinositol, caused by hippocampal disinhibition. Our results are not in line with our predictions, highlighting a potential gap in understanding the mechanisms of underlying changes in MRS neuro-metabolites.

In light of our SPECT study, where ventral hippocampus disinhibition caused marked metabolic activation in the lateral septum, the failure of our MRS measurements to detect any changes in neuro-metabolites in lateral septum under anaesthesia indicates that marked acute metabolic activation in the lateral septum (as detected by SPECT) is not accompanied by neuro-metabolites changes measurable by MRS (possibly reflecting homeostatic metabolic mechanisms). Alternatively, given that the SPECT measurements reflected lateral septum activation in freely moving rats, whereas the MRS measurements were taken under anaesthesia, it is possible that the anaesthesia may have interfered with the lateral septum activation. It may also be the case that different regions (e.g. septum versus PFC) show different links between metabolic activation and MRS neuro-metabolite changes.

3 Further characterisation of the rat striatal disinhibition model: In vivo electrophysiological characterisation of neural activity changes in the striatum under anaesthesia

Declaration: I conducted surgeries, monitored anaesthesia, collected electrophysiological data, removed brains, and analysed and interpreted data. Charlotte Taylor, Jacco Renstrom and Miriam Gwilt contributed to surgery and helped with monitoring anaesthesia.

3.1 Introduction

Tourette's syndrome, characterised by the presence of chronic motor or vocal tics (T. Spencer et al., 1995) has been linked to abnormalities in the cortical-striatal-thalamic-cortical (CSTC) circuit (Albin & Mink, 2006). Particularly, loss of inhibitory GABA function, so called neural disinhibition, in the striatum has been suggested to play a key role, which in turn disinhibits the thalamus and hyperexcites the motor cortex, leading to tics (Gilbert, 2006). Over the last five decades, the effects of neural disinhibition in the striatum have been investigated directly through the use of microinjections of GABA-A antagonists like picrotoxin and bicuculline in rodents (Bronfeld, Yael et al., 2013; Israelashvili & Bar-Gad, 2015; Klaus & Plenz, 2016; McKenzie et al., 1972; Patel & Slater, 1987; Pogorelov et al., 2015; Tarsy et al., 1978; Vinner et al., 2017; Vinner Harduf et al., 2021), as well as in primates (Bronfeld, Yael et al., 2013; Crossman, 1987; McCairn et al., 2009; Worbe et al., 2009). Such pharmacological disinhibition of the striatum produced tic-like movements that manifested several minutes after injection and that lasted up to one hour (Israelashvili & Bar-Gad, 2015).

In contrast to picrotoxin, bicuculline is a competitive GABA-A receptor antagonist, that has shown to have additional effects, namely blocking a current mediated by apamin-sensitive calcium-activated potassium channels underlying the low-threshold spike burst afterhyperpolarisation (AHP) (Debarbieux et al., 1998; Stocker et al., 1999; Pflieger et al., 2002). Electrophysiological recordings show that bicuculline increases firing frequency significantly and changes bursting patterns (lengthening bursts: tonic firing), which may be a consequence of the reduction in AHP (Pflieger et al., 2002). In addition to the finding of enhanced low-threshold calcium spike bursts, Debarbieux et al. (1998) found altered intrinsic oscillatory activity, which was not observed after picrotoxin. For this reason, they urged for the discontinuation of bicuculline for the study of inhibition.

Bursts are defined as spike trains with relative high firing rate (Legendy & Salcman, 1985; Pezze et al., 2014). Compared to a single spike, bursts are more likely to result in successful synaptic transmission and they may also allow for selective communication between neurons (Izhikevich et al., 2003). When the pre-synaptic cell fires a burst of action potentials with a specific resonant interspike frequency to the post-synaptic cell, the burst can either be resonant for the post-synaptic cell or not (depending on the resonant frequency of the post-synaptic cell). Therefore, the pre-synaptic cell can selectively affect cells (Izhikevich et al., 2003).

In vivo electrophysiology measures have been used to look at neural activity within the striatum following infusion of GABA-A receptor antagonists (Israelashvili & Bar-Gad, 2015; Klaus & Plenz, 2016). By identifying specific patterns in neural activity, that are related to tic generation (i.e. reliable markers such as frequency changes of a signal), it may be possible to target those patterns and suppress pathological activity (McCairn & Isoda, 2013). High frequency changes which make up spiking activity, can be detected by high-pass filtering the extracellular voltage (typically >300 Hz) (Kreiman et al., 2006; Moran & Bar-Gad, 2010) and are termed multi-unit activity (MUA). The high frequency changes in the signal are thought to decay quickly over distance (Legatt et al., 1980) and thus MUA is considered to reflect the output of local networks (Berens et al., 2008), consisting of the sum of action potentials from multiple neurons around the recording electrode (Keller et al., 2016; Moran & Bar-Gad, 2010). In contrast, low frequency changes in the signal are captured by low-pass filtering the extracellular voltage (<300 Hz) and termed local field potentials (LFPs). Due to the low frequency changes, the signal is thought to be less attenuated over longer distances (Moran & Bar-Gad, 2010; Kreiman et al., 2006; Berens et al., 2008) and thus reflect more remote processes. It has been proposed that the primary component measured by the LFP are the excitatory and inhibitory post-synaptic potentials (Mitzdorf, 1985). LFPs are thought to reflect the summation of the input to the local network (Berens et al., 2008; Moran & Bar-Gad, 2010), however other processes, such as membrane oscillations (Pedemonte et al., 1998; Goto & O'Donnell, 2001) and spike hyperpolarisation (Buzsáki, 2002) have also been identified to influence LFPs (Moran & Bar-Gad, 2010).

In freely moving rats and non-human primates, large amplitude LFP spike-wave discharges, which are LFP spikes that consist of a sharp negative deflection followed by a positive wave in the LFP signal trace or spike-wave discharges of the opposite polarity (i.e. positive spike, negative wave, depending on location of electrodes) have been reported consistently after striatal disinhibition alongside increased neural firing within the striatum (Darbin & Wichmann, 2008; Israelashvili & Bar-Gad, 2015; Jayasinghe et al., 2017; Klaus & Plenz, 2016; McCairn & Isoda, 2013; McKenzie & Viik, 1975; Muramatsu et al., 1990; Tarsy et al., 1978; Vin-

ner Harduf et al., 2021). Such LFP spike-waves have been shown to highly correlate with tics (Israelashvili & Bar-Gad, 2015; McCairn et al., 2009). It is worth noting that McCairn et al. (2013) also found LFP spikes in the basal ganglia, the cerebellum and primary motor cortex (M1) during tic-like movements and also reported LFP spikes in the basal ganglia during inter-tic intervals. The researchers propose that the large LFP spikes waves in the basal ganglia that precede tic-like movements may be a neuronal correlate of the premonitory urge to tic (McCairn & Isoda, 2013) and LFP spikes in the cerebellum and M1 were confined to the period of tic-like movements, and may thus act as a gate to trigger tic-like movements (McCairn et al., 2013).

Furthermore, a recent study using rats found that LFP spikes are not only apparent during the quiet wake state but also persist during sleep, despite the absence of observable tic-like movements (Vinner Harduf et al., 2021). In contrast, MUA was reduced during sleep. Vinner Harduf et al. (2021) provided strong evidence for a dissociation between LFP spikes and tic-like expression. They suggest that LFP spikes are necessary, but not sufficient for tic-like movements. Instead tic-like movements may require local striatal neural activity entrained to the LFP spikes (reflected by a specific temporal relationship of LFP spike-wave discharge and MUA), and because such neural firing entrained to the LFP spike-wave discharges was reduced during sleep, tic-like movements were reduced. With regards to LFP spike-waves being accompanied by MUA following striatal disinhibition, Klaus & Plenz (2016) also reported such findings. MUA are described as being phase-locked to the onset of the LFP spikes (Vinner Harduf et al., 2021) and showed an increase in rate (Klaus & Plenz, 2016).

We examined the effects of striatal disinhibition on neural activity in the vicinity of the infusion site, by combining striatal picrotoxin infusions with multi-unit and LFP recordings, using an infusion cannula attached to a multi-wire array (Gwilt et al., 2020; McGarrity et al., 2017; Pezze et al., 2014).

3.1.1 Aims

We aimed to confirm that striatal picrotoxin infusions (reliably) induced striatal LFP spike-wave discharges similar to those reported by previous studies (e.g. Israelashvili & Bar-Gad (2015), Klaus & Plenz (2016)) and aim to compare them with the spikes recorded during medial prefrontal cortex (mPFC) disinhibition (Pezze et al., 2014). Furthermore, we aimed to characterise the impact of striatal disinhibition on regional multi-unit firing. More specifically, we aimed to examine if striatal disinhibition, similar to disinhibition in mPFC (Pezze et al., 2014) and hippocampus (McGarrity et al., 2017), would specifically enhance burst firing.

3.2 Methods

3.2.1 Rats

In this study, twenty-six male adult Lister hooded rats (Charles River or Envigo, UK), approximately aged 10-11 weeks and weighing between 290 g and 360 g at the time of the experiment were used. In 5 rats, the infusion cannula arrays were misplaced, in 2 rats the correct placement of the infusion cannula array in the striatum could not be verified and in 5 rats, infusion could not be verified (see 3.2.2.2 for verification of successful infusion). In total, 14 rats contributed to the electrophysiology data. Of those, 2 rats had data from specific electrodes excluded due to the electrode placement outside of the striatum. Analysis was always conducted with a minimum of 2 electrodes per rat.

Rats were housed in groups of four in two-level high top cages (462 mm x 403 mm x 404 mm; Techniplast, UK). Food (Teklad global 18% protein diet 2019, Harlan, UK) and water was provided ad libitum. Animals were housed in an altering light/dark cycle of 12 hours per phase (lights were on between 7 am and 7 pm), at a temperature of 21 ± 1.5 °C and a humidity of $50 \pm 8\%$. All experimental work was carried out during the light phase. Prior to the start of any experimental procedures, rats were given at least 5 days to acclimate to the new environment and were handled daily to habituate them to the experimenters. All procedures were conducted in accordance with the requirements of the United Kingdom (UK) Animals (Scientific Procedures) Act 1986. All efforts were made to minimise animal suffering and to reduce the number of animals used. Procedures were carried out under the personal licence number I71997928, granted by the Home Office.

3.2.2 Multiunit and Local Field Potential recordings from dorsal striatum combined with striatal microinfusions under terminal anaesthesia

3.2.2.1 Brief Overview

Rats were anaesthetised with isoflurane and received an implantation of an electrode recording array connected to an infusion cannula into the anterior dorsal striatum. Under anaesthesia, a baseline recording was taken for 30 min followed by a 60 min post-infusion recording (saline/picrotoxin). Measurements were taken from 4 electrodes per rat and analysed in 5 min blocks. No blinding occurred. At the end of the measurements, rats were euthanised and brains extracted for confirmation of placements of the infusion-recording array. The data was examined for a significant infusion x time interaction to assess significant drug effects on the time course of the recording data. Procedure for surgery, recordings and analysis was based on Pezze et al. (2014) and McGarrity et al. (2017).

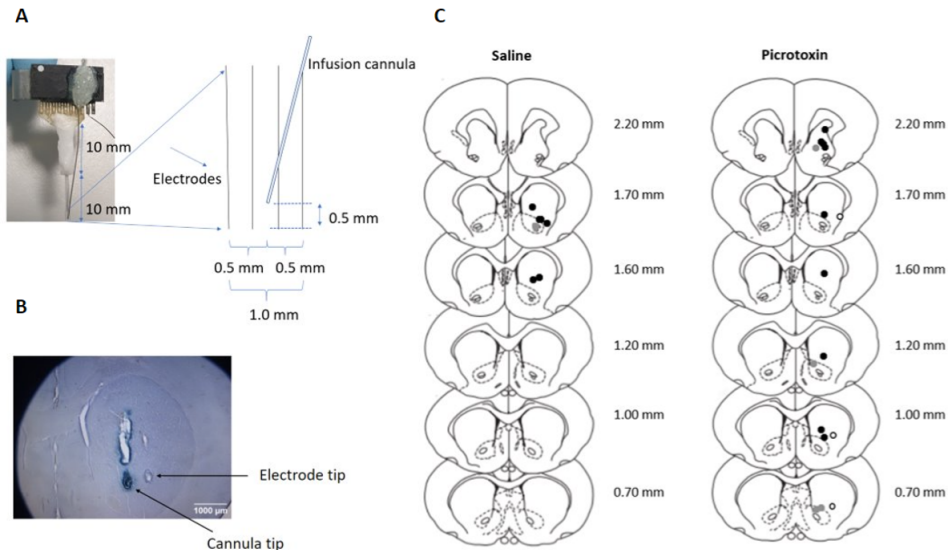
3.2.2.2 Surgery – implantation of recording array and infusion cannula into the striatum

All rats underwent stereotaxic implantation of a 1x4 or 2x4 electrode recording array with an infusion cannula attached (see further detail below and Figure 16A), into the anterior dorsal striatum. Rats were induced with 4% isoflurane in 600 ml/min medical oxygen (1%) and isoflurane levels were adapted according to breathing rate. The breathing rate provides an indication of the depth of anaesthesia and was kept around 60 breathes per minute. Every 5 min, breathing rate was recorded, and isoflurane levels were maintained at 2-3% throughout the experiment. Rats were transferred to a stereotaxic frame and EMLA cream, containing a local anaesthetic (lidocaine, prilocaine, 5%, AstraZeneca, UK), was applied onto the ear bars to minimise the risk of pain. Throughout the experiment, rectal temperature was measured using a rectal probe and maintained at $\sim 37^{\circ}\text{C}$ using a homeothermic blanket control unit (Harvard Apparatus Ltd). After scalp incision, bregma and lambda were aligned horizontally. The coordinates of the infusion cannula for the striatum were taken from bregma as follows: 1.5 mm anterior, 2.5 mm lateral from the skull surface and -4.5 mm ventral from the dura (after removing the bone with a drill over the right anterior dorsal striatum). Coordinates were based on previous studies in other rat strains (Israelashvili & Bar-Gad, 2015; Klaus & Plenz, 2016) and adapted using the in vivo MR Atlas of the Lister hooded rat brain (Prior et al., 2021). The exposed brain was kept moist with 0.9% saline.

We used a custom-made assembly of a 33-gauge stainless-steel infusion cannula and a 1x4- or 2x4 electrode microwire recording array (NB Labs, MicroProbes, Plexon). The arrays consisted of four or eight 50 μm Teflon-coated stainless-steel wires, with a stainless-steel groundwire (Figure 16). The array was connected via a head stage to the recording system. The cannula tip about touched the electrodes and was positioned about 0.5 mm above the tips of the central electrodes. The end of the cannula was connected to a 1 μl Hamilton syringe via flexible Teflon tubing (0.65 mm OD x 0.12 mm ID) (Bioanalytical Systems, Inc). The Hamilton syringe (1 μl) was filled with 0.75 μl distilled water and 0.25 μl air before it was connected to the Teflon tubing. The syringe was then pushed to 0.5 μl , before being pulled back to 0.75 μl . This method creates a small air bubble at the end of the infusion cannula tip to prevent leakage and drug diffusion before the infusion and another bubble at the end of the syringe where it meets the tubing. The latter bubble is monitored for movement (which indicates successful infusion). Infusion cannula and tubing were filled with the infusion solution (picrotoxin in saline or saline) before the infusion-recording assembly was inserted into the brain. The assembly was fixed to the arm of the stereotaxic frame, such that the electrode array was perpendicular to the midline of the brain and anterior to the infusion cannula. The infusion-recording assembly was slowly lowered so that the

infusion cannula tip would reach target coordinates in the striatum. Upon reaching the target, there was at least a 30 min stabilisation period before recording started to stabilise the anaesthetic level and breathing rate.

Figure 16: Electrode and infusion cannula placements



Note: **A:** Photograph showing the assembly of one of our infusion cannulae and 2x4 microwire-electrode array (NB Labs) used to measure the effects of drug microinfusions on striatal multiunit and LFP activity. The array was arranged perpendicular to the midline of the brain, with the infusion cannula located in the centre of the array, about 0.5 mm above the electrode tips. Sketch shows dimensions of multiwire array. **B:** Coronal section of the striatum shows electrolytic lesions of the cannula (left) and most lateral electrode (right) placement. **C:** Approximate locations of markings in the striatum for the tips of the most medial (grey dot) and lateral (white dot with black outline) electrodes as well as the cannulae (black dot) of rats that are included in the analysis. Placements are separated for the different experimental groups that received infusions of saline or picrotoxin. Locations are shown on coronal plates adapted from the atlas by Paxinos & Watson (1998), with numbers indicating distance from bregma in millimeters, as shown in the atlas.

3.2.2.3 Multiunit and Local Field Potential recordings

To record extracellular measures of neural activity, the electrode array was connected to a multichannel preamplifier (Plexon, Inc.) via a unity-gain multichannel headstage. The preamplifier amplified the analogue signal from the electrodes by a factor of 1000 and band-pass filtered the signal into multiunit spikes (250 Hz to 8 kHz) and LFP signals (0.7 Hz to 170 Hz). All recordings were made against ground, with the ground wire of the array clamped to the ear bars of the stereotaxic frame using

a crocodile clip and a lead linking the stereotaxic frame to the ground jack on the amplifier. The analogue signals were then processed by a multichannel acquisition processor system (Plexon, Inc.). This allowed for an additional computer-controllable amplification of up to 32,000, further filtering of multiunit data (500 Hz - 5 kHz), digitisation of spikes at 40 kHz (providing 25 μ s precision on each channel at 12-bit resolution) and of LFP data at 1 kHz.

Multiunit data were displayed on an analogue-digital oscilloscope and monitored using a loudspeaker. Multiunit data and LFP data could then be viewed later online using Real-Time Acquisition System Programs for Unit Timing in Neuroscience (RASPUTIN) software (Plexon, Inc.). RASPUTIN was also used to record neural activity data for the baseline and post-infusion period. LFP data were recorded continuously, and multiunit spikes were recorded when it exceeded a predefined amplitude threshold of -240 μ V.

3.2.2.4 Drugs and microinfusion procedure

Picrotoxin (Sigma-Aldrich) was dissolved in saline at 300 ng/0.5 μ l, aliquoted and kept frozen (not longer than 1 year) until use for infusion where they were then thawed. Previously, Klaus & Plenz (2016) used 0.8-1.5 μ l of 1 mM=603 ng/ μ l picrotoxin solution for striatal infusions and reported marked LFP spike-wave discharges and tic-like movements. Moreover, Morgenstern et al. (1984) reported occasional convulsions and marked locomotor hyperactivity with bilateral infusions of picrotoxin at 500 ng/1 μ l/side into the ventral striatum, but only locomotor hyperactivity at 250 ng/1 μ l/side. Finally, in our own studies in the medial prefrontal cortex, we found pronounced behavioural effects without any evidence for seizures in awake rats, as well as marked spike-wave LFP discharges and increased multi-unit burst firing under anaesthesia with bilateral infusions of 0.5 μ l of 600 ng/ μ l picrotoxin (i.e., 300 ng/0.5 μ l/per side) (Pezze et al., 2014). Overall, these findings suggest that unilateral infusion of 300 ng picrotoxin/0.5 μ l into the right striatum will have robust neural and behavioural effects, while not causing seizures or other adverse effects. (Our behavioural study in awake rats in Chapter 4 also confirmed that a dose of 300 ng picrotoxin/0.5 μ l reliably causes tic-like movements.)

Baseline neural activity was recorded for 30 min. This was followed by moving the piston of the 1 μ l Hamilton syringe at a slow speed (about 0.5 μ l/min) to remove the 0.25 μ l air plug from the infusion cannula tip and to inject 0.5 μ l of picrotoxin/saline into the striatum. Movement of the air bubble that was trapped between infusion tubing and syringe, was monitored to verify successful infusion. Start and end times of the infusion were noted. Data recorded during the infusion period was removed and start time for post-infusion was identified for the data analysis. After completion of the infusion, recordings continued for a minimum of 60min.

3.2.2.5 Histology - verification of electrode and infusion cannula placements in the anterior dorsal striatum

At the end of each experiment, rats were overdosed by increasing the isoflurane levels. With a lesion marker (GRASS Instruments, Model D.C. LM5A) a constant current (1 mA, 10s) was passed through the stainless-steel electrodes. Usually, the most lateral and medial electrode as well as the cannula, were chosen to mark their location and to deposit ferric ions at the tip of the positive electrode and cannula. The infusion-recording assembly was then removed, and rats were overdosed by anaesthesia. Brains were extracted and stored in a 4% paraformaldehyde solution with 4% potassium ferrocyanide for at least 2 days. Brains were sliced into 80 μm thick coronal sections using a vibratome (Leica VT1000 S) and placed onto microscope slides for verification and documentation of the electrode placements using a Leica light microscope (Leica DM1000, Leica DFC295, 1.25x/0.04 with a Leica HCX PL Fluotar 1.25x/0.04 microscope objective) (Figure 16B). Electrode placements were mapped onto coronal sections of a rat brain atlas (Paxinos & Watson, 1998) (Figure 16C). Some slides were stained with cresyl violet and coverslipped to take photos, captured with a Zeiss Axioplan light microscope using a QImaging MicroPublishers 5.0 RTV and the Micro Manager software. Images were taken using a 1.25x/0.035NA objective. The images were then white balanced and a scale bar applied using the FIJI software.

3.2.2.6 Data analysis

Analysis was carried out using NeuroExplorer version 4 (Nex Technologies, Plexon) software to calculate firing rate and burst parameters from the multiunit data and power spectral densities from the LFP data. Parameters were measured from up to 4 electrodes per rat and were normalised within each channel by dividing the values recorded in each 5 min time block by the average of the baseline values recorded in blocks 1 to 6 (30 min). Large activity variations between channels of a single rat were common, likely due to different electrode placements, with some channels showing little to no spiking (potentially due to placement into white matter tracts) and others showing more consistent activity. Values were averaged across all channels per individual rat, to produce one set of 18 blocks (6 pre- and 12 post-infusion blocks) per rat, which were then used to analyse drug infusion effects. Using ANOVA with groups as the between-subjects variable (saline versus picrotoxin) and time points (5 min time blocks) as the repeated measures factor, the data was examined for significant differences between the groups. We focused on the interaction infusion x time to assess significant drug effects on the time course of the recording data. Significance threshold was set at $p < 0.05$. Based on previous studies demonstrating the impact of hippocampal and prefrontal picrotoxin infusions on neural activity in the vicinity of the infusion site (McGarrity et al., 2017; Pezze et al., 2014), we expected that reliable

conclusions could be drawn with $n=8$ rats per group and $n=8$ was our target sample size at the outset of the study. The experiment was run in multiple batches with the aim to complete successful recordings in the target sample size. Due to exclusion of rats based on the histological verification of cannula and electrode placements, our saline group included only $n=6$ rats. For each batch, rats were randomly allocated to a drug group. The drug allocation was counterbalanced, so that each batch had equal numbers of rats infused with saline or picrotoxin.

3.2.2.7 Multiunit data and burst analysis

To detect striatal bursts, we used the Poisson surprise method, similar to previous studies (Homayoun et al., 2005; Pezze et al., 2014; Stevenson et al., 2007). Bursts are defined as epochs of relative high firing rate (Legendy & Salcman, 1985; Pezze et al., 2014). Legendy & Salcman (1985) assigned the bursts to a quantitative measure, called Poisson surprise (S) to evaluate how improbable it is that the burst happened by chance. The method compares the surprising (i.e. improbable) nature of a burst of neuronal spikes to the average spike rate during the rest of the analysis window (5 min). The surprise value (S) of a burst is defined as the negative natural logarithm of the probability that a relatively high burst firing rate occurs due to chance. Only bursts with a surprise value of greater than 3 were included in our analysis (Pezze et al., 2014; Stevenson et al., 2007). This value means that there is an approximate probability of 0.05 for similar spike patterns to occur by chance as part of a random spike train:

$$\begin{aligned}
 S &= -\ln(x) \\
 3 &= -\ln(x) \\
 x &= \frac{1}{e^3} = 0.05
 \end{aligned}$$

The following burst parameters were calculated for each 5 min block: mean spike frequency per block, number of bursts per block, bursts per minute, percentage spikes in bursts, mean burst duration, mean spikes in burst, mean spike frequency in burst per block, mean peak spike frequency in burst, mean interburst interval per block and mean burst surprise. For the analysis of mean burst duration, mean interburst interval per block and mean spike frequency in burst per block, any channel was excluded if the number of bursts was 0 in at least one 5 min block. This led to the exclusion of 1 rat for the analysis of mean interburst interval per block.

3.2.2.8 LFP data analysis with AUC

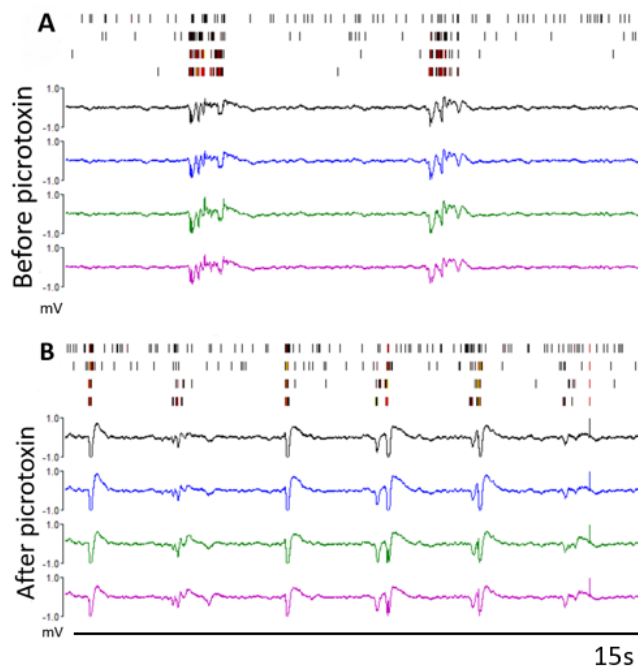
Power spectral density analysis was used in Neuroexplorer version 4, which applies fast Fourier transform analysis to the LFP signal. We calculated the area under the curve (AUC) of the power spectral density function (PSD) from 0.7-40 Hz as a measure of overall LFP power for every 5 min block of the pre-infusion and post-infusion recording periods (methods adopted from Pezze et al. (2014)).

3.3 Results

3.3.1 Qualitative description of LFP and multi-unit activity patterns induced by striatal disinhibition

Following picrotoxin infusion there were changes in the multi-unit firing pattern and local field potentials (LFP) that were evident based on visual inspection (Figure 17). There were large LFP spike-wave discharges, consisting of a single negative spike followed by a positive wave, and intensified multi-unit bursts during the negative spike in five out of eight rats. Our experiment did not reveal the LFP characteristics of seizures that may be induced by local GABA-A antagonists (a fast sequence of sharp negative deflections (10-15 Hz) in LFP patterns (Neckelmann et al., 1998; Steriade & Contreras, 1998)).

Figure 17: Enhanced LFP spike-wave discharges and multiunit burst-firing



Note: LFP spike-wave discharges and intensified multiunit burst-firing pattern within the striatum after picrotoxin infusion. Multiunit recording traces (top, electrodes 1-4) and LFP traces (bottom, electrodes 1-4) from one exemplary experiment involving infusion of 300 ng picrotoxin. Baseline recording ~ 10 -15 min before infusion (A). Post-infusion recordings ~ 10 -15 min after picrotoxin infusion (B). Following infusion there are observable changes in the multi-unit firing pattern and LFP. There are large LFP spike-wave discharges, consisting of a single negative spike followed by a positive wave, and sharp multi-unit bursts during the negative spike.

3.3.2 Mean baseline values of electrophysiological parameters

The mean baseline values for all analyses (mean spike frequency per block, number of burst per block, percentage spikes in burst, mean burst duration, mean spikes in burst, mean spike frequency in burst per block, mean peak spike frequency in burst, mean interburst interval per block, mean burst surprise and mean baseline overall LFP power (measured as AUC of PSD) showed no statistically significant difference between infusion groups (all $t < 0.576$, $p > 0.277$).

Table 2 includes all baseline values for saline and picrotoxin from our present study in the striatum and compares them to our previous studies in the medial prefrontal cortex (mPFC) and ventral hippocampus (McGarrity et al., 2017; Pezze et al., 2014). **Mean spike frequency per block** in the striatum is about a quarter to half as high as in the mPFC and ventral hippocampus (prospective saline groups, 10.7 vs 17.5 vs 42.1; prospective picrotoxin groups, 9.8 vs 39.1 vs 35.4). **Bursts per minute** was about 10 to 15 times less in the striatum than in the hippocampus (prospective saline groups, 20.24 vs 265.5; prospective picrotoxin groups, 16.13 vs 251.11). **Mean spike frequency in burst per block** was about two to four times smaller in the striatum compared to the mPFC and hippocampus (prospective saline groups, 106.68 vs 223.3 vs 381.3; prospective picrotoxin groups, 102.12 vs 199.9 vs 401.8). **Mean interburst interval per block** was about double in the striatum compared to the mPFC and hippocampus (prospective saline groups, 12.47 vs 6.8 vs 6.6; prospective picrotoxin groups, 10.41 vs 5.9 vs 4.4). Overall, this suggests that burst firing is less intense in the striatum compared to the mPFC and ventral hippocampus.

Table 2: Baseline values of multi-unit and LFP parameters recorded from the dorsal striatum in the present study, alongside values recorded previously from medial prefrontal cortex (Pezze et al., 2014) and ventral hippocampus (McGarrity et al., 2017)

Parameter	Prospective infusion group	Striatum, present study		Medial prefrontal cortex, Pezze et al. (2014)		Ventral hippocampus, McGarrity et al. (2017)	
		Mean	SEM	Mean	SD	Mean	SEM
Mean spike frequency per block (1/s)	Saline	10.74	4.40	17.5	5.9	42.1	11.8
	Picrotoxin (150 ng)			15.6	4.3		
	Picrotoxin (300 ng)	9.76	2.29	39.1	14.3	35.4	3.4
Number of bursts per block	Saline	101.22	58.90	132.4	57.7		
	Picrotoxin (150 ng)			117.4	38.6		
	Picrotoxin (300 ng)	80.64	22.06	236.6	67.8		
Bursts per minute	Saline	20.24	11.78			265.5	75.5
	Picrotoxin (150 ng)						
	Picrotoxin (300 ng)	16.13	4.41			251.11	27.7
Percentage of spikes fired within bursts	Saline	38.38	7.11	69.3	4.1	28.8	3.9
	Picrotoxin (150 ng)			72.3	4.6		
	Picrotoxin (300 ng)	43.18	4.90	52.8	7.8	25.6	1.6
Mean burst duration (s)	Saline	0.30	0.09	0.23	0.03	0.01	0.0005
	Picrotoxin (150 ng)			0.23	0.03		
	Picrotoxin (300 ng)	0.30	0.04	0.19	0.04	0.0092	0.0002
Mean spikes in burst	Saline	16.40	2.20				
	Picrotoxin (150 ng)						
	Picrotoxin (300 ng)	16.85	1.82				
Mean spike frequency in burst per block (1/s)	Saline	106.68	32.05	223.3	33.3	381.3	6.1
	Picrotoxin (150 ng)			218.5	22.0		
	Picrotoxin (300 ng)	102.12	22.39	199.9	34.6	401.8	4.9
Mean peak spike frequency in burst (1/s)	Saline	484.60	49.60				
	Picrotoxin (150 ng)						
	Picrotoxin (300 ng)	501.59	46.02				
Mean interburst interval per block (s)	Saline	12.47	4.41	6.8	2.3	6.6	1.7
	Picrotoxin (150 ng)			5.8	0.97		
	Picrotoxin (300 ng)	10.41	2.59	5.9	2.1	4.4	0.08
Mean burst surprise	Saline	13.61	2.32				
	Picrotoxin (150 ng)						
	Picrotoxin (300 ng)	12.27	1.46				
Mean LFP AUC of PSD (μV^2)	Saline	0.020	0.005	0.015	0.004	0.0411	0.0035
	Picrotoxin (150 ng)			0.013	0.002		
	Picrotoxin (300 ng)	0.020	0.004	0.024	0.006	0.0303	0.0025

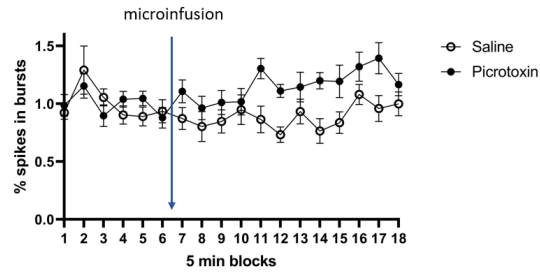
Note: Mean baseline values and standard error of means (SEM) of electrophysiological parameters compared between the prospective saline and picrotoxin infusion groups across studies.

3.3.3 Striatal picrotoxin infusion enhances burst firing in the vicinity of the infusion site

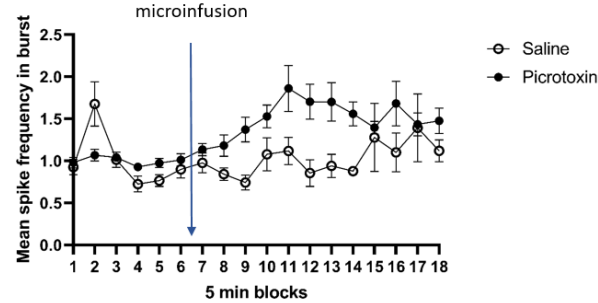
Normalised data for percentage of spikes in bursts (Figure 18a), mean spike frequency in burst per 5 min block (Figure 18b) and mean peak spike frequency in burst (Figure 18c) were significantly increased by picrotoxin in the striatum compared to saline. This was supported by ANOVAs of these parameters showing significant interactions drug x 5 min block (all $F < 2.897$, all $p > 0.044$). Whereas, the normalised mean interburst interval per block was slightly decreased (and stayed around 1) by picrotoxin and was strongly increased with saline infusion (around 3) (Figure 18d). An ANOVA showed a significant interaction of drug x 5 min block ($F_{(17,204)} = 1.840$, $p = 0.025$). Normalised data for number of burst per block also appeared to increase following infusion in the picrotoxin group, whereas the parameter was similar before and after infusion in the saline group (Figure 18e). However, the ANOVA only revealed a main effect of group across pre- and post-infusion 5 min blocks ($F_{(1,12)} = 5.193$, $p = 0.042$), but no interaction ($F_{(17,204)} = 1.422$, $p = 0.129$) or main effect involving 5 min blocks ($F_{(17,204)} = 1.459$, $p = 0.113$). Normalised data for mean burst duration (Figure 19a), LFPs (Figure 19b), mean spikes in burst (Figure 19c), mean spike frequency per block (Figure 19d) and mean burst surprise (Figure 19e) showed no picrotoxin related changes (all $F < 1.430$ and $p > 0.125$), although for mean spikes in burst and mean spike frequency per block there was an overall effect of 5 min block ($F_{(17,204)} = 1.801$, $p < 0.030$) and ($F_{(17,204)} = 1.696$, $p < 0.046$) respectively, and a trend for such an effect for mean burst surprise ($F_{(17,204)} = 1.567$, $p < 0.076$).

Figure 18: Enhanced burst firing

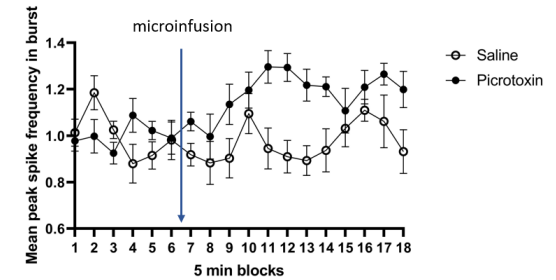
(a) Percentage spikes in burst



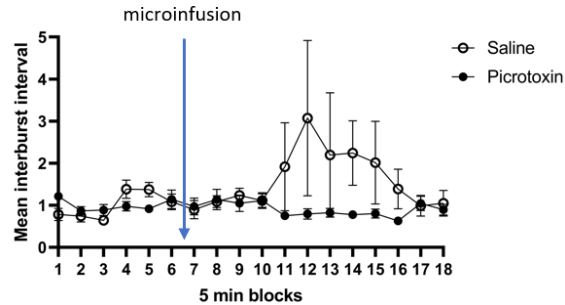
(b) Mean spike frequency in burst per block



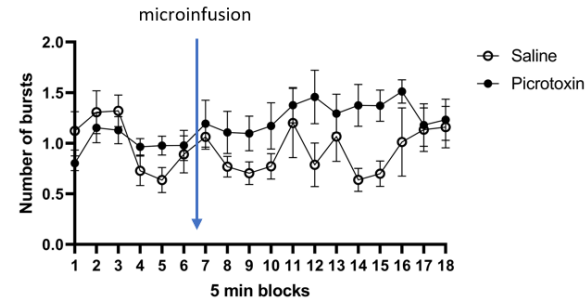
(c) Mean peak spike frequency in burst



(d) Mean interburst interval per block



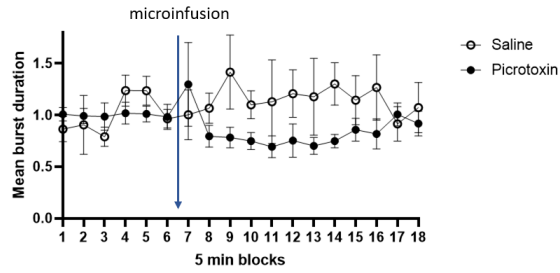
(e) Number of bursts



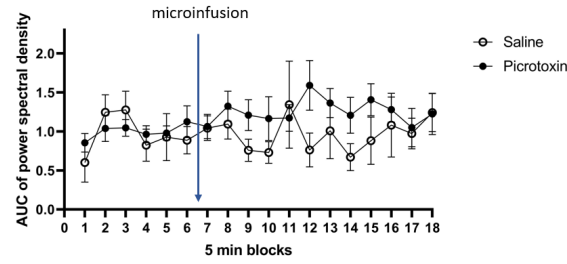
Note: Time courses of percentage spikes in bursts (18a), mean spike frequency in burst per block (18b), mean peak spike frequency in burst (18c), mean interburst interval per block (18d) and number of bursts (18e). Values are normalised to the average of the 6 baseline 5 min blocks and are presented in mean \pm SEM. The vertical blue line after 6 indicates time of infusion.

Figure 19: No picrotoxin related changes

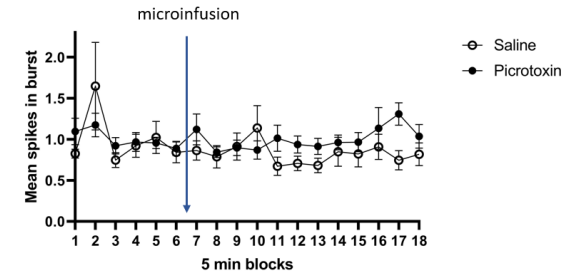
(a) Mean burst duration



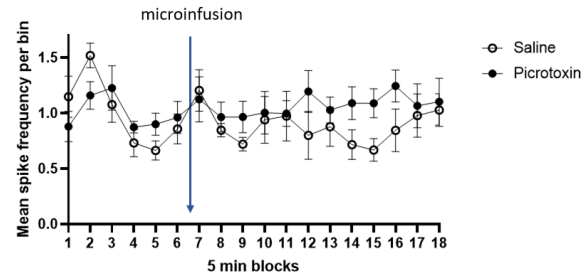
(b) LFP (measured as AUC of PSD)



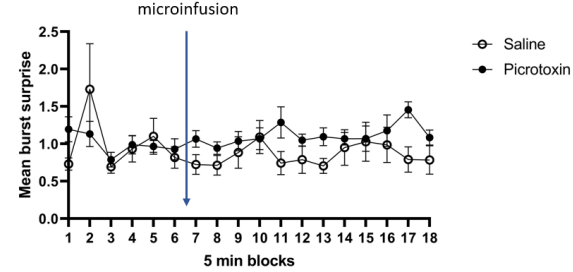
(c) Mean spikes in burst



(d) Mean spike frequency per block



(e) Mean burst surprise



Note: Time courses of mean burst duration (19a), LFP, measured as Area under the Curve of power spectral density (19b), mean spikes in burst (19c), mean spike frequency per block (19d) and mean burst surprise (19e). Values are normalised to the average of the 6 baseline 5 min blocks and are presented in mean \pm SEM. The vertical blue line after 6 indicates time of infusion.

3.4 Discussion

Visual inspection revealed striking changes in the local field potential (LFP) spike-wave discharges and multiunit firing pattern particularly during LFP spikes following picrotoxin infusion into the striatum, which were not visible following saline infusion. We found marked spike-wave discharges and enhanced burst firing under anaesthesia, following picrotoxin infusion.

3.4.1 LFP changes

In line with previous studies in freely moving rats (e.g. Israelashvili & Bar-Gad (2015); Klaus & Plenz (2016); Vinner Harduf et al. (2021)), striatal disinhibition caused large LFP spike-wave discharges, consisting of a single negative spike followed by a positive wave. Although picrotoxin infusion numerically increased overall LFP power (by up to roughly a factor of 2.5 compared to saline), as reflected by the AUC of the PSD, there was no statistical support for change in AUC measure. This may partly reflect variability of the AUC measure and limited statistical power, although we previously found a significant and much larger increase of LFP AUC following local disinhibition in the mPFC (Pezze et al., 2014), which caused similar spike-wave discharges to those observed in striatum. When comparing our data with disinhibition in the mPFC (Pezze et al., 2014), we find that the baseline LFP activity in the striatum is higher than in the mPFC and there are less periods with spike-wave discharges in our data, which may explain the less pronounced AUC difference. It is also worth noting that in our current study, negative spikes of the LFP spikes were clipped following picrotoxin infusion into the striatum, indicating that the spike amplitude was outside of the recording range of our system, which thus likely led to a slight underestimation of the effect.

3.4.2 Multi-unit changes

We observed sharp multi-unit bursts during the negative LFP spikes. Our study is the first to characterise changes in striatal multi-unit measurements caused by striatal disinhibition, showing that disinhibition specifically enhances burst firing, reflected by significant increases in mean spike frequency in burst per block, mean peak spike frequency in burst and percentage spikes and by increased frequency in which bursts occur, reflected by significant decreases of mean interburst interval per block after picrotoxin infusion into the striatum. This is a new finding in the striatum and is consistent with disinhibition induced enhancement of burst firing that we previously reported in the prefrontal cortex and hippocampus (Pezze et al., 2014; McGarrity et al., 2017), suggesting that in all these regions, GABA-A receptor mediated inhibition is particularly important to control neural burst firing. Our baseline values suggest that burst firing is less pronounced in the striatum compared to mPFC and hippocampus, po-

tentially reflecting regional differences. Furthermore, bursts were defined differently for the hippocampus (based on inter-spike interval instead of Poisson Surprise method). Hippocampal bursts were defined as having at least 2 spikes with an interspike interval shorter than 6 ms (Royer et al., 2012; McGarrity et al., 2017). Alternatively, such difference may indicate unreliable measurement values that may be due to our sample size of $n = 6-8$ per group and the large inter-rat and intra-rat (i.e. channels) variability.

Enhanced burst firing in the striatum following striatal disinhibition, which causes tic-like movements in rats (e.g. Bronfeld, Yael et al. (2013); Klaus & Plenz (2016), Chapter 4), fits well with literature showing enhanced burst firing of striatal projection (medium spiny) neurons in rats with lesioned (Tseng et al., 2001; Nisenbaum et al., 1986) or blocked dopaminergic input to the striatum. Such a blockade came from, for example, haloperidol (Frank & Schmidt, 2003), a drug that has been used to model aspects of Parkinson’s disease (Waku et al., 2021). Interestingly, when Frank & Schmidt (2003) injected rats with haloperidol, it caused catalepsy, and tetanus of the forelimb muscle alongside enhanced striatal burst firing. The tetanus of the forelimb muscle correlated highly (70%) with burst activity in projection (medium spiny) neurons of the lateral striatum. Taken together, it is plausible that enhanced burst firing in the striatum is partly responsible for both hypokinetic syndromes (such as Parkinson’s disease) and hyperkinetic syndromes (such as Tourette Syndrome). It may be the case, that extensive burst firing causes akinesia and catalepsy (i.e. reduced movement) and more specific increased firing, may drive specific muscle groups selectively and cause distinct tic-like movements.

3.4.3 Anaesthetised versus freely moving recordings

A major confounding variable is the use of anaesthesia. Anaesthetics have shown to decrease neural activity (Heinke & Koelsch, 2005; Moreland, 2014), modulate synaptic activity (Aksenov et al., 2015), suppress neurotransmitters (Shichino et al., 1997) and reduce the amplitude of evoked field potentials (Masamoto et al., 2007). Additionally, anaesthetics are thought to enhance GABA-A receptor mediated inhibition (Garcia et al., 2010; Nishikawa & MacIver, 2001). Together, these findings suggest that anaesthetic use during electrophysiological measurements could potentially mask infusion related effects on neural activity.

Nevertheless, our findings, as well as our previous studies (Pezze et al., 2014; McGarrity et al., 2017; Gwilt et al., 2020), identify changes in LFPs and multi-unit activity using acute pharmacological infusions under anaesthesia. Furthermore, the use of terminal anaesthesia also has advantages and allows examination of neural mechanisms independent from behavioural modulation, meaning that we can determine if a certain neural

change is caused directly by a certain drug (e.g. picrotoxin, GABA-A receptor antagonist). In spite of marked LFP spike-wave discharges, that have previously been observed during tic-like movements in freely moving rats in previous striatal disinhibition studies, we did not see tic-like movements under anaesthesia. This finding, supports Vinner Harduf et al. (2021) who reported LFP spikes during sleep, following continuous bicuculline infusion, despite the absence of observable tic-like movements. We may conclude that the LFPs are therefore not just an effect of tic-like movements but may be a direct phenomenon of striatal disinhibition.

3.4.4 Conclusion

Our study found large local field potential (LFP) spike-wave discharges, in line with previous studies in freely moving rats, and complemented the previous findings by showing that these occur without the occurrence of tic-like movements under anaesthesia and alongside enhanced burst firing, indicating that striatal spike-wave discharges do not necessarily cause tic-like movements.

4 Further characterisation of the rat striatal disinhibition model: tic-like movements

Declaration: I conducted surgeries, monitored anaesthesia, collected data, perfused rats, and analysed and interpreted data. Charlotte Taylor contributed to surgery, data collection and perfusion. Luke O'Hara helped with monitoring anaesthesia during surgery.

4.1 Introduction

Over the last five decades, the effects of neural disinhibition in the striatum have been investigated directly, through the use of microinfusions of a GABA-A antagonist, like picrotoxin and bicuculline in rodents (McKenzie et al., 1972; Tarsy et al., 1978; Patel & Slater, 1987; Bronfeld, Yael et al., 2013; Israelashvili & Bar-Gad, 2015; Pogorelov et al., 2015; Klaus & Plenz, 2016; Vinner et al., 2017; Vinner Harduf et al., 2021), as well as in primates (Crossman, 1987; McCairn et al., 2009; Worbe et al., 2009; Bronfeld, Israelashvili & Bar-Gad, 2013). Earlier research classified the movements caused by striatal disinhibition as 'hyperkinetic syndrome' (McKenzie et al., 1972), or described them with more specific terms like 'choreiform movements' (McKenzie et al., 1972), 'myoclonus' (Tarsy et al., 1978; Patel & Slater, 1987) and/or 'dyskinesia' (Crossman, 1987; Muramatsu et al., 1990). Although some early animal studies discussed involuntary movements caused by picrotoxin in the context of Tourette Syndrome (and Huntington's chorea) (McKenzie et al., 1972), the striatal disinhibition model has only been highlighted as a model of Tourette Syndrome over the last few years (Yael et al., 2016). The first to describe such movements as tics were Bronfeld, Yael et al. (2013). An overview of previous literature that elicited tic-like movements in limbs, by manipulating the striatum in rodents, is presented in Table 3. In this chapter, movements are described as tic-like (based on previous literature), however the relationship of these movements to tics in patients with Tourette Syndrome, is critically considered in the Discussion (Section 4.4.2).

Tic-like movements are expressed on the contralateral side of the disinhibited area and are mostly confined to a single body part, depending on the somatotopic location of the striatal infusion (Bronfeld, Israelashvili & Bar-Gad, 2013). For example, bicuculline infusions into the anterior striatum cause tic-like forelimb movements, whereas infusions into the posterior striatum cause tic-like hindlimb movements in rats (Bronfeld, Yael et al., 2013). Yael et al. (2016) and Israelashvili et al. (2015) also looked at bicuculline infusions into the nucleus accumbens and found hyperactivity as well as tic-like movements in some of rats, potentially due to spread of the drug along the cannula (Yael et al., 2016). Tic-like movements

begin to manifest several minutes after microinfusions, typically occur at an interval of 1-4 s, and subside within about 1 h of the acute striatal infusion (Bronfeld, Yael et al., 2013; Israelashvili & Bar-Gad, 2015).

Importantly, even when animals express tic-like movements, they appear to continue with their normal ongoing behaviours, such as exploration and grooming (Bronfeld, Yael et al., 2013). These findings are important, as tics typically do not interfere with voluntary movements (Sanger et al., 2010) (although in some people, tics may be disabling and interfering with daily living (Ohm, 2006)). Furthermore, it indicates that striatal disinhibition in animals is not grossly debilitating.

4.1.1 Aims

We aimed to confirm that striatal disinhibition, by local microinfusion of the GABA-A receptor antagonist picrotoxin (300 ng or 200 ng of picrotoxin in 0.5 µl saline), causes tic-like movements in Lister hooded rats. We investigated reliability of such movements following picrotoxin infusion and characterised the time course and some key features of tic-like movements.

Table 3: Rodent studies reporting tic-like limb movements, caused by striatal disinhibition, caused by intra-striatal drug microinfusions

Study	Rat/Mouse strain	Region of striatum	Coordinates	Drug and dose	Term used to refer to movement
McKenzie, Gordon & Viik (1972)	Long Evans rats	Anterior neostriatum	Not provided	Picrotoxin: 5-10 µg in saline with 1 µg/ml of ascorbic acid <i>Volume:</i> 10 µl	Choreiform activity
Tarsy et al. (1978)	Wistar rats	Anterior caudate nucleus	AP: 8.5, ML: ± 2.5	Picrotoxin (Unilateral): 0.1-2 µg infused in 1-3 µl 0.9% saline Picrotoxin (Bilateral): 1 µg	Repetitive myoclonus, rhythmic jerking movement, retrocollis
		Posterior caudate nucleus	AP: 6.7, ML: ± 3.8	DL-c-allylglycine: 100-150 µg in 2-3 µl 0.9% saline Bicuculline: 1-3 µg in saline (pH adjusted to 6.5)	
		Centre of caudate nucleus	AP: 3.7, ML: ± 2.5	Benzy-penicillin: 1 unit in 2 µl <i>Volume not specified</i>	
Patel & Slater (1987)	Sprague Dawley rats	Striatum	AP: 8.5, H: - 1.0, L: 1.0	Picrotoxin: 0.5-2 µg <i>Volume and vehicle solution not specified</i>	Myoclonus, rhythmic and sustained jerking, dyskinesia
Muramatsu et al. (1990)	Wistar albino rats	Striatum	AP: 1.4, ML: 3.5, DV: 5 (from cerebral cortex)	Picrotoxin: <i>Concentration:</i> 1 mg in 1 ml of saline <i>Amount:</i> 1 µg <i>Volume:</i> 1 µl	Dyskinesia, rapid flexion and extension of limb
Bronfeld et al. (2013)	Sprague Dawley rats	Anterior striatum	AP: 1.5, ML: ± 2.5, DV: 5	Bicuculline methiodide: 1 µg/µl in physiological saline or artificial CSF (aCSF contained [in mM]: 145 NaCl, 15 Hepes, 2.5 KCl, 2MgCl ₂ , 1.2 CaCl ₂ , PH 7.4 with NaOH) <i>Volume:</i> 0.5-1 µl	Motor tics
		Posterior Striatum	AP: -0.4 to 0.5, ML: ± 3.5, DV: 5		
Israelashvili & Bar-Gad (2015)	Long Evans rats	Anterior striatum	AP: 1.4, ML: 2.5, DV: 4.6	Bicuculline methiodide: 1 µg/µl in artificial CSF <i>Volume:</i> 0.35 -0.7 µl	Focal tics, tics
Pogorelov et al. (2015)	C57Bl/6 mice	Dorsal lateral striatum	AP: 0.5, ML: -2.2, DV: 3.2	Picrotoxin: 0.1 and 0.2 µg infused in 0.2µl saline <i>Volume:</i> 0.2 µl	Tic-like movements, tics
		Central striatum	AP: 0.4, ML: -1.7, DV: 3.5		
Klaus & Plenz (2016)	Sprague-Dawley rats	Dorsal striatum	AP: 0.9-1.5, ML: 2.2-2.6, DV: 4.2-5.5	Picrotoxin: 1 mM (602.583 ng/µl) in 0.8-1.5 µl sterile drug solution IEM-1460: 0.5 mM (227.165 ng/µl) and 5 mM (2271.65 ng/µl) in 0.8-1.5 µl sterile drug solution <i>Volume not specified</i>	Stereotypical, Involuntary movements
Vinner et al. (2017)	Long Evans rats	Dorsolateral striatum	AP: 0.25, ML: 2.75, DV: 4	Bicuculline methiodide: 1 or 2 µg/µl in artificial CSF (aCSF contained (in mM): 145 NaCl, 15 HEPES, 2.5 KCl, 2MgCl ₂ , 1.2 CaCl ₂ , PH 7.4 with NaOH) <i>Volume:</i> 200 µl, release rate 1 µl/hr, 7 days or 200 µl, release rate 0.5 µl/hr, 14 days	Motor tics
Yael et al. (2019)	Long Evans rats	Nucleus accumbens core	AP: 1.5, ML: 2.2, DV: 7.0	Bicuculline methiodide: 1 µg/µl in artificial CSF (concentrations (in mM): 145 NaCl, 15 Hepes, 2.5 KCl, 2MgCl ₂ , 1.2 CaCl ₂ , PH 7.4 with NaOH) at a concentration of 1 µg/µl <i>Volume:</i> 0.5µl	Motor tics
Israelashvili, Yael et al. (2020)	Long Evans rats	Anterior striatum	AP: 1.4; ML: 2.5; DV: 4.6 AP:1; ML: 2.5 DV: 5	Bicuculline methiodide: 1 µg/µl in artificial CSF <i>Median volume</i> (anterior): 0.35 µl <i>Median volume</i> (ventral): 0.5 µl	Motor tics
		Nucleus accumbens core	AP: 1.5; ML: 2.2; DV: 7		
Vinner et al. (2021)	Long Evans rats	Dorsolateral striatum	AP: 1.0, ML: 2.5, DV: 5	Bicuculline methiodide: 1 or 2 µg/µl in artificial CSF (aCSF contained (in mM): 145 NaCl, 15 Hepes, 2.5 KCl, 2MgCl ₂ , 1.2 CaCl ₂ , pH 7.4 with NaOH)	Motor tics

Note: Papers identified using google scholar search terms “striatum” “tics” “rat” “mice”. Last performed search in October 2022. **Mechanisms of the drug:** Picrotoxin, Bicuculline and Penicillin: GABA-A receptor antagonist, DL-c-allylglycine: Glutamic acid decarboxylase inhibitor, IEM-1460: antagonist of GluR2-lacking AMPA receptors.

4.2 Methods

4.2.1 Rats

We used eight male adult Lister hooded rats (Charles Rivers, UK), weighing between 290 g and 340 g and aged approximately 10-11 weeks, at the time of surgery. The sample size of $n=8$ was chosen, because we expected that this would allow us to confirm the substantial increase in tic-like movements, which we expected to be caused by striatal disinhibition, as well as to estimate the robustness of these increases (i.e., which proportion of rats showed tic-like movements).

Rats were housed in groups of four in two-level high top cages (462 mm x 403 mm x 404 mm; Techniplast, UK). To minimize the risk of damaging cannula implants, food hoppers were removed and replaced with pots standing on the floor after surgery. Food (Teklad global 18% protein diet 2019, Harlan, UK) and water was provided ad libitum. Rats were housed in an alternating light/dark cycle of 12 h per phase (lights were on between 7 am and 7 pm), at a temperature of $21 \pm 1.5^\circ\text{C}$ and a humidity of $50 \pm 8\%$. All experimental work was carried out during the light phase. Prior to surgery, rats were given at least 7 days to acclimate to the new environment and were handled daily to habituate them to the experimenters. All procedures were conducted in accordance with the requirements of the United Kingdom (UK) Animals (Scientific Procedures) Act 1986. All efforts were made to minimise animal suffering and to reduce the number of animals used. Procedures were carried out under the personal licence number I71997928, granted by the Home Office.

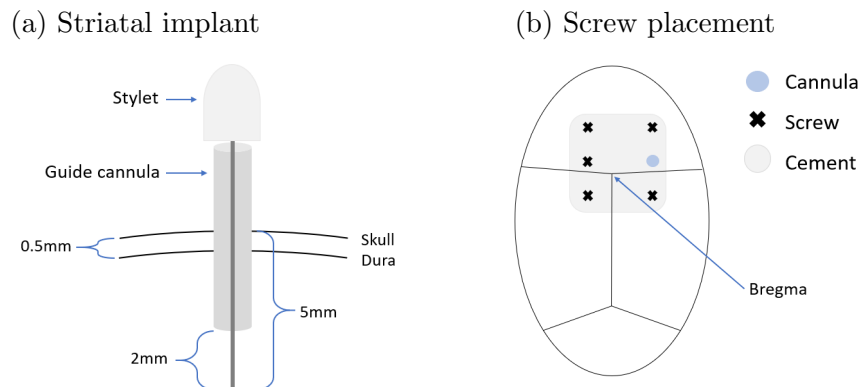
4.2.2 Implantation of the guide cannula into the anterior dorsal striatum

All rats underwent stereotaxic surgery to implant an infusion guide cannula into the anterior dorsal striatum. Rats were anaesthetised with isoflurane in oxygen (induced with 3% and maintained at 1.5–3%; flow rate 1 L/min). Following induction of anaesthesia, rats were subcutaneously injected with an analgesic (Rimadyl large animal solution, 1:9 dilution, 0.1 ml/100 g, s.c., Zoetis, UK) and an antibiotic (Synylox, 14% Amoxicillin, Zoetis, UK, 0.2 ml/ 100g) to act as a prophylactic against infections. Rats were positioned in a stereotaxic frame. EMLA cream, containing a local anaesthetic (lidocaine, prilocaine, 5%, AstraZeneca, UK), was applied onto the ear bars to reduce pain, and an eye gel (Lubrithal, Dechra, Denmark) was used to prevent ocular drying. An incision was made in the scalp, the skull was exposed and bregma and lambda were aligned horizontally. A hole was drilled unilaterally above the infusion site, 1.5 mm anterior to bregma and 2.5 mm right from the midline. Through the hole, an infusion guide cannula (C315G-SPC guide, 26 gauge, 4.4 mm below pedestal, Plastics One Inc., USA), with a stainless-steel stylet (C315DC/Spc to fit 4.4 mm 315G with 2.0 mm projection, Plastics One

Inc, USA) was inserted into the brain, to prevent occlusion of the guide cannula. The tip of the infusion cannula, which protruded 2.0 mm from the tip of the guide was aimed at a coordinate of 5.0 mm ventral from the skull (Figure 20a). Because the infusion cannula would also protrude 2.0 mm from the guide, this would result in an infusion target coordinate of 1.5 mm anterior to bregma, 2.5 mm right from the midline and 5.0 mm ventral from the skull. These coordinates, to target the anterior striatum, were chosen using an MR atlas of the male Lister hooded rat brain ‘Ratlas-LH’ (Prior et al., 2021) and are based on Bronfeld, Yael et al. (2013) and Klaus & Plenz (2016) who used similar injection sites to induce tic-like forelimb movements in rats.

The guide cannulae was secured in place to the skull using dental acrylic (flowable composite; Henry Schein, Germany) and 5 stainless-steel screws. Screws were placed in front, behind and just to the side of the cannula, to ensure stabilisation of the unilateral implant (Figure 20b). The open wound was then stitched to reduce its size. Rats received an intraperitoneal injection of saline (1 ml) for rehydration and were monitored as they recovered from the anaesthesia. Following surgery, rats were checked, weighed, and injected with antibiotic (Synulox, 14% Amoxicillin, Zoetis, UK, 0.2 ml/100 g), as well as habituated to handling necessary for the infusion, daily. Rats were given at least 7 days to recover before commencing the experiment.

Figure 20: Graphical visualisation of cannula, screw and stylet implants



Note: **(a)** Sketch showing guide cannula and stylet position in the head (not to scale). **(b)** Sketch indicating screw placement for unilateral right anterior dorsal striatum cannula implant.

4.2.3 Microinfusion procedure and drugs for behavioural studies

Rats were gently restrained to remove dummies and to insert infusion cannulae (C315I/SPC internal 33 gauge to fit 4.4 mm C315G with 2 mm projection, Plastics One Inc., USA) into the guides. The infusion cannula tip extended 2 mm below the guide into the right anterior dorsal striatum (DV: -5 mm infusion tip from skull). The infusion cannula was connected through polyethylene tubing (PE50 tubing Product code: C313CT (PE50), Bilaney Consultants, Germany) to a 5 μ l syringe mounted on a microinfusion pump. 0.9 % sterile saline (control) (0.5 μ l) or picrotoxin (either 300 ng/0.5 μ l or 200 ng/0.5 μ l in sterile saline) was delivered over 1 min. The dose of 300 ng/0.5 μ l was based on the study by Klaus & Plenz (2016) who used 0.8 to 1.5 μ l of 1 mM (603 ng/ μ l) picrotoxin solution for striatal infusions and reported tic-like movements, and our electrophysiology study (Chapter 3) where we observed large LFP spike wave discharges and enhanced multi-unit burst firing, without electrophysiological seizure signs, after striatal infusion of 300 ng picrotoxin in 0.5 μ l saline. No blinding occurred.

To identify successful infusion into the brain, a bubble was included in the tubing and monitored for movement. Following infusion, the infusion cannula remained for an additional minute to allow further absorption of the drug into the brain tissue. The infusion cannula was then replaced by the stylet and the rat was immediately placed into an opaque plastic rectangular box (dimensions 38 x 40 x 53 cm, Tontarelli) for up to two and a half hours. 4 rats at a time were placed into 4 boxes for recording (Figure 22). Onset of tic-like movements was determined in reference to the rat being placed in the box. Initially, recordings of the rat were planned to be for 60 min, however, this was prolonged to a time until rats stopped showing tic-like movements for 30 min. Rats were recorded for up to 150 min.

Picrotoxin was dissolved in saline at a concentration of 300 ng/0.5 μ l before it was aliquoted and kept frozen until use (not longer than 1 year). On the day of infusion, aliquots were thawed. For the final infusion (day 8), the aliquots were diluted to 200 ng/0.5 μ l in saline.

4.2.4 Study of tic-like movements caused by striatal disinhibition

Following surgery and recovery, the study lasted 8 days (Figure 21). On day 1, rats were habituated to the observation boxes (dimensions 38 x 40 x 53 cm, Tontarelli) for 30 min (duration of all habituation sessions). This was followed by seven additional days, consisting of four infusion days, separated by washout days to avoid carry-over effects from the preceding infusion day. On infusion days, following a 30 min habituation period in the boxes, rats received striatal picrotoxin or saline infusions, before they were placed in the boxes. Their behaviour was recorded for up to 150 min. An overhead camera (HD PRO Webcam C920, 1080p, 720p pixels, Logitech) was placed centrally over four boxes that were positioned side by side (Figure 22), and was used to record the rats' behaviour during the 30 min habituation period and the post-infusion period (up to 150 min) on infusion days. All rats were carefully monitored visually for tic-like behaviour and any gross adverse side effects.

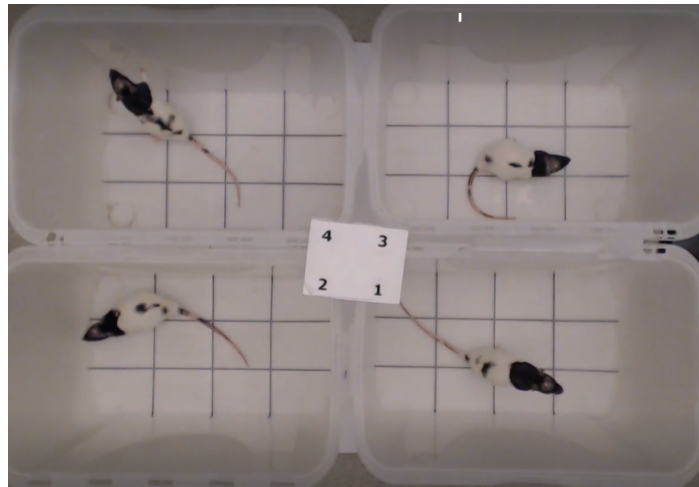
Figure 21: Study timeline of tic-like movements caused by striatal disinhibition



Note: The first two picrotoxin infusions were with 300 ng of picrotoxin in 0.5 μ l saline and the latter was with 200 ng of picrotoxin in 0.5 μ l saline.

On the first infusion day (day 2), rats received 300 ng picrotoxin in 0.5 μ l saline, to investigate whether picrotoxin infusion (300 ng in 0.5 μ l saline) causes marked tic-like movements of the contralateral forelimb, without seizures or any other gross adverse side effects. For the second infusion day (day 4), rats were infusion with 0.5 μ l saline, to demonstrate that saline alone does not cause any behavioural changes, and to confirm that tic-like movements are caused by striatal disinhibition, rather than non-specific infusion effects. On the third infusion day (day 6), rats received the same picrotoxin dose again, to investigate whether marked tic-like movements can be caused reliably within the same rat. Lastly, on the fourth infusion day (day 8), we observed the effects of a lower dose of picrotoxin (200 ng in 0.5 μ l saline) to test if such dose still reliably causes tic-like movements.

Figure 22: Set up of recording for tic-like movements



Note: An overhead camera recorded 4 rats at a time in individual boxes.

4.2.5 Analysis

Using the video recordings, individual tic-like movements of each rat were counted manually in 5 min blocks. A movement was counted as a tic-like movement when the movement was abrupt and when it was not part of the rats' normal behaviour. Because recordings were made with an overhead camera, the rats' head and rest of the body may have obstructed detection of very slight limb or face movements. When a movement was more intense and involved rotation of the body around the long axis, a 'body twists', it was noted and counted additionally.

4.2.6 Histology

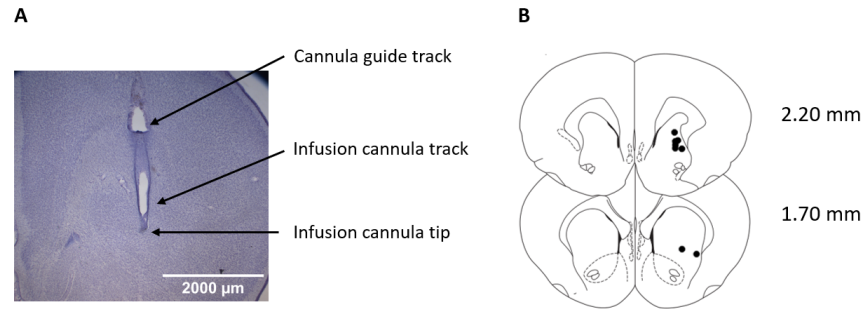
Following completion of the experiment, rats were overdosed with sodium pentobarbital (Dolethal, Vetoquinol, UK) and transcardially perfused using 0.9% saline followed by 4% paraformaldehyde (PFA) solution. Brains were extracted and stored in 4% PFA. They were sliced into 80 μm thick coronal sections using a vibratome (Leica VT1000 S) and placed onto microscope slides. Infusion cannula placements were verified using a Leica light microscope (Leica DM1000, Leica DFC295, 1.25x/0.04 with a Leica HCX PL Fluotar 1.25x/0.04 microscope objective) and mapped onto coronal sections adapted from the rat brain atlas by Paxinos & Watson (1998). Some slides were stained with cresyl violet and coverslipped to take photos, captured with a Zeiss Axioplan light microscope using a QImaging MicroPublishers 5.0 RTV and the Micro Manager software. Images were taken using a 1.25x/0.035NA objective. The images were then white balanced and a scale bar applied using the FIJI software.

4.3 Results

4.3.1 Histology - infusion cannula placements in the anterior dorsal striatum

In all eight rats, cannula tips were located between 1.70 mm and 2.20 mm anterior to bregma within the striatum (Figure 23).

Figure 23: Infusion sites in the anterior dorsal striatum



Note: **A:** Photograph of a coronal brain section showing guide cannula track (top), infusion cannula track (middle) and trace left by the infusion cannula tip (bottom). **B:** Approximate locations of infusion tips in the striatum using light microscopy. Locations are shown on coronal plates adapted from the atlas by Paxinos & Watson (1998), with numbers indicating distance from bregma in millimeters as shown in the atlas.

4.3.2 Description of tic-like movements

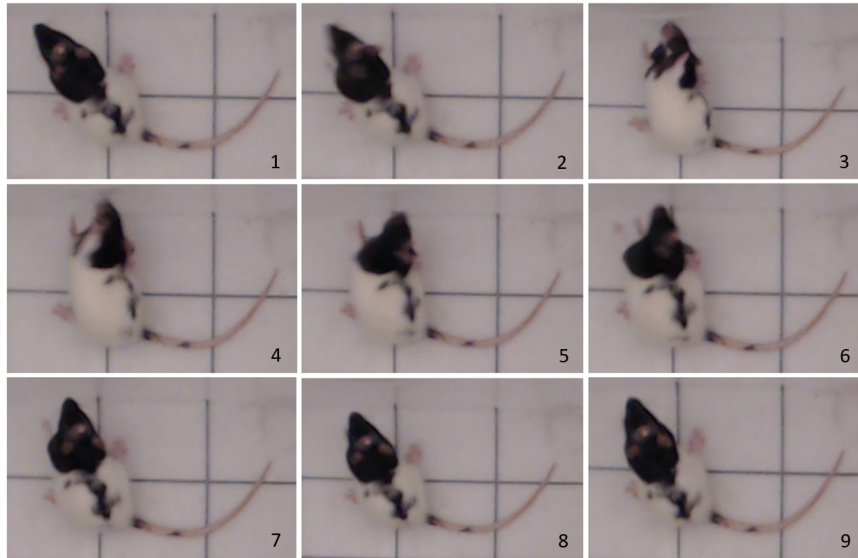
Tic-like movements, caused by striatal picrotoxin infusion, were observed in all rats. 23 out of 24 picrotoxin infusions evoked tic-like movements. Tic-like movements varied in intensity throughout a session, between rats and between infusion days. For example, some rats started having very subtle tic-like movements that became "stronger" and more obvious with time (judged by visual inspection). The number of tic-like movements also varied, as well as the expression of tic-like movements. Figure 24a shows screenshots of a tic-like movement recorded in a rat after infusion of 300 ng picrotoxin on the second picrotoxin infusion day (day 6). The rat lifts its left forelimb, thereby rotating its head and torso to the right around the body's long axis, before putting the left forelimb back down again, and thereby moving its head and torso into its starting position.

There were also some more pronounced forelimb movements that lasted for several seconds and led to a whole rotation of the body around its long axis. An example of such twisting is illustrated in Figure 24b. Screenshots are taken from a rat after infusion of 300 ng picrotoxin, on the first infusion day (day 2). The rats' head moves to the right side and the left forelimb moves forcefully backwards, twisting its upper body (2-3). The right forelimb is stretched out, while the left forelimb moves back

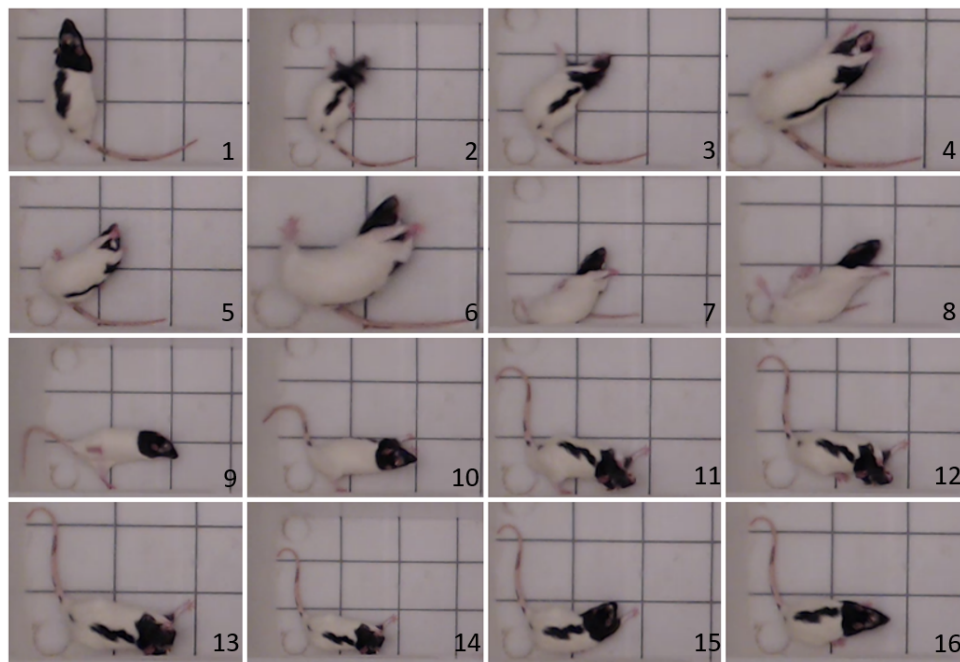
and forth (2-8). The face is facing upwards (4). The whole body starts moving backwards (5) and the head twists further to the right (6). The left hindlimb swings from left to right and the right hindlimb and tail move along (6-9), resulting in a non-twisted body posture (10). The right forelimb is stretched out again on the floor and the left forelimb is moving back and forth with high frequency while the head is twisted to the right (judged by visual inspection) (11). The head starts moving with the left forelimb, it appears as though the rat is licking its left paw (13-15). The amplitude of the left forelimb movements becomes smaller. The head moves to its normal position (15), the right forelimb returns to its normal body position and the rat continues with normal behaviour (16).

Figure 24: Screenshots from the video recording showing tic-like movements

(a)



(b)



Note: Screenshots from video clips recording tic-like movements. **(a)** A less intense forelimb movement that involves lifting the left forelimb, rotating the head and torso and returning to normal body posture. **(b)** A more pronounced forelimb movement that lasted for several seconds and led to a whole rotation of the body around its long axis.

4.3.3 Time course of tic-like movements

Individual tic-like movements were counted in 5 min blocks. Following striatal disinhibition by 300 ng (Figure 25a & 25b) and 200 ng (Figure 25c) of picrotoxin, rats started showing tic-like movements within 5 min and the number of tic-like movements peaked from about 5 min to 35 min after infusion. Figure 25 shows tic-like movements for up to 60 min, to facilitate comparison between infusions. Some rats had tic-like movements for longer than 60 min following the first and second picrotoxin infusion. See Figure 27 for number of tic-like movements per rat per infusion and Table 4 for duration of tic-like movements. All three picrotoxin infusions (day 2, 6 & 8) caused similar numbers of tic-like movements for the 12 x 5 min blocks. A two-way repeated measures ANOVA revealed no significant difference in the number of tic-like movements ($F_{(2,14)} = 1.349, p = 0.291$) and no significant interaction between infusion and time ($F_{(22,154)} = 0.947, p = 0.543$). However, there was a significant main effect of time ($F_{(11,77)} = 10.665, p < 0.001$). Additionally, there was no significant difference of tic-like movements between the two 300 ng picrotoxin infusions ($F_{(1,7)} = 1.694, p = 0.234$) and no significant interaction between infusion and time ($F_{(11,77)} = 1.098, p = 0.374$). However, there was a significant time effect ($F_{(11,77)} = 5.159, p < 0.001$). Following saline infusion, no tic-like movements were observed, nor any other changes in behaviour (data not shown).

When comparing onset and duration of tic-like movements between all three picrotoxin infusions (day 2, 6 and 8), repeated measures ANOVAs showed no significant difference between infusions for onset ($F_{(2,12)} = 0.157, p = 0.857$) and duration ($F_{(2,12)} = 1.860, p = 0.198$). Rat 5 was removed for both analyses as it did not show any tic-like movements following the 2nd picrotoxin infusion (day 6) (Figure 27e). For descriptive information see Table 4.

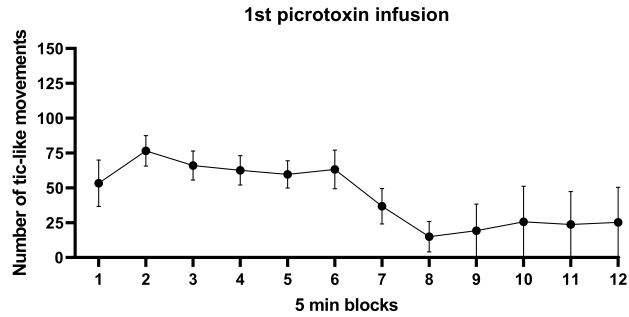
Table 4: Comparing tic onset and duration between picrotoxin infusions

		1 st picrotoxin infusion	2 nd picrotoxin infusion	3 rd picrotoxin infusion
Tic onset	Mean	198.57	165.43	157.29
	Min	12.00	44.00	0.00
	Max	452.00	291.00	345.00
Tic duration	Mean	1991.29	3335.14	2182.00
	Min	546.00	1978.00	1627.00
	Max	4391.00	7726.00	2842.00

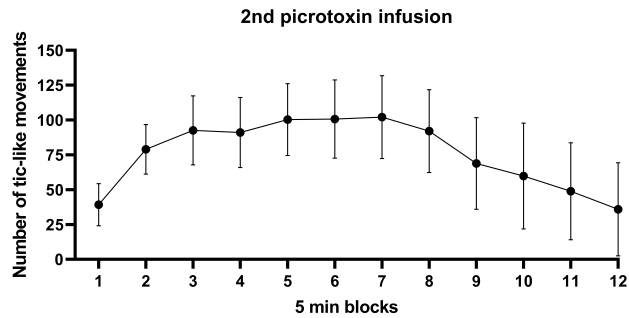
Note: 1st and 2nd picrotoxin infusion are of 300 ng picrotoxin in 0.5 µl saline and 3rd picrotoxin infusion is of 200 ng picrotoxin in 0.5 µl saline. Time is shown in seconds.

Figure 25: Time course of tic-like movements following striatal disinhibition by picrotoxin

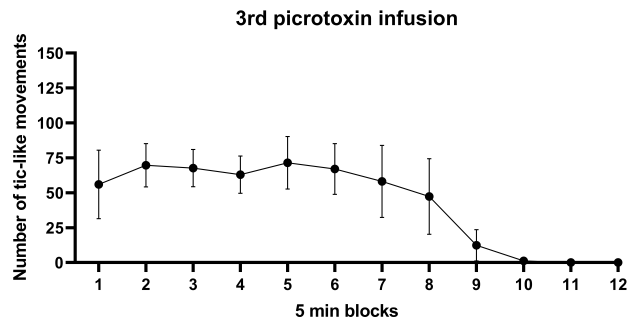
(a) Day 2: 300 ng of picrotoxin



(b) Day 6: 300 ng of picrotoxin



(c) Day 8: 200 ng of picrotoxin



Note: Tic-like movements (mean \pm SEM) are shown in 5 min blocks, following striatal disinhibition by 300 ng (**a & b**) or 200 ng (**c**) of picrotoxin in 0.5 μ l saline. 1 on the x-axis indicates 0-5 min post picrotoxin infusion. The data show the average tic-like movements counted after an infusion. Regardless of the dose, tic-like movements were peaking from around 5 min (block 1) to about 30 min (block 6). To facilitate comparison, the number of tic-like movements are shown for 12 blocks (60 min).

4.3.4 Pronounced tic-like movements involving rotation of the body around long axis - 'body twists'

Rats had up to 53 tic-like movements that involved rotation of the body around its long axis following infusion. There was high inter-rat and inter-infusion variability. Some rats had no such movements following one infusion and displayed some rotation movements after a different infusion with greater or lesser frequency. Although there is a numerical tendency for the higher dose to induce more of the full body rotations than the lower dose (see Table 5), this was not supported statistically using a repeated measures ANOVA ($F_{(2,12)} = 2.118, p = 0.163$).

Table 5: Number of body twisting per infusion

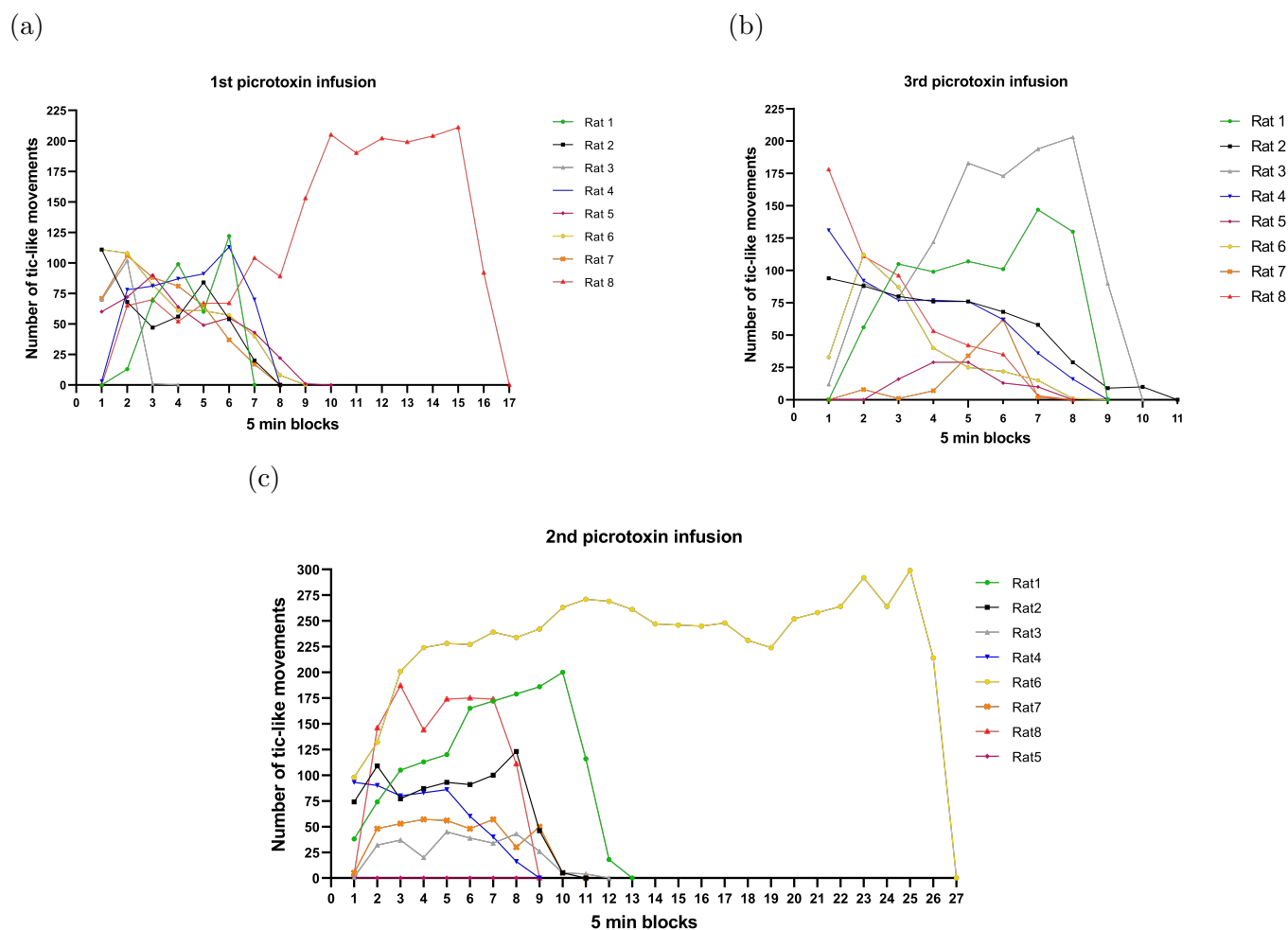
	1st picrotoxin infusion	2nd picrotoxin infusion	3rd picrotoxin infusion
Mean	14.86	11.43	1.71
SEM	7.85	5.37	0.68
Min	0	0	0
Max	53	39	5

Note: 1st and 2nd picrotoxin infusion are of 300 ng picrotoxin in 0.5 μ l saline and 3rd picrotoxin infusion is of 200 ng picrotoxin in 0.5 μ l saline. Highest and lowest number of full body rotations is following the first and last picrotoxin infusion respectively.

4.3.5 Consideration of between- and within-subjects variability in number of tic-like movements following striatal disinhibition

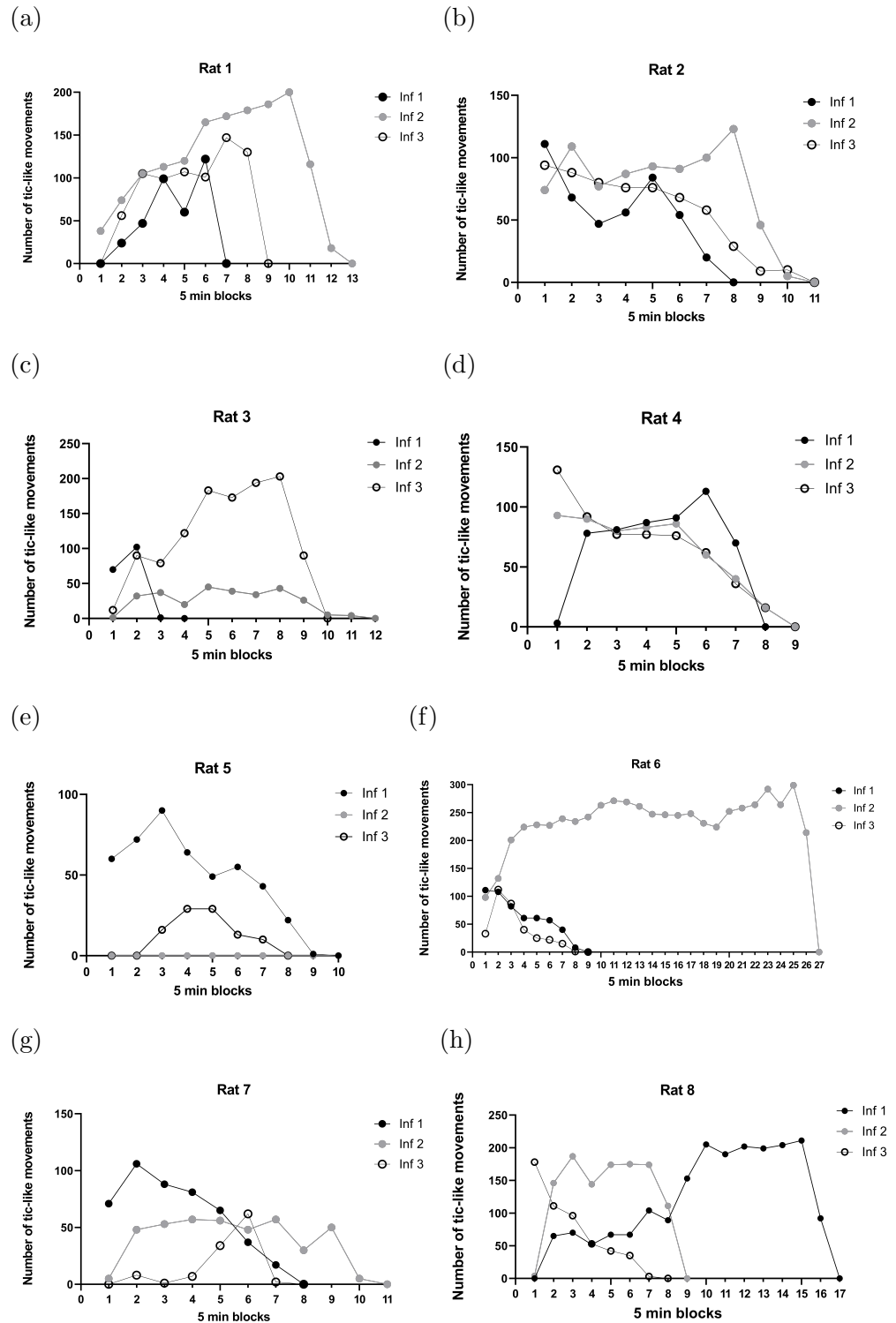
There was substantial inter-rat variability of number of tic-like movements following picrotoxin infusion (Figure 26). For example, one rat had in total 286 tic-like movements and another 6173. There was also high intra-rat variability with the same rat showing highly variable numbers of tic-like movements after each picrotoxin infusion (e.g. 363 vs 1486 vs 745) (Figure 27).

Figure 26: Between-subjects variability in number of tic-like movements following striatal disinhibition



Note: Comparing number of tic-like movements following picotoxin infusion with 300 ng (26a, 26c) and 200 ng (26b) in 0.5 μ l of saline into the right anterior dorsal striatum between rats. X-axis length based on duration of longest tic-like movements.

Figure 27: Comparing number of tic-like movements between infusions per rat



Note: Comparing three picrotoxin infusions per rat. First two infusions were with 300 ng per 0.5 μ l in saline and the third was with 200 ng per 0.5 μ l in saline.

4.4 Discussion

Right anterior dorsal striatal microinfusions of picrotoxin caused tic-like movements in the left forelimb in all rats. These tic-like movements were reliably and repeatedly induced within the same rat, with further infusions. The number of tic-like movements varied between rats and between session, however most rats expressed highest tic-like movements within the first 5 min to 35 min.

4.4.1 Reliably inducing tic-like movements

We successfully caused tic-like movements in the left forelimb in all rats, following picrotoxin infusion to the right anterior dorsal striatum. This is in line with previous experiments (e.g. Pogorelov et al. (2015); Klaus & Plenz (2016)). As similarly described by Bronfeld, Yael et al. (2013), the "strength" (judged by visual inspection) of the movement varied (often becoming stronger with time) before decreasing. After our first successful infusion, we confirmed that tic-like movements can be reliably and repeatedly induced within the same rat, with a second dose of 300 ng picrotoxin in 0.5 μ l saline. Following the second picrotoxin infusion, one rat did not express tic-like movements, however expressed tic-like movements after a third infusion with a lower dose of 200 ng picrotoxin in 0.5 μ l saline on a different day. It is likely that the absence of tic-like movements was due to an unsuccessful infusion of picrotoxin, rather than due to it being rat specific or it being delivered to the wrong brain area. With the final infusion, we were able to confirm that a lower dose of picrotoxin also reliability causes tic-like movements. Furthermore, no significant difference in number of tic-like movements was found with a lower dose, contrasting Pogorelov et al. (2015) findings. As expected, saline infusion did no produce tic-like movements nor any other behavioural changes.

There was substantial inter-rat variability and the number of tic-like movements per 5 min block also varied between rats. However, most rats expressed highest tic-like movements within the first 5 min to 35 min, which is in line with Patel & Slater (1987). There was also big intra-rat variability, with the same rat having different amounts of tic-like movements after each infusion. Although the infusion pump is set to deliver 300 ng in 0.5 μ l, it may be the case that different amounts of picrotoxin reached the dorsal striatum during different infusions.

4.4.2 Comparison of tic-like movements following striatal disinhibition in rats with tics in Tourette syndrome

It is challenging to classify a movement as a simple tic or as some other hyperkinetic movement by solely the phenotype. Different hyperkinetic disorders have often quite similar expression, with definitions overlapping (Zinner & Mink, 2010) and in some patients, different movement disorders also co-existing (Martino & Hedderly, 2019), such as tics disorders

and stereotypies (Zinner & Mink, 2010), making differentiation harder. Moreover, in patients with Tourette syndrome, further information such as the presence of a premonitory urge to move, having a temporal relief following tic expression (Martino et al., 2013), being able to control, defer, and suppress the expression of tics to some extent (Bortolato & Pittenger, 2017), as well as comorbidities and effective treatment, help classify the movement disorder. However, due to the lack of comprehension of animals' vocalisation, and the difficulty of measuring some of these features in animals, it makes it challenging to distinguish and classify a movement as a simple tic or as some other hyperkinetic movement by solely the phenotype. Nevertheless, it is essential, that future animal studies describe their animals' behaviour carefully, as different hyperkinetic disorders in humans may require different treatment plans (Sanger et al., 2010).

In our study, the abnormal movements (i.e. movements that were misplaced in context and time) following striatal disinhibition in rats were sudden, involuntary, repetitive, and stereotyped and therefore, misplaced in context and time, fitting with descriptions of tics in Tourette Syndrome (Cohen et al., 2013; Zinner & Mink, 2010). There were also some movements that involved twisting of the body for a longer period of time, alongside high frequency back-and-forth movements of the left forelimb (judged by visual inspection). Such movements, the twisting of the body, are also apparent in Tourette Syndrome (Dueck et al., 2009; Shute et al., 2016; Jankovic, 1997). As we only targeted a region in the right anterior dorsal striatum, we mainly produced tic-like movements in the left forelimb, due to the somatotopic organization in the striatum (Bronfeld, Israelashvili & Bar-Gad, 2013). However, tics in the disorder may occur as brief bouts throughout the day, tend to wax and wane in frequency and severity and often change anatomical location (Gilbert et al., 2014) and therefore, our model does not capture the complexity of the disorder.

4.4.3 Conclusion

We confirmed that right anterior dorsal striatal disinhibition, by local microinfusion of the GABA-A receptor antagonist picrotoxin, causes tic-like movements in the left forelimb as previously reported (e.g., Pogorelov et al. (2015); Klaus & Plenz (2016)). We characterised the time course and some key features of tic-like movements. We confirmed that tic-like movements can be reliably and repeatedly induced within the same rat and described variability of tic-like movements between infusions as well as between rats. The movements observed in this study were compared to tics in Tourette syndrome.

5 Further characterisation of the rat striatal disinhibition model: No deficit in prepulse inhibition of the acoustic startle response, and increased locomotor activity

Declaration: I conducted surgeries, monitored anaesthesia, collected data, perfused rats, and analysed and interpreted data. Charlotte Taylor and Luke O'Hara contributed to surgery and monitoring anaesthesia. Charlotte Taylor and Rachel Grasmeder Allen contributed to data collection and perfusion.

5.1 Introduction

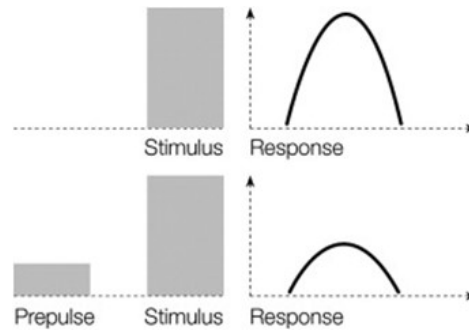
Prepulse inhibition (PPI) and locomotor activity (LMA) may be important markers of basal ganglia dysfunction; both disrupted PPI and increased locomotor activity have been previously associated with similar striatal dysfunction in rodent models. However, how distinct types of striatal dysfunction, related to distinct disorders, affect these measures, still remains largely to be clarified. Our study contributes to addressing this gap, focusing on striatal disinhibition, which has been linked to Tourette Syndrome. This introduction starts by describing sensorimotor gating and PPI (Section 5.1.1), followed by PPI disruption in Tourette Syndrome (Section 5.1.2) and brain regions involved in PPI (Section 5.1.3). Lastly, striatal control over locomotor activity is described (Section 5.1.4).

5.1.1 Sensorimotor gating and prepulse inhibition

Sensorimotor gating refers to mechanisms protecting the early pre-attentive processing of information (e.g., the prepulses in PPI experiments), by attenuating motor responses to other sensory stimuli (e.g., the startle response to startle pulses in PPI experiments) (Bast & Feldon, 2003). Prepulse inhibition of the startle reflex is often used as a measure of sensorimotor gating (Baldan Ramsey et al., 2011) and can be tested on rodents (Willott et al., 1994; Paylor & Crawley, 1997), monkeys (Davis et al., 2008; Linn et al., 2003; Winslow et al., 2002), as well as humans (Zebardast et al., 2013; Castellanos et al., 1996). Acoustic PPI occurs when a weaker, non-startling pre-pulse immediately prior (30-500 ms) to the stronger startling pulse inhibits the startle response (Figure 28). The amount of PPI is thought to reflect sensorimotor gating, and a loss of PPI is commonly used to show dysfunction in the sensorimotor gating mechanism (Swerdlow et al., 1999). The startle reflex is often a twitch of facial or body muscles to a sudden stimulus (Koch, 1999; Kohl et al., 2013; Swerdlow et al., 1999). In rodents, the acoustic startle reflex is

measured through the downward force of the muscles that follows contraction (Swerdlow, 2013). It is thought to be a primitive and protective body response against predators or a blow, as well as a preparation of a flight/fight response (Koch, 1999). PPI is measured using the startle magnitude and compares trials that include a prepulse and that do not (Swerdlow, Karban et al., 2001).

Figure 28: Prepulse inhibition of the startle response



Note: Prepulse inhibition occurs when a weaker, non-startling pre-pulse immediately prior to the stronger startling pulse inhibits the startle response. Figure taken from Kohl et al. (2013).

5.1.2 PPI disruption in Tourette Syndrome

A number of neuropsychiatric disorders are characterised by sensorimotor gating deficits, including Tourette Syndrome (Baldan Ramsey et al., 2011). Swerdlow and colleagues suggested that motor or vocal tics are due to failed automatic gating of sensory information (experienced as unwanted and bothersome premonitory urges) (Swerdlow, 2013; Swerdlow & Sutherland, 2005). Many studies reported deficits in PPI in patients with Tourette syndrome, looking at eye blink responses (following supra-orbital nerve electrical stimulation (Castellanos et al., 1996; S. J. Smith & Lees, 1989) or air puffs (Swerdlow, Karban et al., 2001)) or using electromyography (following acoustic startle (Swerdlow et al., 1994)). However, Zebardast et al. (2013) did not find a significant deficit in PPI of the tactile startle response, elicited by an air puff to the throat, in adult Tourette patients.

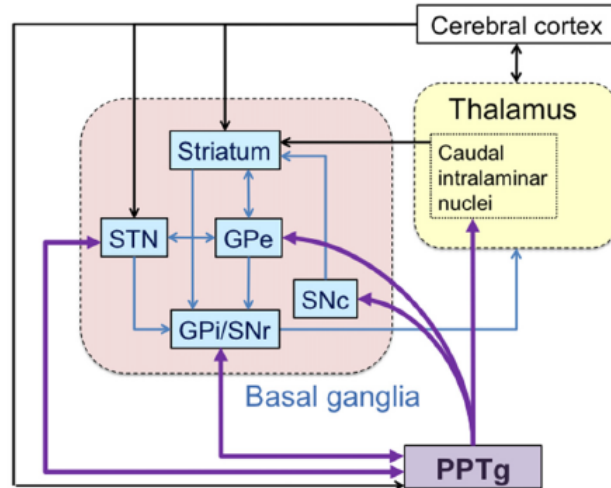
The suggested link between tic-like movements and PPI disruption in Tourette syndrome (Swerdlow, 2013; Swerdlow & Sutherland, 2005) is also supported by reports of disrupted PPI in transgenic mouse models that show tic-like movements and are relevant to Tourette Syndrome. One of those mouse models is the HDC knockout mouse. Previously, Ercan-Sencicek et al. (2010) reported about a family, where the father and all eight offspring met the criteria for Tourette syndrome and who all carried a rare mutation in the HDC gene encoding L-histidine decarboxylase

(Ercan-Sencicek et al., 2010). The HDC knockout mice had tic-like movements as well as PPI impairments, of which the latter was similar to patients that carried the HDC mutation and that had a tic disorder (Castellan Baldan et al., 2014). The D1CT-7 transgenic mouse model, developed by Campbell et al. (1999), is one of the best-characterised genetic models of Tourette Syndrome (Santangelo et al., 2018) and has also shown PPI deficits (Godar et al., 2016).

5.1.3 Brain regions involved in PPI

Although PPI is mediated by brainstem circuits, with the pedunculo-pontine tegmental nucleus (PPTg) playing a key role, it is modulated by a range of forebrain regions, including ventral and dorsal striatum (Koch & Schnitzler, 1997; Kumari et al., 2005). The PPTg when lesioned, has shown to reduce PPI (Swerdlow & Geyer, 1993). It projects to the thalamus and as well as a range of brain regions in the basal ganglia, including the subthalamic nucleus (STN), internal globus pallidus (GPi), substantia nigra pars reticulata (SNr), external globus pallidus (GPe), and substantia nigra pars compacta (SNc) (Figure 29). With the first three projections being bilateral connections, both the PPTg and basal ganglia can have a widespread influence over one another (Mena-Segovia et al., 2004).

Figure 29: Connectivity between PPTg, basal ganglia and thalamus



Note: Figure taken from Mori et al. (2016).

From this strong connectivity, it is not surprising that structures within the basal ganglia also affect PPI. In particular the striatum, a key brain region in Tourette syndrome (Albin & Mink, 2006; Draper et al., 2015; Berardelli et al., 2003; Felling & Singer, 2011), has shown to directly affect PPI. For example, reductions in PPI are reported when the central or caudodorsal striatum (Kodsi & Swerdlow, 1995), nucleus accumbens (Kodsi & Swerdlow, 1997) or dorso-medial striatum (Baldan Ramsey et

al., 2011) is lesioned. Moreover, there is substantial evidence that dopamine transmission negatively modulates PPI (Mansbach et al., 1988; Swerdlow et al., 1986; Swerdlow, Geyer & Braff, 2001), with this effect being, at least partly, mediated by dopamine receptors in the nucleus accumbens (Swerdlow, Braff, Masten & Geyer, 1990; Swerdlow et al., 1992; Swerdlow, Braff & Geyer, 1990) and the anteriomedial striatum (Swerdlow et al., 1992). An elevation in startle amplitude has been reported following lesions to the ventral (Kodsi & Swerdlow, 1994, 1995) and caudodorsal striatum (Kodsi & Swerdlow, 1995). When low prepulse intensities were used, increased startle amplitudes were found in rats with rostradorsal striatal lesions (Kodsi & Swerdlow, 1995). Baldan Ramsey et al. (2011) on the other hand, reported no effect of dorsomedial striatal lesions in mice on startle.

Based on the findings of patients with Tourette syndrome, the genetic mouse models and previous studies on striatal involvement in PPI as well as its anatomical location within the basal ganglia, which has connectivity to the peduncolopontine tegmentum, we expected that dorsal striatal disinhibition may disrupt PPI.

5.1.4 Striatal control over locomotor activity

The striatum is often divided into a dorsal part (which includes the caudate nucleus and putamen) and a ventral part (which includes the nucleus accumbens and olfactory tubercle) (Robbins & Everitt, 1992; Voorn et al., 2004). Previous studies in rats have strongly implicated the ventral striatum, specifically the nucleus accumbens, in the regulation of open field locomotor activity. Increases in locomotor activity have been reported when the nucleus accumbens was inactivated via permanent lesions (Lorens et al., 1970; D. Wirtshafter et al., 1978; Maldonado-Irizarry & Kelley, 1995) or by local infusions of GABA (Morgenstern et al., 1984; Wong et al., 1991), although nucleus accumbens (core) infusions of the GABA receptor agonist muscimol acutely reduced locomotor activity, followed by hyperactivity after a few days (Pothuizen et al., 2005). Locomotor hyperactivity was also reported when the nucleus accumbens was stimulated with dopamine (Pijnenburg & van Rossum, 1973; D. M. Jackson et al., 1975; Costall & Naylor, 1975; Costall et al., 1984; Jones et al., 1981), 6,7-ADTN, a dopamine agonist (Arnt, 1981), carbachol, a cholinergic agonist (Austin & Kalivas, 1988), glutamatergic receptor agonists such as AMPA (Arnt, 1981), NMDA (M. Wu et al., 1993), DHPG and DCG-IV (C. J. Swanson & Kalivas, 2000), or disinhibited by bicuculline, a GABA receptor antagonist (Yael et al., 2019; Israelashvili et al., 2020). A decrease in locomotor activity was reported when the nucleus accumbens was lesioned with 6-hydroxydopamine (Radhakishun et al., 1988), or injected with AP-5, an NMDA receptor antagonist (Maldonado-Irizarry & Kelley, 1994). These studies support the notion that nucleus accumbens is involved in locomotor activity, with various manipulations of this

region affecting locomotor activity.

Although some authors have mainly highlighted that dorsal striatal disinhibition predominantly causes tic-like movements (Israelashvili et al., 2020; Bronfeld, Yael et al., 2013), there is also some evidence that dorsal striatal disinhibition increases locomotor activity. Indeed, studies in cats reported increased locomotor activity following disinhibition of the caudate nucleus (Yoshida et al., 1991), and numerous studies on dorsal striatal disinhibition in rats have reported increased locomotor activity, alongside specific movements/behaviours that were not part of the normal behaviour repertoire, such as myoclonic jerks (Tarsy et al., 1978; Worbe et al., 2009), forelimb tremors (Morgenstern et al., 1984), stereotyped sniffing (Costall & Naylor, 1975) and tic-like movements (Yael et al., 2016; Bronfeld, Yael et al., 2013; Israelashvili et al., 2020). Further support for the role of the dorsal striatum in locomotor activity comes from Jurado-Parras et al. (2020) who lesioned the dorsal striatum and found decreases in the speed of reward-oriented locomotion, as well as West et al. (1990) who found a region in the dorsolateral striatum that exhibited single-unit correlations with specific locomotor limb movements.

In light of the evidence above, striatal disinhibition targeting the anterior dorsal striatum, may, alongside tic-like movements (as reported by previous literature and shown in Chapter 4), also cause locomotor hyperactivity, although this effect is likely to be weaker than the locomotor hyperactivity caused by nucleus accumbens disinhibition (Yael et al., 2019).

5.1.5 Aims

We aimed to examine the effect of striatal disinhibition, using the GABA-A antagonist picrotoxin on (i) startle and prepulse inhibition and (ii) locomotor activity, in two separate experiments. Based on the studies discussed above, an increase in locomotor activity and a disruption in PPI was expected.

5.2 Methods

5.2.1 Rats

We used sixteen male adult Lister hooded rats (Envigo, UK), weighing between 290 g and 330 g and approximately aged 10-11 weeks at the time of surgery. Our target sample size was $n=10-16$, which would give us a power $> 80\%$ to detect differences between striatal disinhibition and striatal saline infusion that correspond to an effect size of Cohen's d of about 1 or greater, using two-tailed ($p < 0.05$) paired comparisons in a within-subjects study (power analysis conducted with GPower 3.1 (Faul et al., 2007)). Three rats had to be excluded: (i) one rat had a stuck stylet after surgery (before any testing), (ii) one rat had a broken infusion

cannula in the guide cannula on the second infusion day for our PPI experiment, and (iii) one rat was found lying on the floor of the LMA box (during the experiment). It had previously shown tic-like movements, was alive but was unresponsive when found. When picked up, it disliked being held and had blood around the mouth and throat. Moments later it moved both forelimbs, ears and had facial twitches. That rat received picrotoxin previously in the PPI experiment and showed no side effects apart from tic-like movements. Therefore, we had 14 rats in total contributing to the PPI data and 13 rats contributing to the locomotor activity data.

Animal housing and husbandry were as described previously in Chapter 4, Section 4.2.1. All procedures were conducted in accordance with the requirements of the United Kingdom (UK) Animals (Scientific Procedures) Act 1986. All efforts were made to minimise animal suffering and to reduce the number of animals used. Procedures were carried out under the personal licence number I71997928, granted by the Home Office.

5.2.2 Implantation of the guide cannula into the anterior dorsal striatum

All rats underwent stereotaxic surgery to unilaterally implant an infusion guide cannula into the right anterior dorsal striatum. Surgery was conducted as described previously in Chapter 4, Section 4.2.2 and infusion target coordinates of 1.5 mm anterior to bregma, 2.5 mm right from the midline and 5.0 mm ventral from the skull were kept, as they reliably induced tic-like movements, without any gross adverse side effects in Chapter 4. Following surgery, rats were checked, weighed, and injected with antibiotic (Synulox, 14% Amoxicillin, Zoetis, UK, 0.2 ml/100 g), as well as habituated to handling necessary for the infusion, daily. Rats were given at least 7 days to recover before commencing the first experiment.

5.2.3 Microinfusion procedure and drugs for behavioural studies

Rats were gently restrained to remove dummies and to insert infusion cannulae (C315I/SPC internal 33 gauge to fit 4.4 mm C315G with 2 mm projection, Plastics One Inc., USA) into the guides. The infusion cannula tip extended 2 mm below the guide into the right anterior dorsal striatum (DV: -5 mm infusion tip from skull). The infusion cannula was connected through polyethylene tubing (PE50 tubing Product code: C313CT (PE50), Bilaney Consultants, Germany) to a 5 µl syringe mounted on a microinfusion pump. A volume of 0.5 µl of 0.9 % sterile saline (control) or 300 ng picrotoxin in 0.5 µl saline was delivered over 1 min. No blinding occurred. To identify successful infusion into the brain, a bubble was included in the tubing and monitored for movement. Following infusion, the infusion cannula remained for an additional minute to allow further absorption of the drug into the brain tissue, before the infusion

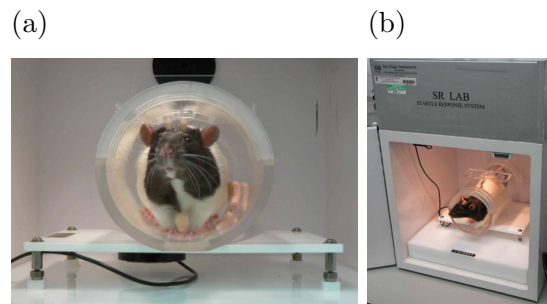
cannula was replaced by the stylet. For PPI, rats were placed immediately into test boxes and doors were closed. Then, testing started once all 4 rats had been infused and placed into their boxes. Startle/PPI sessions started within 1 to 11 min following infusion (mean = 4.24, SEM = 0.61). For LMA testing, rats were placed in boxes as soon as possible after completion of infusion. Photobeam break measurements started immediately. Rats were checked for tic-like movements following picrotoxin infusion randomly throughout the session, providing a positive control for a successful infusion.

Picrotoxin was dissolved in saline at a concentration of 300 ng/0.5 μ l before it was aliquoted and kept frozen until use (not longer than 1 year). On the day of infusion, aliquots were thawed.

5.2.4 Startle and PPI testing

Startle and PPI was measured using four startle response systems (San Diego Instruments), similar to Pezze et al. (2014) (Figure 30). Systems were placed in individual sound-attenuating chambers (39 x 38 x 58 cm³) that were well lit (ranging from 228 to 355 W), ventilated and consisted of a clear Perspex cylinder (8.8 cm diameter, 19.5 cm long) on a solid Perspex base connected to an accelerometer, which connected to Reflex Testing software (San Diego Instruments). The amplitude of the whole body startle response to an acoustic pulse was defined as the average of 100 x 1 ms accelerometer readings collected from pulse onset.

Figure 30: Test chambers to measure startle reflex and prepulse inhibition



Note: Photographs do not show unilateral anterior dorsal striatum implants.

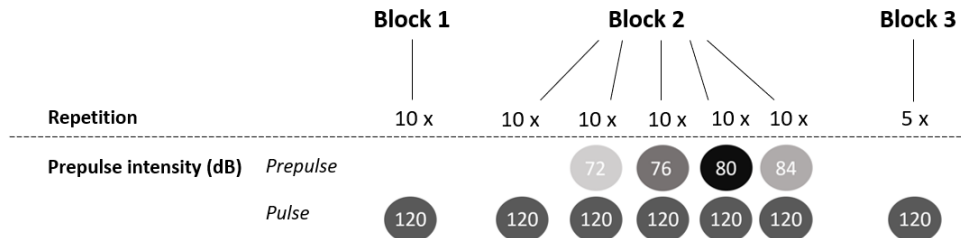
A test session started with a 5 min acclimatisation period of the rat being in the cylinder with a 62 dB(A) background noise level, that continued throughout the session. Following the acclimatisation, there were three test blocks (Figure 31). (1) The first block consisted of 10 individual startle pulses [40 ms, 120 dB(A) broad-band bursts], allowing habituation for the startle response to a relatively stable level for the remainder sessions. (2) The second block consisted of a total of 50 trials (5 different

trial types x 10 times) which were presented in a pseudorandom order and with an intertrial interval that varied between 10 to 20 s in duration (average 15 s). The 5 different trial types consist of one pulse-alone type and four types having a weak 20 ms prepulse of 72, 76, 80, 80 or 84 dB(A) preceding the startle pulse by 100 ms. The percentage of PPI (%PPI) induced by each prepulse intensity was calculated as follows:

$$\%PPI = \frac{(\text{MSA on pulse-alone trials}) - (\text{MSA on prepulse-plus-pulse trials})}{\text{MSA on pulse-alone trial}} \times 100\%$$

where MSA stands for mean startle amplitude. (3) The final block consisted of five startle pulses. Analysis of startle amplitude on pulse-alone trials across all three blocks was conducted to measure startle habituation. The total duration of the test session was 23 min.

Figure 31: Pulse-alone and prepulse-plus-pulse trials



Note: Prepulse was 20 ms long preceding the 40 ms long startle pulse by 100 ms.

5.2.5 Open-field locomotor activity testing

Locomotor activity was measured using 12 clear Perspex chambers (39.5 cm long x 23.5 cm wide x 24.5 cm deep) with metal grid lids placed in a dimly lit chamber (36.6-59.5 lx; measurements taken with lids off), similar to Pezze et al. (2014). The chambers sat in frames containing two levels of a 4 x 8 photobeam configuration (Photobeam Activity System; San Diego Instruments) (Figure 32). A locomotor count was recorded when there was a movement from one beam to another within the lower level of photobeams. Fine movement counts were recorded after a beam was interrupted for the second and subsequent times, with no other beam being interrupted in the meantime. A refractory period was set in place to avoid counting scratching or tail flipping. During the refractory period additional interruptions on a beam were not counted within 1 s. Further interruptions of the same beam during the refractory period restarted the refractory period. When an animal blocked multiple beams due to its size, the system regarded the last interrupted beam as the 'currently interrupted' one. A session started with the placement of the rat into the centre of the chamber and lasted 60 min. Data was analysed for each 5 min block of testing.

Figure 32: Activity boxes with photobeams

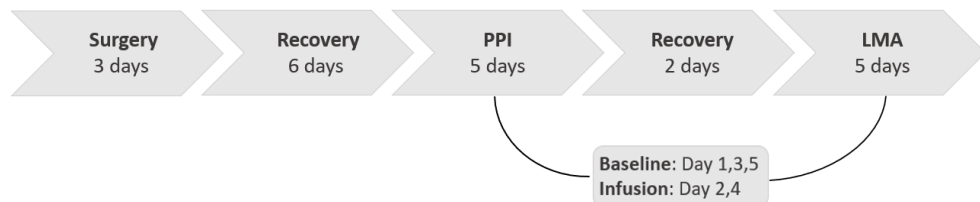


5.2.6 Experimental design and analysis

The effects of striatal neural disinhibition were examined in a within-subjects, counterbalanced, crossover design over both the startle PPI and open-field locomotor activity testing, using two conditions: saline (0.5 μ l) and picrotoxin (300 ng/0.5 μ l) (Sigma-Aldrich, UK). This dose is the same as in Chapters 3 and 4. The study lasted 21 days in total (Figure 33). Both experiments (startle/PPI and locomotor activity) comprised of 5 successive days. On day 1 of each experiment (startle PPI and open-field locomotor activity), rats were tested without infusions to habituate them to the testing procedure and to get baseline measurements. On day 2 and 4, rats received one of the two infusions (saline or picrotoxin). To verify that any drug differences on the infusion day reflected temporary infusion effects, rather than any other confounding factors, rats were re-tested on the days after infusion (day 3 & 5).

Startle/PPI and locomotor activity data was analysed using a two-way repeated measures ANOVA with drugs (saline/picrotoxin) and test blocks or trial types (12 x 5 min blocks for open field testing, three test blocks for startle testing and four different prepulse types for PPI testing) as within-subjects factors. A significance level of $p < 0.05$ was accepted for all statistical tests.

Figure 33: Study timeline for PPI and LMA experiment



Note: Infusion was either with saline (0.5 μ l) or picrotoxin (300 ng/0.5 μ l).

5.2.7 Histology

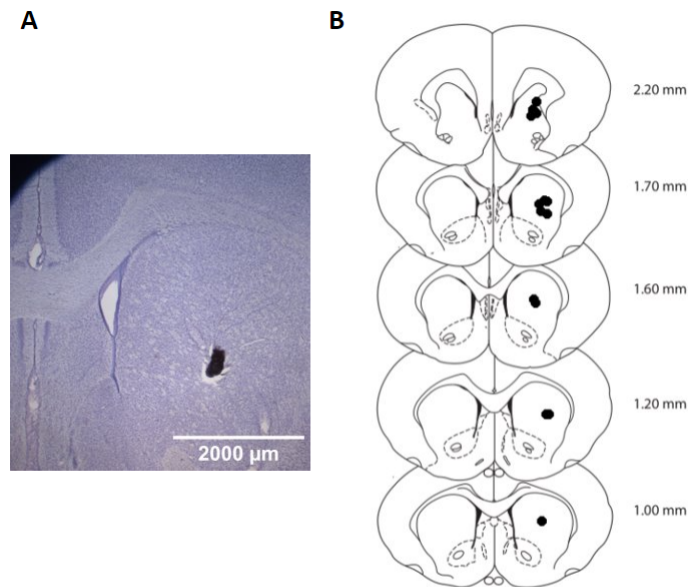
Following completion of the experiments, rats were overdosed with sodium pentobarbital (Dolethal, Vetoquinol, UK) and transcardially perfused using 0.9% saline followed by 4% paraformaldehyde (PFA) solution. Brains were extracted and stored in 4% PFA. They were sliced into 80 μm thick coronal sections using a vibratome (Leica VT1000 S) and placed onto microscope slides. Infusion cannula placements were verified using a Leica light microscope (Leica DM1000, Leica DFC295, 1.25x/0.04 with a Leica HCX PL Fluotar 1.25x/0.04 microscope objective) and mapped onto coronal sections adapted from the rat brain atlas by Paxinos & Watson (1998). Some slides were stained with cresyl violet and coverslipped to take photos, captured with a Zeiss Axioplan light microscope using a QImaging MicroPublishers 5.0 RTV and the Micro Manager software. Images were taken using a 1.25x/0.035NA objective. The images were then white balanced and a scale bar applied using the FIJI software.

5.3 Results

5.3.1 Histology - infusion cannula placements in the anterior dorsal striatum

In total, data from 14 rats was used for analysis of the PPI experiment, and from 13 rats for the LMA experiment. Cannulae tip positions were mapped onto coronal sections of an adapted Paxinos & Watson (1998) rat brain atlas (Figure 34). All cannula tips were located in the striatum between 1.00 mm and 2.20 mm posterior to bregma.

Figure 34: Infusion cannula tip placements in the anterior dorsal striatum



Note: **A:** Photograph of a coronal section showing the infusion cannula tip trace. **B:** Approximate locations of infusion tips in the striatum mapped on coronal plates adapted from the atlas by Paxinos & Watson (1998), with numbers indicating distance from bregma in millimeters, as shown in the atlas.

5.3.2 Tic-like movements in the LMA and PPI experiments

In the startle/PPI experiments, all rats (n=14) infused with picrotoxin into the striatum showed tic-like movements. In the locomotor activity experiment, we could confirm visually that 13 out of 14 rats had tic-like movements following picrotoxin infusion. Data of one rat was excluded (see reason for exclusion in Section 5.2.1).

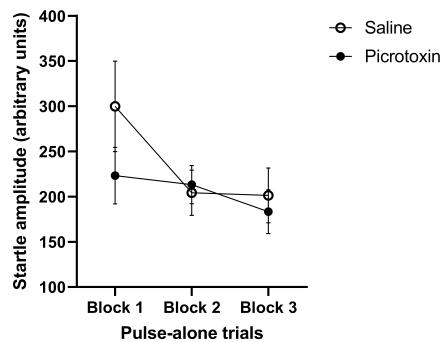
5.3.3 Startle and Prepulse inhibition

5.3.3.1 Picrotoxin in the striatum tended to reduce startle but did not affect PPI

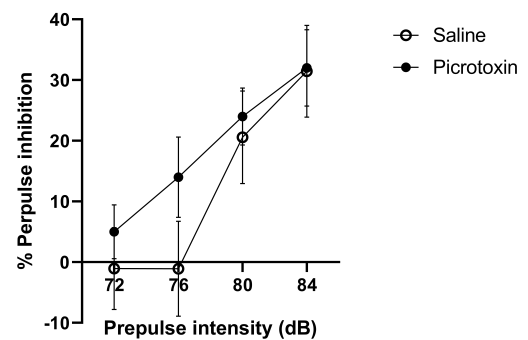
Striatal disinhibition tended to reduce startle during the first test block (1-10 pulses), before habituation led to similarly low startle responses in both infusion conditions (Figure 35a). There was a significant effect of test block ($F_{(2,26)} = 5.543$, $p = 0.010$). There was no significant main effect of drug ($F_{(1,13)} = 0.858$, $p = 0.371$), but a strong trend for an interaction of infusion x pulse-alone trials ($F_{(2,26)} = 3.183$, $p = 0.058$). Striatal disinhibition did not affect percentage prepulse inhibition (Figure 35b). No significant main effect of infusion condition and no significant infusion x prepulse intensity interaction ($F < 1.4$, $p > 0.27$) was found. There was only a significant main effect of prepulse intensity ($F_{(3,39)} = 19.150$, $p < 0.001$), with percentage prepulse inhibition being higher at higher intensities.

Figure 35: Startle and percentage prepulse inhibition following striatal infusion of saline or picrotoxin

(a) Startle



(b) Percentage prepulse inhibition



Note: (a) Block 1 refers to single-pulses in trials 1-10, block 2 to single-pulses in trials 11-60 and block 3 to single-pulses in trials 61-65. Data are shown as mean \pm SEM.

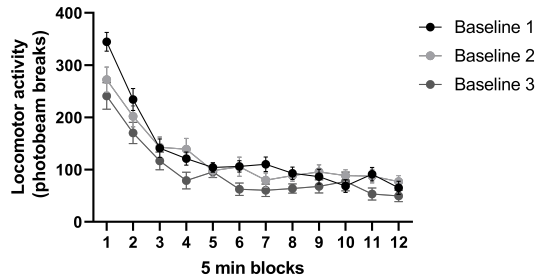
5.3.4 Locomotor activity

5.3.4.1 Habituation within a session and over days

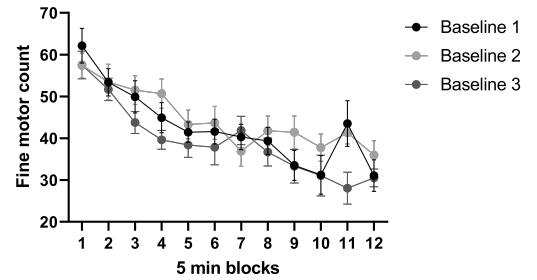
Baseline locomotor and fine movement measurements (taken on day 1, 3 and 5) show habituation to the boxes within a session and over days (decreased activity with time) (Figure 36a). A repeated measures ANOVA of locomotor activity data supported this by revealing a significant interaction of 5 min block x day ($F_{(22,264)} = 2.360$, $p = 0.001$) a significant effect of day (baseline day 1,3,5) ($F_{(2,24)} = 9.319$, $p = 0.001$) and time (5 min blocks) ($F_{(11,132)} = 58.426$, $p < 0.001$). A repeated measures ANOVA for fine movement count on the baseline days revealed a significant effect of time ($F_{(11,132)} = 17.668$, $p < 0.001$), reflecting habituation within a session, a trend for a reduction across days ($F = 3.287$, $p = 0.055$) and no significant interaction ($F = 1.207$, $p = 0.241$).

Figure 36: Baseline measurements of locomotor activity and fine movement activity

(a) Locomotor activity



(b) Fine movement counts



Note: (a) Baseline locomotor activity and (b) fine movement count (mean \pm SEM), measured by photobeam breaks, are shown in 5 min blocks for day 1, 3 and 5. Locomotor activity and fine movement count was higher on the first days. Habituation occurred within a session as well as over days for locomotor activity. Activity is shown for the total recording time of 12 x 5 min blocks (60 min).

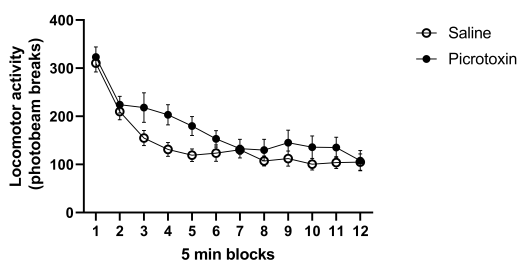
5.3.4.2 Picrotoxin in the striatum increases locomotor activity and fine movement count

Picrotoxin in the striatum significantly increased locomotor activity. A repeated measures ANOVA revealed a significant effect of drug ($F_{(1,12)} = 7.005$, $p = 0.021$), significant effect of time ($F_{(11,132)} = 31.498$, $p < 0.001$) and an interaction (drug x time) that was at trend level ($F_{(11,132)} = 1.687$, $p = 0.083$), which reflected that the locomotor hyperactivity caused by striatal disinhibition was most pronounced between 10 and 25 min (blocks 3-5) after start of the test session (Figure 37a). Picrotoxin increased locomotor activity, from about 5-10 min after the start of the test session. There was a general decrease of locomotor activity over time for both saline and picrotoxin, reflecting habituation. Fine movement count was also increased by picrotoxin, reflected by a significant drug effect ($F_{(1,12)} = 20.036$, $p = 0.001$), significant effect of time ($F_{(11,132)} = 8.337$, $p < 0.001$) and significant interaction of drug x time ($F_{(11,132)} = 3.123$, $p = 0.001$) (Figure 37b). The fine movement count was higher following the picrotoxin infusion than saline infusion for the entirety of the 60 min time course. The first 25 min (blocks 1-6) were marked by an increase of fine movement activity, which gradually decreased over time.

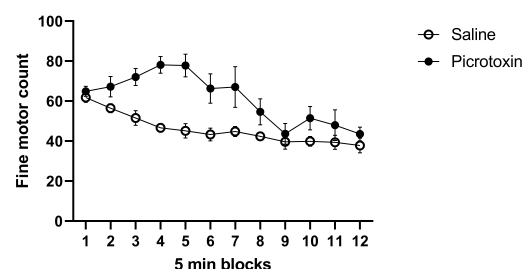
During re-baseline testing following infusion days, there were no carry over effects of the picrotoxin infusion, reflected by no significant main effect or interaction involving the infusion condition on the preceding infusion day (all $F < 1.309$, $p > 0.226$) for both locomotor activity and fine movement count. On re-baseline days, both locomotor and fine movement counts only showed a significant effect of time, reflecting habituation ($F < 32.9$, $p < 0.001$).

Figure 37: Locomotor measurements following saline/picrotoxin

(a) Locomotor activity



(b) Fine movement count



Note: (a) Locomotor activity and (b) fine movement count (mean \pm SEM) are shown in 5 min blocks, following striatal disinhibition by 300 ng of picrotoxin in 0.5 μ l saline. Locomotor activity was higher in the picrotoxin group and decreased with time, reflecting habituation. Fine movement count peaked from \sim 5 min (block 1) to \sim 25 min (block 5). Activity is shown for the total recording time: 12 x 5 min blocks (60 min).

5.4 Discussion

Striatal microinfusion of picrotoxin in Lister hooded rats did not affect PPI but tended to reduce startle. Picrotoxin caused locomotor hyperactivity and increased fine movement counts alongside tic-like movements.

5.4.1 Dorsal striatal disinhibition does not affect prepulse inhibition but causes tic-like movements

Our findings of no change in prepulse inhibition following dorsal striatal disinhibition, are opposed to our hypothesis and are not consistent with previous striatal lesion studies (Kodsi & Swerdlow, 1995, 1997; Baldan Ramsey et al., 2011), nor with genetic mouse models of Tourette Syndrome (Castellan Baldan et al., 2014; Campbell et al., 1999), who reported reductions in PPI. Dorsal striatal disinhibition tended to reduce startle reactivity, contrasting previous striatal lesions studies where an increase in startle amplitude was reported (Kodsi & Swerdlow, 1994, 1995). Our findings indicate that GABAergic inhibition may not be required for prepulse inhibition. Furthermore, the intact PPI after striatal disinhibition does not support a direct contribution of striatal disinhibition to PPI deficits in Tourette Syndrome.

5.4.2 Dorsal striatal disinhibition causes increased locomotor activity and fine movement count alongside tic-like movements

Dorsal striatal disinhibition caused tic-like movements and significantly increased locomotor activity and fine movement count. Highest locomotor activity was observed at the start of a session, which decreased over time due to habituation. The biggest difference of locomotor activity between the drug conditions (picrotoxin vs saline) was 5 min to 35 min after infusion. This corresponds well to our data collected in Chapter 4. The change in the fine movement counts was bigger than of the locomotor activity and had a different temporal pattern. The time course of the fine movement count was similar to the time course of tic-like movements (an increase over the first 25 min vs 30 min before it decreased) and the frequency of fine movement counts and tic-like movements was in a similar range per 5 min block (min: 45 vs 30, max: 80 vs 75). Although information such as the onset and duration of tic-like movements were not collected in this experiment, the similarities of the time courses and counts suggest, that the fine movement count may reflect tic-like movements and that open field photo beam activity boxes could be used as an automated method to quantify tic-like movements.

The findings of locomotor hyperactivity alongside tic-like movements suggest that dorsal striatal activity is not only involved in generating movements of individual body parts, but also in modulating locomotor activity,

consistent with other studies associating dorsal striatum with locomotor control (e.g. Yoshida et al. (1991); West et al. (1990); Jurado-Parras et al. (2020)). The findings also reveal that tic-like movements do not interfere significantly with locomotion and still lead to hyperactivity (in line with (Godar et al., 2016)).

5.4.3 Relating our findings to Tourette Syndrome

Swerdlow and colleagues suggested that motor or vocal tics are due to failed automatic gating of sensory information (Swerdlow, 2013; Swerdlow & Sutherland, 2005). However, our findings reveal that acute dorsal striatal disinhibition causes tic-like movements without PPI deficits, indicating that PPI deficits are not necessary for such movements. It might be the case that PPI deficits observed in patients with Tourette Syndrome may arise from compensatory mechanisms, that would not be present in an acute model. A chronic striatal disinhibition model may provide further answers. Alternatively, other brain changes in Tourette Syndrome may account for the PPI deficits found in individuals.

Our data shows that striatal disinhibition contributes to increased locomotor activity. Hyperactivity is often observed in patients with Tourette Syndrome, with around 60% of TS patients also having Attention deficit hyperactivity disorder (ADHD) (Whittington et al., 2016; Freeman et al., 2000; Robertson, 2015). The increased locomotor activity alongside tic-like movements after striatal disinhibition supports the notion of ADHD and Tourette Syndrome not being distinct disorders, but belonging to a broader spectrum of neurodevelopmental disorders, with abnormal basal ganglia activity (particularly in the striatum) and thus sharing similar brain connectivity issues (Kern et al., 2015; Israelashvili et al., 2020).

5.4.4 Limitations

One limitation of our experiments is the lack of information on onset and duration of tic-like movements. As this was not recorded, we do not know the extent to which tic-like movements impacted prepulse inhibition, locomotor activity and fine movement count (although for PPI, we did not find a significant change with picrotoxin infusion).

Another limitation may be the rat strain that we used for the study. Our previous studies found that prefrontal and hippocampal disinhibition in Lister hooded rats did not affect PPI (Pezze et al., 2014; McGarrity et al., 2017), although these manipulations disrupted PPI in other rat strains, including Wistar and Sprague Dawley rats (Bast et al., 2001a; Japha & Koch, 1999). This suggests that, in Lister hooded rats, PPI may be less susceptible to disruption by forebrain manipulations. Therefore, striatal disinhibition in a different rat strain may cause deficits in PPI.

Lastly, a limitation arises from the activity box set up of counting fine

movements. A fine movement count was triggered when a beam was interrupted (transitioned from unblocked to blocked, rather than a beam continuously being blocked) for a second time (or more), with no other beam being interrupted. Therefore, in order for a fine movement, such as a forelimb tic-like movement to count, the forelimb would have to alternate between blocking and unblocking a photobeam. During the time of unblocking, no other body part would have been able to continuously block the photobeam. From our Chapter 4, a tic-like forelimb movement was often accompanied by a twist of the head at the same time. This may result in the photobeam not being in contact with both the head and forelimb at a given time and may thus count a tic-like movement as a fine movement. However, if the head blocked a photobeam and the forelimb moved, such movement may not have been captured by the system. Additionally, if a rat moved and had tic-like forelimb movements at the same time, multiple beams may have been triggered, and no fine movement count would have been registered.

5.4.5 Conclusion

In our study, picrotoxin infusion caused tic-like movements, had no effect on prepulse inhibition, tended to reduce startle and significantly increased locomotor activity and fine motor count. No PPI deficit following striatal disinhibition indicates that GABAergic inhibition in the dorsal striatum is not critical for prepulse inhibition. Our finding that marked tic-like movements were produced alongside intact PPI does not support the possibility that PPI disruption is necessary for tic-like movements (as suggested by Swerdlow and colleagues). The timeline of the fine motor count was similar to the timeline of the tic-like movements, and therefore, fine motor counts may thus be used as an automated measure of tic-like movements. The locomotor hyperactivity alongside tic-like movements suggest that dorsal striatal activity is not only involved in generating movements of individual body parts, but also in modulating locomotor activity, consistent with other studies associating dorsal striatum with locomotor control (e.g. Yoshida et al. (1991); West et al. (1990); Jurado-Parras et al. (2020)) and suggests that striatal disinhibition that contributes to tic-like movements may also contribute to hyperactivity, which is often comorbid with Tourette Syndrome (Robertson, 2015).

6 Pilot studies to examine the feasibility of resting state functional connectivity MRI and Magnetic Resonance Spectroscopy in the rat striatal disinhibition model

Declaration: I conducted surgeries, monitored anaesthesia, and collected and interpreted rsFC MRI and MRS data. Malcolm Prior operated the scanner. Processing and analysis of rsFC MRI was performed by Tracy Farr. Anaesthesia during surgery was monitored by Jacco Renstrom and Rachel Grasmeder Allen.

6.1 Introduction

Resting-state functional connectivity (rsFC) Magnetic Resonance Imaging (MRI) is a powerful tool to investigate functional connectivity changes in the brain at a resting state (Zhu et al., 2019), by recording low frequency spontaneous fluctuations in the blood oxygenation level-dependent (BOLD) signal (Smitha et al., 2017). This imaging method has been used on patients with Tourette Syndrome to better understand the brain's functional connectivity changes in the disorder (Ganos et al., 2014; Ramkiran et al., 2019; Worbe et al., 2012; Cui et al., 2014; Liu et al., 2017; Tikoo et al., 2020; Openneer et al., 2020).

Magnetic Resonance Spectroscopy (MRS) provides an opportunity to measure neuro-metabolites in vivo and non-invasively (Mahone et al., 2018). This tool has been used to investigate changes in glutamate and GABA in patients with Tourette Syndrome, in areas such as the supplementary motor area (Draper et al., 2014; He et al., 2022), premotor cortex (Mahone et al., 2018), primary sensorimotor cortex (Puts & Edden, 2012; Tinaz et al., 2014), anterior cingulate cortex (Freed et al., 2016; Kanaan et al., 2017), thalamus (Kanaan et al., 2017) and striatum (Kanaan et al., 2017). Those areas are of particular interest, as abnormalities of the cortical-striatal-thalamic-cortical circuit appear to play a central role in Tourette Syndrome (Albin & Mink, 2006) and more specifically, motor tics are thought to arise from the loss of inhibitory function (i.e. GABA) in the striatum, which in turn leads to disinhibition of the thalamus and hyperexcitability of the motor cortex, leading to tics (Gilbert, 2006).

Both MR methods are also useful when used on animals, as human brain networks share similar structural and spatial organisation with other species, including rodents and non-human primates (Smucny et al., 2014). This is of great translational value and may allow the use of functional brain connectivity phenotypes as translational markers, aiding therapeutic drug discovery (N. Dawson et al., 2015). RsFC measurements have been conducted on anaesthetised and non-anaesthetised animals, in-

cluding monkeys (Vincent et al., 2007), rats (Krimmel et al., 2019; Liang et al., 2011; Pawela et al., 2008) and mice (Mechling et al., 2014; Nasrallah et al., 2014). These studies however, did not involve implanting a guide cannula into the brain to deliver a drug.

The striatal disinhibition model of Tourette Syndrome, which has been a main focus of this thesis, involves striatal guide cannula implants and microinfusions of picrotoxin, a GABA-A receptor antagonist in rats. Both the guide cannula and the drug infusion may interfere with rsFC MRI measurements. A previous study, conducted by Mandino et al. (2022) used fMRI and intra-cerebral cannulae in mouse brains and obtained sufficient quality BOLD data, however, we aimed to provide proof of principle that standard rsFC MRI measurements are possible in rats with pre-implanted guide cannulae and microinfusions in the dorsal striatum. We have previously conducted MRS on the prefrontal cortex and septum, following ventral hippocampus disinhibition (e.g. Chapter 2) and therefore did not expect any problems when taking spectra from the motor cortex in rats unilaterally implanted with a striatal guide cannula.

6.1.1 Aims

We aimed to provide proof of principle that standard resting-state functional connectivity MR measurements and MRS measurements of neuro-metabolites, including glutamate and GABA, in the motor cortex are possible in rats with pre-implanted guide cannulae and microinfusions in the dorsal striatum.

6.2 Methods

6.2.1 Rats

Eight male adult Lister hooded rats (Envigo, UK), weighing between 300 g and 330 g, and aged approximately 10-11 weeks, at the time of surgery were used. The study was run in two batches. Of the first four rats, one was left intentionally unoperated to establish that we could obtain good quality rsFC MRI data without guide cannula implant. The other three rats were implanted with unilateral dorsal striatal guide cannulae, but could not be scanned: one rat died in the scanner; in the other two rats, the head caps fell off, before the scanning. Based on the problems with the head caps in the first batch, adaptations were made to the head caps for the second batch (see Section 6.2.2). All four rats of the second batch were scanned.

Rats were housed in groups of four in two-level high top cages (462 mm x 403 mm x 404 mm; Techniplast, UK). To minimize the risk of damaging cannula implants, food hoppers were removed and replaced with pots lying on the floor after surgery. Food (Teklad global 18% protein diet 2019, Harlan, UK) and water was provided ad libitum. Animals were housed in

an altering light/dark cycle of 12 h per phase (lights were on between 7 am and 7 pm), at a temperature of $21 \pm 1.5^\circ\text{C}$ and a humidity of $50 \pm 8\%$. All experimental work was carried out during the light phase. Prior to the start of any experimental procedures, rats were given at least 7 days to acclimate to the new environment and were handled daily to habituate them to the experimenters. All procedures were conducted in accordance with the requirements of the United Kingdom (UK) Animals (Scientific Procedures) Act 1986. All efforts were made to minimise animal suffering and to reduce the number of animals used. Procedures were carried out under the personal licence number I71997928, granted by the Home Office.

6.2.2 Surgery - Stereotaxic implantation of guide cannula into the right anterior dorsal striatum

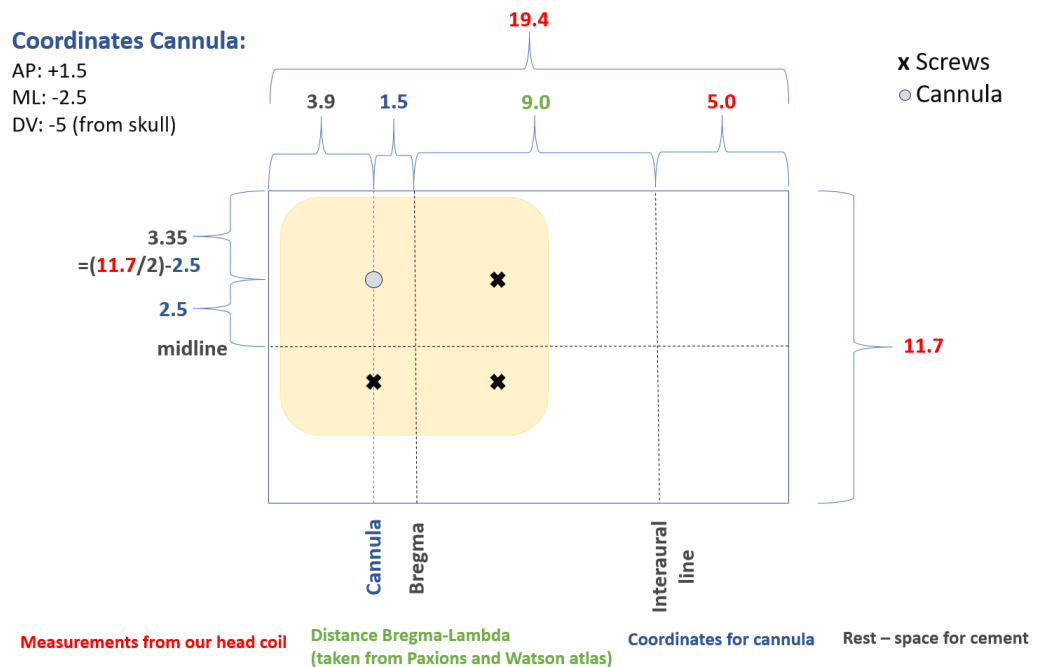
All rats but one, underwent stereotaxic surgery to implant an infusion guide cannula into the anterior dorsal striatum. Rats were anaesthetised with isoflurane in oxygen (induced with 3% and maintained at 1.5–3%; flow rate 1 L/min). Following induction of anaesthesia, rats were subcutaneously injected with an analgesic (Rimadyl large animal solution, 1:9 dilution, 0.1 ml/100g, s.c., Zoetis, UK) and an antibiotic (Synylox, 14% Amoxicillin, Zoetis, UK, 0.2 ml/100 g) to act as a prophylactic against infections. Rats were positioned in a stereotaxic frame. EMLA cream, containing a local anaesthetic (lidocaine, prilocaine, 5%, AstraZeneca, UK), was applied onto the ear bars to reduce pain, and an eye gel (Lub-rithal, Dechra, UK) was used to prevent ocular drying. An incision was made in the scalp, the skull was exposed and bregma and lambda were aligned horizontally. A hole was drilled unilaterally above the infusion site, 1.5 mm anterior to bregma and 2.5 mm right from the midline. Through the hole, an MR compatible infusion guide cannula (PEEK, 26 gauge, 4.4 mm below pedestal; Plastics One, USA), with a stainless-steel stylet (C315DC/Spc to fit 4.4 mm 315G with 2.0 mm projection, Plastics One Inc, USA) was inserted into the brain, to prevent occlusion of the guide cannula. The tip of the stylet, which protruded 2.0 mm from the tip of the guide was aimed at a coordinate of 5.0 mm ventral from the skull. Because the infusion cannula would also protrude 2.0 mm from the guide, this would result in an infusion target coordinate of 1.5 mm anterior to bregma, 2.5 mm right from the midline and 5.0 mm ventral from the skull. These coordinates to target the anterior dorsal striatum were based on our previous studies (Chapters 3, 4, 5).

The guide cannulae was secured in place to the skull using dental cement (Simplex Rapid Powder with Simplex Rapid liquid, Kemdent, UK) and three MR compatible nylon screws (Plastics One, USA). Screws were implanted to the side of, and behind the cannula, to ensure stabilisation of the unilateral implant (Figure 38). For the first batch, screws were purposely implanted not too deep, as our previous MRS study (Chapter 2)

revealed deep screws caused image artefacts. Moreover, the use of cement was minimised at the front of the cannula as well as at the side, due to restricted space from the head coil. Measurements from the head coil were taken to determine the maximal extent of cementing that could be used around the cannula (Figure 38). The open wound was then stitched to reduce its size. Rats received an intraperitoneal injection of saline (1 ml) for rehydration and were monitored as they recovered from the anaesthesia. Following surgery, rats were checked, weighed, and injected with antibiotic (Synylox, 14% Amoxicillin, Zoetis, UK, 0.2 ml/100 g). Rats were given at least 5 days to recover before scanning.

As two out of three rats lost their head caps from the first batch, we adapted our method of cementing and placing screws, for the second batch of rats. To increase stabilisation, screws were implanted deeper (accepting some susceptibility artefacts) and cement was built up on the left side and back of the implant. The head caps for the second batch of rats were stable.

Figure 38: Graphical visualisation of guide cannula and screw implants



Note: Sketch is to scale. Numbers in millimeters.

6.2.2.1 Animal preparation for rsFC MRI and MRS

Rats were initially anaesthetised with 3% isoflurane in oxygen (1%) in an induction area outside the scanner room, and the stainless-steel stylet was removed from the striatal guide cannula. After transporting the rat over to a pre-warmed cradle in the MR scanner room, the head of the rat

was restrained using tooth and ear bars. An eye gel (LubriThal; Dechra, UK) was applied to prevent eyes from drying out during scanning. In the scanner, isoflurane was delivered through a nose cone with a mixture of O₂ and N₂O as carrier gases (in the ratio 0.33:0.66 L/min, respectively). The level of the anaesthetic was adjusted (isoflurane 1-3%) to maintain a stable respiratory rate around 60 ± 10 . Respiratory rate was monitored using an ERT control/gating module (Model 1032, SA Instruments, Stony Brook, USA), of which the sensors were positioned under the abdomen of the rat, below the diaphragm, which detect movement of the rib cages when the animal breathes. A pulse oximeter (SA Instruments, Stony Brook, USA) was positioned onto the rats' foot. The rats' body temperature was measured using a rectal thermal probe and controlled by a water-pump system that was connected to tubing embedded in the base of the rat cradle. Temperature was maintained around $37 \pm 1^\circ\text{C}$. For the rsFC MRI a receive-only single coil with active detuning and curved to fit the rats head was used (Bruker, Germany). For the MRS measurements, a surface receive-only head coil, consisting of 4 channels (Bruker, Germany) was chosen based on previous experiments (e.g. Chapter 2). The MR compatible infusion cannula (PEEK, 33-gauge, to fit the guides with 2 mm protrusion; Plastics One, USA) for the right anterior dorsal striatum infusion was inserted into the guide of the operated rat (Figure 39), before the rat was moved into the scanner bore.

Figure 39: Photograph of head coil set up for rsFC MRI scanning



Note: Overhead view of a rat in the cradle and restrained with ear bars (orange screws). The head coil used for rsFC scanning is placed on the rats' head and an infusion cannula was inserted into the guide.

6.2.3 rsFC MRI and ¹H-MRS acquisition

RsFC MRI and MRS measurements were conducted on a 7 Tesla Bruker Biospec 70/30 USR horizontal bore small animal scanner (Bruker, Germany) running ParaVision 5 and 6. A surface reception coil, consisting of 4 coils, was placed as closely to the guide cannula as possible. To ensure

that the motor cortex was in the centre of the magnet, a quick gradient echo acquisition scan was performed (TE = 6 ms, TR = 100 ms). Anatomical reference images were obtained in three orthogonal planes using a rapid acquisition with relaxation enhancement (RARE) sequence (Hennig et al., 1986) with TR = 5 s, flip angle = 90° and rare factor = 8.

For the *rsFC MRI measurements*, scan slices were lined up with the anterior commissure (corresponding to the AP and ML coordinates of bregma (Prior et al., 2021)). A gradient echo-echo planar imaging (GE-EPI) sequence was used for rsFC MRI (TE = 15 ms, RE = 2000 ms, FOV: 30 x 30, data points: 64 x 64, in plane resolution = 0.469 x 0.469, flip angle: 68°). 300 volumes were acquired.

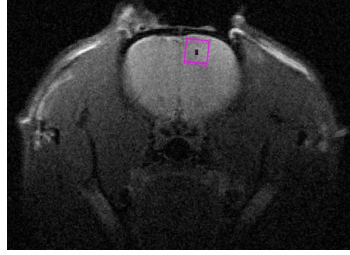
The *MRS measurements* were the same as in Chapter 2: the axial MRI scan slice (which corresponds to coronal view) was with TE = 14 ms, TE_{effective} = 28 ms, FOV = 40x40 mm and spatial resolution = 0.156 x 0.156. The values for the dorso-ventral views were TE = 25 ms, TE_{effective} = 50 ms, FOV = 40 x 40, spatial resolution = 0.156 x 0.156, and for the sagittal views were TE = 25 ms, TE_{effective} = 50 ms, FOV = 50 x 36 mm, spatial resolution = 0.195 x 0.141. For both the rsFC MRI and MRS measurements, axial, sagittal and dorso-ventral slice thickness was 1 mm.

A voxel of 2x2x2 mm³ was positioned in the motor cortex for the acquisition of MRS data (Figure 40). Gradient echo sequence was used to calculate a phase difference, to map the homogeneity of the overall magnetic field, allowing enhancement of B₀ homogeneity. Local magnetic field homogeneity was adjusted within the motor cortex by applying FASTMAP (Gruetter, 1993). Localised proton MR spectroscopy was obtained using a Point Resolved Spectroscopy (PRESS) sequence (Bottomley, 1987) with an acquisition time of 34 min (acquisition parameters: TE = 13.5 ms, TR = 2000 ms, spectral width of 4006.41 Hz with 2048 points and 1024 averages with Eddy current compensation) after water suppression with variable power and optimized relaxation delays (VAPOR) (Tkáč et al., 1999).

6.2.4 rsFC MRI combined with striatal saline microinfusions

Microinfusions were performed as described in Chapter 2 (Section 2.2.5). Here, the infusion cannula tip protruded 2.0 mm below the guides into the dorsal striatum. The air plug (0.25 µl), plus a volume of 0.5 µl of saline was infused unilaterally over the course of approximately 90 s (30 s for air plug + 60 s for saline). Rats underwent pre- and post-infusion rsFC MRI scans, followed by MRS of the motor cortex. After the scans, rats were overdosed with pentobarbital (Dolethal, Vetoquinol, UK), while still under isoflurane anaesthesia.

Figure 40: Coronal view of voxel placement in motor cortex



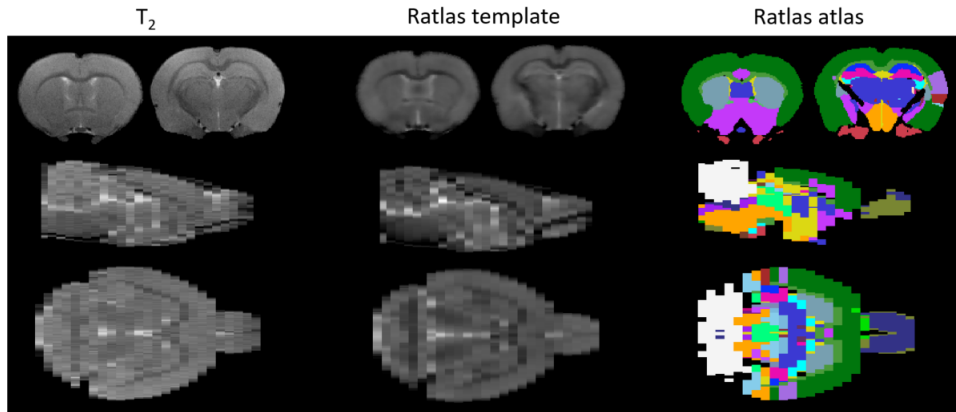
Note: Coronal view (axial slice) of the unoperated rat brain. Purple box shows localisation of the voxel of interest ($2 \times 2 \times 2 \text{ mm}^3$) in the motor cortex and delineates the area in which spectra were acquired. It was used to quantify the relative metabolite concentrations.

6.2.5 Processing and analysis of rsFC MRI & MRS data

RsFC MRI data was converted to NIfTI format using Bru2nii (<https://github.com/neurolabusc/Bru2Nii>) and Brkraw (<https://github.com/BrkRaw/brkraw>) and scaled by a factor of 10. Visual inspection of the images revealed that only the data from the unoperated rat was suitable for rsFC analysis (see Results 6.3.1). The Ratlas-LH brain template and atlas of the young adult male Lister hooded brain (Prior et al., 2021) was registered to the T_2 images of the unoperated rat (Figure 41). Registration was performed using Advanced Normalization Tools (ANTs) (<https://github.com/ANTsX/ANTs>), using a non-linear approach. The Ratlas mask was multiplied by the resting state image to skull strip. The FMRIB Software library (FSL) (www.fmrib.ox.ac.uk/fsl) was used for rsFC MRI data analysis. All data was high passed filtered (as BOLD was low frequency $> 0.01 \text{ Hz}$), nuisance regressed (corrected for scanner drift, motion and physiological rhythms) with MCFLIRT and smoothed by the full width at half maximum (0.7 mm kernel). For the seed-based analysis, a 1 mm sphere was used and dual regression was performed to identify the voxels that were correlated with the seed.

Processing of MRS was done as in Chapter 2. MRS data was analysed using LCModel software (S. W. Provencher, 1993) in a fully automated pipeline. The analysis window ranged from 0.2 to 4.0 ppm . Data was fitted to a basis set containing 21 metabolites: alanine (Ala), aspartate (Asp), creatine (Cr), phosphocreatine (PCr), gamma-aminobutyric acid (GABA), glucose (Glc), glutamine (Gln), glutamate (Glu), glycerophosphorylcholine (GPC), phosphorylcholine (PCh), glutathione (GSH), myo-inositol (m-Ins), lactate (Lac), n-acetyl aspartate (NAA), n-acetyl aspartate glutamate (NAAG), scyllo-inositol (Scyllo), taurine (Tau), total creatine (Cr+PCr), total choline (GPC+PCh), NAA+NAAG (tNAA) and glutamate + glutamine (Glx). Metabolite concentrations were determined as a ratio to total creatine (Cr+PCr) (S. W. Provencher, 1993).

Figure 41: Registration of Ratlas to the unoperated rat brain



Note: Registration of the brain of the unoperated rat in the present study to the template and atlas from Ratlas (Prior et al., 2021)

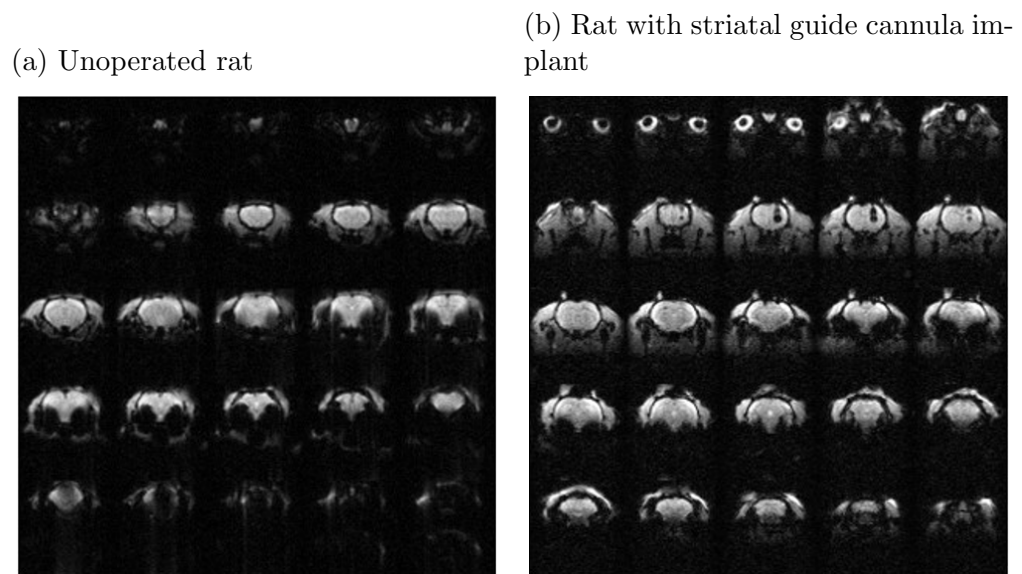
Cramér-Rao lower bounds (CRLB) provide quantitative error estimates for metabolic quantification, to assess reliability of the metabolite concentration (Öz et al., 2014), with CRLB values under 20% deemed as reliable spectra fitting. We included any metabolite measurement with a CRLB of 50%. The following metabolites were undetectable: Asp, PCr, GABA, Glc, PCh, GSH, Lac, Scyllo, -CRCH2, as well as lipids. Macromolecule components were not analysed for this study.

6.3 Results

6.3.1 Identification of default network in unoperated but not operated rat

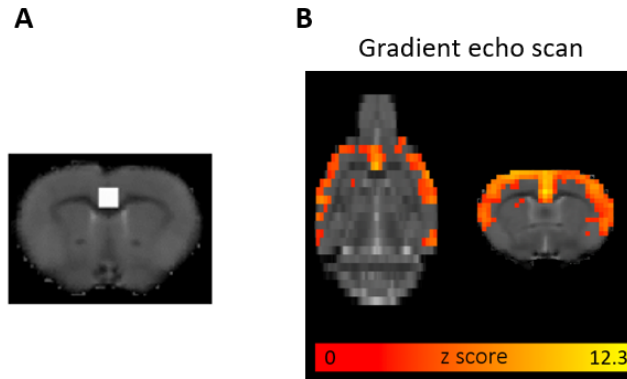
Firstly, gradient echo images were visually inspected to see if they have sufficient signal for the analysis (Figure 42). All cannulated rats (Figure 42b) had big signal dropout, and thus the data could not be used for further analyses. Signal was sufficient for the unoperated rat (Figure 42a).

Figure 42: Coronal view of gradient echo images taken from the unoperated (a) and an operated (b) rat



To see if we could identify the classical default mode network, that had been identified by previous studies (Lu et al., 2012; G. R. Hall et al., 2022), in the unoperated rat, the signal over time of a cluster of voxels in the anterior cingulate was correlated to the time series of the rest of the brain (Figure 43). This revealed statistically similar time series in the cingulate cortex, orbital cortex, prelimbic cortex, retrosplenial cortex, visual cortex, auditory cortex, temporal association cortex, primary and secondary somatosensory cortex, insula cortex and prefrontal cortex (infralimbic and dorsal peduncular cortex). Additionally, we found correlations with the motor cortex and claustrum.

Figure 43: Seed based analysis with the anterior cingulate



Note: **A** Coronal view of seed placement in the anterior cingulate. **B** Axial and coronal view of unoperated rat depicting voxels in orange that had a time series that correlated with the time series of the anterior cingulate.

6.3.2 Poor signal for MRS with cannula implant in the striatum and the motor cortex as ROI

MRS data was acquired of one rat with a guide cannula implant in the right striatum and the motor cortex as region of interest (ROI). Creatine (Cr), total creatine (Cr+PCr), glutamate (glu), glutamate + glutamine (glx), n-acetyl aspartate (NAA) and NAA+NAAG (tNAA) were reliably measured, with a CRLB threshold of under 20%. Alanine (Ala), glutamine (gln), glycerophosphorylcholine (GPC), myo-inositol (m-Ins), n-acetyl aspartate glutamate (NAAG), taurine (tau) and total choline (GPC + PCh) had CRLB values of under 50%. GABA could not be reliably measured, with a CRLB of 55%. For this scan, we had a poor shim value (11.2 Hz) and a low Signal to Noise ratio value for the water signal of the voxel in the motor cortex ($\text{SNR}_{\text{H}_2\text{O}} = 71.8$). From another rat we obtained a shim value of 13.0 Hz and $\text{SNR}_{\text{H}_2\text{O}}$ of 90.1, however, did not continue with a scan, as we deemed the shim value as too high.

6.4 Discussion

We obtained sufficient quality rsFC MRI data to reveal the resting-state default mode network of an unoperated rat, using the anterior cingulate as a seed: The cingulate cortex, orbital cortex, prelimbic cortex, retrosplenial cortex, visual cortex, auditory cortex, temporal association cortex, primary and secondary somatosensory cortex, insula cortex and prefrontal cortex (infralimbic and dorsal peduncular cortex) had time series that correlated with the time series of the anterior cingulate, and have all been previously identified as regions that are part of the rodent default mode network (Lu et al., 2012). Our analysis also revealed the claustrum, a subcortical region previously associated with the salience

network (J. B. Smith et al., 2020). This correlation may be due to high noise at the single subject level which may disappear if more rats were added. Our analysis also showed significant correlations with the motor cortex, a region in very close proximity to the cingulate cortex. Our results are likely due to activity in the cingulate cortex being widespread and covering areas in the medial anterior to posterior direction as well as noise. Overall, our findings support that our imaging sequence and anaesthetic procedure is suitable for good quality rsFC MRI. However, we were unable to obtain any resting-state default mode network of an operated rat, due to the significant signal loss caused by the presence of the guide cannula.

MRS data from the motor cortex was acquired of one rat that had a cannula implanted in the striatum. We reliably measured creatine, total creatine, glutamate, glutamate + glutamine, NAA, and NAA+NAAG (with a CRLB threshold of under 20%). However, our MR signal was quite poor. This contrasted with our previous MRS studies in rats with ventral hippocampal implants, where we disinhibited the ventral hippocampus, measured neuro-metabolites from the prefrontal cortex (PFC) and the septum (Chapter 2), and obtained sufficient signal. One possible explanation for lower signals is the distance between the area with the guide cannula implant and the region of interest (ROI). When calculating distances between the implanted area and the ROI, it is noticeable that the greater the distance, the greater signal we obtain. For our calculations we used a voxel from the ROI, located it in the Ratlas (Prior et al., 2021) and subtracted the coordinates from the target coordinates for the infusion cannula. The following shows the distance between the regions with the signal to noise ratio value for the water signal of the voxel (SNR_H₂O). It is clear that bigger distances had higher SNR_H₂O values (mean \pm SEM):

- **Ventral hippocampus to PFC** distance: 8.50 mm, SNR_H₂O = 284.16 \pm 9.86
- **Ventral hippocampus to septum** distance: 6.55 mm, SNR_H₂O = 185.29 \pm 10.46
- **Dorsal striatum to motor cortex** distance: 1.80 mm, SNR_H₂O = 80.95 \pm 12.94

It is possible, that higher signals are obtained with greater distances, due to the head coil being able to cover the ROI fully, and not being blocked by the guide cannula and cement.

6.4.1 Conclusion

To conclude, our imaging sequence and anaesthetic procedure is suitable to show the resting state network in an unoperated rat. However, for operated rats implanted with an intracerebral guide cannula, the cannula causes too much signal dropout, making rsFC MRI analysis impossible. For MRS measurements, a region at a greater distance from the implant likely leads to higher signals.

7 General discussion

The work in this thesis addressed the effect of hippocampal and striatal disinhibition (i.e. reduced inhibitory GABA transmission) on behaviour, neuro-metabolites in a projection site, and neural activity in the disinhibited region. Hippocampal disinhibition has been implicated in cognitive disorders such as schizophrenia and striatal disinhibition with Tourette Syndrome. Within this thesis, we firstly extended on a previous Single-Photon Emission Computed Tomography (SPECT) experiment that showed that ventral hippocampal disinhibition caused marked metabolic activation in several extra-hippocampal brain sites, including the lateral septum (Williams et al., in preparation). Using Magnetic Resonance Spectroscopy (MRS), we investigated the effects of ventral hippocampal disinhibition on the neuro-metabolites in the septum (Chapter 2). To the best of our knowledge, there are currently no studies that performed region-specific neuronal manipulation and measured its impact on a distal site using MRS. Overall, we were able to robustly acquire a neurochemical profile comparable to previous rodent studies. Our study revealed no clear effects of hippocampal disinhibition on any of the neuro-metabolites measured in the septum, including glutamate, glutamine and GABA. In light of our SPECT study, where ventral hippocampus disinhibition caused marked metabolic activation in the lateral septum, the failure of our MRS measurements to detect any changes in neuro-metabolites in the lateral septum under anaesthesia may indicate that marked acute metabolic activation in the lateral septum (as detected by SPECT) is not accompanied by neuro-metabolites changes measurable by MRS.

Much of this thesis focused on striatal disinhibition. First, we examined the effects of striatal disinhibition, induced by picrotoxin infusions into the anterior dorsal striatum, on neural activity in the vicinity of the infusion site, using electrophysiological measurements in anaesthetised rats (Chapter 3). By combining multi-unit and local field potentials (LFP) recordings, using an infusion cannula attached to a multi-wire array, we confirmed that striatal picrotoxin infusions induced large LFP spike-wave discharges, consisting of a single negative spike followed by a positive wave, similar to previous studies in freely moving rats (e.g., Israelashvili & Bar-Gad (2015); Klaus & Plenz (2016); McCairn & Isoda (2013); Vinner Harduf et al. (2021)) and observed sharp multi-unit bursts during the negative LFP spike. Our study complements these previous findings by showing that these LFP discharges occur without tic-like movements under anaesthesia. To our knowledge, we are the first to characterise changes in striatal multi-unit measurements caused by striatal disinhibition. We showed that disinhibition specifically enhances burst firing, reflected by significant increases in mean spike frequency in burst per bin, mean peak spike frequency in burst and percentage spikes and by increased frequency in which bursts occur, reflected by significant decreases of mean interburst

interval per bin, after picrotoxin infusion into the striatum. This is a new finding in the striatum and is consistent with disinhibition induced enhancement of burst firing that we previously reported in the prefrontal cortex and hippocampus (Pezze et al., 2014; McGarrity et al., 2017), suggesting that in all these regions, GABA-A receptor-mediated inhibition is particularly important to control neural burst firing.

In our following experiment (Chapter 4), we confirmed that striatal disinhibition, by local microinfusion of the GABA-A receptor antagonist picrotoxin causes tic-like movements as previously reported (e.g., Pogorelov et al. (2015); Klaus & Plenz (2016)). Additionally, the time course of the movements was characterised and some key features of tic-like movements, based on visual inspection of the rats, was described. After unilateral local microinfusion of picrotoxin into the right anterior dorsal striatum we successfully caused tic-like movements of the left forelimb in all rats. We confirmed that tic-like movements can be reliably and repeatedly induced within the same rat, with a second and third infusion. The most common tic-like movement involved the rat lifting its left forelimb, thereby rotating its head and torso to the right around the body's long axis, before putting the left forelimb back down again, and thereby moving its head and torso into their starting position. There were also some more pronounced forelimb movement that lasted for several seconds and led to a whole rotation of the body around its long axis. There was substantial inter-rat variability and number of tic-like movements per 5 min block also varied between rats, however most rats expressed highest tic-like movements within the first 5 min to 35 min, which is in line Patel & Slater (1987). There was also substantial intra-rat variability with the same rat showing different intensity (number) and time course of tic-like movements after each infusion.

Following this experiment, we investigated the impact of striatal disinhibition on locomotor activity and prepulse inhibition (PPI) (Chapter 5), as both may be important markers of basal ganglia dysfunction, with disrupted PPI and increased locomotor activity having been previously associated with similar striatal dysfunction in rodent models. However, how distinct types of striatal dysfunction, related to distinct disorders, affect these measures, still remains largely to be clarified. Our study contributes to addressing this gap, focusing on striatal disinhibition, which has been linked to Tourette Syndrome. Our findings reveal that dorsal striatal disinhibition causes tic-like movements, has no effect on prepulse inhibition, reduces startle and significantly increases locomotor activity and fine motor count. Our findings show, that GABAergic inhibition in dorsal striatum is not critical for prepulse inhibition. Intact PPI following acute striatal disinhibition contrasts with PPI disruption in patients with Tourette Syndrome. This may partly reflect differences between acute and chronic disinhibition, but, in view of the marked tic-like movements produced alongside intact PPI, it does not support that PPI deficits

are necessary for tic-like movements (as suggested by Swerdlow and colleagues (Swerdlow, 2013; Swerdlow & Sutherland, 2005). The findings of locomotor hyperactivity alongside tic-like movements suggest that dorsal striatal activity is not only involved in generating movements of individual body parts, but also in modulating locomotor activity and suggests that striatal disinhibition that contributes to tic-like movements may also contribute to hyperactivity, which is often comorbid with Tourette Syndrome (Robertson, 2015).

Lastly, we aimed to provide proof of principle that standard rsfc MRI measurements are possible in rats with pre-implanted guide cannulae and microinfusions in the dorsal striatum (Chapter 6). Although we obtained sufficient quality resting-state functional connectivity MR data to reveal the resting-state default mode network of an unoperated rat, using the anterior cingulate as a seed, we were unable to obtain any resting-state default mode network of an operated rat, due to the significant signal loss from the guide cannula. We also tried to obtain spectra from the motor cortex following striatal disinhibition (using MRS), however, were unable to get good Signal to Noise ratio (SNR) values for the water signal of the voxel. When comparing the SNR values between our studies, it appears that SNR decreases with decreased distance between regions (disinhibited region and ROI for spectrum).

8 Conclusions and future directions

This thesis has demonstrated that ventral hippocampal disinhibition in anaesthetised rats has no clear effect on any neuro-metabolites measured in the septum, including glutamate, glutamine and GABA, despite its marked metabolic activation shown previously with SPECT. More broadly, this finding suggests that marked metabolic activation of a brain region may not result in neuro-metabolite changes as measurable by MRS. Furthermore, we showed that right dorsal striatal disinhibition causes tic-like movements in the left forelimb, increases locomotor activity and fine motor count. The findings suggest that dorsal striatal activity is not only involved in generating movements of individual body parts, but also in modulating locomotor activity. Our studies also revealed that striatal disinhibition does not affect prepulse inhibition and that a deficit in prepulse inhibition is not necessary for the expression of tic-like movements. Electrophysiological studies showed that striatal disinhibition in anaesthetised rats caused enhanced burst firing as well as large LFP spike-wave discharges, consisting of a single negative spike, followed by a positive wave. Striatal disinhibition in anaesthetised rats did not evoke tic-like movements. Lastly, we showed that guide cannula implants cause too much signal loss to obtain resting state functional connectivity Magnetic Resonance Imaging measurements of sufficient quality. Furthermore, when using Magnetic Resonance Spectroscopy, a greater distance between the guide cannula and the region of interest would likely lead to higher signals.

Future experiments could use single photon emission computed tomography (SPECT) imaging (Oelschlegel & Goldschmidt, 2020) to identify the widespread effects of striatal disinhibition on other brain regions in freely moving rats and compare those regions to key regions identified in Tourette Syndrome, such as the cortical-striatal-thalamic-cortical circuit. Using electrophysiological recordings, it would be of great value to measure LFP spike-wave discharges and multi-unit bursting in distal brain regions (potentially regions identified with SPECT) after striatal disinhibition and characterise any changes. In particular, comparing potential changes in the forepaw region of the rodent primary motor and primary somatosensory cortex to the striatum, would allow a clearer understanding of the relationship between the brain regions. Additionally, in previous electrophysiological studies under isoflurane anaesthesia, we were able to measure changes in regional neural activity caused by neuropharmacological manipulations and these changes corresponded well to behavioural changes caused by the same manipulations in awake rats (McGarrity et al., 2017; Pezze et al., 2014). In our studies we tried to clarify by which neural pathways and mechanisms imbalanced neural activity affect behaviour, however, it would also be of great interest to identify neuropharmacological strategies that could be used to restore and maintain balanced neural activity, and hence intact behaviour.

Furthermore, a chronic striatal disinhibition model, where a mini-osmotic pump is implanted subcutaneously in the rat's back for prolonged infusion (Vinner et al., 2017), may provide greater insight into the disorder as it likely captures some compensatory mechanisms. Chronic striatal disinhibition, which causes tic-like movements, will likely cause hyperactivity of remotely connected areas, including the supplementary, primary and secondary motor region. However, as Tourette Syndrome typically follows a developmental time course (Leckman et al., 1998) where many adolescents gain greater control over their tics (Cohen et al., 2013), it has been proposed that this gain in control is due to tonic inhibition. Based on previous studies in patients with Tourette Syndrome, we would predict compensatory changes, with an increase in GABA levels in the SMA (Draper et al., 2014), which can be measured using MRS, as well as a decrease in fMRI BOLD activation in the SMA and primary motor cortex (Draper et al., 2014; J. Jung et al., 2013). Additionally, the increased tonic inhibition likely reduces tic-like movements. Understanding the neurobiological basis for the remission of tics may not only further our understanding of why some individuals with Tourette Syndrome do not gain control over their tics but it is also of fundamental importance for developing treatments for Tourette Syndrome.

References

- Akbarian, S., Kim, J. J., Potkin, S. G., Hagman, J. O., Tafazzoli, A., Bunney, W. E. & Jones, E. G. (1995). Gene Expression for Glutamic Acid Decarboxylase is Reduced without Loss of Neurons in Prefrontal Cortex of Schizophrenics. *Archives of General Psychiatry*, *52*(4), 258–266. doi: 10.1001/archpsyc.1995.03950160008002
- Aksenov, D. P., Li, L., Miller, M. J., Iordanescu, G. & Wyrwicz, A. M. (2015). Effects of anesthesia on BOLD signal and neuronal activity in the somatosensory cortex. *Journal of Cerebral Blood Flow and Metabolism*, *35*(11), 1819–1826. doi: 10.1038/jcbfm.2015.130
- Albin, R. L. & Mink, J. W. (2006). Recent advances in Tourette syndrome research. *Trends in Neurosciences*, *29*(3), 175–182. doi: 10.1016/j.tins.2006.01.001
- Alderton, G. (2020). From animal models to humans. *Science*, *367*(6479), 754B. doi: 10.1126/SCIENCE.367.6479.752-H
- Alkire, M. T., Haier, R. J., Shah, N. K. & Anderson, C. T. (1997). Positron emission tomography study of regional cerebral metabolism in humans during isoflurane anesthesia. *Anesthesiology*, *86*(3), 549–557. doi: 10.1097/00000542-199703000-00006
- Andersen, M. L. & Winter, L. M. (2019). Animal models in biological and biomedical research – experimental and ethical concerns. *Anais da Academia Brasileira de Ciencias*, *91*. doi: 10.1590/0001-3765201720170238
- Arnt, J. (1981). Hyperactivity following injection of a glutamate agonist and 6, 7-ADTN into rat nucleus accumbens and its inhibition by THIP. *Life Sciences*, *28*(14), 1597–1603. doi: 10.1016/0024-3205(81)90314-3
- Austin, M. C. & Kalivas, P. W. (1988). The effect of cholinergic stimulation in the nucleus accumbens on locomotor behavior. *Brain Research*, *441*(1-2), 209–214. doi: 10.1016/0006-8993(88)91400-X
- Baldan Ramsey, L. C., Xu, M., Wood, N. & Pittenger, C. (2011). Lesions of the dorsomedial striatum disrupt prepulse inhibition. *Neuroscience*, *180*, 222–228. doi: 10.1016/j.neuroscience.2011.01.041
- Barré-Sinoussi, F. & Montagutelli, X. (2015). Animal models are essential to biological research: Issues and perspectives. *Future Science OA*, *1*(4). doi: 10.4155/fso.15.63
- Bartha, R., Williamson, P. C., Drost, D. J., Malla, A., Carr, T. J., Cortese, L., ... Neufeld, R. W. (1997). Measurement of glutamate and glutamine in the medial prefrontal cortex of never-treated schizophrenic patients and healthy controls by proton magnetic resonance

- spectroscopy. *Archives of General Psychiatry*, 54(10), 959–965. doi: 10.1001/archpsyc.1997.01830220085012
- Basar-Eroglu, C., Schmiedt-Fehr, C., Mathes, B., Zimmermann, J. & Brand, A. (2009). Are oscillatory brain responses generally reduced in schizophrenia during long sustained attentional processing? *International Journal of Psychophysiology*, 71(1), 75–83. doi: 10.1016/j.ijpsycho.2008.07.004
- Bast, T. & Feldon, J. (2003). Hippocampal modulation of sensorimotor processes. *Progress in Neurobiology*, 70(4), 319–345. doi: 10.1016/S0301-0082(03)00112-6
- Bast, T., Pezze, M. & McGarrity, S. (2017). Cognitive deficits caused by prefrontal cortical and hippocampal neural disinhibition. *British Journal of Pharmacology*, 174(19), 3211–3225. doi: 10.1111/bph.13850
- Bast, T., Zhang, W. N. & Feldon, J. (2001a). Hyperactivity, decreased startle reactivity, and disrupted prepulse inhibition following disinhibition of the rat ventral hippocampus by the GABAA receptor antagonist picrotoxin. *Psychopharmacology*, 156(2-3), 225–233. doi: 10.1007/s002130100775
- Bast, T., Zhang, W. N. & Feldon, J. (2001b). The ventral hippocampus and fear conditioning in rats: Different anterograde amnesias of fear after tetrodotoxin inactivation and infusion of the GABAA agonist muscimol. *Experimental Brain Research*, 139(1), 39–52. doi: 10.1007/s002210100746
- Batista-Brito, R. & Fishell, G. (2009). The Developmental Integration of Cortical Interneurons into a Functional Network. In *Current topics in developmental biology* (Vol. 87, pp. 81–118). doi: 10.1016/S0070-2153(09)01203-4
- Beasley, C. L., Zhang, Z. J., Patten, I. & Reynolds, G. P. (2002). Selective deficits in prefrontal cortical GABAergic neurons in schizophrenia defined by the presence of calcium-binding proteins. *Biological Psychiatry*, 52(7), 708–715. doi: 10.1016/S0006-3223(02)01360-4
- Bender, F., Gorbati, M., Cadavieco, M. C., Denisova, N., Gao, X., Holman, C., ... Ponomarenko, A. (2015). Theta oscillations regulate the speed of locomotion via a hippocampus to lateral septum pathway. *Nature Communications*, 6(1), 1–11. doi: 10.1038/ncomms9521
- Benes, F. M. & Berretta, S. (2001). GABAergic interneurons: Implications for understanding schizophrenia and bipolar disorder. *Neuropsychopharmacology*, 25(1), 1–27. doi: 10.1016/S0893-133X(01)00225-1
- Benes, F. M., Khan, Y., Vincent, S. L. & Wickramasinghe, R. (1996). Differences in the subregional and cellular distribution of GABAA receptor

- binding in the hippocampal formation of schizophrenic brain. *Synapse*, *22*(4), 338–349. doi: 10.1002/(SICI)1098-2396(199604)22:4<338::AID-SYN5>3.0.CO;2-C
- Benes, F. M., Lim, B., Matzilevich, D., Walsh, J. P., Subburaju, S. & Minns, M. (2007). Regulation of the GABA cell phenotype in hippocampus of schizophrenics and bipolars. *Proceedings of the National Academy of Sciences of the United States of America*, *104*(24), 10164–10169. doi: 10.1073/pnas.0703806104
- Benes, F. M. & Todtenkopf, M. S. (1998). Meta-Analysis of nonpyramidal neuron (NP) loss in layer II in anterior cingulate cortex (ACCx-II) from three studies of postmortem schizophrenic brain. *Soc Neurosci Abstr*, *24*(2), 1275.
- Berardelli, A., Currà, A., Fabbrini, G., Gilio, F. & Manfredi, M. (2003). Pathophysiology of tics and Tourette syndrome. *Journal of Neurology*, *250*(7), 781–787. doi: 10.1007/s00415-003-1102-4
- Berens, P., Keliris, G. A., Ecker, A. S., Logothetis, N. K. & Tolias, A. S. (2008). Comparing the feature selectivity of the gamma-band of the local field potential and the underlying spiking activity in primate visual cortex. *Frontiers in Systems Neuroscience*, *2*(JUN). doi: 10.3389/neuro.06.002.2008
- Bernácer, J., Prensa, L. & Giménez-Amaya, J. M. (2012). Distribution of GABAergic interneurons and dopaminergic cells in the functional territories of the human striatum. *PLoS ONE*, *7*(1). doi: 10.1371/journal.pone.0030504
- Berretta, S., Munno, D. W. & Benes, F. M. (2001). Amygdalar activation alters the hippocampal GABA system: "Partial" modelling for postmortem changes in schizophrenia. *Journal of Comparative Neurology*, *431*(2), 129–138. doi: 10.1002/1096-9861(20010305)431:2<129::AID-CNE1060>3.0.CO;2-6
- Binshtok, A. M., Fleidervish, I. A., Sprengel, R. & Gutnick, M. J. (2006). NMDA receptors in layer 4 spiny stellate cells of the mouse barrel cortex contain the NR2C subunit. *Journal of Neuroscience*, *26*(2), 708–715. doi: 10.1523/JNEUROSCI.4409-05.2006
- Bivard, A., Stanwell, P. & Parsons, M. (2013). Stroke and Cerebral Ischemia. In *Magnetic resonance spectroscopy: Tools for neuroscience research and emerging clinical applications* (pp. 183–195). Academic Press. doi: 10.1016/B978-0-12-401688-0.00014-8
- Bloch, M. H., Leckman, J. F., Zhu, H. & Peterson, B. S. (2005). Caudate volumes in childhood predict symptom severity in adults with Tourette syndrome. *Neurology*, *65*(8), 1253–1258. doi: 10.1212/01.wnl.0000180957.98702.69

- Bogerts, B., Meertz, E. & Schönfeldt Bausch, R. (1985). Basal Ganglia and Limbic System Pathology in Schizophrenia: A Morphometric Study of Brain Volume and Shrinkage. *Archives of General Psychiatry*, 42(8), 784–791. doi: 10.1001/archpsyc.1985.01790310046006
- Bohlhalter, S., Goldfine, A., Matteson, S., Garraux, G., Hanakawa, T., Kansaku, K., ... Hallett, M. (2006). Neural correlates of tic generation in Tourette syndrome: An event-related functional MRI study. *Brain*, 129(8), 2029–2037. doi: 10.1093/brain/awl050
- Boretius, S., Tammer, R., Michaelis, T., Brockmüller, J. & Frahm, J. (2013). Halogenated volatile anesthetics alter brain metabolism as revealed by proton magnetic resonance spectroscopy of mice in vivo. *NeuroImage*, 69, 244–255. doi: 10.1016/j.neuroimage.2012.12.020
- Bortolato, M. & Pittenger, C. (2017). Modeling tics in rodents: Conceptual challenges and paths forward. *Journal of Neuroscience Methods*, 292, 12–19. doi: 10.1016/j.jneumeth.2017.02.007
- Bottomley, P. A. (1987). Spatial Localization in NMR Spectroscopy in Vivo. *Annals of the New York Academy of Sciences*, 508(1), 333–348. doi: 10.1111/j.1749-6632.1987.tb32915.x
- Braff, D. L. & Geyer, M. A. (1990). Sensorimotor gating and schizophrenia human and animal model studies. *Archives of General Psychiatry*, 47(2), 181–188. doi: 10.1001/archpsyc.1990.01810140081011
- Braff, D. L., Geyer, M. A. & Swerdlow, N. R. (2001). Human studies of prepulse inhibition of startle: Normal subjects, patient groups, and pharmacological studies. *Psychopharmacology*, 156(2-3), 234–258. doi: 10.1007/s002130100810
- Bronfeld, M., Israelashvili, M. & Bar-Gad, I. (2013). Pharmacological animal models of Tourette syndrome. *Neuroscience and Biobehavioral Reviews*, 37(6), 1101–1119. doi: 10.1016/j.neubiorev.2012.09.010
- Bronfeld, M., Yael, D., Belevsky, K. & Bar-Gad, I. (2013). Motor tics evoked by striatal disinhibition in the rat. *Frontiers in Systems Neuroscience*, 7, 1–10. doi: 10.3389/fnsys.2013.00050
- Brown, R., Colter, N., Corsellis, J. A., Crow, T. J., Frith, C. D., Jago, R., ... Marsh, L. (1986). Postmortem Evidence of Structural Brain Changes in Schizophrenia: Differences in Brain Weight, Temporal Horn Area, and Parahippocampal Gyrus Compared With Affective Disorder. *Archives of General Psychiatry*, 43(1), 36–42. doi: 10.1001/archpsyc.1986.01800010038005
- Bu, D. F., Erlander, M. G., Hitz, B. C., Tillakaratne, N. J., Kaufman, D. L., Wagner-McPherson, C. B., ... Tobin, A. J. (1992). Two human glutamate decarboxylases, 65-kDa GAD and 67-kDa GAD, are each encoded by a single gene. *Proceedings of the National Academy*

- of Sciences of the United States of America*, 89(6), 2115–2119. doi: 10.1073/pnas.89.6.2115
- Buchsbaum, M. S., Haier, R. J., Potkin, S. G., Nuechterlein, K., Bracha, H. S., Katz, M., ... Bunney, W. E. (1992). Frontostriatal Disorder of Cerebral Metabolism in Never-Medicated Schizophrenics. *Archives of General Psychiatry*, 49(12), 935–942. doi: 10.1001/archpsyc.1992.01820120023005
- Bustillo, J. R., Chen, H., Jones, T., Lemke, N., Abbott, C., Qualls, C., ... Gasparovic, C. (2014). Increased glutamine in patients undergoing long-term treatment for schizophrenia: A proton magnetic resonance spectroscopy study at 3 T. *JAMA Psychiatry*, 71(3), 265–272. doi: 10.1001/jamapsychiatry.2013.3939
- Bustillo, J. R., Rowland, L. M., Mullins, P., Jung, R., Chen, H., Qualls, C., ... Lauriello, J. (2010). 1H-MRS at 4 Tesla in minimally treated early schizophrenia. *Molecular Psychiatry*, 15(6), 629–636. doi: 10.1038/mp.2009.121
- Buzsáki, G. (2002, 1). Theta oscillations in the hippocampus. *Neuron*, 33(3), 325–340. doi: 10.1016/S0896-6273(02)00586-X
- Buzsáki, G. (2006). *Rhythms of the Brain*. Oxford university press. doi: 10.1093/acprof:oso/9780195301069.001.0001
- Calandreau, L., Desgranges, B., Jaffard, R. & Desmedt, A. (2010, 9). Switching from contextual to tone fear conditioning and vice versa: The key role of the glutamatergic hippocampal-lateral septal neurotransmission. *Learning and Memory*, 17(9), 440–443. doi: 10.1101/lm.1859810
- Campbell, K. M., De Lecea, L., Severynse, D. M., Caron, M. G., McGrath, M. J., Sparber, S. B., ... Burton, F. H. (1999). OCD-like behaviors caused by a neuropotentiating transgene targeted to cortical and limbic D1+ neurons. *Journal of Neuroscience*, 19(12), 5044–5053. doi: 10.1523/jneurosci.19-12-05044.1999
- Caputi, A., Melzer, S., Michael, M. & Monyer, H. (2013). *The long and short of GABAergic neurons* (Vol. 23) (No. 2). Elsevier Current Trends. doi: 10.1016/j.conb.2013.01.021
- Cardin, J. A., Carlén, M., Meletis, K., Knoblich, U., Zhang, F., Deisseroth, K., ... Moore, C. I. (2009). Driving fast-spiking cells induces gamma rhythm and controls sensory responses. *Nature*, 459(7247), 663–667. doi: 10.1038/nature08002
- Castellan Baldan, L., Williams, K. A., Gallezot, J. D., Pogorelov, V., Rapanelli, M., Crowley, M., ... Pittenger, C. (2014). Histidine Decarboxylase Deficiency Causes Tourette Syndrome: Parallel Findings in Humans and Mice. *Neuron*, 81(1), 77–90. doi: 10.1016/j.neuron.2013.10.052

- Castellanos, F. X., Fine, E. J., Kaysen, D., Marsh, W. L., Rapoport, J. L. & Hallett, M. (1996). Sensorimotor gating in boys with Tourette's syndrome and ADHD: Preliminary results. *Biological Psychiatry*, *39*(1), 33–41. doi: 10.1016/0006-3223(95)00101-8
- Cavanna, A. E., Black, K. J., Hallett, M. & Voon, V. (2017). Neurobiology of the Premonitory Urge in Tourette's Syndrome: Pathophysiology and Treatment Implications. *The Journal of Neuropsychiatry and Clinical Neurosciences*. doi: 10.1176/appi.neuropsych.16070141
- Chauhan, P., Jethwa, K., Rathawa, A., Chauhan, G. & Mehra, S. (2021). The Anatomy of the Hippocampus. In *Cerebral ischemia* (pp. 17–30). doi: 10.36255/exonpublications.cerebralischemia.2021.hippocampus
- Chen, W. Q., Jin, H., Nguyen, M., Carr, J., Lee, Y. J., Hsu, C. C., ... Wu, J. Y. (2001). Role of taurine in regulation of intracellular calcium level and neuroprotective function in cultured neurons. *Journal of Neuroscience Research*, *66*(4), 612–619. doi: 10.1002/jnr.10027
- Cline, H. (2005). Synaptogenesis: A balancing act between excitation and inhibition. *Current Biology*, *15*(6). doi: 10.1016/j.cub.2005.03.010
- Cohen, S. C., Leckman, J. F. & Bloch, M. H. (2013). Clinical Assessment of Tourette Syndrome and Tic Disorders. *Neuroscience and biobehavioral reviews*, *37*(6), 997–1007. doi: 10.1016/j.neubiorev.2012.11.013
- Costall, B., Domeney, A. M. & Naylor, R. J. (1984). Locomotor hyperactivity caused by dopamine infusion into the nucleus accumbens of rat brain: specificity of action. *Psychopharmacology*, *82*(3), 174–180. doi: 10.1007/BF00427768
- Costall, B. & Naylor, R. J. (1975). The behavioural effects of dopamine applied intracerebrally to areas of the mesolimbic system. *European Journal of Pharmacology*, *32*(1), 87–92. doi: 10.1016/0014-2999(75)90326-X
- Crossman, A. R. (1987). Primate models of dyskinesia: The experimental approach to the study of basal ganglia-related involuntary movement disorders. *Neuroscience*, *21*(1), 1–40. doi: 10.1016/0306-4522(87)90322-8
- Cui, Y., Jin, Z., Chen, X., He, Y., Liang, X. & Zheng, Y. (2014). Abnormal baseline brain activity in drug-naïve patients with tourette syndrome: A resting-state fMRI study. *Frontiers in Human Neuroscience*, *7*(JAN). doi: 10.3389/fnhum.2013.00913
- Danielsen, E. R. & Ross, B. (1999). *Magnetic Resonance Spectroscopy Diagnosis of Neurological Diseases*. CRC Press. doi: 10.4324/9780429177200

- Danton, G. H. & Dietrich, W. D. (2005). Neuroprotection: Where Are We Going? In *From neuroscience to neurology: Neuroscience, molecular medicine, and the therapeutic transformation of neurology* (pp. 237–265). Academic Press. doi: 10.1016/B978-012738903-5/50015-1
- Darbin, O. & Wichmann, T. (2008). Effects of striatal GABAA-receptor blockade on striatal and cortical activity in monkeys. *Journal of Neurophysiology*, *99*(3), 1294–1305. doi: 10.1152/jn.01191.2007
- Daskalakis, Z. J., Christensen, B. K., Chen, R., Fitzgerald, P. B., Zipursky, R. B. & Kapur, S. (2002). Evidence for impaired cortical inhibition in schizophrenia using transcranial magnetic stimulation. *Archives of General Psychiatry*, *59*(4), 347–354. doi: 10.1001/archpsyc.59.4.347
- Davis, M., Antoniadis, E. A., Amaral, D. G. & Winslow, J. T. (2008). Acoustic startle reflex in rhesus monkeys: A review. *Reviews in the Neurosciences*, *19*(2-3), 171–185. doi: 10.1515/REVNEURO.2008.19.2-3.171
- Dawson, G. R., Maubach, K. A., Collinson, N., Cobain, M., Everitt, B. J., MacLeod, A. M., ... Atack, J. R. (2006). An inverse agonist selective for $\alpha 5$ subunit-containing GABA A receptors enhances cognition. *Journal of Pharmacology and Experimental Therapeutics*, *316*(3), 1335–1345. doi: 10.1124/jpet.105.092320
- Dawson, N., Morris, B. J. & Pratt, J. A. (2015). Functional brain connectivity phenotypes for schizophrenia drug discovery. *Journal of Psychopharmacology*, *29*(2), 169–177. doi: 10.1177/0269881114563635
- Debarbieux, F., Brunton, J. & Charpak, S. (1998). Effect of bicuculline on thalamic activity: A direct blockade of I(AHP) in reticularis neurons. *Journal of Neurophysiology*, *79*(6), 2911–2918. doi: 10.1152/jn.1998.79.6.2911
- Degreef, G., Bogerts, B., Falkai, P., Greve, B., Lantos, G., Ashtari, M. & Lieberman, J. (1992). Increased prevalence of the cavum septum pellucidum in magnetic resonance scans and post-mortem brains of schizophrenic patients. *Psychiatry Research: Neuroimaging*, *45*(1), 1–13. doi: 10.1016/0925-4927(92)90009-S
- DeLisi, L. E., Hoff, A. L., Kushner, M. & Degreef, G. (1993). Increased prevalence of cavum septum pellucidum in schizophrenia. *Psychiatry Research: Neuroimaging*, *50*(3), 193–199. doi: 10.1016/0925-4927(93)90030-L
- Del Olmo, N., Bustamante, J., Del Río, R. M. & Solís, J. M. (2000). Taurine activates GABAA but not GABAB receptors in rat hippocampal CA1 area. *Brain Research*, *864*(2), 298–307. doi: 10.1016/S0006-8993(00)02211-3

- Draper, A., Jude, L., Jackson, G. M. & Jackson, S. R. (2015). Motor excitability during movement preparation in Tourette syndrome. *Journal of Neuropsychology*, *9*(1), 33–44. doi: 10.1111/jnp.12033
- Draper, A., Stephenson, M. C., Jackson, G. M., Pépés, S., Morgan, P. S., Morris, P. G. & Jackson, S. R. (2014). Increased GABA contributes to enhanced control over motor excitability in tourette syndrome. *Current Biology*, *24*(19), 2343–2347. doi: 10.1016/j.cub.2014.08.038
- Duarte, J. M. & Xin, L. (2019). Magnetic Resonance Spectroscopy in Schizophrenia: Evidence for Glutamatergic Dysfunction and Impaired Energy Metabolism. *Neurochemical Research*, *44*(1), 102–116. doi: 10.1007/s11064-018-2521-z
- Dueck, A., Wolters, A., Wunsch, K., Bohne-Suraj, S., Mueller, J. U., Haessler, F., ... Buchmann, J. (2009). Deep brain stimulation of globus pallidus internus in a 16-year-old boy with severe Tourette syndrome and mental retardation. *Neuropediatrics*, *40*(5), 239–242. doi: 10.1055/s-0030-1247519
- Dursun, S. M., Burke, J. G. & Reveley, M. A. (2000). Antisaccade eye movement abnormalities in Tourette syndrome: Evidence for cortico-striatal network dysfunction? *Journal of Psychopharmacology*, *14*(1), 37–39. doi: 10.1177/026988110001400104
- Dwork, A. J. (1997). Postmortem studies of the hippocampal formation in schizophrenia. *Schizophrenia Bulletin*, *23*(3), 385–402. doi: 10.1093/schbul/23.3.385
- Egerton, A., Brugger, S., Raffin, M., Barker, G. J., Lythgoe, D. J., McGuire, P. K. & Stone, J. M. (2012). Anterior cingulate glutamate levels related to clinical status following treatment in first-episode schizophrenia. *Neuropsychopharmacology*, *37*(11), 2515–2521. doi: 10.1038/npp.2012.113
- Egerton, A., Modinos, G., Ferrera, D. & McGuire, P. (2017). Neuroimaging studies of GABA in schizophrenia: A systematic review with meta-analysis. *Translational Psychiatry*, *7*(6). doi: 10.1038/tp.2017.124
- El Idrissi, A. & Trenkner, E. (1999). Growth factors and taurine protect against excitotoxicity by stabilizing calcium homeostasis and energy metabolism. *Journal of Neuroscience*, *19*(21), 9459–9468. doi: 10.1523/jneurosci.19-21-09459.1999
- El Idrissi, A. & Trenkner, E. (2003). Taurine regulates mitochondrial calcium homeostasis. *Advances in experimental medicine and biology*, *526*, 527–536. doi: 10.1007/978-1-4615-0077-3-63
- Ercan-Sencicek, A. G., Stillman, A. A., Ghosh, A. K., Bilguvar, K., O’Roak, B. J., Mason, C. E., ... State, M. W. (2010). L-Histidine De-

- carboxylase and Tourette's Syndrome. *New England Journal of Medicine*, *362*(20), 1901–1908. doi: 10.1056/nejmoa0907006
- Esclapez, M., Tillakaratne, N. J., Tobin, A. J. & Houser, C. R. (1993). Comparative localization of mRNAs encoding two forms of glutamic acid decarboxylase with nonradioactive in situ hybridization methods. *Journal of Comparative Neurology*, *331*(3), 339–362. doi: 10.1002/cne.903310305
- Eyles, D. W., McGrath, J. J. & Reynolds, G. P. (2002). Neuronal calcium-binding proteins and schizophrenia. *Schizophrenia Research*, *57*(1), 27–34. doi: 10.1016/S0920-9964(01)00299-7
- Falkai, P. & Bogerts, B. (1986). Cell loss in the hippocampus of schizophrenics. *European Archives of Psychiatry and Neurological Sciences*, *236*(3), 154–161. doi: 10.1007/BF00380943
- Faul, F., Erdfelder, E., Lang, A. G. & Buchner, A. (2007). G*Power 3: A flexible statistical power analysis program for the social, behavioral, and biomedical sciences. In *Behavior research methods* (Vol. 39, pp. 175–191). Psychonomic Society Inc. doi: 10.3758/BF03193146
- Feifel, D. & Shilling, P. D. (2010). Promise and pitfalls of animal models of schizophrenia. *Current Psychiatry Reports*, *12*(4), 327–334. doi: 10.1007/s11920-010-0122-x
- Felling, R. J. & Singer, H. S. (2011). Neurobiology of Tourette syndrome: Current status and need for further investigation. *Journal of Neuroscience*, *31*(35), 12387–12395. doi: 10.1523/JNEUROSCI.0150-11.2011
- Ferrarelli, F., Sarasso, S., Guller, Y., Riedner, B. A., Peterson, M. J., Bellesi, M., ... Tononi, G. (2012). Reduced natural oscillatory frequency of frontal thalamocortical circuits in schizophrenia. *Archives of General Psychiatry*, *69*(8), 766–774. doi: 10.1001/archgenpsychiatry.2012.147
- Finis, J., Moczydlowski, A., Pollok, B., Biermann-Ruben, K., Thomalla, G., Heil, M., ... Münchau, A. (2012). Echoes from childhood-imitation in Gilles de la Tourette Syndrome. *Movement Disorders*, *27*(4), 562–565. doi: 10.1002/mds.24913
- Fjodorova, M., Noakes, Z. & Li, M. (2015). How to make striatal projection neurons. *Neurogenesis*, *2*(1). doi: 10.1080/23262133.2015.1100227
- Flashman, L. A., Roth, R. M., Pixley, H. S., Cleavinger, H. B., McAllister, T. W., Vidaver, R. & Saykin, A. J. (2007). Cavum septum pellucidum in schizophrenia: Clinical and neuropsychological correlates. *Psychiatry Research - Neuroimaging*, *154*(2), 147–155. doi: 10.1016/j.psychresns.2006.09.001

- Foos, T. M. & Wu, J. Y. (2002). The role of taurine in the central nervous system and the modulation of intracellular calcium homeostasis. *Neurochemical Research*, *27*(1-2), 21–26. doi: 10.1023/A:1014890219513
- Frank, S. T. & Schmidt, W. J. (2003). Burst activity of spiny projection neurons in the striatum encodes superimposed muscle tetani in cataleptic rats. *Experimental Brain Research*, *152*(4). doi: 10.1007/s00221-003-1644-9
- Freed, R. D., Coffey, B. J., Mao, X., Weiduschat, N., Kang, G., Shungu, D. C. & Gabbay, V. (2016). Decreased Anterior Cingulate Cortex γ -Aminobutyric Acid in Youth With Tourette’s Disorder. *Pediatric Neurology*, *65*, 64–70. doi: 10.1016/j.pediatrneurol.2016.08.017
- Freeman, R. D., Fast, D. K., Burd, L., Kerbeshian, J., Robertson, M. M. & Sandor, P. (2000). An international perspective on Tourette syndrome: Selected findings from 3500 individuals in 22 countries. *Developmental Medicine and Child Neurology*, *42*(7), 436–447. doi: 10.1017/S0012162200000839
- Freund, T. F. & Buzsáki, G. (1996). Interneurons of the Hippocampus. *Hippocampus*, *6*(4), 347–470. doi: 10.1002/(sici)1098-1063(1996)6:4<347::aid-hipo1>3.0.co;2-i
- Friston, K. J., Liddle, P. F., Frith, C. D., Hirsch, S. R. & Frackowiak, R. S. (1992). The left medial temporal region and schizophrenia: A pet study. *Brain*, *115*(2), 367–382. doi: 10.1093/brain/115.2.367
- Fujita, K. & Eidelberg, D. (2017). Imbalance of the direct and indirect pathways in focal dystonia: A balanced view. *Brain*, *140*(12), 3075–3077. doi: 10.1093/brain/awx305
- Galarza, M., Merlo, A. B., Ingrassia, A., Albanese, E. F. & Albanese, A. M. (2004). Cavum Septum Pellucidum and Its Increased Prevalence in Schizophrenia: A Neuroembryological Classification. *Journal of Neuropsychiatry and Clinical Neurosciences*, *16*(1), 41–46. doi: 10.1176/jnp.16.1.41
- Gandal, M. J., Edgar, J. C., Klook, K. & Siegel, S. J. (2012). Gamma synchrony: Towards a translational biomarker for the treatment-resistant symptoms of schizophrenia. *Neuropharmacology*, *62*(3), 1504–1518. doi: 10.1016/j.neuropharm.2011.02.007
- Ganos, C., Kahl, U., Brandt, V., Schunke, O., Bäumer, T., Thomalla, G., ... Kühn, S. (2014). The neural correlates of tic inhibition in Gilles de la Tourette syndrome. *Neuropsychologia*. doi: 10.1016/j.neuropsychologia.2014.08.007
- Garcia, P., Kolesky, S. & Jenkins, A. (2010). General Anesthetic Actions on GABAA Receptors. *Current Neuropharmacology*, *8*(1), 2–9. doi: 10.2174/157015910790909502

- Georgiou, N., Bradshaw, J. L., Phillips, J. G., Bradshaw, J. A. & Chiu, E. (1995). The simon effect and attention deficits in gilles de la tourette's syndrome and huntington's disease. *Brain*, *118*(5), 1305–1318. doi: 10.1093/brain/118.5.1305
- Gerfen, C. R. & Bolam, J. P. (2010). The Neuroanatomical Organization of the Basal Ganglia. In *Handbook of behavioral neuroscience* (Vol. 20, pp. 3–28). Elsevier. doi: 10.1016/B978-0-12-374767-9.00001-9
- Gerfen, C. R. & Surmeier, D. J. (2011). Modulation of striatal projection systems by dopamine. *Annual Review of Neuroscience*, *34*, 441–466. doi: 10.1146/annurev-neuro-061010-113641
- Gerfen, C. R. & Wilson, C. J. (1996). Chapter II The basal ganglia. *Handbook of Chemical Neuroanatomy*, *12*, 371–468. doi: 10.1016/S0924-8196(96)80004-2
- Gilani, A. I., Chohan, M. O., Inan, M., Schobel, S. A., Chaudhury, N. H., Samuel, P., ... Moore, H. (2014). Interneuron precursor transplants in adult hippocampus reverse psychosis-relevant features in a mouse model of hippocampal disinhibition. *Proceedings of the National Academy of Sciences of the United States of America*, *111*(20), 7450–7455. doi: 10.1073/pnas.1316488111
- Gilbert, D. L. (2006). Motor cortex inhibitory function in Tourette syndrome, attention deficit disorder, and obsessive compulsive disorder: studies using transcranial magnetic stimulation. *Advances in neurology*, *99*, 107–114.
- Gilbert, D. L., Budman, C. L., Singer, H. S., Kurlan, R. & Chipkin, R. E. (2014). A D1 receptor antagonist, ecopipam, for treatment of tics in Tourette syndrome. *Clinical Neuropharmacology*, *37*(1), 26–30. doi: 10.1097/WNF.0000000000000017
- Gilmour, G., Dix, S., Fellini, L., Gastambide, F., Plath, N., Steckler, T., ... Tricklebank, M. (2012). NMDA receptors, cognition and schizophrenia - Testing the validity of the NMDA receptor hypofunction hypothesis. *Neuropharmacology*, *62*(3), 1401–1412. doi: 10.1016/j.neuropharm.2011.03.015
- Gittis, A. H., Leventhal, D. K., Fensterheim, B. A., Pettibone, J. R., Berke, J. D. & Kreitzer, A. C. (2011). Selective inhibition of striatal fast-spiking interneurons causes Dyskinesias. *Journal of Neuroscience*, *31*(44), 15727–15731. doi: 10.1523/JNEUROSCI.3875-11.2011
- Gittis, A. H., Nelson, A. B., Thwin, M. T., Palop, J. J. & Kreitzer, A. C. (2010). Distinct roles of GABAergic interneurons in the regulation of striatal output pathways. *Journal of Neuroscience*, *30*(6), 2223–2234. doi: 10.1523/JNEUROSCI.4870-09.2010

- Glickstein, S. B., Moore, H., Slowinska, B., Racchumi, J., Suh, M., Chuhma, N. & Ross, M. E. (2007). Selective cortical interneuron and GABA deficits in cyclin D2-null mice. *Development*, *134*(22), 4083–4093. doi: 10.1242/dev.008524
- Glykys, J. & Mody, I. (2007). Activation of GABAA Receptors: Views from Outside the Synaptic Cleft. *Neuron*, *56*(5), 763–770. doi: 10.1016/j.neuron.2007.11.002
- Godar, S. C., Mosher, L. J., Strathman, H. J., Gochi, A. M., Jones, C. M., Fowler, S. C. & Bortolato, M. (2016). The D1CT-7 mouse model of Tourette syndrome displays sensorimotor gating deficits in response to spatial confinement. *British Journal of Pharmacology*, *173*(13), 2111–2121. doi: 10.1111/bph.13243
- Gogtay, N., Vyas, N. S., Testa, R., Wood, S. J. & Pantelis, C. (2011). Age of onset of schizophrenia: Perspectives from structural neuroimaging studies. *Schizophrenia Bulletin*, *37*(3), 504–513. doi: 10.1093/schbul/sbr030
- Goldberg, J. A. & Wilson, C. J. (2016). The Cholinergic Interneuron of the Striatum. In *Handbook of behavioral neuroscience* (Vol. 24, pp. 137–155). Elsevier. doi: 10.1016/B978-0-12-802206-1.00007-6
- Goto, Y. & O'Donnell, P. (2001). Network synchrony in the nucleus accumbens in vivo. *Journal of Neuroscience*, *21*(12), 4498–4504. doi: 10.1523/jneurosci.21-12-04498.2001
- Grabli, D., McCairn, K., Hirsch, E. C., Agid, Y., Féger, J., François, C. & Tremblay, L. (2004). Behavioural disorders induced by external globus pallidus dysfunction in primates: I. Behavioural study. *Brain*, *127*(9), 2039–2054. doi: 10.1093/brain/awh220
- Gray, J. A. & McNaughton, N. (1983). Comparison between the behavioural effects of septal and hippocampal lesions: A review. *Neuroscience and Biobehavioral Reviews*, *7*(2), 119–188. doi: 10.1016/0149-7634(83)90014-3
- Gruetter, R. (1993). Automatic, localized in Vivo adjustment of all first- and second-order shim coils. *Magnetic Resonance in Medicine*, *29*(6), 804–811. doi: 10.1002/mrm.1910290613
- Grunze, H. C., Rainnie, D. G., Hasselmo, M. E., Barkai, E., Hearn, E. F., McCarley, R. W. & Greene, R. W. (1996). NMDA-dependent modulation of CA1 local circuit inhibition. *Journal of Neuroscience*, *16*(6), 2034–2043. doi: 10.1523/jneurosci.16-06-02034.1996
- Grützner, C., Wibrall, M., Sun, L., Rivolta, D., Singer, W., Maurer, K. & Uhlhaas, P. J. (2013). Deficits in High- (bigger than 60 Hz) Gamma-Band Oscillations during Visual Processing in Schizophrenia. *Frontiers in Neuroengineering*, *7*, 88. doi: 10.3389/fnhum.2013.00088

- Guidotti, A., Auta, J., Davis, J. M., Gerevini, V. D., Dwivedi, Y., Grayson, D. R., ... Costa, E. (2000). Decrease in reelin and glutamic acid decarboxylase67 (GAD67) expression in schizophrenia and bipolar disorder: A postmortem brain study. *Archives of General Psychiatry*, *57*(11), 1061–1069. doi: 10.1001/archpsyc.57.11.1061
- Guo, H., Liu, J., Van Shura, K., Chen, H. Z., Flora, M. N., Myers, T. M., ... McCabe, J. T. (2015). N-acetyl-aspartyl-glutamate and inhibition of glutamate carboxypeptidases protects against soman-induced neuropathology. *NeuroToxicology*, *48*, 180–191. doi: 10.1016/j.neuro.2015.03.010
- Gwilt, M., Bauer, M. & Bast, T. (2020). Frequency- and state-dependent effects of hippocampal neural disinhibition on hippocampal local field potential oscillations in anesthetized rats. *Hippocampus*, *30*(10), 1021–1043. doi: 10.1002/hipo.23212
- Haenschel, C., Bittner, R. A., Waltz, J., Haertling, F., Wibrall, M., Singer, W., ... Rodriguez, E. (2009). Cortical oscillatory activity is critical for working memory as revealed by deficits in early-onset schizophrenia. *Journal of Neuroscience*, *29*(30), 9481–9489. doi: 10.1523/JNEUROSCI.1428-09.2009
- Haensel, J. X., Spain, A. & Martin, C. (2015). A systematic review of physiological methods in rodent pharmacological MRI studies. *Psychopharmacology*, *232*(3), 489–499. doi: 10.1007/s00213-014-3855-0
- Hall, G. R., Boehm-Sturm, P., Dirnagl, U., Finke, C., Foddis, M., Harms, C., ... Farr, T. D. (2022). Long-Term Connectome Analysis Reveals Reshaping of Visual, Spatial Networks in a Model with Vascular Dementia Features. *Stroke*, *53*(5), 1735–1745. doi: 10.1161/STROKEAHA.121.036997
- Hall, M. H., Taylor, G., Salisbury, D. F. & Levy, D. L. (2011). Sensory gating event-related potentials and oscillations in schizophrenia patients and their unaffected relatives. *Schizophrenia Bulletin*, *37*(6), 1187–1199. doi: 10.1093/schbul/sbq027
- Hammen, T. & Kuzniecky, R. (2012). Magnetic resonance spectroscopy in epilepsy. *Handbook of Clinical Neurology*, *107*, 399–408. doi: 10.1016/B978-0-444-52898-8.00025-2
- Hattori, R., Kuchibhotla, K. V., Froemke, R. C. & Komiyama, T. (2017). Functions and dysfunctions of neocortical inhibitory neuron subtypes. *Nature Neuroscience*, *20*(9), 1199–1208. doi: 10.1038/nn.4619
- He, J. L., Mikkelsen, M., Huddleston, D. A., Crocetti, D., Cecil, K. M., Singer, H. S., ... Puts, N. A. (2022). Frequency and Intensity of Premonitory Urges-to-Tic in Tourette Syndrome Is Associated With Sup-

- plementary Motor Area GABA+ Levels. *Movement Disorders*, 37(3), 563–573. doi: 10.1002/mds.28868
- Heckers, S., Heinsen, H., Geiger, B. & Beckmann, H. (1991). Hippocampal Neuron Number in Schizophrenia: A Stereological Study. *Archives of General Psychiatry*, 48(11), 1002–1008. doi: 10.1001/archpsyc.1991.01810350042006
- Heckers, S. & Konradi, C. (2015). *GABAergic mechanisms of hippocampal hyperactivity in schizophrenia* (Vol. 167) (No. 1-3). Elsevier. doi: 10.1016/j.schres.2014.09.041
- Heckers, S., Rauch, S. L., Goff, D., Savage, C. R., Schacter, D. L., Fishman, A. J. & Alpert, N. M. (1998). Impaired recruitment of the hippocampus during conscious recollection in schizophrenia. *Nature Neuroscience*, 1(4), 318–323. doi: 10.1038/1137
- Heckers, S., Stone, D., Walsh, J., Shick, J., Koul, P. & Benes, F. M. (2002). Differential hippocampal expression of glutamic acid decarboxylase 65 and 67 messenger RNA in bipolar disorder and schizophrenia. *Archives of General Psychiatry*, 59(6), 521–529. doi: 10.1001/archpsyc.59.6.521
- Heinke, W. & Koelsch, S. (2005). The effects of anesthetics on brain activity and cognitive function. *Current Opinion in Anaesthesiology*, 18(6), 625–631. doi: 10.1097/01.aco.0000189879.67092.12
- Héja, L., Nyitrai, G., Kékesi, O., Dobolyi, , Szabó, P., Fiáth, R., ... Kardos, J. (2012). Astrocytes convert network excitation to tonic inhibition of neurons. *BMC Biology*, 10. doi: 10.1186/1741-7007-10-26
- Hennig, J., Nauerth, A. & Friedburg, H. (1986). RARE imaging: A fast imaging method for clinical MR. *Magnetic Resonance in Medicine*, 3(6), 823–833. doi: 10.1002/mrm.1910030602
- Hirschtritt, M. E., Lee, P. C., Pauls, D. L., Dion, Y., Grados, M. A., Illmann, C., ... Barr, C. L. (2015). Lifetime prevalence, age of risk, and genetic relationships of comorbid psychiatric disorders in tourette syndrome. *JAMA Psychiatry*, 72(4), 325–333. doi: 10.1109/BIBM.2017.8217796
- Ho, N. F., Iglesias, J. E., Sum, M. Y., Kuswanto, C. N., Sitoh, Y. Y., De Souza, J., ... Holt, D. J. (2017, 1). Progression from selective to general involvement of hippocampal subfields in schizophrenia. *Molecular Psychiatry*, 22(1), 142–152. doi: 10.1038/mp.2016.4
- Hollis, C., Pennant, M., Cuenca, J., Glazebrook, C., Kendall, T., Whittington, C., ... Stern, J. (2016). Clinical effectiveness and patient perspectives of different treatment strategies for tics in children and adolescents with tourette syndrome: A systematic review and qualitative analysis. *Health Technology Assessment*, 20(4). doi: 10.3310/hta20040

- Holt, D. J., Kunkel, L., Weiss, A. P., Goff, D. C., Wright, C. I., Shin, L. M., ... Heckers, S. (2006). Increased medial temporal lobe activation during the passive viewing of emotional and neutral facial expressions in schizophrenia. *Schizophrenia Research*, *82*(2-3), 153–162. doi: 10.1016/j.schres.2005.09.021
- Holt, D. J., Weiss, A. P., Rauch, S. L., Wright, C. I., Zalesak, M., Goff, D. C., ... Heckers, S. (2005). Sustained activation of the hippocampus in response to fearful faces in schizophrenia. *Biological Psychiatry*, *57*(9), 1011–1019. doi: 10.1016/j.biopsych.2005.01.033
- Homayoun, H., Jackson, M. E. & Moghaddam, B. (2005). Activation of metabotropic glutamate 2/3 receptors reverses the effects of NMDA receptor hypofunction on prefrontal cortex unit activity in awake rats. *Journal of Neurophysiology*, *93*(4). doi: 10.1152/jn.00875.2004
- Homayoun, H. & Moghaddam, B. (2007). NMDA receptor hypofunction produces opposite effects on prefrontal cortex interneurons and pyramidal neurons. *Journal of Neuroscience*, *27*(43), 11496–11500. doi: 10.1523/JNEUROSCI.2213-07.2007
- Iltis, I., Koski, D. M., Eberly, L. E., Nelson, C. D., Deelchand, D. K., Valette, J., ... Henry, P. G. (2009). Neurochemical changes in the rat prefrontal cortex following acute phencyclidine treatment: An in vivo localized ¹H MRS study. *NMR in Biomedicine*, *22*(7), 737–744. doi: 10.1002/nbm.1385
- Impagnatiello, F., Guidotti, A. R., Pesold, C., Dwivedi, Y., Caruncho, H., Pisu, M. G., ... Costa, E. (1998). A decrease of reelin expression as a putative vulnerability factor in schizophrenia. *Proceedings of the National Academy of Sciences of the United States of America*, *95*(26), 15718–15723. doi: 10.1073/pnas.95.26.15718
- Isaacson, J. S. & Scanziani, M. (2011). How inhibition shapes cortical activity. *Neuron*, *72*(2), 231–243. doi: 10.1016/j.neuron.2011.09.027
- Israelashvili, M. & Bar-Gad, I. (2015). Corticostriatal divergent function in determining the temporal and spatial properties of motor tics. *Journal of Neuroscience*, *35*(50), 16340–16351. doi: 10.1523/JNEUROSCI.2770-15.2015
- Israelashvili, M., Loewenstern, Y. & Bar-Gad, I. (2015). Abnormal neuronal activity in tourette syndrome and its modulation using deep brain stimulation. *Journal of Neurophysiology*, *114*(1), 6–20. doi: 10.1152/jn.00277.2015
- Israelashvili, M., Yael, D., Vinner, E., Belevsky, K. & Bar-Gad, I. (2020). Common neuronal mechanisms underlying tics and hyperactivity. *Cortex*, *127*, 231–247. doi: 10.1016/j.cortex.2020.02.010

- Izhikevich, E. M., Desai, N. S., Walcott, E. C. & Hoppensteadt, F. C. (2003). Bursts as a unit of neural information: Selective communication via resonance. *Trends in Neurosciences*, *26*(3), 161–167. doi: 10.1016/S0166-2236(03)00034-1
- Jackson, D. M., Andén, N. E. & Dahlström, A. (1975). A functional effect of dopamine in the nucleus accumbens and in some other dopamine-rich parts of the rat brain. *Psychopharmacologia*, *45*(2), 139–149. doi: 10.1007/BF00429052
- Jackson, G. M., Draper, A., Dyke, K., Pépés, S. E. & Jackson, S. R. (2015). Inhibition, Disinhibition, and the Control of Action in Tourette Syndrome. *Trends in Cognitive Sciences*, *19*(11), 655–665. doi: 10.1016/j.tics.2015.08.006
- Jackson, G. M., Mueller, S. C., Hambleton, K. & Hollis, C. P. (2007). Enhanced cognitive control in Tourette Syndrome during task uncertainty. *Experimental Brain Research*, *182*(3), 357–364. doi: 10.1007/s00221-007-0999-8
- Jackson, S. R., Parkinson, A., Jung, J., Ryan, S. E., Morgan, P. S., Hollis, C. & Jackson, G. M. (2011). Compensatory neural reorganization in Tourette syndrome. *Current Biology*, *21*(7), 580–585. doi: 10.1016/j.cub.2011.02.047
- Jankovic, J. (1997). Phenomenology and classification of tics. *Neurologic Clinics*, *15*(2), 267–275. doi: 10.1016/S0733-8619(05)70311-X
- Japha, K. & Koch, M. (1999). Picrotoxin in the medial prefrontal cortex impairs sensorimotor gating in rats: Reversal by haloperidol. *Psychopharmacology*, *144*(4), 347–354. doi: 10.1007/s002130051017
- Jayasinghe, V. R., Flores-Barrera, E., West, A. R. & Tseng, K. Y. (2017). Frequency-Dependent Corticostriatal Disinhibition Resulting from Chronic Dopamine Depletion: Role of Local Striatal cGMP and GABA-AR Signaling. *Cerebral Cortex*, *27*(1), 625–634. doi: 10.1093/cercor/bhv241
- Jessen, F., Fingerhut, N., Sprinkart, A. M., Kühn, K. U., Petrovsky, N., Maier, W., ... Träber, F. (2013). N-acetylaspartylglutamate (NAAG) and N-acetylaspartate (NAA) in patients with schizophrenia. *Schizophrenia Bulletin*, *39*(1), 197–205. doi: 10.1093/schbul/sbr127
- Jessen, F., Scheef, L., Germeshausen, L., Tawo, Y., Kockler, M., Kuhn, K. U., ... Heun, R. (2003). Reduced hippocampal activation during encoding and recognition of words in schizophrenia patients. *American Journal of Psychiatry*, *160*(7), 1305–1312. doi: 10.1176/appi.ajp.160.7.1305
- Jones, D. L., Mogenson, G. J. & Wu, M. (1981). Injections of dopaminergic, cholinergic, serotonergic and gabaergic drugs into the nucleus

- accumbens: effects on locomotor activity in the rat. *Neuropharmacology*, *20*(1), 29–37. doi: 10.1016/0028-3908(81)90038-1
- Jung, J., Jackson, S. R., Parkinson, A. & Jackson, G. M. (2013). Cognitive control over motor output in Tourette syndrome. *Neuroscience and Biobehavioral Reviews*, *37*(6), 1016–1025. doi: 10.1016/j.neubiorev.2012.08.009
- Jung, J. Y., Jackson, S. R., Nam, K., Hollis, C. & Jackson, G. M. (2015). Enhanced saccadic control in young people with Tourette syndrome despite slowed pro-saccades. *Journal of Neuropsychology*, *9*(2), 172–183. doi: 10.1111/jnp.12044
- Jurado-Parras, M. T., Safaie, M., Sarno, S., Louis, J., Karoutchi, C., Berret, B. & Robbe, D. (2020). The Dorsal Striatum Energizes Motor Routines. *Current Biology*, *30*(22), 4362–4372. doi: 10.1016/j.cub.2020.08.049
- Just, N. & Faber, C. (2019). Probing activation-induced neurochemical changes using optogenetics combined with functional magnetic resonance spectroscopy: a feasibility study in the rat primary somatosensory cortex. *Journal of Neurochemistry*, *150*(4), 402–419. doi: 10.1111/jnc.14799
- Kalanithi, P. S. A., Zheng, W., Kataoka, Y., DiFiglia, M., Grantz, H., Saper, C. B., . . . Vaccarino, F. M. (2005). Altered parvalbumin-positive neuron distribution in basal ganglia of individuals with Tourette syndrome. *Proceedings of the National Academy of Sciences*, *102*(37), 13307–13312. doi: 10.1073/pnas.0502624102
- Kalkman, H. O. & Loetscher, E. (2003). GAD67: The link between the GABA-deficit hypothesis and the dopaminergic- and glutamatergic theories of psychosis. *Journal of Neural Transmission*, *110*(7), 803–812. doi: 10.1007/s00702-003-0826-8
- Kanaan, A. S., Gerasch, S., García-García, I., Lampe, L., Pampel, A., Anwander, A., . . . Müller-Vahl, K. (2017). Pathological glutamatergic neurotransmission in Gilles de la Tourette syndrome. *Brain*, *140*(1), 218–234. doi: 10.1093/brain/aww285
- Kasai, K., McCarley, R. W., Salisbury, D. F., Onitsuka, T., Demeo, S., Yurgelun-Todd, D., . . . Shenton, M. E. (2004). Cavum septi pellucidi in first-episode schizophrenia and first-episode affective psychosis: An MRI study. *Schizophrenia Research*, *71*(1), 65–76. doi: 10.1016/j.schres.2003.12.010
- Kataoka, Y., Kalanithi, P. S., Grantz, H., Schwartz, M. L., Saper, C., Leckman, J. F. & Vaccarino, F. M. (2010). Decreased number of parvalbumin and cholinergic interneurons in the striatum of individuals

- with tourette syndrome. *Journal of Comparative Neurology*, 518(3), 277–291. doi: 10.1002/cne.22206
- Kawasaki, Y., Maeda, Y., Sakai, N., Higashima, M., Urata, K., Yamaguchi, N. & Kurachi, M. (1994). Evaluation and interpretation of symptom structures in patients with schizophrenia. *Acta Psychiatrica Scandinavica*, 89(6), 399–404. doi: 10.1111/j.1600-0447.1994.tb01536.x
- Kawasaki, Y., Suzuki, M., Maeda, Y., Urata, K., Yamaguchi, N., Matsuda, H., ... Takashima, T. (1992). Regional cerebral blood flow in patients with schizophrenia - A preliminary report. *European Archives of Psychiatry and Clinical Neuroscience*, 241(4), 195–200. doi: 10.1007/BF02190252
- Kee, T., Sanda, P., Gupta, N., Stopfer, M. & Bazhenov, M. (2015). Feed-Forward versus Feedback Inhibition in a Basic Olfactory Circuit. *PLoS Computational Biology*, 11(10). doi: 10.1371/journal.pcbi.1004531
- Kegeles, L. S., Mao, X., Stanford, A. D., Girgis, R., Ojeil, N., Xu, X., ... Shungu, D. C. (2012). Elevated prefrontal cortex γ -aminobutyric acid and glutamate-glutamine levels in schizophrenia measured in vivo with proton magnetic resonance spectroscopy. *Archives of General Psychiatry*, 69(5), 449–459. doi: 10.1001/archgenpsychiatry.2011.1519
- Keller, C. J., Chen, C., Lado, F. A. & Khodakhah, K. (2016). The limited utility of multiunit data in differentiating neuronal population activity. *PLoS ONE*, 11(4). doi: 10.1371/journal.pone.0153154
- Kern, J. K., Geier, D. A., King, P. G., Sykes, L. K., Mehta, J. A. & Geier, M. R. (2015). Shared Brain Connectivity Issues, Symptoms, and Comorbidities in Autism Spectrum Disorder, Attention Deficit/Hyperactivity Disorder, and Tourette Syndrome. *Brain Connectivity*, 5(6), 321–335. doi: 10.1089/brain.2014.0324
- Kikuchi, M., Hashimoto, T., Nagasawa, T., Hirosawa, T., Minabe, Y., Yoshimura, M., ... Koenig, T. (2011). Frontal areas contribute to reduced global coordination of resting-state gamma activities in drug-naïve patients with schizophrenia. *Schizophrenia Research*, 130(1-3), 187–194. doi: 10.1016/j.schres.2011.06.003
- Kim, T., Capps, R. A., Hamade, K. C., Barnett, W. H., Todorov, D. I., Latash, E. M., ... Molkov, Y. I. (2019). The functional role of striatal cholinergic interneurons in reinforcement learning from computational perspective. *Frontiers in Neural Circuits*, 13, 10. doi: 10.3389/fncir.2019.00010
- Klaus, A. & Plenz, D. (2016). A Low-Correlation Resting State of the Striatum during Cortical Avalanches and Its Role in Movement Suppression. *PLoS Biology*, 14(12), 1–30. doi: 10.1371/journal.pbio.1002582

- Koch, M. (1999). The neurobiology of startle. *Progress in Neurobiology*, 59(2), 107–128. doi: 10.1016/S0301-0082(98)00098-7
- Koch, M. & Schnitzler, H. U. (1997). The acoustic startle response in rats - Circuits mediating evocation, inhibition and potentiation. *Behavioural Brain Research*, 89(1-2), 35–49. doi: 10.1016/S0166-4328(97)02296-1
- Kodsi, M. H. & Swerdlow, N. R. (1994). Quinolinic acid lesions of the ventral striatum reduce sensorimotor gating of acoustic startle in rats. *Brain Research*, 643(1-2), 59–65. doi: 10.1016/0006-8993(94)90008-6
- Kodsi, M. H. & Swerdlow, N. R. (1995). Prepulse Inhibition in the Rat Is Regulated by Ventral and Caudodorsal Striato-Pallidal Circuitry. *Behavioral Neuroscience*, 109(5), 912–928. doi: 10.1037/0735-7044.109.5.912
- Kodsi, M. H. & Swerdlow, N. R. (1997). Reduced prepulse inhibition after electrolytic lesions of nucleus accumbens subregions in the rat. *Brain Research*, 773(1-2), 45–52. doi: 10.1016/S0006-8993(97)00869-X
- Kohl, S., Heekeren, K., Klosterkötter, J. & Kuhn, J. (2013). Prepulse inhibition in psychiatric disorders - Apart from schizophrenia. *Journal of Psychiatric Research*, 47(4), 445–452. doi: 10.1016/j.jpsychires.2012.11.018
- Konradi, C., Yang, C. K., Zimmerman, E. I., Lohmann, K. M., Gresch, P., Pantazopoulos, H., ... Heckers, S. (2011). Hippocampal interneurons are abnormal in schizophrenia. *Schizophrenia Research*, 131(1-3), 165–173. doi: 10.1016/j.schres.2011.06.007
- Kreiman, G., Hung, C. P., Kraskov, A., Quiroga, R. Q., Poggio, T. & DiCarlo, J. J. (2006). Object selectivity of local field potentials and spikes in the macaque inferior temporal cortex. *Neuron*, 49(3), 433–445. doi: 10.1016/j.neuron.2005.12.019
- Kreitzer, A. C. (2009). *Physiology and pharmacology of striatal neurons* (Vol. 32). doi: 10.1146/annurev.neuro.051508.135422
- Krimmel, S. R., Qadir, H., Hesselgrave, N., White, M. G., Reser, D. H., Mathur, B. N. & Seminowicz, D. A. (2019). Resting state functional connectivity of the rat claustrum. *Frontiers in Neuroanatomy*, 13, 22. doi: 10.3389/fnana.2019.00022
- Krishnan, G. P., Hetrick, W. P., Brenner, C. A., Shekhar, A., Steffen, A. N. & O'Donnell, B. F. (2009). Steady state and induced auditory gamma deficits in schizophrenia. *NeuroImage*, 47(4), 1711–1719. doi: 10.1016/j.neuroimage.2009.03.085
- Kumar, J., Liddle, E. B., Fernandes, C. C., Palaniyappan, L., Hall, E. L., Robson, S. E., ... Liddle, P. F. (2020). Glutathione and glutamate in

- schizophrenia: a 7T MRS study. *Molecular Psychiatry*, 25(4), 873–882. doi: 10.1038/s41380-018-0104-7
- Kumari, V., Antonova, E., Zachariah, E., Galea, A., Aasen, I., Ettinger, U., ... Sharma, T. (2005). Structural brain correlates of prepulse inhibition of the acoustic startle response in healthy humans. *NeuroImage*, 26(4), 1052–1058. doi: 10.1016/j.neuroimage.2005.03.002
- Kwon, J. S., Shenton, M. E., Hirayasu, Y., Salisbury, D. F., Fischer, I. A., Dickey, C. C., ... McCarley, R. W. (1998). MRI study of cavum septi pellucidi in schizophrenia, affective disorder, and schizotypal personality disorder. *American Journal of Psychiatry*, 155(4), 509–515. doi: 10.1176/ajp.155.4.509
- Lakhan, S. E., Caro, M. & Hadzimidichalis, N. (2013). NMDA receptor activity in neuropsychiatric disorders. *Frontiers in Psychiatry*, 4, 52. doi: 10.3389/fpsyt.2013.00052
- Leckman, J. F., Riddle, M. A., Hardin, M. T., Ort, S. I., Swartz, K. L., Stevenson, J. & Cohen, D. J. (1989). The Yale Global Tic Severity Scale: Initial Testing of a Clinician-Rated Scale of Tic Severity. *Journal of the American Academy of Child and Adolescent Psychiatry*, 28(4), 566–573. doi: 10.1097/00004583-198907000-00015
- Leckman, J. F., Vaccarino, F. M., Kalanithi, P. S. & Rothenberger, A. (2006). Annotation: Tourette syndrome: A relentless drumbeat - Driven by misguided brain oscillations. *Journal of Child Psychology and Psychiatry and Allied Disciplines*, 47(6), 537–550. doi: 10.1111/j.1469-7610.2006.01620.x
- Leckman, J. F., Walker, D. E. & Cohen, D. J. (1993). Premonitory urges in Tourette's syndrome. *American Journal of Psychiatry*, 150(1), 98–102. doi: 10.1176/ajp.150.1.98
- Leckman, J. F., Zhang, H., Vitale, A., Lahnin, F., Lynch, K., Bondi, C., ... Peterson, B. S. (1998). Course of tic severity in Tourette syndrome: the first two decades. *Pediatrics*, 102(1), 14–19.
- Ledoux, A. A., Boyer, P., Phillips, J. L., Labelle, A., Smith, A. & Bohbot, V. D. (2014). Structural hippocampal anomalies in a schizophrenia population correlate with navigation performance on a way-finding task. *Frontiers in Behavioral Neuroscience*, 8, 88. doi: 10.3389/fnbeh.2014.00088
- Legatt, A. D., Arezzo, J. & Vaughan, H. G. (1980). Averaged multiple unit activity as an estimate of phasic changes in local neuronal activity: effects of volume-conducted potentials. *Journal of Neuroscience Methods*, 2(2), 203–217. doi: 10.1016/0165-0270(80)90061-8

- Legendy, C. R. & Salzman, M. (1985). Bursts and recurrences of bursts in the spike trains of spontaneously active striate cortex neurons. *Journal of Neurophysiology*, *53*(4), 926–939. doi: 10.1152/jn.1985.53.4.926
- Leke, R. & Schousboe, A. (2016). The glutamine transporters and their role in the glutamate/GABA-glutamine cycle. *Advances in Neurobiology*, *13*(1), 223–257. doi: 10.1007/978-3-319-45096-4-8
- Lemos, J. C., Shin, J. H. & Alvarez, V. A. (2019). Striatal cholinergic interneurons are a novel target of corticotropin releasing factor. *Journal of Neuroscience*, *39*(29), 5647–5661. doi: 10.1523/JNEUROSCI.0479-19.2019
- Lenington, J. B., Coppola, G., Kataoka-Sasaki, Y., Fernandez, T. V., Palejev, D., Li, Y., . . . Vaccarino, F. M. (2016). Transcriptome Analysis of the Human Striatum in Tourette Syndrome. *Biological Psychiatry*, *79*(5), 372–382. doi: 10.1016/j.biopsych.2014.07.018
- Leonard, B. E. (2002). Neuropsychopharmacology? The fifth generation of progress. Edited by K. L. Davis, D. Charney, J. T. Coyle, C. Nemeroff. Lippincott, Williams and Wilkins: Philadelphia, 2002. ISBN: 0-7817-2837-1. Pages: 2080. *Human Psychopharmacology: Clinical and Experimental*, *17*(8), 433–433. doi: 10.1002/hup.431
- Leranth, C., Deller, T. & Buzsáki, G. (1992). Intraseptal connections redefined: lack of a lateral septum to medial septum path. *Brain Research*, *583*(1-2), 1–11. doi: 10.1016/S0006-8993(10)80004-6
- Lerner, A., Bagic, A., Simmons, J. M., Mari, Z., Bonne, O., Xu, B., . . . Hallett, M. (2012). Widespread abnormality of the γ -aminobutyric acid-ergic system in Tourette syndrome. *Brain*, *135*(6), 1926–1936. doi: 10.1093/brain/aws104
- Leroy, F., Park, J., Asok, A., Brann, D. H., Meira, T., Boyle, L. M., . . . Siegelbaum, S. A. (2018). A circuit from hippocampal CA2 to lateral septum disinhibits social aggression. *Nature*, *564*(7735), 213–218. doi: 10.1038/s41586-018-0772-0
- Letzkus, J. J., Wolff, S. B. & Lüthi, A. (2015). Disinhibition, a Circuit Mechanism for Associative Learning and Memory. *Neuron*, *88*(2), 264–276. doi: 10.1016/j.neuron.2015.09.024
- Lévesque, M. & Parent, A. (2005). The striatofugal fiber system in primates: A reevaluation of its organization based on single-axon tracing studies. *Proceedings of the National Academy of Sciences of the United States of America*, *102*(33), 11888–11893. doi: 10.1073/pnas.0502710102
- Lewis, S. W. & Mezey, G. C. (1985). Clinical correlates of septum pellucidum cavities: An unusual association with psychosis. *Psychological Medicine*, *15*(1), 43–54. doi: 10.1017/S0033291700020912

- Li, B. S., Wang, H. & Gonen, O. (2003). Metabolite ratios to assumed stable creatine level may confound the quantification of proton brain MR spectroscopy. *Magnetic Resonance Imaging*, *21*(8), 923–928. doi: 10.1016/S0730-725X(03)00181-4
- Liang, Z., King, J. & Zhang, N. (2011). Uncovering intrinsic connectional architecture of functional networks in awake rat brain. *Journal of Neuroscience*, *31*(10), 3776–3783. doi: 10.1523/JNEUROSCI.4557-10.2011
- Lichter, D. G. & Finnegan, S. G. (2015). Influence of gender on Tourette syndrome beyond adolescence. *European Psychiatry*, *30*(2), 334–340. doi: 10.1016/j.eurpsy.2014.07.003
- Liddle, P. F., Friston, K. J., Frith, C. D., Hirsch, S. R., Jones, T. & Frackowiak, R. S. (1992). Patterns of cerebral blood flow in schizophrenia. *British Journal of Psychiatry*, *160*(2), 179–186. doi: 10.1192/bjp.160.2.179
- Lieberman, J. A., Girgis, R. R., Brucato, G., Moore, H., Provenzano, F., Kegeles, L., ... Small, S. A. (2018). Hippocampal dysfunction in the pathophysiology of schizophrenia: a selective review and hypothesis for early detection and intervention. *Molecular Psychiatry*, *23*(8), 1764–1772. doi: 10.1038/mp.2017.249
- Liemburg, E., Sibeijn-Kuiper, A., Bais, L., Pijnenborg, G., Knegtering, H., Van Der Velde, J., ... Aleman, A. (2016). Prefrontal NAA and Glx Levels in Different Stages of Psychotic Disorders: A 3T 1 H-MRS Study. *Scientific Reports*, *6*(1), 1–8. doi: 10.1038/srep21873
- Linn, G. S., Negi, S. S., Gerum, S. V. & Javitt, D. C. (2003). Reversal of phencyclidine-induced prepulse inhibition deficits by clozapine in monkeys. *Psychopharmacology*, *169*(3-4), 234–239. doi: 10.1007/s00213-003-1533-8
- Lisman, J. E., Coyle, J. T., Green, R. W., Javitt, D. C., Benes, F. M., Heckers, S. & Grace, A. A. (2008). Circuit-based framework for understanding neurotransmitter and risk gene interactions in schizophrenia. *Trends in Neurosciences*, *31*(5), 234–242. doi: 10.1016/j.tins.2008.02.005
- Liu, Y., Wang, J., Zhang, J., Wen, H., Zhang, Y., Kang, H., ... Peng, Y. (2017). Altered Spontaneous Brain Activity in Children with Early Tourette Syndrome: A Resting-state fMRI Study. *Scientific Reports*, *7*(1). doi: 10.1038/s41598-017-04148-z
- Lodge, D. J., Behrens, M. M. & Grace, A. A. (2009). A loss of parvalbumin-containing interneurons is associated with diminished oscillatory activity in an animal model of schizophrenia. *Journal of Neuroscience*, *29*(8), 2344–2354. doi: 10.1523/JNEUROSCI.5419-08.2009

- Lopes, E. F., Roberts, B. M., Siddorn, R. E., Clements, M. A. & Cragg, S. J. (2019). Inhibition of nigrostriatal dopamine release by striatal GABA A and GABA B receptors. *Journal of Neuroscience*, *39*(6). doi: 10.1523/JNEUROSCI.2028-18.2018
- Lorens, S. A., Sorensen, J. P. & Harvey, J. A. (1970). Lesions in the nuclei accumbens septi of the rat: Behavioral and neurochemical effects. *Journal of Comparative and Physiological Psychology*, *73*(2), 284–290. doi: 10.1037/h0030204
- Lovett-Barron, M., Turi, G. F., Kaifosh, P., Lee, P. H., Bolze, F., Sun, X. H., ... Losonczy, A. (2012). Regulation of neuronal input transformations by tunable dendritic inhibition. *Nature Neuroscience*, *15*(3), 423–430. doi: 10.1038/nn.3024
- Lu, H., Zou, Q., Gu, H., Raichle, M. E., Stein, E. A. & Yang, Y. (2012). Rat brains also have a default mode network. *Proceedings of the National Academy of Sciences of the United States of America*, *109*(10), 3979–3984. doi: 10.1073/pnas.1200506109
- Mahone, E. M., Puts, N. A., Edden, R. A., Ryan, M. & Singer, H. S. (2018). GABA and glutamate in children with Tourette syndrome: A 1 H MR spectroscopy study at 7 T. *Psychiatry Research - Neuroimaging*, *273*, 46–53. doi: 10.1016/j.psychresns.2017.12.005
- Malaspina, D., Harkavy-Friedman, J., Corcoran, C., Mujica-Parodi, L., Printz, D., Gorman, J. M. & Van Heertum, R. (2004, 12). Resting neural activity distinguishes subgroups of schizophrenia patients. *Biological Psychiatry*, *56*(12), 931–937. doi: 10.1016/j.biopsych.2004.09.013
- Maldonado-Irizarry, C. S. & Kelley, A. E. (1994). Differential behavioral effects following microinjection of an NMDA antagonist into nucleus accumbens subregions. *Psychopharmacology*, *116*(1), 65–72. doi: 10.1007/BF02244872
- Maldonado-Irizarry, C. S. & Kelley, A. E. (1995). Excitotoxic lesions of the core and shell subregions of the nucleus accumbens differentially disrupt body weight regulation and motor activity in rat. *Brain Research Bulletin*, *38*(6), 551–559. doi: 10.1016/0361-9230(95)02030-2
- Mallet, N., Leblois, A., Maurice, N. & Beurrier, C. (2019). Striatal cholinergic interneurons: How to elucidate their function in health and disease. *Frontiers in Pharmacology*, *10*, 1488. doi: 10.3389/fphar.2019.01488
- Mandino, F., Vrooman, R. M., Foo, H. E., Yeow, L. Y., Bolton, T. A., Salvan, P., ... Grandjean, J. (2022). A triple-network organization for the mouse brain. *Molecular Psychiatry*, *27*(2), 865–872. doi: 10.1038/s41380-021-01298-5

- Mansbach, R. S., Geyer, M. A. & Braff, D. L. (1988). Dopaminergic stimulation disrupts sensorimotor gating in the rat. *Psychopharmacology*, *94*(4), 507–514. doi: 10.1007/BF00212846
- Marín, O. (2012). Interneuron dysfunction in psychiatric disorders. *Nature Reviews Neuroscience*, *13*(2), 107–120. doi: 10.1038/nrn3155
- Markram, H., Toledo-Rodriguez, M., Wang, Y., Gupta, A., Silberberg, G. & Wu, C. (2004). Interneurons of the neocortical inhibitory system. *Nature Reviews Neuroscience*, *5*(10), 793–807. doi: 10.1038/nrn1519
- Marsman, A., Mandl, R. C., Klomp, D. W., Bohlken, M. M., Boer, V. O., Andreychenko, A., . . . Hulshoff Pol, H. E. (2014). GABA and glutamate in schizophrenia: A 7 T 1H-MRS study. *NeuroImage: Clinical*, *6*, 398–407. doi: 10.1016/j.nicl.2014.10.005
- Martino, D. & Hedderly, T. (2019). Tics and stereotypies: A comparative clinical review. *Parkinsonism and Related Disorders*, *59*, 117–124. doi: 10.1016/j.parkreldis.2019.02.005
- Martino, D., Madhusudan, N., Zis, P. & Cavanna, A. E. (2013). An introduction to the clinical phenomenology of tourette syndrome. *International Review of Neurobiology*, *112*, 1–33. doi: 10.1016/B978-0-12-411546-0.00001-9
- Masamoto, K. & Kanno, I. (2012). Anesthesia and the quantitative evaluation of neurovascular coupling. *Journal of Cerebral Blood Flow and Metabolism*, *32*(7), 1233–1247. doi: 10.1038/jcbfm.2012.50
- Masamoto, K., Kim, T., Fukuda, M., Wang, P. & Kim, S. G. (2007). Relationship between neural, vascular, and BOLD signals in isoflurane-anesthetized rat somatosensory cortex. *Cerebral Cortex*, *17*(4), 942–950. doi: 10.1093/cercor/bhl005
- McCairn, K. W., Bronfeld, M., Belelovsky, K. & Bar-Gad, I. (2009). The neurophysiological correlates of motor tics following focal striatal disinhibition. *Brain*, *132*(8), 2125–2138. doi: 10.1093/brain/awp142
- McCairn, K. W., Iriki, A. & Isoda, M. (2013). Global dysrhythmia of cerebro-basal ganglia-cerebellar networks underlies motor tics following striatal disinhibition. *Journal of Neuroscience*, *33*(2), 697–708. doi: 10.1523/JNEUROSCI.4018-12.2013
- McCairn, K. W. & Isoda, M. (2013). Pharmacological animal models of tic disorders. *International Review of Neurobiology*, *112*, 179–209. doi: 10.1016/B978-0-12-411546-0.00007-X
- McGarrity, S., Mason, R., Fone, K. C., Pezze, M. & Bast, T. (2017). Hippocampal neural disinhibition causes attentional and memory deficits. *Cerebral Cortex*, *27*(9), 4447–4462. doi: 10.1093/cercor/bhw247

- McKenzie, G. M., Gordon, R. J. & Viik, K. (1972). Some biochemical and behavioural correlates of a possible animal model of human hyperkinetic syndromes. *Brain Research*, *47*(2), 439–456. doi: 10.1016/0006-8993(72)90651-8
- McKenzie, G. M. & Viik, K. (1975). Chemically induced choreiform activity: Antagonism by GABA and EEG patterns. *Experimental Neurology*, *46*(1). doi: 10.1016/0014-4886(75)90045-X
- Mechling, A. E., Hübner, N. S., Lee, H. L., Hennig, J., von Elverfeldt, D. & Harsan, L. A. (2014). Fine-grained mapping of mouse brain functional connectivity with resting-state fMRI. *NeuroImage*, *96*, 203–215. doi: 10.1016/j.neuroimage.2014.03.078
- Medoff, D. R., Holcomb, H. H., Lahti, A. C. & Tamminga, C. A. (2001). Probing the human hippocampus using rCBF: Contrasts in schizophrenia. *Hippocampus*, *11*(5), 543–550. doi: 10.1002/hipo.1070
- Mena-Segovia, J., Bolam, J. P. & Magill, P. J. (2004). Pedunculo-pontine nucleus and basal ganglia: Distant relatives or part of the same family? *Trends in Neurosciences*, *27*(10), 585–588. doi: 10.1016/j.tins.2004.07.009
- Merritt, K., Egerton, A., Kempton, M. J., Taylor, M. J. & McGuire, P. K. (2016). Nature of glutamate alterations in schizophrenia a meta-analysis of proton magnetic resonance spectroscopy studies. *JAMA Psychiatry*, *73*(7), 665–674. doi: 10.1001/jamapsychiatry.2016.0442
- Miao, J., Zhang, J., Zheng, L., Yu, X., Zhu, W. & Zou, S. (2012). Taurine attenuates *Streptococcus uberis*-induced mastitis in rats by increasing T regulatory cells. *Amino Acids*, *42*(6), 2417–2428. doi: 10.1007/s00726-011-1047-3
- Minzenberg, M. J., Firl, A. J., Yoon, J. H., Gomes, G. C., Reinking, C. & Carter, C. S. (2010). Gamma oscillatory power is impaired during cognitive control independent of medication status in first-episode schizophrenia. *Neuropsychopharmacology*, *35*(13), 2590–2599. doi: 10.1038/npp.2010.150
- Mitzdorf, U. (1985). Current source-density method and application in cat cerebral cortex: Investigation of evoked potentials and EEG phenomena. *Physiological Reviews*, *65*(1), 37–100. doi: 10.1152/physrev.1985.65.1.37
- Modinos, G., Şimşek, F., Azis, M., Bossong, M., Bonoldi, I., Samson, C., ... McGuire, P. (2018). Prefrontal GABA levels, hippocampal resting perfusion and the risk of psychosis. *Neuropsychopharmacology*, *43*(13), 2652–2659. doi: 10.1038/s41386-017-0004-6
- Moffett, J. R., Arun, P., Ariyannur, P. S. & Namboodiri, A. M. (2013). *N-Acetylaspartate reductions in brain injury: Impact on post-injury neur-*

- oenergetics, lipid synthesis, and protein acetylation* (Vol. 5). Frontiers Research Foundation. doi: 10.3389/fnene.2013.00011
- Moran, A. & Bar-Gad, I. (2010). Revealing neuronal functional organization through the relation between multi-scale oscillatory extracellular signals. *Journal of Neuroscience Methods*, *186*(1), 116–129. doi: 10.1016/j.jneumeth.2009.10.024
- Moreland, N. C. (2014). Fundamentals of Neuroanesthesia: A Physiologic Approach to Clinical Practice. *Anesthesiology*, *121*(4), 908–909. doi: 10.1097/aln.0000000000000309
- Morgenstern, R., Mende, T., Gold, R., Lemme, P. & Oelssner, W. (1984, 10). Drug-induced modulation of locomotor hyperactivity induced by picrotoxin in nucleus accumbens. *Pharmacology Biochemistry and Behavior*, *21*(4), 501–506. doi: 10.1016/S0091-3057(84)80030-1
- Mori, F., Okada, K. I., Nomura, T. & Kobayashi, Y. (2016). The pedunculopontine tegmental nucleus as a motor and cognitive interface between the cerebellum and basal ganglia. *Frontiers in Neuroanatomy*, *10*, 109. doi: 10.3389/fnana.2016.00109
- Mozrzymas, J. W., Zarmowska, E. D., Pytel, M. & Mercik, K. (2003). Modulation of GABAA receptors by hydrogen ions reveals synaptic GABA transient and a crucial role of the desensitization process. *Journal of Neuroscience*, *23*(22), 7981–7992. doi: 10.1523/jneurosci.23-22-07981.2003
- Mueller, S. C., Jackson, G. M., Dhalla, R., Datsopoulos, S. & Hollis, C. P. (2006). Enhanced cognitive control in young people with Tourette's syndrome. *Current Biology*, *16*(6), 570–573. doi: 10.1016/j.cub.2006.01.064
- Müller, C. & Remy, S. (2018, 9). Septo-hippocampal interaction. *Cell and Tissue Research*, *373*(3), 565–575. doi: 10.1007/s00441-017-2745-2
- Muramatsu, S., Yoshida, M. & Nakamura, S. (1990). Electrophysiological study of dyskinesia produced by microinjection of picrotoxin into the striatum of the rat. *Neuroscience Research*, *7*(4), 369–380. doi: 10.1016/0168-0102(90)90011-3
- Nakazawa, K. & Sapkota, K. (2020). The origin of NMDA receptor hypofunction in schizophrenia. *Pharmacology and Therapeutics*, *205*, 107426. doi: 10.1016/j.pharmthera.2019.107426
- Napolitano, A., Shah, K., Schubert, M. I., Porkess, V., Fone, K. C. & Auer, D. P. (2014). In vivo neurometabolic profiling to characterize the effects of social isolation and ketamine-induced NMDA Antagonism: A rodent study at 7.0 T. *Schizophrenia Bulletin*, *40*(3), 566–574. doi: 10.1093/schbul/sbt067

- Nasrallah, F. A., Tay, H. C. & Chuang, K. H. (2014). Detection of functional connectivity in the resting mouse brain. *NeuroImage*, *86*, 417–424. doi: 10.1016/j.neuroimage.2013.10.025
- Natsubori, T., Inoue, H., Abe, O., Takano, Y., Iwashiro, N., Aoki, Y., ... Yamasue, H. (2014). Reduced frontal glutamate + glutamine and N-acetylaspartate levels in patients with chronic schizophrenia but not in those at clinical high risk for psychosis or with first-episode schizophrenia. *Schizophrenia Bulletin*, *40*(5), 1128–1139. doi: 10.1093/schbul/sbt124
- Neckelmann, D., Amzica, F. & Steriade, M. (1998). Spike-wave complexes and fast components of cortically generated seizures. III. Synchronizing mechanisms. *Journal of Neurophysiology*, *80*(3), 1480–1494. doi: 10.1152/jn.1998.80.3.1480
- Nespoli, E., Rizzo, F., Boeckers, T. M., Hengerer, B. & Ludolph, A. G. (2016). Addressing the complexity of Tourette’s syndrome through the use of animal models. *Frontiers in Neuroscience*, *10*, 133. doi: 10.3389/fnins.2016.00133
- Nisenbaum, E. S., Stricker, E. M., Zigmond, M. J. & Berger, T. W. (1986). Long-term effects of dopamine-depleting brain lesions on spontaneous activity of type II striatal neurons: Relation to behavioral recovery. *Brain Research*, *398*(2). doi: 10.1016/0006-8993(86)91481-2
- Nishikawa, K. & MacIver, M. B. (2001). Agent-selective effects of volatile anesthetics on GABAA receptor-mediated synaptic inhibition in hippocampal interneurons. *Anesthesiology*, *94*(2), 340–347. doi: 10.1097/00000542-200102000-00025
- Nopoulos, P., Swayze, V., Flaum, M., Ehrhardt, J. C., Yuh, W. T. & Andreasen, N. C. (1997). Cavum septi pellucidi in normals and patients with schizophrenia as detected by magnetic resonance imaging. *Biological Psychiatry*, *41*(11), 1102–1108. doi: 10.1016/S0006-3223(96)00209-0
- Nordahl, T. E., Kusubov, N., Carter, C., Salamat, S., Cummings, A. M., O’Shora-Celaya, L., ... Budinger, T. F. (1996). Temporal lobe metabolic differences in medication-free outpatients with schizophrenia via the PET-600. *Neuropsychopharmacology*, *15*(6), 541–554. doi: 10.1016/S0893-133X(96)00098-X
- Oelschlegel, A. M. & Goldschmidt, J. (2020). Functional Neuroimaging in Rodents Using Cerebral Blood Flow SPECT. *Frontiers in Physics*, *8*, 152. doi: 10.3389/fphy.2020.00152
- Ohm, B. (2006). The effect of Tourette syndrome on the education and social interactions of a school-age child. *The Journal of neuroscience*

nursing : journal of the American Association of Neuroscience Nurses, 38(3). doi: 10.1097/01376517-200606000-00009

- Oja, S. S. & Saransaari, P. (1996). Taurine as osmoregulator and neuromodulator in the brain. *Metabolic Brain Disease*, 11(2), 153–164. doi: 10.1007/BF02069502
- Öngür, D., Prescott, A. P., McCarthy, J., Cohen, B. M. & Renshaw, P. F. (2010). Elevated gamma-aminobutyric acid levels in chronic schizophrenia. *Biological Psychiatry*, 68(7), 667–670. doi: 10.1016/j.biopsych.2010.05.016
- Oorschot, D. E. (1996). Total number of neurons in the neostriatal, pallidal, subthalamic, and substantia nigral nuclei of the rat basal ganglia: A stereological study using the cavalieri and optical disector methods. *Journal of Comparative Neurology*, 366(4), 580–599. doi: 10.1002/(SICI)1096-9861(19960318)366:4<580::AID-CNE3>3.0.CO;2-0
- Openner, T. J., Marsman, J. B. C., van der Meer, D., Forde, N. J., Akkermans, S. E., Naaijen, J., ... Hoekstra, P. J. (2020). A graph theory study of resting-state functional connectivity in children with Tourette syndrome. *Cortex*, 126, 63–72. doi: 10.1016/j.cortex.2020.01.006
- Öz, G., Alger, J. R., Barker, P. B., Bartha, R., Bizzi, A., Boesch, C., ... Kauppinen, R. A. (2014). Clinical proton MR spectroscopy in central nervous system disorders. *Radiology*, 270(3), 658–679. doi: 10.1148/radiol.13130531
- Ozonoff, S., Strayer, D. L., McMahon, W. M. & Filloux, F. (1998). Inhibitory deficits in Tourette syndrome: A function of comorbidity and symptom severity. *Journal of Child Psychology and Psychiatry and Allied Disciplines*, 39(8), 1109–1118. doi: 10.1017/S0021963098003230
- Patel, S. & Slater, P. (1987). Analysis of the brain regions involved in myoclonus produced by intracerebral picrotoxin. *Neuroscience*, 20(2), 687–693. doi: 10.1016/0306-4522(87)90119-9
- Pawela, C. P., Biswal, B. B., Cho, Y. R., Kao, D. S., Li, R., Jones, S. R., ... Hyde, J. S. (2008). Resting-state functional connectivity of the rat brain. *Magnetic Resonance in Medicine*, 59(5), 1021–1029. doi: 10.1002/mrm.21524
- Paxinos, G. & Watson, C. (1998). *The Rat Brain in Stereotaxic Coordinates* (4th ed.). Academic Press.
- Paylor, R. & Crawley, J. N. (1997). Inbred strain differences in prepulse inhibition of the mouse startle response. *Psychopharmacology*, 132(2), 169–180. doi: 10.1007/s002130050333
- Pedemonte, M., Barrenechea, C., Nuñez, A., Gambini, J. P. & García-Austt, E. (1998). Membrane and circuit properties of lateral septum

- neurons: Relationships with hippocampal rhythms. *Brain Research*, 800(1), 145–153. doi: 10.1016/S0006-8993(98)00517-4
- Pelkey, K. A., Chittajallu, R., Craig, M. T., Tricoire, L., Wester, J. C. & McBain, C. J. (2017). Hippocampal gabaergic inhibitory interneurons. *Physiological Reviews*, 97(4), 1619–1747. doi: 10.1152/physrev.00007.2017
- Perälä, J., Suvisaari, J., Saarni, S. I., Kuoppasalmi, K., Isometsä, E., Pirkola, S., ... Lönnqvist, J. (2007). Lifetime prevalence of psychotic and bipolar I disorders in a general population. *Archives of General Psychiatry*, 64(1), 19–28. doi: 10.1001/archpsyc.64.1.19
- Perry, T. L., Buchanan, J., Kish, S. J. & Hansen, S. (1979). Γ -Aminobutyric-Acid Deficiency in Brain of Schizophrenic Patients. *The Lancet*, 313(8110), 237–239. doi: 10.1016/S0140-6736(79)90767-0
- Perry, W. & Braff, D. L. (1994). Information-processing deficits and thought disorder in schizophrenia. *American Journal of Psychiatry*, 151(3), 363–367. doi: 10.1176/ajp.151.3.363
- Perry, W., Geyer, M. A. & Braff, D. L. (1999). Sensorimotor gating and thought disturbance measured in close temporal proximity in schizophrenic patients. *Archives of General Psychiatry*, 56(3), 277–281. doi: 10.1001/archpsyc.56.3.277
- Peterson, B. S., Staib, L., Scahill, L., Zhang, H., Anderson, C., Leckman, J. F., ... Webster, R. (2001). Regional brain and ventricular volumes in Tourette syndrome. *Archives of General Psychiatry*, 58(5), 427–440. doi: 10.1001/archpsyc.58.5.427
- Peterson, B. S., Thomas, P., Kane, M. J., Scahill, L., Zhang, H., Bronen, R., ... Staib, L. (2003). Basal ganglia volumes in patients with Gilles de la Tourette syndrome. *Archives of General Psychiatry*, 60(4), 415–424. doi: 10.1001/archpsyc.60.4.415
- Pezze, M., McGarrity, S., Mason, R., Fone, K. C. & Bast, T. (2014). Too little and too much: Hypoactivation and disinhibition of medial prefrontal cortex cause attentional deficits. *Journal of Neuroscience*, 34(23), 7931–7946. doi: 10.1523/JNEUROSCI.3450-13.2014
- Pfieger, J. F., Clarac, F. & Vinay, L. (2002). Picrotoxin and bicuculline have different effects on lumbar spinal networks and motoneurons in the neonatal rat. *Brain Research*, 935(1-2), 81–86. doi: 10.1016/S0006-8993(02)02469-1
- Pijnenburg, A. J. & van Rossum, J. M. (1973). Stimulation of locomotor activity following injection of dopamine into the nucleus accumbens. *Journal of Pharmacy and Pharmacology*, 25(12), 1003–1005. doi: 10.1111/j.2042-7158.1973.tb09995.x

- Plenz, D. (2003). When inhibition goes incognito: Feedback interaction between spiny projection neurons in striatal function. *Trends in Neurosciences*, *26*(8), 436–443. doi: 10.1016/S0166-2236(03)00196-6
- Plessen, K. J., Bansal, R. & Peterson, B. S. (2009). Imaging evidence for anatomical disturbances and neuroplastic compensation in persons with Tourette syndrome. *Journal of Psychosomatic Research*, *67*(6), 559–573. doi: 10.1016/j.jpsychores.2009.07.005
- Pogorelov, V., Xu, M., Smith, H. R., Buchanan, G. F. & Pittenger, C. (2015). Corticostriatal interactions in the generation of tic-like behaviors after local striatal disinhibition. *Experimental Neurology*, *265*, 122–128. doi: 10.1016/j.expneurol.2015.01.001
- Pothuizen, H. H., Jongen-Rêlo, A. L. & Feldon, J. (2005). The effects of temporary inactivation of the core and the shell subregions of the nucleus accumbens on prepulse inhibition of the acoustic startle reflex and activity in rats. *Neuropsychopharmacology*, *30*(4), 683–696. doi: 10.1038/sj.npp.1300643
- Pouwels, P. J. & Frahm, J. (1997). Differential distribution of NAA and NAAG in human brain as determined by quantitative localized proton MRS. *NMR in Biomedicine*, *10*(2), 73–78. doi: 10.1002/(SICI)1099-1492(199704)10:2<73::AID-NBM448>3.0.CO;2-4
- Prior, M. J. W., Bast, T., McGarrity, S., Goldschmidt, J., Vincenz, D., Seaton, A., ... Pitiot, A. (2021). Ratlas-LH: An MRI template of the Lister hooded rat brain with stereotaxic coordinates for neurosurgical implantations. *Brain and Neuroscience Advances*, *5*, 239821282110363. doi: 10.1177/23982128211036332
- Provencher, S. (2021). LCMModel & LCMgui User’s Manual. , *1LCModel V*. Retrieved from <http://lcmmodel.ca/lcm-manual.shtml>
- Provencher, S. W. (1993). Estimation of metabolite concentrations from localized in vivo proton NMR spectra. *Magnetic Resonance in Medicine*, *30*(6), 672–679. doi: 10.1002/mrm.1910300604
- Puts, N. A. & Edden, R. A. (2012). In vivo magnetic resonance spectroscopy of GABA: A methodological review. *Progress in Nuclear Magnetic Resonance Spectroscopy*, *60*, 29–41. doi: 10.1016/j.pnmrs.2011.06.001
- Radhakishun, F. S., Wolterink, G. & van Ree, J. M. (1988). The response of apomorphine administered into the accumbens in rats with bilateral lesions of the nucleus accumbens, induced with 6-hydroxydopamine. *Neuropharmacology*, *27*(11), 1111–1116. doi: 10.1016/0028-3908(88)90005-6
- Ramkiran, S., Heidemeyer, L., Gaebler, A., Shah, N. J. & Neuner, I. (2019). Alterations in basal ganglia-cerebello-thalamo-

- cortical connectivity and whole brain functional network topology in Tourette's syndrome. *NeuroImage: Clinical*, *24*, 101998. doi: 10.1016/j.nicl.2019.101998
- Rao, S. G., Williams, G. V. & Goldman-Rakic, P. S. (2000). Destruction and creation of spatial tuning by disinhibition: GABA(A) blockade of prefrontal cortical neurons engaged by working memory. *Journal of Neuroscience*, *20*(1), 485–494. doi: 10.1523/jneurosci.20-01-00485.2000
- Reddy-Thootkur, M., Kraguljac, N. V. & Lahti, A. C. (2022). The role of glutamate and GABA in cognitive dysfunction in schizophrenia and mood disorders – A systematic review of magnetic resonance spectroscopy studies. *Schizophrenia Research*, *249*, 74–84. doi: 10.1016/j.schres.2020.02.001
- Reid, M. A., Salibi, N., White, D. M., Gawne, T. J., Denney, T. S. & Lahti, A. C. (2019). 7T Proton Magnetic Resonance Spectroscopy of the Anterior Cingulate Cortex in First-Episode Schizophrenia. *Schizophrenia Bulletin*, *45*(1), 180–189. doi: 10.1093/schbul/sbx190
- Risold, P. Y. & Swanson, L. W. (1997). Connections of the rat lateral septal complex. *Brain Research Reviews*, *24*(2-3), 115–195. doi: 10.1016/S0165-0173(97)00009-X
- Robbins, T. W. & Everitt, B. J. (1992). Functions of dopamine in the dorsal and ventral striatum. *Seminars in Neuroscience*, *4*(2), 119–127. doi: 10.1016/1044-5765(92)90010-Y
- Robertson, M. M. (2015). A personal 35 year perspective on Gilles de la Tourette syndrome: Prevalence, phenomenology, comorbidities, and coexistent psychopathologies. *The Lancet Psychiatry*, *2*(1), 68–87. doi: 10.1016/S2215-0366(14)00132-1
- Roeske, M. J., Konradi, C., Heckers, S. & Lewis, A. S. (2021). Hippocampal volume and hippocampal neuron density, number and size in schizophrenia: a systematic review and meta-analysis of postmortem studies. *Molecular Psychiatry*, *26*(7), 3524–3535. doi: 10.1038/s41380-020-0853-y
- Rowland, L. M., Kontson, K., West, J., Edden, R. A., Zhu, H., Wijtenburg, S. A., ... Barker, P. B. (2013). In vivo measurements of glutamate, GABA, and NAAG in schizophrenia. *Schizophrenia Bulletin*, *39*(5), 1096–1104. doi: 10.1093/schbul/sbs092
- Royer, S., Zemelman, B. V., Losonczy, A., Kim, J., Chance, F., Magee, J. C. & Buzsáki, G. (2012). Control of timing, rate and bursts of hippocampal place cells by dendritic and somatic inhibition. *Nature Neuroscience*, *15*(5), 769–775. doi: 10.1038/nn.3077

- Rutter, L., Carver, F. W., Holroyd, T., Nadar, S. R., Mitchell-Francis, J., Apud, J., ... Coppola, R. (2009). Magnetoencephalographic gamma power reduction in patients with schizophrenia during resting condition. *Human Brain Mapping, 30*(10), 3254–3264. doi: 10.1002/hbm.20746
- Sanger, T. D., Chen, D., Fehlings, D. L., Hallett, M., Lang, A. E., Mink, J. W., ... Valero-Cuevas, F. (2010). Definition and classification of hyperkinetic movements in childhood. *Movement Disorders, 25*(11), 1538–1549. doi: 10.1002/mds.23088
- Santangelo, A., Bortolato, M., Mosher, L. J., Crescimanno, G., Di Giovanni, G., Cassioli, E., ... Casarrubea, M. (2018). Behavioral fragmentation in the D1CT-7 mouse model of Tourette’s syndrome. *CNS Neuroscience and Therapeutics, 24*(8), 703–711. doi: 10.1111/cns.12789
- Sarwar, M. (1989). The septum pellucidum: Normal and abnormal. *American Journal of Neuroradiology, 10*(5), 989–1005.
- Schaffer, S., Takahashi, K. & Azuma, J. (2000). Role of osmoregulation in the actions of taurine. *Amino Acids, 19*(3-4), 527–546. doi: 10.1007/s007260070004
- Scharf, J. M., Miller, L. L., Gauvin, C. A., Alabiso, J., Mathews, C. A. & Ben-Shlomo, Y. (2015). Population prevalence of Tourette syndrome: A systematic review and meta-analysis. *Movement Disorders, 30*(2), 221–228. doi: 10.1002/mds.26089
- Schmitt, A., Steyskal, C., Bernstein, H. G., Schneider-Axmann, T., Parlapani, E., Schaeffer, E. L., ... Falkai, P. (2009). Stereologic investigation of the posterior part of the hippocampus in schizophrenia. *Acta neuropathologica, 117*(4), 395–407. doi: 10.1007/s00401-008-0430-y
- Schobel, S. A., Chaudhury, N. H., Khan, U. A., Paniagua, B., Styner, M. A., Asllani, I., ... Small, S. A. (2013). Imaging Patients with Psychosis and a Mouse Model Establishes a Spreading Pattern of Hippocampal Dysfunction and Implicates Glutamate as a Driver. *Neuron, 78*(1), 81–93. doi: 10.1016/j.neuron.2013.02.011
- Schobel, S. A., Lewandowski, N. M., Corcoran, C. M., Moore, H., Brown, T., Malaspina, D. & Small, S. A. (2009). Differential targeting of the CA1 subfield of the hippocampal formation by schizophrenia and related psychotic disorders. *Archives of General Psychiatry, 66*(9), 938–946. doi: 10.1001/archgenpsychiatry.2009.115
- Sheehan, T. P., Chambers, R. A. & Russell, D. S. (2004, 8). Regulation of affect by the lateral septum: Implications for neuropsychiatry. *Brain Research Reviews, 46*(1), 71–117. doi: 10.1016/j.brainresrev.2004.04.009
- Shenton, M. E., Kikinis, R., Jolesz, F. A., Pollak, S. D., LeMay, M., Wible, C. G., ... McCarley, R. W. (1992, 8). Abnormal-

- ities of the Left Temporal Lobe and Thought Disorder in Schizophrenia. *New England Journal of Medicine*, 327(9), 604–612. doi: 10.1056/nejm199208273270905
- Shichino, T., Murakawa, M., Adachi, T., Nakao, S., Shinomura, T., Kurata, J. & Mori, K. (1997). Effects of isoflurane on in vivo release of acetylcholine in the rat cerebral cortex and striatum. *Acta Anaesthesiologica Scandinavica*, 41(10), 1335–1340. doi: 10.1111/j.1399-6576.1997.tb04654.x
- Shioiri, T., Oshitani, Y., Kato, T., Murashita, J., Hamakawa, H., Inubushi, T., ... Takahashi, S. (1996). Prevalence of cavum septum pellucidum detected by MRI in patients with bipolar disorder, major depression and schizophrenia. *Psychological Medicine*, 26(2), 431–434. doi: 10.1017/s0033291700034838
- Shute, J. B., Okun, M. S., Opri, E., Molina, R., Rossi, P. J., Martinez-Ramirez, D., ... Gunduz, A. (2016). Thalamocortical network activity enables chronic tic detection in humans with Tourette syndrome. *NeuroImage: Clinical*, 12, 165–172. doi: 10.1016/j.nicl.2016.06.015
- Singer, H. S., Reiss, A. L., Brown, J. E., Aylward, E. H., Shih, B., Chee, E., ... Denckla, M. B. (1993). Volumetric mri changes in basal ganglia of children with tourette’s syndrome. *Neurology*, 43(5), 950–956. doi: 10.1212/wnl.43.5.950
- Sitskoorn, M. M., Aleman, A., Ebisch, S. J., Appels, M. C. & Kahn, R. S. (2004). Cognitive deficits in relatives of patients with schizophrenia: A meta-analysis. *Schizophrenia Research*, 71(2-3), 285–295. doi: 10.1016/j.schres.2004.03.007
- Smith, J. B., Lee, A. K. & Jackson, J. (2020). The claustrum. *Current Biology*, 30(23), R1401-R1406. doi: 10.1016/j.cub.2020.09.069
- Smith, S. J. & Lees, A. J. (1989). Abnormalities of the blink reflex in Gilles de la Tourette syndrome. *Journal of Neurology, Neurosurgery and Psychiatry*, 52(7), 895–898. doi: 10.1136/jnnp.52.7.895
- Smith, Y., Bevan, M. D., Shink, E. & Bolam, J. P. (1998). Microcircuitry of the direct and indirect pathways of the basal ganglia. *Neuroscience*, 86(2), 353–387. doi: 10.1016/S0306-4522(98)00004-9
- Smitha, K. A., Akhil Raja, K., Arun, K. M., Rajesh, P. G., Thomas, B., Kapilamoorthy, T. R. & Kesavadas, C. (2017). Resting state fMRI: A review on methods in resting state connectivity analysis and resting state networks. *Neuroradiology Journal*, 30(4), 305–317. doi: 10.1177/1971400917697342
- Smucny, J., Wylie, K. P. & Tregellas, J. R. (2014). Functional magnetic resonance imaging of intrinsic brain networks for translational drug

- discovery. *Trends in Pharmacological Sciences*, 35(8), 397–403. doi: 10.1016/j.tips.2014.05.001
- Soares, D. P. & Law, M. (2009). Magnetic resonance spectroscopy of the brain: review of metabolites and clinical applications. *Clinical Radiology*, 64(1), 12–21. doi: 10.1016/j.crad.2008.07.002
- Soghomonian, J. J. & Martin, D. L. (1998). Two isoforms of glutamate decarboxylase: Why? *Trends in Pharmacological Sciences*, 19(12), 500–505. doi: 10.1016/S0165-6147(98)01270-X
- Sohal, V. S., Zhang, F., Yizhar, O. & Deisseroth, K. (2009). Parvalbumin neurons and gamma rhythms enhance cortical circuit performance. *Nature*, 459(7247), 698–702. doi: 10.1038/nature07991
- Somogyi, P. & Klausberger, T. (2005). Defined types of cortical interneurone structure space and spike timing in the hippocampus. *Journal of Physiology*, 562(1), 9–26. doi: 10.1113/jphysiol.2004.078915
- Sonnewald, U., Kortner, T. M., Qu, H., Olstad, E., Suñol, C., Bak, L. K., ... Waagepetersen, H. S. (2006). Demonstration of extensive GABA synthesis in the small population of GAD positive neurons in cerebellar cultures by the use of pharmacological tools. *Neurochemistry International*, 48(6-7), 572–578. doi: 10.1016/j.neuint.2006.01.005
- Sowell, E. R., Kan, E., Yoshii, J., Thompson, P. M., Bansal, R., Xu, D., ... Peterson, B. S. (2008). Thinning of sensorimotor cortices in children with Tourette syndrome. *Nature Neuroscience*, 11(6), 637–639. doi: 10.1038/nn.2121
- Spencer, K. M., Nestor, P. G., Niznikiewicz, M. A., Salisbury, D. F., Shenton, M. E. & McCarley, R. W. (2003). Abnormal neural synchrony in schizophrenia. *Journal of Neuroscience*, 23(19), 7407–7411. doi: 10.1523/jneurosci.23-19-07407.2003
- Spencer, T., Biederman, J., Harding, M., Wilens, T. & Faraone, S. (1995). The Relationship between Tic Disorders and Tourette's Syndrome Revisited. *Journal of the American Academy of Child and Adolescent Psychiatry*, 34(9), 1133–1139. doi: 10.1097/00004583-199509000-00009
- Stagg, C. J., Bachtiar, V. & Johansen-Berg, H. (2011). What are we measuring with GABA Magnetic Resonance Spectroscopy? *Communicative & Integrative Biology*, 4(5), 573–575. doi: 10.4161/cib.16213
- Stan, A. D., Ghose, S., Zhao, C., Hulsey, K., Mihalakos, P., Yanagi, M., ... Tamminga, C. A. (2015). Magnetic resonance spectroscopy and tissue protein concentrations together suggest lower glutamate signaling in dentate gyrus in schizophrenia. *Molecular Psychiatry*, 20(4). doi: 10.1038/mp.2014.54

- Steen, R. G., Mull, C., McClure, R., Hamer, R. M. & Lieberman, J. A. (2006). Brain volume in first-episode schizophrenia: Systematic review and meta-analysis of magnetic resonance imaging studies. *British Journal of Psychiatry*, *188*(6), 510–518. doi: 10.1192/bjp.188.6.510
- Steriade, M. & Contreras, D. (1998). Spike-wave complexes and fast components of cortically generated seizures. I. Role of neocortex and thalamus. *Journal of Neurophysiology*, *80*(3), 1439–1455. doi: 10.1152/jn.1998.80.3.1439
- Stern, E., Silbersweig, D. A., Chee, K. Y., Holmes, A., Robertson, M. M., Trimble, M., . . . Dolan, R. J. (2000). Functional neuroanatomy of tics in Tourette syndrome. *Archives of General Psychiatry*, *57*(8), 741–748. doi: 10.1001/archpsyc.57.8.741
- Stevenson, C. W., Halliday, D. M., Marsden, C. A. & Mason, R. (2007). Systemic administration of the benzodiazepine receptor partial inverse agonist FG-7142 disrupts corticolimbic network interactions. *Synapse*, *61*(8), 646–663. doi: 10.1002/syn.20414
- Stocker, M., Krause, M. & Pedarzani, P. (1999). An apamin-sensitive Ca²⁺-activated K⁺ current in hippocampal pyramidal neurons. *Proceedings of the National Academy of Sciences of the United States of America*, *96*(8), 4662–4667. doi: 10.1073/pnas.96.8.4662
- Stone, D. J., Walsh, J. & Benes, F. M. (1999). Localization of cells preferentially expressing GAD67 with negligible GAD65 transcripts in the rat hippocampus. A double in situ hybridization study. *Molecular Brain Research*, *71*(2), 201–209. doi: 10.1016/S0169-328X(99)00185-0
- Sullivan, M. A., Chen, H. & Morikawa, H. (2008). Recurrent inhibitory network among striatal cholinergic interneurons. *Journal of Neuroscience*, *28*(35), 8682–8690. doi: 10.1523/JNEUROSCI.2411-08.2008
- Sun, M., Zhao, Y., Gu, Y. & Xu, C. (2012). Anti-inflammatory mechanism of taurine against ischemic stroke is related to down-regulation of PARP and NF- κ B. *Amino Acids*, *42*(5), 1735–1747. doi: 10.1007/s00726-011-0885-3
- Swanson, C. J. & Kalivas, P. W. (2000). Regulation of locomotor activity by metabotropic glutamate receptors in the nucleus accumbens and ventral tegmental area. *Journal of Pharmacology and Experimental Therapeutics*, *292*(1), 406–414.
- Swanson, L. W. (1977). The anatomical organization of septo-hippocampal projections. *Ciba Foundation symposium*(58), 25–48. doi: 10.1002/9780470720394.ch4
- Sweatt, J. D. (2007). Long-term potentiation: A candidate cellular mechanism for information storage in the CNS. In *Learning and*

memory: A comprehensive reference (Vol. 4, pp. 295–326). Elsevier.
doi: 10.1016/B978-012370509-9.00016-4

- Swerdlow, N. R. (2013). Update: Studies of prepulse inhibition of startle, with particular relevance to the pathophysiology or treatment of Tourette Syndrome. *Neuroscience and Biobehavioral Reviews*, *37*(6), 1150–1156. doi: 10.1016/j.neubiorev.2012.09.002
- Swerdlow, N. R., Braff, D. L. & Geyer, M. A. (1990). GABAergic projection from nucleus accumbens to ventral pallidum mediates dopamine-induced sensorimotor gating deficits of acoustic startle in rats. *Brain Research*, *532*(1-2), 146–150. doi: 10.1016/0006-8993(90)91754-5
- Swerdlow, N. R., Braff, D. L. & Geyer, M. A. (1999). Cross-species studies of sensorimotor gating of the startle reflex. *Annals of the New York Academy of Sciences*, *877*, 202–216. doi: 10.1111/j.1749-6632.1999.tb09269.x
- Swerdlow, N. R., Braff, D. L., Geyer, M. A. & Koob, G. F. (1986). Central dopamine hyperactivity in rats mimics abnormal acoustic startle response in schizophrenics. *Biological Psychiatry*, *21*(1), 23–33. doi: 10.1016/0006-3223(86)90005-3
- Swerdlow, N. R., Braff, D. L., Masten, V. L. & Geyer, M. A. (1990). Schizophrenic-like sensorimotor gating abnormalities in rats following dopamine infusion into the nucleus accumbens. *Psychopharmacology*, *101*(3), 414–420. doi: 10.1007/BF02244063
- Swerdlow, N. R., Caine, S. B. & Geyer, M. A. (1992). Regionally selective effects of intracerebral dopamine infusion on sensorimotor gating of the startle reflex in rats. *Psychopharmacology*, *108*(1-2), 189–195. doi: 10.1007/BF02245306
- Swerdlow, N. R. & Geyer, M. A. (1993). Prepulse Inhibition of Acoustic Startle in Rats After Lesions of the Pedunculopontine Tegmental Nucleus. *Behavioral Neuroscience*, *107*(1), 104–117. doi: 10.1037/0735-7044.107.1.104
- Swerdlow, N. R., Geyer, M. A. & Braff, D. L. (2001). Neural circuit regulation of prepulse inhibition of startle in the rat: Current knowledge and future challenges. *Psychopharmacology*, *156*(2-3), 194–215. doi: 10.1007/s002130100799
- Swerdlow, N. R., Karban, B., Ploum, Y., Sharp, R., Geyer, M. A. & Eastvold, A. (2001). Tactile prepuff inhibition of startle in children with Tourette's syndrome: In search of an "fMRI-friendly" startle paradigm. *Biological Psychiatry*, *50*(8), 578–585. doi: 10.1016/S0006-3223(01)01164-7

- Swerdlow, N. R. & Sutherland, A. N. (2005). Using animal models to develop therapeutics for Tourette Syndrome. *Pharmacology and Therapeutics*, *108*(3), 281–293. doi: 10.1016/j.pharmthera.2005.05.003
- Swerdlow, N. R., Weber, M., Qu, Y., Light, G. A. & Braff, D. L. (2008). Realistic expectations of prepulse inhibition in translational models for schizophrenia research. *Psychopharmacology*, *199*(3), 331–388. doi: 10.1007/s00213-008-1072-4
- Swerdlow, N. R., Zinner, S., Hartston, H., Filion, D. & Magulac, M. (1994). Central inhibitory deficits in OCD and Tourette syndrome. *Biological Psychiatry*, *35*(9), 664. doi: 10.1016/0006-3223(94)90835-4
- Talati, P., Rane, S., Kose, S., Blackford, J. U., Gore, J., Donahue, M. J. & Heckers, S. (2014). Increased hippocampal CA1 cerebral blood volume in schizophrenia. *NeuroImage: Clinical*, *5*, 359–364. doi: 10.1016/j.nicl.2014.07.004
- Tamminga, C. A., Thaker, G. K., Buchanan, R., Kirkpatrick, B., Alphas, L. D., Chase, T. N. & Carpenter, W. T. (1992). Limbic System Abnormalities Identified in Schizophrenia using Positron Emission Tomography with Fluorodeoxyglucose and Neocortical Alterations with Deficit Syndrome. *Archives of General Psychiatry*, *49*(7), 522–530. doi: 10.1001/archpsyc.1992.01820070016003
- Tarsy, D., Pycoc, C. J., Meldrum, B. S. & Marsden, C. D. (1978). Focal contralateral myoclonus produced by inhibition of gaba action in the caudate nucleus of rats. *Brain*, *101*(1), 143–162. doi: 10.1093/brain/101.1.143
- Tebartz Van Elst, L., Valerius, G., Büchert, M., Thiel, T., Rüsç, N., Bubl, E., ... Olbrich, H. M. (2005). Increased prefrontal and hippocampal glutamate concentration in schizophrenia: Evidence from a magnetic resonance spectroscopy study. *Biological Psychiatry*, *58*(9), 724–730. doi: 10.1016/j.biopsycho.2005.04.041
- Tepper, J. M., Abercrombie, E. D. & Bolam, J. P. (2007). Basal ganglia macrocircuits. In *Progress in brain research* (Vol. 160, pp. 3–7). doi: 10.1016/S0079-6123(06)60001-0
- Tepper, J. M. & Bolam, J. P. (2004). Functional diversity and specificity of neostriatal interneurons. *Current Opinion in Neurobiology*, *14*(6), 685–692. doi: 10.1016/j.conb.2004.10.003
- Tepper, J. M., Wilson, C. J. & Koós, T. (2008). Feedforward and feedback inhibition in neostriatal GABAergic spiny neurons. *Brain Research Reviews*, *58*(2), 272–281. doi: 10.1016/j.brainresrev.2007.10.008
- Théberge, J., Bartha, R., Drost, D. J., Menon, R. S., Malla, A., Takhar, J., ... Williamson, P. C. (2002). Glutamate and glutamine measured with 4.0 T proton MRS in never-treated patients with schizophrenia and

- healthy volunteers. *American Journal of Psychiatry*, 159(11), 1944–1946. doi: 10.1176/appi.ajp.159.11.1944
- Théberge, J., Williamson, K. E., Aoyama, N., Drost, D. J., Manchanda, R., Malla, A. K., ... Williamson, P. C. (2007). Longitudinal grey-matter and glutamatergic losses in first-episode schizophrenia. *British Journal of Psychiatry*, 191(4), 325–334. doi: 10.1192/bjp.bp.106.033670
- Tikoo, S., Cardona, F., Tommasin, S., Gianni, C., Conte, G., Upadhyay, N., ... Pantano, P. (2020). Resting-state functional connectivity in drug-naive pediatric patients with Tourette syndrome and obsessive-compulsive disorder. *Journal of Psychiatric Research*, 129, 129–140. doi: 10.1016/j.jpsychires.2020.06.021
- Tinaz, S., Belluscio, B. A., Malone, P., van der Veen, J. W., Hallett, M. & Horovitz, S. G. (2014). Role of the sensorimotor cortex in tourette syndrome using multimodal imaging. *Human Brain Mapping*, 35(12), 5834–5846. doi: 10.1002/hbm.22588
- Tinaz, S., Malone, P., Hallett, M. & Horovitz, S. G. (2015). Role of the right dorsal anterior insula in the urge to tic in tourette syndrome. *Movement Disorders*, 30(9), 1190–1197. doi: 10.1002/mds.26230
- Tingley, D. & Buzsáki, G. (2018). Transformation of a Spatial Map across the Hippocampal-Lateral Septal Circuit. *Neuron*, 98(6), 1229–1242. doi: 10.1016/j.neuron.2018.04.028
- Tkac, I., Henry, P. G., Zacharoff, L., Wedel, M., Gong, W., Deelchand, D. K., ... Dubinsky, J. M. (2012). Homeostatic adaptations in brain energy metabolism in mouse models of Huntington disease. *Journal of Cerebral Blood Flow and Metabolism*, 32(11), 1977–1988. doi: 10.1038/jcbfm.2012.104
- Tkáč, I., Starčuk, Z., Choi, I. Y. & Gruetter, R. (1999). In vivo 1H NMR spectroscopy of rat brain at 1 ms echo time. *Magnetic Resonance in Medicine*, 41(4), 649–656. doi: 10.1002/(SICI)1522-2594(199904)41:4<649::AID-MRM2>3.0.CO;2-G
- Torrey, E. F., Barci, B. M., Webster, M. J., Bartko, J. J., Meador-Woodruff, J. H. & Knable, M. B. (2005). Neurochemical markers for schizophrenia, bipolar disorder, and major depression in postmortem brains. *Biological Psychiatry*, 57(3), 252–260. doi: 10.1016/j.biopsych.2004.10.019
- Toth, K., Borhegyi, Z. & Freund, T. F. (1993). Postsynaptic targets of GABAergic hippocampal neurons in the medial septum-diagonal band of Broca complex. *Journal of Neuroscience*, 13(9), 3712–3724. doi: 10.1523/jneurosci.13-09-03712.1993

- Toyama, H., Ichise, M., Liow, J. S., Vines, D. C., Seneca, N. M., Modell, K. J., ... Innis, R. B. (2004). Evaluation of anesthesia effects on [18F]FDG uptake in mouse brain and heart using small animal PET. *Nuclear Medicine and Biology*, *31*(2), 251–256. doi: 10.1016/S0969-8051(03)00124-0
- Tregellas, J. R. (2014). Neuroimaging biomarkers for early drug development in schizophrenia. *Biological Psychiatry*, *76*(2), 111–119. doi: 10.1016/j.biopsych.2013.08.025
- Tregellas, J. R., Smucny, J., Harris, J. G., Olincy, A., Maharajh, K., Kronberg, E., ... Freedman, R. (2014). Intrinsic hippocampal activity as a biomarker for cognition and symptoms in schizophrenia. *American Journal of Psychiatry*, *171*(5), 549–556. doi: 10.1176/appi.ajp.2013.13070981
- Tremblay, L., Worbe, Y., Thobois, S., Sgambato-Faure, V. & Féger, J. (2015). Selective dysfunction of basal ganglia subterritories: From movement to behavioral disorders. *Movement disorders : official journal of the Movement Disorder Society*, *30*(9), 1155–1170. doi: 10.1002/mds.26199
- Trenkner, E. (1990). Possible role of glutamate with taurine in neuron-glia interaction during cerebellar development. *Progress in clinical and biological research*, *351*, 133–140.
- Tseng, K. Y., Kasanetz, F., Kargieman, L., Riquelme, L. A. & Murer, M. G. (2001). Cortical slow oscillatory activity is reflected in the membrane potential and spike trains of striatal neurons in rats with chronic nigrostriatal lesions. *Journal of Neuroscience*, *21*(16). doi: 10.1523/jneurosci.21-16-06430.2001
- Uhlhaas, P. J., Linden, D. E., Singer, W., Haenschel, C., Lindner, M., Maurer, K. & Rodriguez, E. (2006). Dysfunctional long-range coordination of neural activity during gestalt perception in schizophrenia. *Journal of Neuroscience*, *26*(31), 8168–8175. doi: 10.1523/JNEUROSCI.2002-06.2006
- Uhlhaas, P. J. & Singer, W. (2010). Abnormal neural oscillations and synchrony in schizophrenia. *Nature Reviews Neuroscience*, *11*(2), 100–113. doi: 10.1038/nrn2774
- Uhlhaas, P. J. & Singer, W. (2013). High-frequency oscillations and the neurobiology of schizophrenia. *Dialogues in Clinical Neuroscience*, *15*(3), 301–313. doi: 10.31887/dcns.2013.15.3/puhlhaas
- Vaccarino, F. M., Kataoka-Sasaki, Y. & Lenington, J. B. (2013). Cellular and Molecular Pathology in Tourette Syndrome. In *Tourette syndrome* (pp. 205–220). Oxford University Press. doi: 10.1093/med/9780199796267.003.0010

- van Os, J. & Kapur, S. (2009). Schizophrenia. *The Lancet*, *374*(9690), 635–645. doi: 10.1016/S0140-6736(09)60995-8
- Vargas, T., Dean, D. J., Osborne, K. J., Gupta, T., Ristanovic, I., Ozturk, S., ... Mittal, V. A. (2018). Hippocampal subregions across the psychosis spectrum. *Schizophrenia Bulletin*, *44*(5), 1091–1099. doi: 10.1093/schbul/sbx160
- Vincent, J. L., Patel, G. H., Fox, M. D., Snyder, A. Z., Baker, J. T., Van Essen, D. C., ... Raichle, M. E. (2007). Intrinsic functional architecture in the anaesthetized monkey brain. *Nature*, *447*(7140), 83–86. doi: 10.1038/nature05758
- Vinner, E., Israelashvili, M. & Bar-Gad, I. (2017). Prolonged striatal disinhibition as a chronic animal model of tic disorders. *Journal of Neuroscience Methods*, *292*, 20–29. doi: 10.1016/j.jneumeth.2017.03.003
- Vinner Harduf, E., Matzner, A., Belevsky, K. & Bar-Gad, I. (2021). Dissociation of tic generation from tic expression during the sleep-wake cycle. *iScience*, *24*(4). doi: 10.1016/j.isci.2021.102380
- Vogels, T. P. & Abbott, L. F. (2009). Gating multiple signals through detailed balance of excitation and inhibition in spiking networks. *Nature Neuroscience*, *12*(4), 483–491. doi: 10.1038/nn.2276
- Volk, D. W., Austin, M. C., Pierri, J. N., Sampson, A. R. & Lewis, D. A. (2000). Decreased glutamic acid decarboxylase67 messenger RNA expression in a subset of prefrontal cortical γ -aminobutyric acid neurons in subjects with schizophrenia. *Archives of General Psychiatry*, *57*(3), 237–245. doi: 10.1001/archpsyc.57.3.237
- Volk, D. W., Pierri, J. N., Fritschy, J. M., Auh, S., Sampson, A. R. & Lewis, D. A. (2002). Reciprocal alterations in pre- and post-synaptic inhibitory markers at chandelier cell inputs to pyramidal neurons in schizophrenia. *Cerebral Cortex*, *12*(10), 1063–1070. doi: 10.1093/cercor/12.10.1063
- Voorn, P., Vanderschuren, L. J., Groenewegen, H. J., Robbins, T. W. & Pennartz, C. M. (2004). Putting a spin on the dorsal-ventral divide of the striatum. *Trends in Neurosciences*, *27*(8), 468–474. doi: 10.1016/j.tins.2004.06.006
- Vouimba, R. M., Garcia, R. & Jaffard, R. (1998). Opposite effects of lateral septal LTP and lateral septal lesions on contextual fear conditioning in mice. *Behavioral Neuroscience*, *112*(4), 875–884. doi: 10.1037/0735-7044.112.4.875
- Waku, I., Magalhães, M. S., Alves, C. O. & de Oliveira, A. R. (2021). Haloperidol-induced catalepsy as an animal model for parkinsonism: A systematic review of experimental studies. *European Journal of Neuroscience*, *53*(11). doi: 10.1111/ejn.15222

- Walker, M. A., Highley, J. R., Esiri, M. M., McDonald, B., Roberts, H. C., Evans, S. P. & Crow, T. J. (2002). Estimated neuronal populations and volumes of the hippocampus and its subfields in schizophrenia. *American Journal of Psychiatry*, *159*(5), 821–828. doi: 10.1176/appi.ajp.159.5.821
- Wang, D., Guo, Q., Zhou, Y., Xu, Z., Hu, S. W., Kong, X. X., ... Cao, J. L. (2021). GABAergic Neurons in the Dorsal-Intermediate Lateral Septum Regulate Sleep-Wakefulness and Anesthesia in Mice. *Anesthesiology*, *135*(3), 463–481. doi: 10.1097/ALN.0000000000003868
- Wang, R. & Reddy, P. H. (2017). Role of Glutamate and NMDA Receptors in Alzheimer’s Disease. *Journal of Alzheimer’s Disease*, *57*(4), 1041–1048. doi: 10.3233/JAD-160763
- Wei, W., Zhang, N., Peng, Z., Houser, C. R. & Mody, I. (2003). Perisynaptic Localization of δ Subunit-Containing GABAA Receptors and Their Activation by GABA Spillover in the Mouse Dentate Gyrus. *Journal of Neuroscience*, *23*(33), 10650–10661. doi: 10.1523/jneurosci.23-33-10650.2003
- Weiss, A. P., Zalesak, M., DeWitt, I., Goff, D., Kunkel, L. & Heckers, S. (2004). Impaired hippocampal function during the detection of novel words in schizophrenia. *Biological Psychiatry*, *55*(7), 668–675. doi: 10.1016/j.biopsych.2004.01.004
- Wenneberg, C., Glenthøj, B. Y., Hjorthøj, C., Buchardt Zingenberg, F. J., Glenthøj, L. B., Rostrup, E., ... Nordentoft, M. (2020). Cerebral glutamate and GABA levels in high-risk of psychosis states: A focused review and meta-analysis of 1H-MRS studies. *Schizophrenia Research*, *215*, 38–48. doi: 10.1016/j.schres.2019.10.050
- West, M. O., Carelli, R. M., Pomerantz, M., Cohen, S. M., Gardner, J. P., Chapin, J. K. & Woodward, D. J. (1990). A region in the dorsolateral striatum of the rat exhibiting single-unit correlations with specific locomotor limb movements. *Journal of Neurophysiology*, *64*(4), 1233–1246. doi: 10.1152/jn.1990.64.4.1233
- Whittington, C., Pennant, M., Kendall, T., Glazebrook, C., Trayner, P., Groom, M., ... Hollis, C. (2016). Practitioner Review: Treatments for Tourette syndrome in children and young people – a systematic review. *Journal of Child Psychology and Psychiatry and Allied Disciplines*, *57*(9), 988–1004. doi: 10.1111/jcpp.12556
- Whitworth, A. B., Honeder, M., Kremser, C., Kemmler, G., Felber, S., Hausmann, A., ... Fleischhacker, W. W. (1998). Hippocampal volume reduction in male schizophrenic patients. *Schizophrenia Research*, *31*(2-3), 73–81. doi: 10.1016/S0920-9964(98)00013-9

- Wijtenburg, S. A., Wright, S. N., Korenic, S. A., Gaston, F. E., Ndubizu, N., Chiappelli, J., ... Rowland, L. M. (2017). Altered Glutamate and Regional Cerebral Blood Flow Levels in Schizophrenia: A 1 H-MRS and pCASL study. *Neuropsychopharmacology*, *42*(2), 562–571. doi: 10.1038/npp.2016.172
- Williams, L. E., Blackford, J. U., Luksik, A., Gauthier, I. & Heckers, S. (2013). Reduced habituation in patients with schizophrenia. *Schizophrenia Research*, *151*(1-3), 124–132. doi: 10.1016/j.schres.2013.10.017
- Williams, S. A., Gwilt, M., Hock, R., Taylor, C., Loayza, J., Stevenson, C. W., ... Bast, T. (2022). Hippocampal Disinhibition Reduces Contextual and Elemental Fear Conditioning While Sparing the Acquisition of Latent Inhibition. *eNeuro*, *9*(1). doi: 10.1523/ENEURO.0270-21.2021
- Willott, J. F., Carlson, S. & Chen, H. (1994). Prepulse inhibition of the startle response in mice: Relationship to hearing loss and auditory system plasticity. *Behavioral Neuroscience*, *108*(4), 703–713. doi: 10.1037/0735-7044.108.4.703
- Winslow, J. T., Parr, L. A. & Davis, M. (2002). Acoustic startle, prepulse inhibition, and fear-potentiated startle measured in rhesus monkeys. *Biological Psychiatry*, *51*(11), 859–866. doi: 10.1016/S0006-3223(02)01345-8
- Wirtshafter, D., Asin, K. E. & Kent, E. W. (1978). Nucleus accumbens lesions reduce amphetamine hyperthermia but not hyperactivity. *European Journal of Pharmacology*, *51*(4), 449–452. doi: 10.1016/0014-2999(78)90437-5
- Wirtshafter, H. S. & Wilson, M. A. (2019). Locomotor and Hippocampal Processing Converge in the Lateral Septum. *Current Biology*, *29*(19), 3177–3192. doi: 10.1016/j.cub.2019.07.089
- Wobrock, T., Schneider, M., Kadovic, D., Schneider-Axmann, T., Ecker, U. K., Retz, W., ... Falkai, P. (2008). Reduced cortical inhibition in first-episode schizophrenia. *Schizophrenia Research*, *105*(1-3), 252–261. doi: 10.1016/j.schres.2008.06.001
- Wong, L. S., Eshel, G., Dreher, J., Ong, J. & Jackson, D. M. (1991). Role of dopamine and GABA in the control of motor activity elicited from the rat nucleus accumbens. *Pharmacology, Biochemistry and Behavior*, *38*(4), 829–835. doi: 10.1016/0091-3057(91)90250-6
- Woods, D. W., Walther, M. R., Bauer, C. C., Kemp, J. J. & Conelea, C. A. (2009). The development of stimulus control over tics: A potential explanation for contextually-based variability in the symptoms

- of Tourette syndrome. *Behaviour Research and Therapy*, *47*(1), 41–47. doi: 10.1016/j.brat.2008.10.013
- Worbe, Y., Baup, N., Grabli, D., Chaigneau, M., Mounayar, S., McCairn, K., ... Tremblay, L. (2009). Behavioral and movement disorders induced by local inhibitory dysfunction in primate striatum. *Cerebral Cortex*, *19*(8), 1844–1856. doi: 10.1093/cercor/bhn214
- Worbe, Y., Malherbe, C., Hartmann, A., Péligrini-Issac, M., Messé, A., Vidailhet, M., ... Benali, H. (2012). Functional immaturity of cortico-basal ganglia networks in Gilles de la Tourette syndrome. *Brain*, *135*(6), 1937–1946. doi: 10.1093/brain/aws056
- Wu, M., Brudzynski, S. M. & Mogenson, G. J. (1993). Functional interaction of dopamine and glutamate in the nucleus accumbens in the regulation of locomotion. *Canadian Journal of Physiology and Pharmacology*, *71*(5-6), 407–413. doi: 10.1139/y93-061
- Wu, Z. Y. & Xu, T. L. (2003). Taurine-evoked chloride current and its potentiation by intracellular Ca²⁺ in immature rat hippocampal CA1 neurons. *Amino Acids*, *24*(1-2), 155–161. doi: 10.1007/s00726-002-0314-8
- Yael, D., Israelashvili, M. & Bar-Gad, I. (2016). Animal models of Tourette syndrome—from proliferation to standardization. *Frontiers in Neuroscience*, *10*, 132. doi: 10.3389/fnins.2016.00132
- Yael, D., Tahary, O., Gurovich, B., Belelovsky, K. & Bar-Gad, I. (2019). Disinhibition of the nucleus accumbens leads to macro-scale hyperactivity consisting of micro-scale behavioral segments encoded by striatal activity. *Journal of Neuroscience*, *39*(30), 5897–5909. doi: 10.1523/JNEUROSCI.3120-18.2019
- Yin, H. H. (2017). The Basal Ganglia in Action. *Neuroscientist*, *23*(3), 299–313. doi: 10.1177/1073858416654115
- Yoshida, M., Nagatsuka, Y., Muramatsu, S. & Nijima, K. (1991). Differential roles of the caudate nucleus and putamen in motor behavior of the cat as investigated by local injection of GABA antagonists. *Neuroscience Research*, *10*(1), 34–51. doi: 10.1016/0168-0102(91)90018-T
- Zebardast, N., Crowley, M. J., Bloch, M. H., Mayes, L. C., Wyk, B. V., Leckman, J. F., ... Swain, J. E. (2013). Brain mechanisms for prepulse inhibition in adults with Tourette syndrome: Initial findings. *Psychiatry Research - Neuroimaging*, *214*(1), 33–41. doi: 10.1016/j.psychresns.2013.05.009
- Zhang, Z. J. & Reynolds, G. P. (2002). A selective decrease in the relative density of parvalbumin-immunoreactive neurons in the hippocampus in schizophrenia. *Schizophrenia Research*, *55*(1-2), 1–10. doi: 10.1016/S0920-9964(01)00188-8

- Zhong, C., Luo, Q. & Jiang, J. (2014). Blockade of N-acetylaspartylglutamate peptidases: A novel protective strategy for brain injuries and neurological disorders. *International Journal of Neuroscience*, *124*(12), 867–873. doi: 10.3109/00207454.2014.890935
- Zhu, F., Tang, L., Zhu, P., Lin, Q., Yuan, Q., Shi, W., ... Shao, Y. (2019). Resting-state functional magnetic resonance imaging (fMRI) and functional connectivity density mapping in patients with corneal ulcer. *Neuropsychiatric Disease and Treatment*, *15*, 1833–1844. doi: 10.2147/NDT.S210658
- Zinner, S. H. & Mink, J. W. (2010). Movement disorders I: Tics and stereotypies. *Pediatrics in Review*, *31*(6), 223–233. doi: 10.1542/pir.31-6-223